# Characterization of primary cilia in patient-derived glioma stem cells

Inaugural Dissertation

zur

Erlangung des Doktorgrades
Dr. nat. med.

der Medizinischen Fakultät
und
der Mathematisch-Naturwissenschaftlichen Fakultät
der Universität zu Köln

vorgelegt von

Gladiola Goranci-Buzhala

aus Gjakovë, Kosovo

Copy-Star
Köln
2020

| | |
|---|---|
| Betreuer: | Prof. Dr. Jay Gopalakrishnan |
| Referent/Referentin: | Prof. Dr. Mirka Uhlirova |
| | Prof. Dr. Bernhard Schermer |
| Datum der mündlichen Prüfung: | 10.06.2020 |

## Table of contents

**Abbreviations** ..... **3**

**List of figures** ..... **7**

**List of tables** ..... **9**

**Abstract** ..... **10**

**Zusammenfassung** ..... **11**

**1. Introduction** ..... **13**

**1.1 Cilium is a conserved eukaryotic cellular structure** ..... **13**

**1.2 Historical aspects of the primary cilium** ..... **15**

**1.3 Ciliogenesis** ..... **15**

1.3.1 Stages of cilium biogenesis ..... 16

**1.4 Cilium assembly** ..... **17**

1.4.1 Initiation of cilium assembly ..... 18

1.4.2 Maintenance of ciliary length ..... 19

**1.5 Cilium disassembly** ..... **20**

1.5.1 Aurora-A/HDAC6 dependent cilium disassembly ..... 21

1.5.2 NEK2/KIF24 dependent cilium disassembly ..... 23

1.5.3 CPAP mediated cilium disassembly ..... 25

**1.6 The cilium functions as a signaling hub** ..... **25**

1.6.1 Hedgehog signaling pathway ..... 26

1.6.2 PDGFR-α signaling pathway ..... 27

**1.7 Primary cilia in the regulation of neural stem cell proliferation and brain development** ..... **28**

**1.8 Primary cilia in human cancers** ..... **29**

**1.9 Glioblastoma multiforme** ..... **31**

1.9.1 Current evidence for role of primary cilia in glioblastoma ..... 32

**2. Objectives and Aims** ..... **35**

**3. Results** ..... **36**

**3.1 Patient-derived GSCs exhibit suppressed ciliogenesis** ..... **36**

**3.2 GSCs have an elevated level of CDC that contains NEK2 and KIF24 as crucial components** ..... **40**

**3.3 Depletion of CDC components induces cilia in GSCs** ..... **43**

**3.4 Ciliogenesis is associated with reduced recruitment of CDC** ..... **47**

**3.5 Perturbing CDC recruitment can induce functional cilia in GSCs** ..... **50**

**3.6 Inducing ciliogenesis triggers GSCs differentiation** ..... **52**

**3.7 GSCs differentiation is a cilium-dependent process** ..... **54**

**3.8 PDGFR-α signaling is regulated through primary cilia** ..... **56**

**3.9 Global transcriptome analysis reveals differentiation toward neuronal lineage** ..... **60**

**3.10 Infiltration assay in 3D brain organoids ..... 62**
3.10.1 Assay 1: co-culture iPSCs and GSCs ..... 62
3.10.2 Assay 2: supplying GSCs to organoids ..... 65
3.10.3 Assay3: fusion of GSCs spheres with mature organoids ..... 69
**3.11 Ciliated GSCs fail to invade into brain organoids ..... 71**
**3.12 Cilium induction triggers differentiation of GSCs within 3D organoids ..... 74**
**4. Discussion ..... 76**
**4.1 Glioma stem cells have suppressed ciliogenesis ..... 76**
**4.2 Elevated levels of CDC complex suppress ciliogenesis in GSCs ..... 77**
**4.3 Targeting CDC complex is a potential mechanism to induce ciliogenesis in GSCs ..... 77**
4.3.1 CDC proteins promote cell cycle progression in cancer cells ..... 78
**4.4 Newly induced cilia in GSCs are functional ..... 79**
4.4.1 Dual role of cilia in brain tumors ..... 79
**4.5 Cilium induction triggers GSCs to switch from a stemness to a differentiation state ..... 80**
**4.6 Cilium induction sequesters elevated level of PDGFR-α ..... 81**
**4.7 Human brain organoid as a tool to study GSCs invasion assay ..... 82**
**4.8 Future perspectives ..... 84**
**5. Material and Methods ..... 85**
**5.1 Material ..... 85**
**5.2 Instruments and Apparatus ..... 88**
**5.3 Cell lines ..... 89**
**5.4 Antibodies ..... 90**
**5.5 Solutions and mixtures ..... 93**
**5.6 Molecular biology ..... 94**
5.6.1 Polymerase chain reaction (PCR) ..... 94
5.6.2 Gel electrophoresis ..... 95
5.6.3 Restriction digest ..... 95
5.6.4 Ligation ..... 95
**5.7 2D cell culture ..... 96**
5.7.1 Culturing and maintenance of patient-derived GSCs ..... 96
5.7.2 Lentiviral production and transduction of target cells ..... 96
5.7.3 Culturing and maintenance of human iPSC culture ..... 97
5.7.4 Derivation of neural progenitor cells (NPCs) from iPSCs ..... 97
5.7.5 Astrocyte generation from neural progenitor cells ..... 97
5.7.6 Small interfering (si)RNA transfection ..... 98
5.7.7 Immuno-staining and light microscopy analysis of 2D cells ..... 98
**5.8 3D cell culture ..... 99**
5.8.1 Establishment of different assay conditions to model patient-derived GSCs in brain organoids ..... 99
5.8.2 Whole organoid tissue clearing ..... 100

5.8.3 Immunofluorescence microscopy and time-lapse imaging of organoids ..... 101
5.8.4 Organoid Immunostaining ..... 101
**5.9 Biochemistry ..... 102**
5.9.1 Protein concentration ..... 102
5.9.2 Denaturing SDS-polyacrylamide gel electrophoresis (SDS-PAGE) and western blot ..... 102
5.9.3 FLAG-immunoprecipitation (FLAG-IP) ..... 103
**5.10 RNA sequencing and analysis ..... 103**
**5.11 Statistical analysis ..... 103**
**References ..... 104**
**List of publications ..... 119**
**Curriculum vitae ..... 120**
**Acknowledgment ..... 122**
**Appendix ..... 124**
**Erklärung ..... 169**

# Abbreviations

| | |
|---|---|
| ADP | Adenosine diphosphate |
| AKNA | Microtubule organization protein AKNA |
| AKT | AKT serine/threonine kinase 1 |
| AMP | Adenosine monophosphate |
| ARL13B | ADP-ribosylation factor-like protein 13B |
| ASCL1 | Achaete-scute homolog 1 |
| ATP | Adenosine triphosphate |
| bFGF | Basic fibroblast growth factor |
| BSA | Bovine serum albumin |
| C2CD3 | C2 domain-containing protein 3 |
| Cc2d2a | Coiled-coil and C2 domain-containing protein 2A |
| CD133 | Prominin1 |
| CD15 | Fucosyltransferase 4 |
| CDK20 | Cyclin dependent kinase 20 |
| CDKN2A | Cyclin dependent kinase inhibitor 2A |
| cDNA | Complementary DNA |
| CEP120 | Centrosomal protein of 120 kDa |
| CEP164 | Centrosomal protein of 164 kDa |
| CEP83 | Centrosomal protein of 83 kDa |
| CEP89 | Centrosomal protein of 89 kDa |
| CEP97 | Centrosomal protein of 97 kDa |
| CHI3L1 | Chitinase 3-like 1 |
| CIP2A | Cancerous inhibitor of protein phosphatase 2A |
| CP110 | Centriolar coiled-coil protein of 110 kDa |
| CPAP | Centrosomal P4.1-associated protein |
| CRL3 | Interleukin-31 receptor subunit alpha |
| CRMP5 | Dihydropyrimidinase-related protein 5 |
| Cx43 | Gap junction alpha-1 protein |
| DAPI | 4',6-diamidino-2-phenylindole |
| dd $H_2O$ | Double distilled water |
| DMEM | Dulbecco’s modified eagle’s medium |
| DMSO | Dimethylsulfoxide |
| DNA | Deoxyribonucleic acid |
| ECM | Extracellular matrix |

| | |
|---|---|
| EDTA | Ethylenediaminetetraacetic acid |
| EdU | 5-ethynyl-2'-deoxyuridine |
| EGF | Epidermal growth factor |
| EM | Electron microscopy |
| FBF1 | Fas-binding factor 1 |
| FGFr1 | Fibroblast growth factor receptor 1 |
| FUCCI | Fluorescent ubiquitination-based cell cycle indicator |
| GABRA1 | Gamma-aminobutyric acid type A receptor alpha1 subunit |
| GBM | Glioblastoma multiforme |
| GFAP | Glial fibrillary acidic protein |
| GFP | Green fluorescent protein |
| GLI1 | GLI family zinc finger 1 |
| GLI2 | GLI family zinc finger 2 |
| GLI3 | GLI family zinc finger 3 |
| GSC | Glioblastoma stem cell |
| GSK3β | Glycogen synthase kinase-3 beta |
| GT335 | Glutamine amidotransferase like class 1 domain containing 3A |
| HDAC2 | Histone deacetylase 2 |
| HDAC6 | Histone deacetylase |
| Hh | Hedgehog signaling pathway |
| IDH1 | Isocitrate dehydrogenase (NADP(+) 1) |
| IFT20 | Intraflagellar transport 20 |
| IFT88 | Intraflagellar transport 88 |
| IGF-1 | Insulin-like growth factor 1 |
| IP | Immunoprecipitation |
| iPSC | Induced pluripotent stem cell |
| KCTD17 | BTB/POZ domain-containing protein KCTD17 |
| kDa | Kilodalton |
| KIF24 | Kinesin family member 24 |
| KIF2A | Kinesin family member 2A |
| KIF3A | Kinesin family member 3A |
| KIF7 | Kinesin family member 7 |
| LIMK2 | LIM domain kinase 2 |
| *MDM2* | Mouse double minute 2 homolog |
| *MET* | MET proto-oncogene, receptor tyrosine kinase |
| mRNA | Messenger RNA |
| MTOC | Microtubule organizing center |
| mTOR | Mammalian target of rapamycin |

| | |
|---|---|
| MYO5A | Myosin-Va |
| n. s. | Not significant |
| NaCl | Natrium/ sodium chloride |
| NDE1 | Nude neurodevelopment protein 1 |
| NEDD9 | Enhancer of filamentation |
| *NEFL* | Neurofilament light |
| NEK2 | NIMA related kinase 2 |
| NES | Nestin |
| NEURL4 | Neuralized-like protein 4 |
| NF-κB | Nuclear factor kappa B |
| NF1 | Neurofibromin 1 |
| NIMA | Never In Mitosis Gene A |
| OFD1 | Oral-facial-digital syndrome 1 protein |
| pAKT | Phosphorylated AKT serine/threonine kinase 1 |
| PBS | Phosphate buffer solution |
| PBST | PBS with 0.1% Triton-X |
| PCR | Polymerase chain reaction |
| PDGFR-α | Platelet-derived growth factor receptor alpha |
| PDGFR-β | Platelet-derived growth factor receptor beta |
| PIFO | Protein pitchfork |
| PLK1 | Polo-like kinase 1 |
| PMSF | Phenylmethane sulfonyl fluoride |
| PTCH1 | Protein patched homolog 1 |
| PTEN | Phosphatase and tensin homolog |
| RNA | Ribonucleic acid |
| RNAi | RNA interference |
| RPE | Retinal pigment epithelium cells |
| rpm | Revolutions per minute |
| RT | Room temperature |
| RTK | Receptor tyrosine kinase |
| S.D. | Standard deviation |
| SEM | Standard error |
| S100β | S100 calcium binding protein B |
| SCLT | Sodium channel and clathrin linker 1 |
| SLC12A5 | Solute carrier family 12 member 5 |
| SMO | Smoothened, frizzled class receptor |
| STED | Stimulated emission depletion |
| STIL | Sil, SCL/TAL1 interrupting locus |

| | |
|---|---|
| SUFU | SUFU negative regulator of hedgehog signaling |
| SYT1 | Synaptotagmin 1 |
| TAE | Tris base, acetic acid and EDTA |
| Tctex-1 | Dynein light chain Tctex-1 |
| Tctn1 | Tectonic-1 |
| Tctn2 | Tectonic-2 |
| TESK1 | Dual specificity testis-specific kinase 1 |
| Tmem67 | Meckelin |
| TMZ | Temozolomide |
| *TNF* | Tumor necrosis factor |
| *TP53* | Tumor protein P53 |
| Trichoplein | Trichoplein keratin filament-binding protein |
| Tris | 2-amino-2-(hydroxymethyl)1,3-propandiol |
| TTBK2 | Tau-tubulin kinase 2 |
| TUJ | Tubulin beta 3 class III |
| UBE3C | Ubiquitin-protein ligase E3C |
| *VHL* | von Hippel-Lindau disease tumor suppressor |
| WHO | World health organization |
| γ-TUBULIN | Gamma tubulin |

# List of figures

Figure 1.1. Ciliary structure. ..... 14
Figure 1.2. Biogenesis of the cilium. ..... 17
Figure 1.3. Cilium dynamics in cell cycle. ..... 21
Figure 1.4. Cilium disassembly. ..... 22
Figure 1.5. Schematic diagrams indicating KIF24 and NEK2 domains. ..... 24
Figure 1.6. Schematic diagram indicating CPAP different domains. ..... 25
Figure 1.7. Hedgehog signaling at the primary cilium. ..... 26
Figure 3.1. Patient-derived GSCs exhibit suppressed ciliogenesis. ..... 37
Figure 3.2. Suppressed ciliogenesis promotes cell proliferation. ..... 39
Figure 3.3. NEK2 and KIF24 co-purify with CDC proteins. ..... 40
Figure 3.4. GSCs have elevated levels of CDC components. ..... 42
Figure 3.5. Depletion of CDC components induce cilia in patient-derived GSC cell line. ..... 44
Figure 3.6. Overexpression of NEK2-KD induce cilia in proneural subtype of GSCs. ..... 45
Figure 3.7. Overexpression of NEK2-KD induces cilia and prevents cell proliferation. ..... 46
Figure 3.8. Ciliogenesis is irreversibly induced in GSCs after NEK2-KD overexpression. ..... 47
Figure 3.9. Overexpression of NEK2-KD impairs CDC recruitment to the newly induced cilia in GSCs. ..... 49
Figure 3.10. Induced cilia in GSCs are structurally and functionally normal. ..... 51
Figure 3.11. Induced cilia in GSCs can transduce Hh signaling upon SAG activation. ..... 52
Figure 3.12. Cilia induction trigger GSCs differentiation. ..... 53
Figure 3.13. Depletion of IFT88 prevents cilium assembly in GSC cell line. ..... 55
Figure 3.14. NEK2-KD induced GSCs differentiation is cilium-dependent process. ..... 56
Figure 3.15. Cilium induction relocates PDGFR-α to newly induced cilia. ..... 58
Figure 3.16. PDGFR-α in proneural GSCs is constitutively active. ..... 59
Figure 3.17. NEK2-KD induces GSC expression profiles indicative of cilium-dependent cell differentiation. ..... 61
Figure 3.18. Time-lapse confocal imaging of GSCs invasion in brain organoid using assay 1. ..... 63
Figure 3.19. Tissue cleared confocal imaging of GSCs invasion in brain organoid using assay 1. ..... 64
Figure 3.20. Time-lapse confocal imaging of GSCs invasion in brain organoid using assay 2. ..... 66
Figure 3.21. Tissue cleared confocal imaging of GSCs invasion in brain organoid using assay 2. ..... 67
Figure 3.22. iPSC-derived brain organoids express mature neural marker. ..... 68
Figure 3.23. Tissue cleared confocal imaging of fussed GSCs spheres to brain organoids using assay 3. ..... 70
Figure 3.24. Time-lapse confocal imaging shows that cilium induction prevents GSCs invasion into brain organoids. ..... 72

Figure 3.25. Tissue cleared confocal imaging shows that cilium induction prevents GSCs invasion into brain organoids. .....73
Figure 3.26. Differentiated GSCs impairs invasion into brain organoids. .....74

# List of tables

Table 1. Cancer types and pathways that results in suppressed ciliogenesis. ....31
Table 2. Primary cilia in glioblastoma cells. ....33
Table 3. List of materials ....85
Table 4. ATCC cell lines ....89
Table 5. Human induced pluripotent stem cells ....89
Table 6. Patient-derived GSCs ....89
Table 7. Targeted GSC lines ....90
Table 8. Primary antibodies ....90
Table 9. Secondary antibodies ....92
Table 10. Buffers ....93
Table 11. List of oligonucleotide sequences used for cloning. ....95
Table 12. List of upregulated gene expression levels (FPKM; >0.6 log2-fold change, FDR<0.01) in U3047MG naïve), ciliated GSCs (U3047MG NEK2-KD) cells ....124
Table 13. List of downregulated gene expression levels (FPKM; >0.6 log2-fold change, FDR<0.01) in U3047MG naïve), ciliated GSCs (U3047MG NEK2-KD) cells. ....146

# Abstract

Primary cilia are highly conserved eukaryotic organelles that serve as a ‘’cellular antenna’’ for signaling functions. Dysfunctions or defects in primary cilia are associated with numerous human diseases. Typically, the mother centriole, transforms into a structure called basal body, which then templates the formation of the primary cilium. Abnormal cilia are implicated in cancer progressions such as in breast, pancreatic, brain, and prostate cancers. Glioblastoma multiforme (GBM) is one of the most frequent lethal primary brain tumors.

GBM is characterized by extreme heterogeneity, rapid growth, and efficient invasion of neoplastic cells, called Glioblastoma Stem-like Cells (GSCs). GSCs represent a subpopulation of the cells that are resistant to treatment and are suspected to be driving forces for the disease recurrence. Until now, there is no effective treatment for GBM. The average median survival time of the patients from the initial diagnosis is 12-15 months. GBM cells appear to lose cilia, which can contribute to the malignant phenotype. However, the mechanism of suppressed ciliogenesis is not fully characterized yet. Thus, the aims of this thesis were **(i)** to understand the possible mechanisms that can suppress the ciliogenesis in GSCs, **(ii)** to investigate the pathways that could restore the ciliogenesis and, **(iii)** characterize GSCs after cilium induction.

Primary cilium assembly and disassembly are a dynamic process, which is coupled with the cell cycle. At the onset of cilium disassembly, the Centrosomal-P4.1-associated protein (CPAP) provides a scaffold for the cilium-disassembly complex (CDC) proteins, including NDE1, OFD1, NEK2, and CPAP. These proteins are recruited to the ciliary base to ensure timely cilium disassembly and promote cell cycle progression. Hence, using multidisciplinary approaches, the current doctoral thesis investigated primary cilia dynamics in multiple patient-derived GSCs. The experiments revealed that elevated levels and recruitment of CDC components lead to suppressing of the ciliogenesis and an increase in the cell cycle progression.

Moreover, depletion of different CDC proteins induced ciliogenesis in GSCs in which PDGFR-α level is elevated. Among the CDC proteins, NEK2 depletion induced the maximum frequencies of ciliation in GSCs. Furthermore, inducible overexpression of the catalytically inactive NEK2 in GSCs was sufficient to induce cilia irreversibly. Importantly, both functional, including transcriptomic analyzes, showed that cilium induction switched GSCs from self-renewal to differentiation state. Taken together, the current work provides evidence for a novel mechanism to induce ciliogenesis in patient-derived GSCs and suggests that the cilium induction can potentially serve as a new strategy to intervene in GSCs proliferation.

# Zusammenfassung

Primäre Zilien sind hochkonservierte eukaryote Organellen, die als „zelluläre Antennen“ für die Signalfunktionen dienen. Fehlfunktionen oder Defekte in primären Zilien sind mit verschiedenen humanen Erkrankungen assoziiert. Die Formation des primären Ziliums erfolgt typischerweise durch die “Mutter-Zentriole”, die den Basalkörper des Ziliums formt. Abnormale Zilien spielen eine Rolle in der Progression bei z.B. Brust-, Pankreas-, Hirn-, und Prostata-Krebs. Das Glioblastom (GBM) ist einer der am häufigsten vorkommenden letalen primären Gehirntumore. Das GBM ist äußerst heterogen und durch ein rapides Wachstum und eine effiziente Invasion der neoplastischen Zellen, den sogenannten Glioblastom-Stammzell-ähnlichen Zellen (in engl. GSCs = Glioblastoma Stem-like Cells), gekennzeichnet. Die GSCs repräsentieren eine Untergruppe derjenigen Zellen, die behandlungsresistent sind und für die treibende Kraft beim Relaps dieser Erkrankung gehalten werden.

Bis heute gibt es keine wirksame Therapie für das GBM. Die durchschnittliche Überlebenszeit der Patienten von der anfänglichen Diagnose beträgt zwischen 12 und 15 Monaten. GBM-Zellen scheinen das primäre Zilium zu verlieren, und dieser Verlust kann zu malignen Phänotypen beitragen. Der Mechanismus dieser supprimierten Ziliogenese ist jedoch noch nicht vollständig beschrieben. Aus diesem Grund war das Ziel dieser Arbeit **(i)** den möglichen Mechanismus zu verstehen, der die Ziliogenese unterdrückt, **(ii)** zu untersuchen, wie man die Ziliogenese wieder induzieren kann, und **(iii)** die GSCs nach dieser Induktion zu charakterisieren. Der Aufbau und Abbau des primären Ziliums ist ein dynamischer Prozess, der mit dem Zellzyklus gekoppelt ist. Zu Beginn des Zilium-Abbaus bildet das Centrosomal-P4.1-associated Protein (CPAP) ein Gerüst für die Proteine des Zilium-Abbau-Komplexes (Cilium-Disassembly-Complex, CDC), wie zum Beispiel Nde1, OFD1, NEK2 und CPAP. Diese Proteine werden dann an die Basis des Ziliums rekrutiert, um dessen Abbau sicherzustellen und das Voranschreiten des Zellzyklus zu fördern. Anhand multidisziplinärer Ansätze habe ich die Dynamik des primären Ziliums in mehreren von Patienten abstammenden GSCs untersucht. Mit meinen Experimenten konnte ich zeigen, dass erhöhte Level der CDC und dessen Rekrutierung zu einer Unterdrückung der Ziliogenese und zu einer Zunahme der Zellzyklus-Progression führten. Dagegen konnte die Abnahme der verschiedenen CDC-Proteine die Ziliogenese in den GSCs induzieren, in welchen das PDGFR-α Level erhöht war. Unter den CDC-Proteinen wurde die höchste Anzahl an ziliierten GSCs induziert, wenn NEK2 unterdrückt wurde. Des Weiteren reichte die induzierbare Überexpression des katalytisch inaktiven NEK2-Proteins in GSCs aus, um die Zilien irreversibel zu induzieren. Sowohl funktionelle als auch transkriptionelle Analysen zeigten, dass durch die Induktion der Zilien die GSCs aus dem Selbsterneuerungs-Modus in den Differenzierungs-Modus umschalten. Schließlich demonstrierte ich anhand eines auf *in vitro* humanen Hirn-Organoiden basierenden GSCs-Invasions-Assays, dass die Zilium-Induktion die Differenzierung triggert, und dabei die Infiltrierung der GSCs in die Hirn-Organoide verhindert.

Zusammenfassend liefert diese Arbeit wichtige Erkenntnisse auf einen neuen Mechanismus zur Induktion der Zilien in Patienten-abstammenden GSCs und gibt Hinweise, wie die Induktion des Ziliums potentiell als neue Strategie dazu dienen kann, die GSCs-Proliferation zu beeinflussen.

# 1. Introduction

## 1.1 Cilium is a conserved eukaryotic cellular structure

Eukaryotic cells display a complex and extensive intracellular compartmentalization based on numerous organelles. In contrast to prokaryotes, approximately half of the volume of eukaryotic cytoplasm consists of a variety of membrane-enclosed organelles, such as the nucleus, endoplasmic reticulum, Golgi apparatus, mitochondria, endosomes, lysosomes, and cilium. Extensive studies have identified the biogenesis mechanisms, functions, and dysfunctions of most of these organelles. However, the cellular structure and function of cilium is less explored, although it is an evolutionary conserved eukaryotic organelle, ranging from green algae to higher metazoans, including human cells (Alberts et al., 2002, Carvalho-Santos et al., 2011). Centrosomes are the major microtubule-organizing centers of animal cells essential for accurate cell division. At their core, a centrosome consists of a pair of centrioles surrounded by a protein network of peri-centriolar material (PCM). Within a centrosome, the mature centriole functions as a basal body to template a cilium, a microtubule-based structure that protrudes from the surface of virtually all eukaryotic interphase cells, playing key roles in signaling pathways, cellular differentiation, and organism development (Avidor-Reiss and Gopalakrishnan, 2012, Nigg and Raff, 2009).

Historically, cilia have been classified as either motile or immotile (primary cilia). The primary cilium is formed on the apical surface of most of the polarized vertebrate cells. The primary cilium is immotile, and it can sense physical and biochemical signals. On the other hand, the motile cilia are present on trachea and oviduct epithelial cell surfaces and collectively beat in wave-like patterns to promote fluid movement (Ishikawa and Marshall, 2011).

Differences in structure, motility, and morphology define the different cilia types, namely the primary and motile cilia. The differences are especially evident for motile cilia that occur as bundles on epithelial cells versus the single motile sperm flagellum, or specialized sensory cilia like the photoreceptors and the prototypical primary cilium **(Figure 1.1).** Motile cilia (or flagella on unicellular organisms) are present on specialized cells such as sperm cells to control cell movement. However, almost all vertebrate cells exhibit a primary cilium that is a solitary non-motile or sensory cilium.

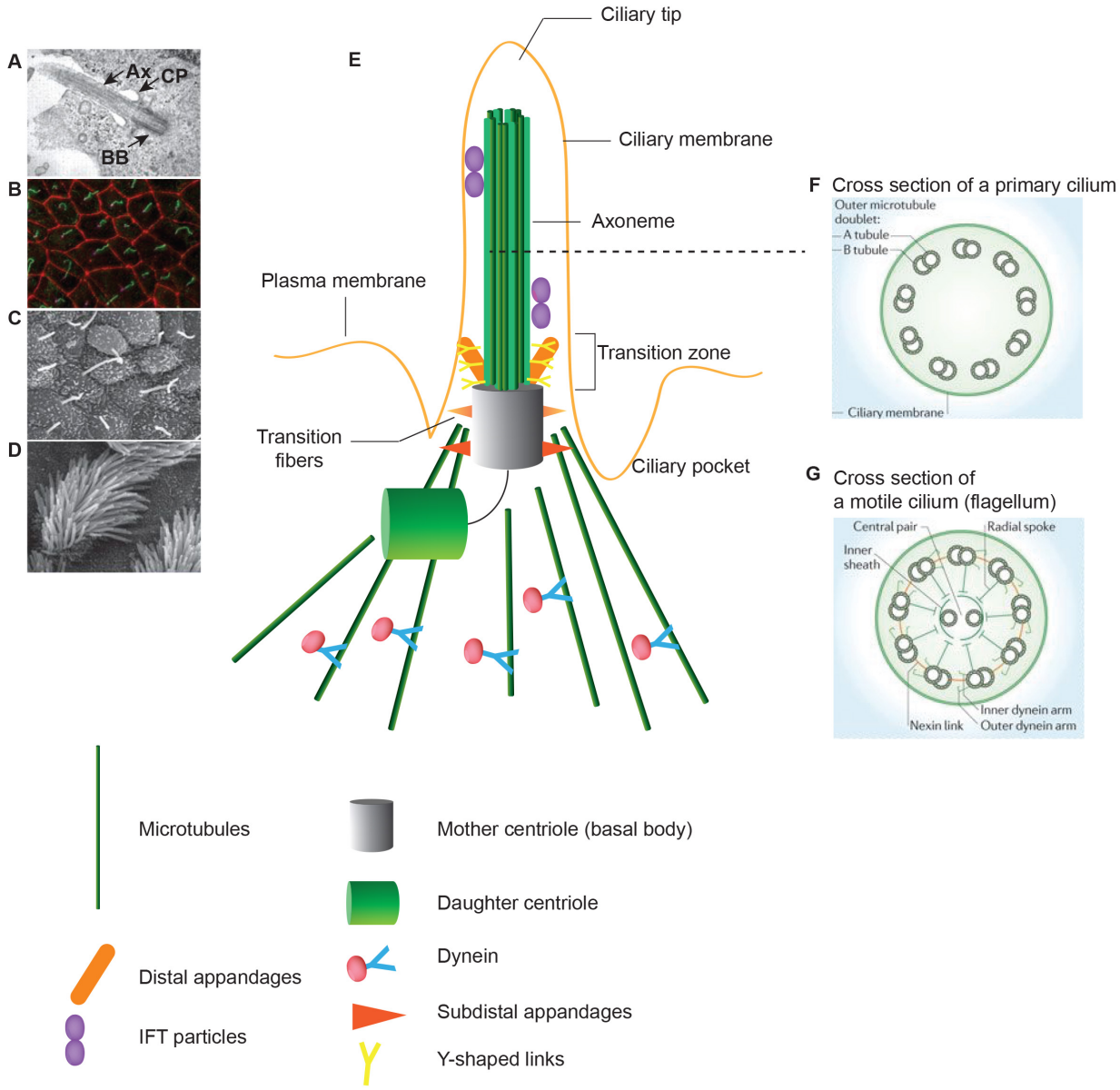


**Figure 1.1. Ciliary structure.**
**A.** Electron microscopy (EM) image of a primary cilium in retinal-pigmented epithelial (RPE) cells. Ciliary structure elements are labeled with arrows. BB (basal body); CP (ciliary pocket); Ax (axoneme).
**B**. Immunofluorescence image of primary cilia in inner medullary collecting duct (IMCD3) cells. Primary cilia are shown in green, cell junctions are shown in red.
**C** and **D**. Scanning electron microgram (SEM) of mouse nodal motile cilia.
**E.** The core structure of a primary cilium is composed of microtubule bundles (ciliary axoneme) extending from the basal body, a microtubule-based structure derived from the mother centriole. The ciliary membrane is continuous with the plasma membrane.
**F and G**. Cross-section diagrams of a primary cilium (with a 9+0 axoneme), and a motile cilium (with 9+2 axoneme).
Images in **A-D**, and **F-G** are adopted from Ishikawa and Marshall review (Ishikawa and Marshall, 2011). The primary cilium graphical illustration **E** is modified from Wang and Dynlacht review (Wang and Dynlacht, 2018).

## 1.2 Historical aspects of the primary cilium

In 1898, Zimmerman first visualized the primary cilium as a hair-like structure organelle in rabbit kidney tubule epithelial cells. However, the term “primary cilium” was first used in 1968 by Sorokin, who studied the ciliogenesis in human pulmonary development (Sorokin, 1968a, Satir et al., 2010). The primary cilium (hereafter referred to as cilium) had not been considered as important but rather rudimentary until studies discovered that it serves as a sensory antenna and play a crucial role in various signaling pathways (Hirokawa et al., 2006, Fliegauf et al., 2007, Satir and Christensen, 2007, Gerdes et al., 2009). Since then, the physiological relevance of the cilium has been recognized in a variety of human cells such as stem cells, epithelial, endothelial, kidney tubule, bile duct, photoreceptor, and pancreatic cells (Fliegauf et al., 2007). Importantly, defects in the cilium formation or function can cause a wide range of human disorders collectively termed ciliopathies (Badano et al., 2006, Waters and Beales, 2011, Seeger-Nukpezah et al., 2013). In this regard, the cilium has been particularly gaining attention and attracting many questions and thoughts about its role in human health and diseases, especially in cancer. However, the role of cilium in cancer development and progression is still not fully elucidated.

## 1.3 Ciliogenesis

The mother and the daughter centrioles are therefore important structures that govern future cilium formation. The centrioles and their surrounding proteins, called the pericentriolar material (PCM) are called centrosomes, which are basically tiny, non-membranous organelles involved in cell division. Ciliogenesis describes the assembly of the cilium when the cell is exiting the cell cycle. During ciliogenesis, the older mother centriole docks at the plasma membrane and functions as a basal body to initiate the cilium formation. The basal body nucleates the microtubule doublets to form the ciliary axoneme (Sorokin, 1968b, Vertii et al., 2016). The axoneme is the main skeleton of the cilium and emanates from the apical side of the basal body. The axoneme consists of nine doublet peripheral microtubules, either with or without a pair of singlet microtubules **(Figure 1.2F and G)** (Satir and Christensen, 2007). The 9+0 microtubule configuration in the non-motile primary cilium lacks dynein motors required for a ciliary movement. In contrast, motile cilia contain an additional pair of microtubules in the center (9+2), which provide cilia with motility **(Figure 1F and G)**. Complex molecules of inner, outer dynein arms, radial spokes, and nexin links enable ciliary movement and beating (Satir et al., 2007, Satir et al., 2010, Lindemann and Lesich, 2010).

The ciliary membrane closely sheaths the ciliary axoneme, which continues with the plasma membrane **(Figure 1.1E)** (Satir and Christensen, 2007, Sanchez and Dynlacht, 2016). Presumably, the ciliary membrane shares the same biochemical origins with the plasma membrane (Nachury et al., 2010, Garcia et al., 2018). However, it has been demonstrated that the ciliary membrane

constitutes at least 600 different proteins. But, until now, there is no evidence to prove that protein synthesis occurs within the cilium (Pazour et al., 2005, Ishikawa et al., 2012).
The basal body's distal end functions as a permeability barrier between cilium and cytoplasm, called as 'ciliary gate', consisting of two subregions that include transition fibers and the transition zone **(Figure 1.1E)** (Garcia-Gonzalo and Reiter, 2012). Transition fibers, also named distal appendages, anchor the mature mother centriole to the plasma membrane through the recruitment of Centrosomal protein 164 kDa (CEP164) and Outer dense fiber protein 2 (ODF2) (Pitaval et al., 2010). Furthermore, the transition fibers can also mediate the assembling of intraflagellar transport complexes and are believed to form a ‘ciliary pore complex’ that may provide size-dependent ciliary protein trafficking. The transition zone controls the intracellular trafficking of biomolecules along the ciliary axoneme **(Figure 1.1E)**. The ciliary pocket is another compartment of a membrane domain at the cilium base acting as a platform for ciliary endocytic activity, vesicular trafficking, and links the cilium to the actin cytoskeleton. Y-shaped linkers at the transition zone, called the ciliary necklace, also act as a permeability barrier, separate the cilium and cytoplasm components.

Despite similar structure and morphology throughout the human body, the prototypic cilium shows tissue-specific functions. Mutations causing defects in ciliary structure or function result in the tissue-specific phenotypes: they typically do not affect all ciliated cells. The specificity seems to be dependent on the mutation, cilia, and cell type. For example, loss of transition zone proteins (Tctn1, Tctn2, Tmem67 or Cc2d2a) in the worms, mice, or human cells have been shown to affect cilia and ciliary signaling in different tissues to a different extent (Wiegering et al., 2018, Garcia-Gonzalo et al., 2011, Williams et al., 2011). Likewise, depletion of a newly identified Microtubule organization protein AKNA (AKNA) did not affect cilia in neural stem cells, but rather ependymal cells of the brain, harboring motile cilia in the adult neural stem cell niche (Camargo Ortega et al., 2019).

### 1.3.1 Stages of cilium biogenesis

The process of cilium formation in vertebrate cells occurs through distinct routes, either extracellular or intracellular route, depending on whether the ciliogenesis starts at the cell surface or within the cytoplasm. The intracellular route of cilium formation occurs through a series of orchestrated events beginning with the mother centriole's maturation into a basal body and docking of the basal body at the plasma membrane (Westlake et al., 2011). In vitro experiments with mouse 3T3 fibroblast and retinal-pigmented epithelial (RPE) cells have contributed to the elucidation of ciliogenesis's critical aspects. In those models, the intracellular route's initial steps start with the formation of small cytoplasmic vesicles (pre-ciliary vesicles) that originate from the Golgi and the recycling endosome, accumulating in the proximity of mother centriole and distal appendages **(Figure 1.2 B, C, and D)**. The vesicle that docks at the mother centriole initiates the mother centriole transition to the basal body. Then, the basal body docks with the distal appendages' help at the plasma membrane and

initiates an axoneme formation **(Figure 1.2 E and F)** (Kobayashi et al., 2014, Lu et al., 2015, Schmidt et al., 2012, Sorokin, 1968b).

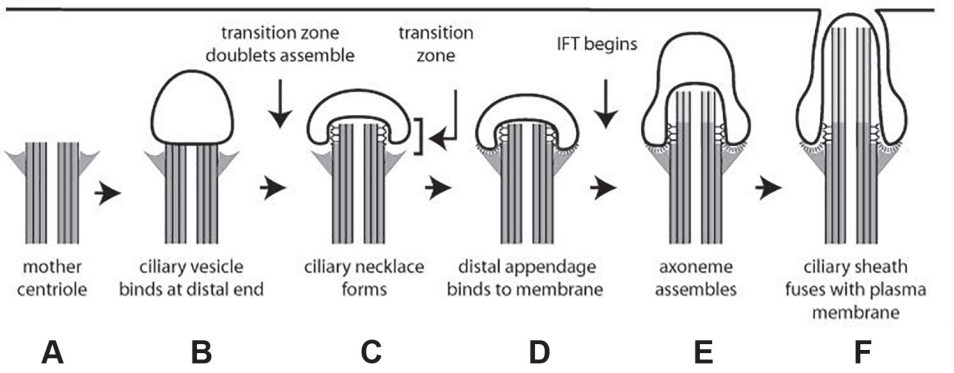


**Figure 1.2. Biogenesis of the cilium.**
Multiple stages of ciliogenesis. **A**. The transition of mother centriole to the basal body. **B**. Golgi-derived ciliary vesicle localizes to the mother centriole (basal body) and invaginates the nascent axoneme. **C**. The appearance of transition structures (Y-shaped linkers). **D**. Distal appendages help the basal body to dock to the plasma membrane. **E**. IFT-dependent axoneme elongation. **F**. Ciliary vesicles fuse with the new membrane to form a sheath that surrounds the elongating axonemal. Adopted from Sorokin (Sorokin, 1968b).

The extracellular route differs from the intracellular one in a way that centrioles do not capture vesicles in the cytoplasm. Initially, mother centriole migrates to the cell surface and docks at the plasma membrane with the help of distal appendage proteins, microtubules, and the actin cytoskeletons (Pitaval et al., 2017, Pitaval et al., 2010, Avidor-Reiss and Gopalakrishnan, 2013, Kobayashi and Dynlacht, 2011). After the docking event, the microtubule-based axoneme extends from the cell surface and forms the transition zone together with the trafficking machinery. However, it remains unclear how cells decide for either the intracellular or extracellular route, and whether this determines the ciliary function. Fibroblasts, RPE cells, and neural precursor cells template the cilium formation through Golgi-derived ciliary vesicle (intracellular route) (Baudoin et al., 2012). Polarized epithelial cells, on the other hand, form cilia through the direct fusion of the basal body to the plasma membrane (extracellular route) (Sung and Leroux, 2013, Sorokin, 1968b, Molla-Herman et al., 2010). The process of ciliogenesis may play a role in the cilium position, which can influence the functionality of the mature cilium. Importantly, in vertebrates, ciliogenesis is tightly coupled with cell division as centrioles are released from the plasma membrane to function as the spindle apparatus during mitosis. How cilia assembly and disassembly are coupled to the cell cycle, and the molecular players regulating cilia assembly and disassembly dynamics remain poorly understood.

## 1.4 Cilium assembly

During the cell cycle, newly formed centrioles are assembled from the existing mother and older (grandmother) centriole during the S-phase. Newly formed daughter centrioles are distinguished by the recruitment of daughter centriolar proteins such as Centrosomal protein of 120 kDA (CEP120),

Centrobin, and Neutralized-like protein 4 (NEURL4) (Li et al., 2012, Mahjoub et al., 2010, Zou et al., 2005). In the following cell cycle, the newly formed centrioles in each of the two daughter cells mature and will become mother centrioles, through the loss of daughter centriole proteins (CEP120, Centrobin, and NEURL4) at the $G_1$-S phase and followed by the gaining of distal appendages and subdistal appendages in the late $G_2$ phase. The distal and subdistal appendage proteins (CEP83, CEP89, SCLT, CEP164, and FBF1) are recruited to the distal end of the mother centriole (basal body) to promote the initial step of cilium assembly **(Figure 1.2)** (Sanchez and Dynlacht, 2016). The distal appendages are crucial for the initiation of the ciliogenesis, starting with vesicle docking and for the recruitment of intraflagellar transport (IFT) machinery during the axoneme formation. Subdistal appendages, on the other hand, determine cilium positioning by anchoring centrioles to the cytoplasmic microtubule network **(Figure 1.2)** (Sanchez and Dynlacht, 2016, Yang et al., 2018).

### 1.4.1 Initiation of cilium assembly

In the initial step of ciliogenesis, the periciliary vesicle is transported to the mother centriole (basal body), together with microtubules in kinesin and dynein-dependent manner **(Figure 1.2).** The Kinesin family member C1 (KIFC1) is recruited to Golgi to transport periciliary vesicle to the mother centriole. It was shown that the depletion of KIFC1 in RPE cells interrupts the trafficking of the ciliary membrane proteins to centrioles. As a result, they accumulate at the Golgi, suggesting that KIFC1 mediates the transport of vesicles from the Golgi to the mother centrioles to promote ciliogenesis (Lee et al., 2018). Another study demonstrated that the periciliary vesicle transport to the distal appendages is also mediated via the motor protein Myosin-Va (MYO5A) (Wu et al., 2018). The depletion of the MYO5A in RPE and 3T3 cells disrupts the centrosomal actin network, which leads to the blockade of periciliary vesicles docking.

Furthermore, growing evidence suggests that the centrosomes, besides functioning as microtubule organizers, also act as an actin-organizing center (Farina et al., 2016). Ciliary membrane-associated proteome demonstrated the presence of actin-binding proteins as dynamic components inside the cilium in mammalian cells (Kohli et al., 2017). The actin cytoskeleton remodeling factors LIM domain kinase 2 (LIMK2) and Dual specificity testis-specific protein kinase 1 (TESK1), both serine/threonine kinases are present in the vicinity of the centrioles and control ciliogenesis via remodeling actin cytoskeleton (Kim et al., 2015a). Moreover, components of centriolar satellites, electron-dense cytoplasmic structures, in particular, C2 domain-containing protein 3 (C2CD3) and Oral-facial-digital syndrome 1 protein (OFD1), play an essential role in the periciliary vesicle trafficking, fusion, extension, and assembling distal appendages (Singla et al., 2010, Ye et al., 2014). Altogether the data suggests that the tightly regulated ciliogenesis is a very dynamic process.

After ciliary vesicle formation, CEP164 recruits Tau tubulin kinase 2 (TTBK2) to the distal end of the basal body (mother centriole) to initiate cilium formation, triggering the removal of the centrosomal

protein CP110-CEP97 complex (Goetz et al., 2012, Cajanek and Nigg, 2014). A crucial mechanism that controls the basal body to cilium transition is supported by the reduced recruitment of Centrosomal protein of 110 kDa (CP110) and Centrosomal protein of 97 kDa (CEP97) at the distal end of the mother centriole, which promotes the cilium formation (Spektor et al., 2007). Indeed, the TTBK2 null mouse mutant lacks cilia and has defects in the sonic hedgehog (Hh) signaling. This phenotype could be due to the defects in the anchoring of the basal body and the recruitment of IFT machinery proteins essential for the trafficking, axoneme growth, and maintenance (Goetz et al., 2012). Additionally, TTBK2 knockout cells retain CP110 at the basal body, proving that TTBK2 is a key player in removing CP110 from the mother centriole (basal body) and initiating the ciliogenesis.

The centrosomal protein TALPID3 has been demonstrated to be essential for ciliary vesicle docking during ciliogenesis (Kobayashi et al., 2014). Recently, a study identified that TALPID3 interacts with the C2 domain-containing protein 3 (C2CD3) at the distal ends of the centrioles resulting in centriole maturation and distal appendages assembly (Wang et al., 2018). Subsequently, a recent report demonstrated that CEP120, besides its role in centriole elongation, regulates ciliogenesis. Depletion of CEP120 in RPE cells impaired recruitment of C2CD3 and TALPID3 to the distal end of the centriole, resulting in defective centriole elongation and cilium formation (Tsai et al., 2019).

### 1.4.2 Maintenance of ciliary length

During the axoneme growth, extensive amounts of tubulin dimers enter the cilium from the cytoplasm. The bidirectional cargo transport is provided via the IFT machinery that supports a mechanism for the cilium formation, maintenance, and function (Satir and Christensen, 2007, Ishikawa and Marshall, 2017). Directly after the IFT complex recruitment to the mother centriole, the transition zone, and the basal body begin to form. IFT proteins are divided into two large complexes, IFT-A (retrograde transport) and IFT-B (anterograde transport).
The IFT-B is associated with kinesin II and mediates anterograde transport of molecules from base to the cilium tip, known as an anterograde transporter. The IFT-A is associated with dynein and mediates retrograde movement from the tip to the base of the cilium (Pedersen et al., 2008). Pazour and colleagues discovered that mutations in the IFT machinery, specifically the IFT88 knockout in *Chlamydomonas,* results in a loss of the flagella. Moreover, the same knockout studies in mice resulted in ciliary defects, which lead to polycystic kidney disease (Pazour et al., 2000). Defects in the IFT transport proteins or tubulin can perturb axoneme growth and cilium length. In agreement with this idea, studies in *Chlamydomonas* and mammalian cells revealed that increasing soluble tubulin affects cilium length, whereas stabilization of tubulin leads to shorter cilium (Sharma et al., 2011, Wang et al., 2013b). Furthermore, the rate of IFT transport along with the axoneme has an impact on the cilium length. Therefore, increased and decreased anterograde transport rate is associated with longer or shorter cilium, respectively (Marshall and Rosenbaum, 2001, Marshall et al., 2005). Since the mother centriole (basal body) templates the cilium, it is possible that

centrosomal proteins can also interact with cytoplasmic tubulin and play a crucial role in regulating tubulin during the ciliary axoneme growth. Indeed, Centrosomal-P4.1-associated-protein (CPAP) binds tubulin via its PN2-3 domain, regulating ciliary length. Interestingly, mutations in PN2-3 CPAP (F375A) exhibit strongly reduced tubulin interaction, causing shorter cilia. Together this data suggests that CPAP defines ciliary microtubule length through binding and releasing the cytoplasmic tubulin to determine ciliary-microtubule lengths (Zheng et al., 2016, Sharma et al., 2016).

The ciliary membrane also plays an essential role in the axoneme elongation during the cilium formation. Studies have demonstrated that overexpression of active small GTPases Rabin8 (Rab8a) in mammalian cells can affect ciliary membrane growth, resulting in the shorter cilia. The Rab8a forms a complex with the octameric protein complex BBSome and potentially cooperates with other unknown factors to organize ciliary membrane assembly (Nachury et al., 2007, Westlake et al., 2011). Once the cilium is assembled and elongated, a selective mechanism that operates at the cilium base enables it to retain its composition. In particular, a soluble protein barrier, the transition zone functions to maintain the protein composition of the cilium (Jensen and Leroux, 2017, Nachury and Mick, 2019). Finally, it is noteworthy to emphasize that the cilium's length is also under the control of cilium disassembly pathways, which prevent assembly pathways during the cell cycle re-entry (see below).

## 1.5 Cilium disassembly

In contrast to cilium assembly, the mechanisms involved in cilium disassembly have not been well characterized. Thus, recent studies have begun to uncover the mechanisms linking cilium disassembly to cell cycle re-entry and identified proteins crucial for cilium disassembly. Experiments in mammalian cultured cells suggest that the cilium disassembles in two waves. The first wave occurs in the G1 phase of the cell cycle, shortly after the quiescent cells' mitogenic stimulation. In contrast, the second wave occurs before cells enter the mitosis **(Figure 1.3)** (Pugacheva et al., 2007, Tucker et al., 1979). In cycling cells, the cilium assembly occurs during the cell cycle exit ($G_1$-$G_0$) or quiescent state, whereas the cilium disassembly coincides with the cell cycle re-entry ($G_1$-S to M) **(Figure 1.3)**. Cilium disassembly and cell-cycle re-entry require the destabilization and depolymerization of axonemal microtubules **(Figure1.3)**. Several studies have demonstrated numerous key regulator proteins that mediate cilium disassembly, a process that has an extensive implication in human disease, in particular cancer.

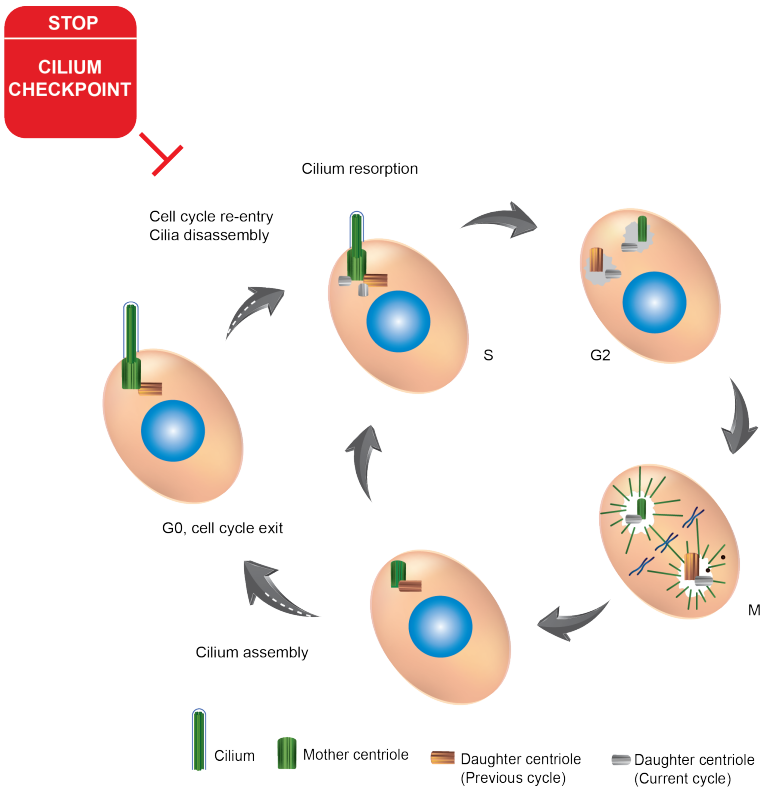


**Figure 1.3. Cilium dynamics in cell cycle.**
Cilium checkpoint. The mother centriole serves as a template for the cilium formation during the cell cycle exit in the $G_0$ phase. Cilium disassembly starts at the S phase when centrioles duplicates. Cilium disassembles at the $G_2$ phase when cells continue to mitotic progression. Modified from Gabriel et al., 2016 (Gabriel et al., 2016)

### 1.5.1 Aurora-A/HDAC6 dependent cilium disassembly

The mitotic kinase Aurora-A plays a key role during both waves of cilium disassembly (Pugacheva et al., 2007). Aurora-A is a serine/threonine kinase essential for the cilium length and deciliation at the onset of cell cycle re-entry, as well as centrosome duplication, maturation, and spindle assembly (Pugacheva et al., 2007, Pan et al., 2004). The initial indication that Aurora-A controls the cilium's length was demonstrated in Chlamydomonas reinhardtii biflagellate alga (Pan et al., 2004). In cultured mammalian cells, upon cell cycle re-entry, Aurora-A is recruited to the basal body, which phosphorylates and activates Histone deacetylase 6 (HDAC6), which deacetylases and destabilizes tubulin polymer within the ciliary axoneme **(Figure 1.4)**. Activation of Aurora-A is a complex process, stringently controlled by different signaling pathways, including calcium influx, which in turn induces binding of the calmodulin to the Aurora-A and its partner Enhancer of filamentation 1 (NEDD9). Another protein that regulates cilium disassembly via control of Aurora-A activation at the basal body is Trichoplein keratin filament-binding protein **(Figure 1.4)**. In quiescent cells ($G_1$-$G_0$ phase), Trichoplein is absent from the basal body and localizes to the centrosome in proliferating RPE cells (Inoko et al., 2012). Additionally, the HDAC6 can promote cilium disassembly through another substrate, which is the Polo-like kinase1 (PLK1) (Wang et al., 2013a, Lee et al., 2012) **(Figure 1.4)**. PLK1 is a G2-M phase kinase. It is recruited to the pericentriolar matrix before the cell cycle re-entry

and then activates the HDAC6 to promote its function for ciliary deacetylation resorption (Lee and Rhee, 2011) (Wang et al., 2013a) (Ramani et al., 2018).

Protein pitchfork (PIFO) through binding to the beta-tubulin activates Aurora-A, promoting the cilium disassembly. Interestingly, *Pifo* heterozygous mutant mice display ciliopathy-related phenotypes, highlighting the consequences of perturbing cilium disassembly **(Figure 1.3)** (Kinzel et al., 2010). More recently, it has been recently shown that another Histone deacetylase 2 (HDAC2) plays an important role during the cilium disassembly (Kobayashi et al., 2017). Altogether the data illustrate that both HDAC6 and Aurora-A can regulate the cilium disassembly through different substrates and mechanisms. A delay or failure in cilium disassembly retains cells in the $G_0$-$G_1$ phase and transiently prevents the cell cycle progression (Pugacheva et al., 2007, Jackson, 2011, Kim et al., 2011). It has been demonstrated that cilium must be disassembled before the cell re-enter the cell cycle such that the mother centriole can be released from the plasma membrane to participate in organizing the mitotic spindle (Paridaen et al., 2013, Guemez-Gamboa et al., 2014).

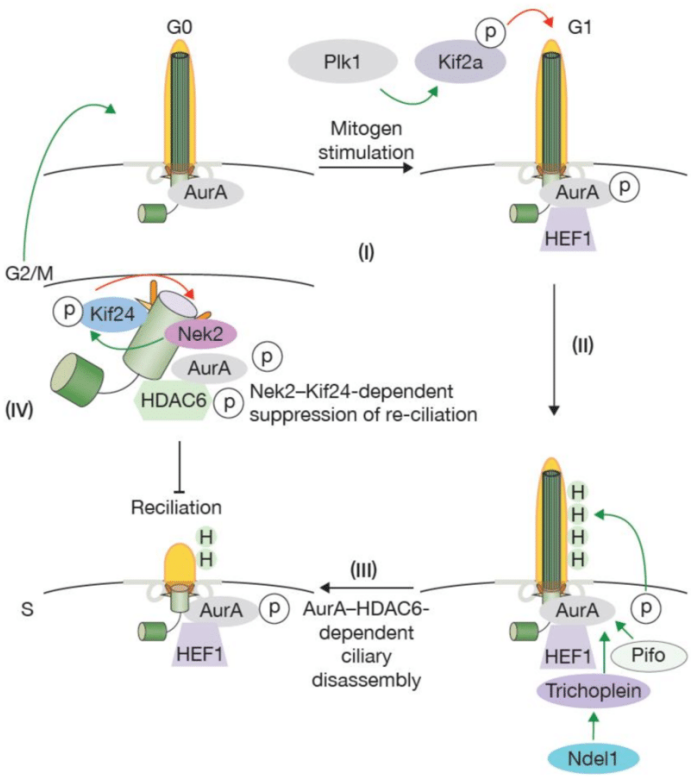


**Figure 1.4. Cilium disassembly.**
Cell cycle re-entry requires the inhibition of axoneme growth and the recruitment of several regulatory proteins to trigger cilium disassembly. HEF1 is recruited and activates Aurora-A at the basal body, which then stimulates and activates HDAC6 (green H), and tubulin de-acetylation. This leads to axoneme disassembly. Pitchfork (Pifo) and Trichoplein are recruited to activate Aurora-A, and Ndel1 (same as NDE1) stabilizes Trichoplein at the basal body to inhibit ciliogenesis. **(I-III)**. After mitogen stimulation, PLK1-mediated phosphorylation of kinesin KIF2A, which stimulates the depolymerization of axonemal microtubules. In the second wave of the cilium disassembly, NEK2 is expressed which then stimulates and activates another depolymerizing kinesin, KIF24. Activation of KIF24 prevents re-ciliation through the S-$G_2$-M transition, ensuring that centrioles replicates in the S-phase and assemble a mitotic spindle in the M-phase (Sanchez and Dynlacht, 2016).

Additional centrosomal proteins are also engaged at the onset of cilium disassembly and cell cycle re-entry (S-phase) such as Nuclear distribution gene E homologue 1 (NDE1) and Dynein light chain Tctex-type1 (Tctex-1 or DYNLT1). NDE1 is a negative regulator of the ciliary length, and recruitment to the basal body initiates cilium disassembly (Kim et al., 2011). The depletion of *Nde1* in mouse fibroblast NIH-3T3 cells resulted in the longer cilium formation and delay in the cell cycle progression (S-phase) via the CDK5 phosphorylation, which in turn ubiquitinylates F-box protein/WD repeat-containing protein (Fbw7) as the E3 ligase that mediates the destruction of Nde1 (Alkuraya et al., 2011).

Furthermore, the Tctex-1 is phosphorylated and recruited to the ciliary transition zone before the S-phase entry and promotes cilium disassembly and the cell cycle re-entry. The depletion of Tctex-1 leads to persistent ciliation and retains cells in the $G_1$-S phase. Exogenously expression of phosphor-mimic Tctex-1 (T94E) mutant protein increases cilium disassembly and the S-phase entry. The potential mechanism of Tctex-1 to regulate cilium disassembly is mediated through actin dynamics (Li et al., 2011). These results support a model in which the cilium acts as a brake to prevent the cell-cycle progression.

### 1.5.2 NEK2/KIF24 dependent cilium disassembly

There are two kinesin 13 family members, Kinesin-like protein 2a (KIF2A) and Kinesin-like protein 24 (KIF24). Both kinesins are implicated in cilium disassembly via destabilization or depolymerization of the axoneme microtubules for mitotic entry (Kim et al., 2015b, Kobayashi et al., 2011). KIF2A is recruited to the subdistal appendages of mother centrioles at the proximal ends of both centrioles and phosphorylates PLK1 during $G_2$ - M phase. Recruitment of this kinesin promotes cell proliferation and microtubule-depolymerizing activity at the mother centrioles to disassemble cilium. The depletion of KIF2A in RPE cells showed an impaired cilium disassembly and cell cycle progression (Miyamoto et al., 2015).

KIF24 was identified as a negative regulator of cilium assembly, which interacts with CP110 at the distal end of centrioles (Kobayashi et al., 2011). The depletion of this kinesin protein in RPE cells enhances cilia assembly, implicating the role of KIF24 during cilia disassembly (Kim et al., 2015b). In this study by Kim and colleagues revealed that KIF24 is a substrate for NEK2, co-expressed with the wild type form of NEK2 (NEK2-WT), but not with the catalytically inactive mutant NEK2-KD (amino acid site 37) (**Figure 1.5).** The phosphorylation sites in KIF24 are restricted to the carboxyl-terminal kinesin domain (548-825), which is flanked by NEK2-binding surfaces **(Figure1.5).**

NEK2 is a 445 amino acid (48kDA) protein comprising the N-terminal kinase domain and the C-terminal non-catalytic regulatory domain **(Figure 1.5).** The kinase domain has all the motifs typical of serine/threonine protein kinases (Hanks and Hunter, 1995). The more C-terminal region contains the non-catalytic and coiled-coil regions. The central leucine zipper domain promotes

homodimerization, which leads to autophosphorylation (Fry et al., 1998). NEK2 is localized to the distal part of the mother centriole and functions in both cilium disassembly and centrosome duplication before mitosis, indicating the crucial role of NEK2 in cell cycle control (Spalluto et al., 2012, Fry et al., 1995). Interestingly, similar to KIF24, the depletion of NEK2 also causes an increased ciliation in RPE cells (Spalluto et al., 2012). Overall, the cell cycle-specific phosphorylation of KIF24 by NEK2 is an essential step to provide a safeguard mechanism against an aberrant assembly of the cilium upon cell cycle re-entry.

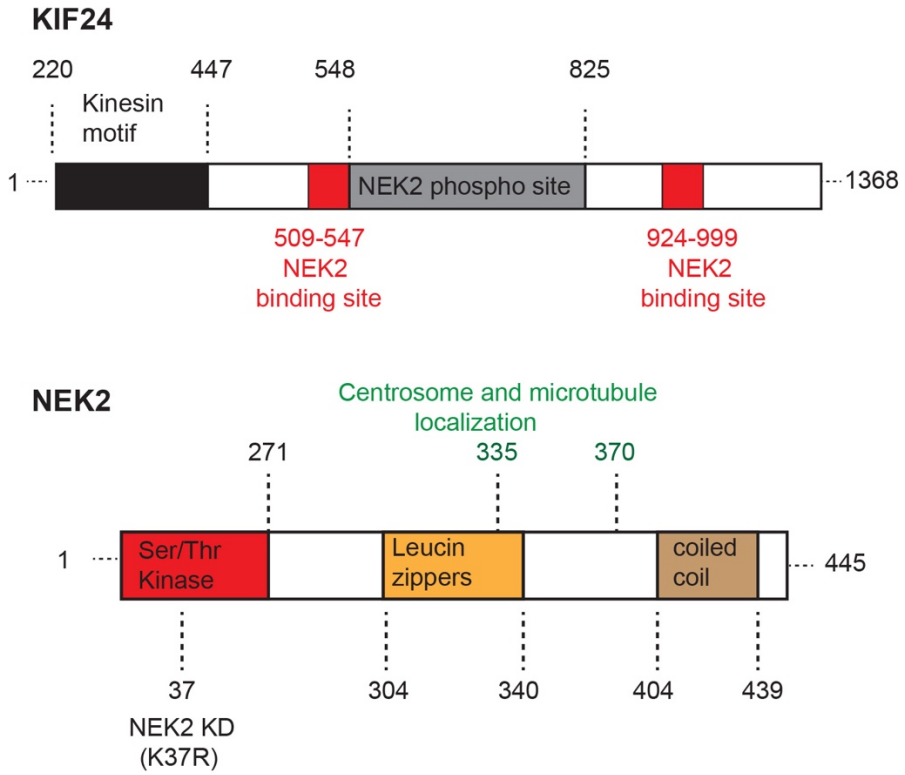


**Figure 1.5. Schematic diagrams indicating KIF24 and NEK2 domains.**
Top: a schematic representation of the human KIF24 protein structure. Kinesin motif (black), NEK2 binding sites (509-547, 924-999), NEK2 phosphorylation site (grey) are shown.
Bottom: a schematic representation of the human NEK2 protein structure. The relative positions of the catalytic domain (Ser/Thr kinase, red), leucin zipper (yellow), coiled-coil (brown), K37R (NEK2-KD) indicates a mutant site, where the amino acid has been exchanged to prevent phosphorylation of KIF24. The numbers above and below the domains indicate amino acid positions.

### 1.5.3 CPAP mediated cilium disassembly

The centrosome plays a dual role, existing as a microtubule-nucleating center and as the basal body to template the cilium. CPAP, a conserved centrosomal protein, plays a role in centriole formation and provides a scaffold for protein complexes during centrosome assembly (Hayward et al., 2004, Gopalakrishnan et al., 2011, Lin et al., 2013, Zheng et al., 2016). CPAP contains both, a tubulin dimer-binding domain (PN2-3, 311–422 aa) and microtubule-binding domain (A5N, 423-607aa) (Hsu et al., 2008, Zheng et al., 2016, Cormier et al., 2009). The CC5 domain at the C-terminal CPAP provides a scaffold for CDC proteins to promote cilium disassembly (Gabriel et al., 2016). The C-terminus of CPAP also includes a highly conserved region known as the G-box or TCP domain, providing crucial protein-protein interactions and might serve as a tethering site for centrosomal proteins (Zheng et al., 2014).


**Figure 1.6. Schematic diagram indicating CPAP different domains.**
PN2-3 (magenta) tubulin dimer-binding domain, MBD (blue) microtubule-binding domain, CC5 (green), and TCP (yellow) domain. The numbers indicate amino acid positions (Zheng et al., 2016).

A recent study uncovered that CPAP is a negative regulator of ciliary length independent of its centrosome biogenesis role. During cilium disassembly, the CPAP's CC5 domain provides a scaffold for the cilium disassembly complex (CDC), which comprises NDE1, Aurora-A, and OFD1 that are recruited to the ciliary base for timely cilium disassembly. Mutated CPAP lacking the CC5 domain fails to localize at the ciliary base, resulting in inefficient CDC recruitment causing retarded cilium disassembly, and delayed cell cycle re-entry (Gabriel et al., 2016). Based on this, the cilium disassembly provides a conceptually novel ‘cilium checkpoint’ regulating the cell cycle progression. Consistently, cilium disassembly proteins are associated with pathological processes such as cancer (Chefetz et al., 2011, Kim et al., 2015b, Tang et al., 2013, Kobayashi et al., 2017). However, the exact role of the cilium disassembly molecules in this context still needs to be determined.

## 1.6 The cilium functions as a signaling hub

The sensory role of cilium depends on the spatiotemporal localization of the specific receptors and associated signaling modules in the ciliary membrane. More specifically, the cilium coordinates signal transduction pathways such as Hh signaling, Platelet-derived growth factor receptor alpha (PDGFR-α), Notch, and Wnt signaling pathways. Moreover, cilium provides photo-, mechano- and osmo-sensing functions that transduce information from the extracellular environment (Christensen et al., 2012, Bangs and Anderson, 2017).

### 1.6.1 Hedgehog signaling pathway

The Hh signaling is a well-studied signaling pathway that acts through the cilium. In vertebrates, the cilium plays a major role in transducing the Hh signaling pathway that plays a vital role in embryonic development and stem cell maintenance (McMahon et al., 2003, Machold et al., 2003). Dysregulation of the pathway can cause various birth defects, including polydactyly, skeletal malformations, and human cancer (Goetz and Anderson, 2010). The first evidence linking cilium and Hh signaling stem from a phenotype-based genetic screen in the mouse that identified a set of proteins required to form the cilium (Huangfu et al., 2003). The relationship between ciliary function and mammalian Hh signaling has a complex and direct relevance for human diseases such as Kartagener syndrome, pulmonary dysfunction, polycystic kidney disease, retinal degeneration, infertility, hydrocephalus, holoprosencephaly, polydactyly and cancer (Bale, 2002). Most interestingly, the Hh signal transduction relies on the localization of Hh proteins to the cilium. In mammals, binding of Hh ligands Sonic (Shh), Indian (Ihh), and Desert (Dhh) to the patched-1 protein (PTCH1) receptors activate the Hh signaling pathway **(Figure1.7)** (Bangs and Anderson, 2017, Rohatgi et al., 2007). Upon Hh stimulation, the inhibitory effect of PTCH1 on GPCR-like protein Smoothened (SMO) is abolished, resulting in SMO translocation to the cilium. Accumulation of SMO allows for cilium-mediated signal transduction via the ciliary localized glioma transcription factors (GLI). Subsequently, GLI activates the expression of Hh target genes. Together these studies suggest that Hh signaling requires maintenance and function of cilia to sense Hh ligands and activates downstream signals, which are critical for development, carcinogenesis, and stem cell function **(Figure1.6, panel "ON")** (Humke et al., 2010, Wen et al., 2010). Furthermore, both inactive GLI and suppressor of fused homolog (SUFU) localize to the ciliary tip.

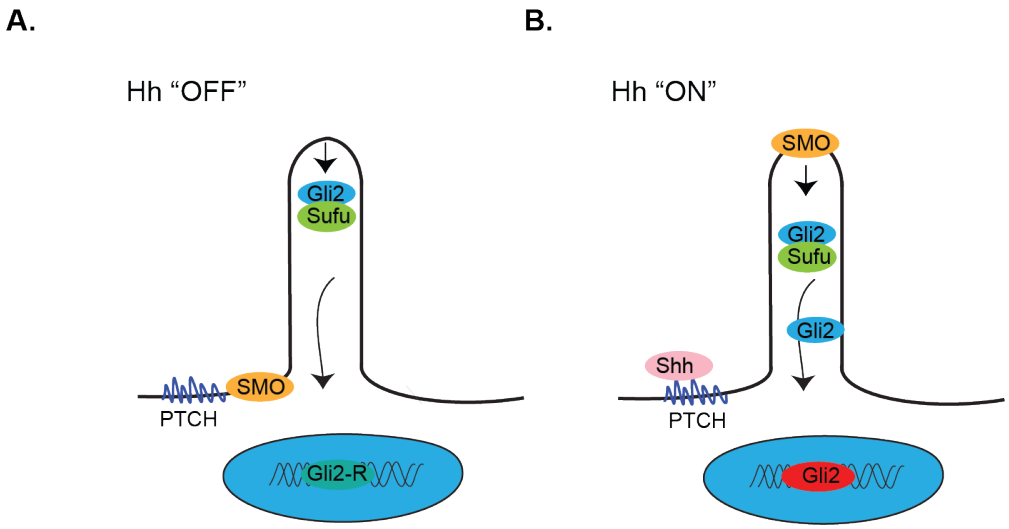


**Figure 1.7. Hedgehog signaling at the primary cilium.**
**A.** In the unstimulated state, PTCH1 localizes to the ciliary membrane and represses SMO from translocating into the cilium. GLI transcription factors are sequestered and suppressed by SUFU at the tip of the primary cilium, generating GLI3 repressor (GLI3R), which moves to the nucleus and represses expression of Hh target genes. **B.** In the activated state of Hh signaling, upon binding of the Hh ligand to

PTCH1, the repression of SMO from Ptch1 is relieved, allowing SMO to translocate into the cilium where it can activate downstream signaling. This then allows SMO to disassociate the GLI/SUFU complex and the transport of the GLI2 activator to the nucleus to activate the expression of downstream target genes. Modified from (Gladiola Goranci-Buzhala, 2017).

Interestingly, the IFT proteins Ift172/Wimple and Ift88/Polaris, and Kif3a mouse mutants displayed abnormal embryonic morphogenesis at neural tube levels, coinciding with reduced aberrant Hh signaling (Huangfu et al., 2003). In addition, a partial loss of function of Ift52, as well as mutated retrograde dynein IFT molecules revealed a similar aberrant phenotype during embryonic development in mice. It was also demonstrated that IFT function in mutant mice is essential to control both Gli2-R (repressor) and Gli2 (activator) transcriptional activities, which are essential for the Hh signaling cascade (Zhang et al., 2016, Liu et al., 2005). Altogether these elegant findings suggest that the primary cilium and IFT are required a proper Hh signaling pathway. However, whether IFT molecules directly participate in transporting Hh components still remains an open question.

The ADP ribosylation factor-like GTPase 13B (Arl13B), mediates trafficking of Hh signaling components within the cilium. Mutation in mouse embryonic fibroblast Arl13B$_{hnn}$ (hnn cell types within the neural tube) did not respond upon Hh ligand stimulation. It displayed an altered distribution of Hh signaling components, such as Gli2, Gli3, Sufu, and Smo. These components are localized along with the cilium in healthy cells. Thus, loss of Arl13b results in the ligand-independent SMO activation, suggesting that Arl13b acts downstream of the known tumor resistance mechanism. Mutations in the Hh signaling components (Ptch, Sufu, and Smo) are considered oncogenic drivers in basal cell carcinoma and medulloblastoma tumors (Taylor et al., 2002). Loss of Arl13b reduces Hh-dependent transcription and proliferation, and inhibits tumor formation in a mouse model of medulloblastoma (Bay et al., 2018). Further, in a subset of Hh signaling-dependent tumors, cilium regulates either tumor formation or suppression depending on the mutation of Hh signaling proteins (e.g., SmoM2 and activated Gli2) (Wong et al., 2009). These results demonstrate that cilium plays a dual role in both activation and inactivation of the Hh signaling pathway, also functioning either as a mediator or suppressor of tumorigenesis depending on the genetic background.

### 1.6.2 PDGFR-α signaling pathway

Signaling via PDGFs and their receptors play an essential role in cell survival, growth control, proliferation, cell migration, embryonic development, and tissue homeostasis (Heldin and Westermark, 1999, Andrae et al., 2008). Lih et al discovered a functional link between PDGFR-α and cilium for the first time (Lih et al., 1996). Subsequent reports have demonstrated that the cilium partially coordinates PDGFR-α signaling in cultured mouse embryonic and NIH3T3 fibroblast cells (Schneider et al., 2005, Schneider et al., 2010). PDGFR-α forms homodimers and localizes to the cilium during the $G_0$ phase (quiescence phase) (Fredriksson et al., 2004). Likewise, embryonic fibroblasts of *orpk* mutant mice (IFT88$_{Tg737Rpw}$) failed to form a normal cilium and were not able to

upregulate PDGFR-α during cell cycle arrest upon serum-starvation, in contrast to wild type embryonic fibroblast. These data indicate that localization of PDGFR-α along the cilium is necessary for proper signal transduction (Schneider et al., 2005). In contrast to PDGFR-α, the PDGFR-β signaling was not alerted in *orpk* mutant mice since the activation of PDGFR-β does not occur in the cilium. These findings support the conclusion that PDGFR-α signaling is coordinated through the cilium, which can control cell cycle and tissue homeostasis during the development of different cells and tissues (Christensen et al., 2012, Christensen et al., 2008).

Pieces of evidence suggest that PDGFR-α signaling is associated with the cilium. The ligand PDGFR-AA activates PDGFR-α through phosphorylation (at the amino acid sites 720, 742, and 745) and localization at the cilium. Once PDGFR-α is activated, it induces the downstream signaling pathways such as Mek1/Erk1/2 and Akt pathways near the cilium base. Activated signaling subsequently phosphorylates Retinoblastoma protein (Rb) and Cyclin-dependent kinase 1 (CDC2 of CDK1), which initiates cell cycle progression (Schneider et al., 2005). Deregulation of PDGFR-α signaling has been implicated in cancer development, and studies have indicated that gastrointestinal stromal tumors express elevated levels of PDGFR-α signaling (Andrae et al., 2008, Corless et al., 2011). Thus, it is conceivable that the cilium suppression could be beneficial for preventing cancer cell growth. Even though the role of PDGFR-α signaling/primary cilium in cancer progression remains still uncovered, to understand if the loss of primary cilium can lead either with signal activation or inhibition indicates that PDGFR-α demands primary cilium to function correctly.

## 1.7 Primary cilia in the regulation of neural stem cell proliferation and brain development

Neural progenitor cells (NPCs) are characterized by their ability of self-renewal and differentiation into neuronal cell types. A balance between self-renewal and differentiation is achieved through a controlled symmetric and asymmetric cell division to maintaining proper tissue homeostasis and the stem cell pool. During symmetric division, the cell divides two stem cells while in asymmetric division cell divides one stem cell and one differentiated cell. Defects during the asymmetric cell division may cause premature depletion of the stem cell pool and abnormal development (Shitamukai and Matsuzaki, 2012, Gomez-Lopez et al., 2014). During the quiescence state ($G_0$ phase), NPCs assemble cilium responsible for sensing and transmitting signals into the cells. The symmetric division of NPCs during the development is regulated by the dynamic control of proteins that initiates cilium assembly and disassembly, together with downstream signaling cascades, responsible for cell lineage differentiation (Izawa et al., 2015, Goetz and Anderson, 2010). The precise timing of cilium disassembly ensures the length of $G_1$-S transition and the self-renewal property of NPCs (Gabriel et al., 2016, Li et al., 2011, Kim et al., 2011). It has been demonstrated that Ift88 and Kif3a deficient mice exhibit suppressed ciliogenesis resulting in defective expansion of neural progenitor and

cerebellum development (Chizhikov et al., 2007, Spassky et al., 2008). Furthermore, conditional homozygous mouse mutants for ciliary genes (e.g., *Ift88* or *Stumpy*) display cilia loss leading to aberrant Hh signaling and increased proliferation of progenitors (Breunig et al., 2008, Kumamoto et al., 2012).

Recent studies have emerged, demonstrating an essential role of cilia in brain development (Gabriel et al., 2016, Lepanto et al., 2016). In brief, during the early stages of the neural epithelium development, NPCs rapidly self-renew and expand through symmetrical cell division. Neuroepithelium expansion is a rate-limiting step to generate a sufficient pool with enough NPCs, fundamental for brain development. Neuroepithelial polarity during the brain development process is tightly regulated between symmetric proliferation and asymmetric differentiation of NPCs (Gabriel et al., 2016). Thus, factors that can instruct NPCs to either self-renew or differentiate are tightly regulated. Lately, it has been identified that the CDC proteins are essential for timely cilium disassembly and stem cell pool maintenance. The impaired function of CDC proteins can affect the cilium disassembly and prevent NPCs from entering into mitosis. Prolonged $G_1$-S transition leads to premature neural differentiation, depleting the NPC pools (Gabriel et al., 2016). These observations are consistent with previous work demonstrating that lengthening of the $G_1$ phase by depletion of Cdk4/CyclinD1 in mouse cortical progenitors is sufficient to switch neural progenitors to the differentiation stage (neurogenesis) (Lange et al., 2009). Furthermore, another study has demonstrated that disruption of the cilium function via shRNA constructs targeting Kif3a in mice embryo, has resulted in a defective NPCs differentiation, additionally supporting a crucial role of cilium in the neurodevelopment (Chen et al., 2019). Together, these studies have identified the cilium's key roles in controlling NPCs' homeostasis during brain development.

## 1.8 Primary cilia in human cancers

Hallmarks of cancer include uncontrolled cell proliferation, disruption of the cell cycle, and altered signaling pathways that support tumorigenesis. How cilia control tumor initiation or progression, potentially through cell cycle regulation, is not fully understood yet. A growing body of evidence supports the notion that many cancer cells from different tissues with increased proliferation rates exhibit suppressed ciliogenesis (Fang and Zhang, 2016, Goranci-Buzhala et al., 2017, Plotnikova et al., 2008, Egeberg et al., 2012). However, it is not clear whether cilium loss is the cause or the consequence of cellular transformation.

Intriguingly, the CDC's components are elevated in various cancer types and suggest that they could play a vital role in tumorigenesis (Egeberg et al., 2012, Dere et al., 2015, Fang and Zhang, 2016). There are numerous examples linking cilium loss to elevated expression levels of the CDC components. PLK1 is a mitotic kinase that regulates mitotic events by phosphorylating serine/threonine rich proteins of centrosomes, kinetochores, mitotic spindle, midbody, and cilium

disassembly (Kishi et al., 2009). PLK1 also plays a critical role in cilium disassembly. PLK1 forms a complex with Disheveled segment polarity protein 2 (Dvl2). It activates one of the non-canonical Wnt pathways, which also initiates cilium disassembly upon activation of Aurora-A through the Human Enhancer of Filamentation 1 (HEF1) (Lee et al., 2012). Plk1 is also reported to be a proto-oncogene. It is highly expressed in human colon and lung cancer cells suggesting that the elevated levels of Plk1 may accelerate cell cycle progression via maintaining cilium in a suppressed state (Raab et al., 2018, Weichert et al., 2005).

Aurora-A is a mitotic kinase that localizes to centrosomes and regulates entry to the S phase, which initiates the cilium disassembly process (see cilia disassembly section) (Gradilone et al., 2013, Xiang et al., 2017). Ovarian and clear cell renal carcinoma cells show increased expression levels of Aurora-A as well as a defect in cilium formation (Egeberg et al., 2012, Dere et al., 2015) **(refer to Table 1)**. In line with these findings, other studies have demonstrated that inhibition of HDAC6 restored ciliogenesis in chondrosarcoma and cholangiocarcinoma cancer cells and impaired capacity of cell proliferation and invasion (Xiang et al., 2017) **(**T**able 1)**.

NEK2 is a multifunctional protein kinase that regulates mitotic progression, centrosome duplication, separation, microtubule stabilization, kinetochore attachment, and the spindle assembly checkpoint (Jeong et al., 2007, Sonn et al., 2009, Boekhout and Wolthuis, 2015).
Recently, NEK2 has been shown to play a role as a proto-oncogene affecting drug resistance, tumor progression, and metastasis (Cappello et al., 2014, Hayward et al., 2004, Zhou et al., 2013) Furthermore, it was demonstrated that mouse melanoma xenografts with shRNA-mediated depletion of Nek2 could overcome drug resistance (Zhou et al., 2013). NEK2 overexpression has also been identified in a wide range of human cancers, but it has not yet been determined whether NEK2 is part of a CDC component. However, NEK2 plays a prominent role in the final stage of the cilium disassembly through the phosphorylation of KIF24 (see cilia disassembly section 1.4), thus both proteins are attractive targets to restore ciliation as a mean to impair the cell cycle proliferation. This idea is supported by studies in which perturbing NEK2 impaired the proliferation of human breast cancer cells (Kim et al., 2015b). Altogether, these studies indicate a suppressive role of cilia in cell cycle progression, raising the possibility that cilia loss promotes unrestricted cell cycle progression in cancer cells.

**Table 1. Cancer types and pathways that result in suppressed ciliogenesis.**

| **Cancer types** (Exhibiting suppressed ciliogenesis) | **Potential mechanism for suppressed ciliogenesis** | **Reference** |
|---|---|---|
| Pancreas | Activation of KRAS pathway | (Seeley et al., 2009, Emoto et al., 2014) |
| Breast | Unknown | (Yuan et al., 2010, Nobutani et al., 2014) |
| Melanoma | EZH2 overexpression | (Zingg et al., 2018) |
| Renal cell carcinoma | Aurora-A, Nek8 overexpression | (Schraml et al., 2009, Basten et al., 2013, Ding et al., 2015) |
| Chondrosarcoma and Cholangiocarcinoma | HDAC6 overexpression | (Gradilone et al., 2013, Razumilava et al., 2014, Xiang et al., 2017) |
| Glioblastoma | CCRK upregulation | (Yang et al., 2013) |
| Ovarian | Aurora-A overexpression | (Egeberg et al., 2012, Dere et al., 2015) |
| Chondrosarcoma/Enchondromas | Gli2 overexpression | (Ho et al., 2013) |
| Rhabdomyosarcoma | Unknown | (Fu et al., 2014) |

## 1.9 Glioblastoma multiforme

Glioblastoma multiforme (GBM) is the most aggressive type of adult brain tumor, and the World Health Organization (WHO) categorizes it as a grade IV stage tumor (Matsukado et al., 1961, Ostrom et al., 2014). The nature of the GBM is highly infiltrative and invasive. Patients have a poor prognosis and median survival of 12–15 months, with a maximum survival rate of less than 5% for five years. Upon initial diagnosis, GBM patients receive a harsh treatment that combines surgery, radiotherapy, and temozolomide (TMZ) prescription (Stupp et al., 2005, Johnson and O'Neill, 2012, Tanaka et al., 2013). Classification of GBM obtained from genomic, and transcriptome analysis by The Cancer Genome Atlas Network (TCGA) is based on a genetic signature. According to this, there are four distinct GBM subclasses: classical, mesenchymal, proneural, and neural (Verhaak et al., 2010, Xie et al., 2015).

The classical subtype is characterized by an increased expression level of EGFR, deletion of PTEN, CDKN2A, TP53 loss, increased expression of neural stem cell markers, and constitutively activated Hh signaling. The loss of NF1 characterizes the mesenchymal subtype, mutations in PTEN, expression of mesenchymal markers such as CHI3L1 and MET, Mitogen-activated protein kinase (MAPK) activation and an elevated expression of genes involved in Tumor necrosis factor (TNF) and Nuclear factor-kappa B (NF-kB) pathways. The proneural subtype is classified based on amplification, mutation, and overexpression of genes such as PDGFR-α, IDH1, and TP53. This subtype is also characterized by the activation of the Phosphatidylinositol-3 kinase (PI3K) pathway. The final subtype is the neural subtype, and it has not been well characterized for a specific genetic profile. However, compared to other subtypes, the neural subtype expresses elevated levels of neural markers such as NEFL, GABRA1, SYT1, and SLC12A5 (Verhaak et al., 2010, Xie et al., 2015). All of the subclasses of GBM are highly untreatable, and thus, considered as intractable cancer types. There are numerous reasons accounting for this, which include morphological, cellular, genetic, and intertumoral heterogeneity. The characterization of GBM subtypes could help in identifying the factors that underlie therapy resistance and tumor relapse.

Regardless of the subtypes, all GBM types possess highly tumorigenic, self-renewing glioma stem cells (GSCs), contributing to tumor initiation, maintenance, resistance, and relapse (Lathia et al., 2015, Rich and Eyler, 2008, Jacob et al., 2020). GSCs possess neural stem cell attributes exhibiting uncontrolled self-renewal properties, which might have been acquired or reactivated upon therapy resistance (Park et al., 2017, Rajakulendran et al., 2019). Nevertheless, it remains unclear if there is an alteration in cellular structures like centrosomes and cilium related to cell cycle control, self-renewal, and differentiation. Intense effort is being made to understand the mechanism of GSCs proliferation, which can then be targeted to control GSCs proliferation as a potential therapeutic intervention. So far, only a few studies have emerged showing that the cilium is lost in cultured GBM cells, raising the question of whether loss of cilia is a cell culture artifact or a result of suppressed ciliogenesis is due to the uncontrolled cell cycle.

### 1.9.1 Current evidence for role of primary cilia in glioblastoma

Most of the altered signaling pathways in GBM are closely related to signals that are mediated through cilia especially the PDGFR-α, Hh, Wnt, TGF-ß and Notch pathways (Christensen et al., 2012, Bangs and Anderson, 2017, Christensen et al., 2017, Ezratty et al., 2011, Wallingford and Mitchell, 2011). Therefore, it can be assumed that cilium is involved in the deregulation of cellular signaling in many GBM patients. Since the EGFR and PDGFR-α pathways are profoundly affected in GBMs, it is possible that the altered cilia-mediated signaling could deregulate cell cycle progression, self-renewal, and differentiation leading to tumor formation.

Moser and colleagues' initial works characterized the stages of primary cilium biogenesis in healthy astrocytes, astrocytoma, and GBM cells (Table 2), where they showed that the cilium structure is disrupted at the early stages of ciliogenesis. As a result, GBM cells were not able to form functional cilia. Moreover, the authors have identified the presence of GBM cells with the abnormal configuration of distal/subdistal appendages structure. By performing similar ultra-structural analysis in biopsy samples, the authors have characterized that GBM tissues also display structural defects in cilia (Moser et al., 2009b), (Moser et al., 2014). Taken together, these data indicate that GBM cells and tumor tissues have defects in ciliogenesis. Another study supported that cilia loss can determine cancer progression in eight cancer types, including GBM. Shpak and colleagues reported the downregulation of cilia-related genes, based on The Cancer Genome Atlas (TCGA) gene expression annotations (Shpak et al., 2014).

Apart from correlative data, little evidence is provided whether GBM development is cilium-dependent, and if reintroducing cilium can affect GBM proliferation. The depletion of the cell-cycle related kinase (CDK20/CCRK) can induce cilia in a small fraction of serum-starved U251MG cells **(Table 1 and 2)** (Yang et al., 2013). However, it is unclear whether the small fraction of ciliated cells was due to the depletion of the kinase or serum-starvation culture condition. Hence, addressing this question requires low-passage patient-derived GSCs and increase human cohorts. Since the mechanism of cilium loss was only shown in commercial cell lines, do not precisely reflect the characteristics of cells in GBM patients. Another study revealed that lysophosphatidic acid (LPA) could mediate signaling through cilia and impact the GBM cell proliferation (Loskutov and Pugacheva, 2019, Loskutov et al., 2018). LPA is a lipid-based mitogen highly expressed in the brain and increases proliferation and invasion of the GBM cells. A receptor of LPA (LPAR1) was found to accumulate at the cilium in human astrocytes. Loskutov and colleagues demonstrated that suppressed ciliogenesis increases cell proliferation of GBM and astrocytes through a LPA-dependent mechanism involving primary cilium **(Table 2)**. Targeting LPA-signaling using the inhibitor Ki16425 efficiently decreased the proliferation of astrocytes and GBM cells (Loskutov and Pugacheva, 2019, Loskutov et al., 2018).

**Table 2. Primary cilia in glioblastoma cells.**

| Cell line used | Source | Culture condition | Cilia | Reference |
|---|---|---|---|---|
| U87MG, T98G, U373MG, U138MG | Commercial ATCC | Serum | lost | (Moser et al., 2009a) |
| U251MG | Commercial ATCC | Serum | lost | (Moser et al., 2009b) (Yang et al., 2013) |
| Line 0, Line1, Line2, SN179(S2), SN186 (S3) | patient derived cells | Serum-free and growth factors | lost | (Sarkisian et al., 2014) |

Besides these initial studies in Table 2, only little is known regarding cilia's functional significance in GBM initiation and progression. One study demonstrated that smaller fraction (from 8 to 15%) of GBM cells are ciliated, and this fraction of cells express Zinc finger E-box binding homeobox 1(ZEB1) protein (Sarkisian et al., 2014). ZEB1 is a transcription factor for epithelial-mesenchymal-transition (EMT) in GBM. It is expressed in invasive GBM cells, particularly in patient cells with shorter survival and poor response to adjuvant chemotherapy TMZ treatment. Furthermore, EMT in GBM can lead to tumorigenesis, invasion, and chemoresistance demonstrated in GBM cells and xenograft mouse models (Siebzehnrubl et al., 2013). This study suggested that ZEB1 might be a good target in recurrent tumor cells since it is mainly expressed in the invasive GBM that also displays a poor response to treatment with TMZ. Similarly, the lack of cilia in both PCM1 and KIF3a depleted GBM cells, increases sensitivity to TMZ, suggesting that ciliary proteins which mediate ciliogenesis (PCM1 and KIF3a) can modulate GBM resistance (Hoang-Minh et al., 2016a). Altogether, these data suggest that most GBM cells fail to assemble cilia, and only small subpopulations are ciliated cells in primary GBM tumor biopsies.

Given that an increased cell cycle progression is one of the major features of GBM tumor invasion and propagation, the possibility of controlling cilia and, therefore, the cell cycle, would have great medical relevance. Hence, further studies, specifically in patient-derived primary cultures, could lead to a better understanding of the largely unexplored m cilia function mechanism, and could potentially contribute to discovering novel targets for GBM therapy.

# 2. Objectives and Aims

The role of primary cilia in tumorigenesis has only begun to emerge, and due to its importance in cell cycle progression and proliferation, it has already received significant attention (Moser et al., 2014, Goranci-Buzhala et al., 2017, Seeger-Nukpezah et al., 2013, Gradilone et al., 2017) Since cilia play decisive roles in regulating cell cycle progression and cellular signaling, suppressed ciliogenesis is anticipated to contribute to cancer initiation, invasion, and tumorigenesis (Michaud and Yoder, 2006, Gradilone et al., 2013, Plotnikova et al., 2008, Emoto et al., 2014). To better understand the basics of cilia biology in GBM, I sought to achieve the following aspects in the doctoral thesis:

1. Does suppressed ciliogenesis play a role in cell cycle progression of patient-derived GSCs?
   a) What is the prevalence of primary cilia in patient-derived GSCs and biopsies?
   b) Does suppressed ciliogenesis promotes cell cycle progression in GSCs?
   c) What is the molecular mechanism underlying the suppressed ciliogenesis in GSCs?

2. What are the molecular mechanisms that regulate ciliogenesis and restrict cell cycle progression in GSCs?
   a) Which protein complexes are required to induce cilia in GSCs?
   b) Functional characterization of newly induced primary cilia in GSCs.
   c) To examine the cell fate decision of GSCs after cilium induction.

3. Does induce ciliogenesis prevents GSCs invasion in a human brain organoid model?
   a) Develop a suitable assay to study GSCs invasion in the human brain organoids.
   b) Is induction of ciliogenesis in GSCs sufficient to prevent invasion in human brain organoids?

# 3. Results

## 3.1 Patient-derived GSCs exhibit suppressed ciliogenesis

Since primary ciliogenesis is disrupted at an early stage in the majority of human GBM tumors (Moser et al., 2009), eight patient-derived GSCs (isolated cells) and nine different clinical tissues (fixed biopsy tumor section) were analyzed. Patient-derived GSCs were used from three subtypes based on their genetic background **(Table 6)** such as mesenchymal (U3024MG), classical (U3056MG), proneural (U3047MG, U3082MG, U3033MG, MGG87, MGG8, #275, #454). Most importantly, all of the samples represent the three subtypes of GBM characterized by specific genetic defects and altered signaling pathways **(see introduction 1.8)**. Since the cellular origin of glioblastoma (GBM) might originate from neuroprogenitor cells (NPCs), NPCs-derived astrocytes, and oligodendrocyte precursor cells (Stiles and Rowitch, 2008, Yao et al., 2018). Therefore, patient-derived GSCs were compared to iPSCs-derived astrocytes and NPCs. Cilia were identified ciliary membrane marker ARL13B and centrosomal protein marker γ-Tubulin using immunofluorescence analyses. Our results demonstrate an overall suppressed ciliogenesis in patient-derived GSCs **(Figure 3.1A, B)**. Additionally, the quantification of ciliated cells, comparing the astrocytes and NPCs, to GSCs exhibit a significant decrease in ciliation **(Figure 3.1C)**.

Similar to patient-derived GSCs, nine independent, GBM patient biopsies show an overall suppressed ciliogenesis. **(Figure 3.1C-D)**. To visualize the tumor tissue cancer cells, Collapsin response mediator protein (CRMP5) is used along with the ciliary membrane marker (ARL13B)**.** CRMP5 is expressed in cytoplasm and nucleus in GBM, predicting lower patient survival and tumor proliferation (Moutal et al., 2015). Tumor cells were scored based on CRMP5, and ciliogenesis was quantified by counting cilia in 500 tumor cells from three independent experiments.

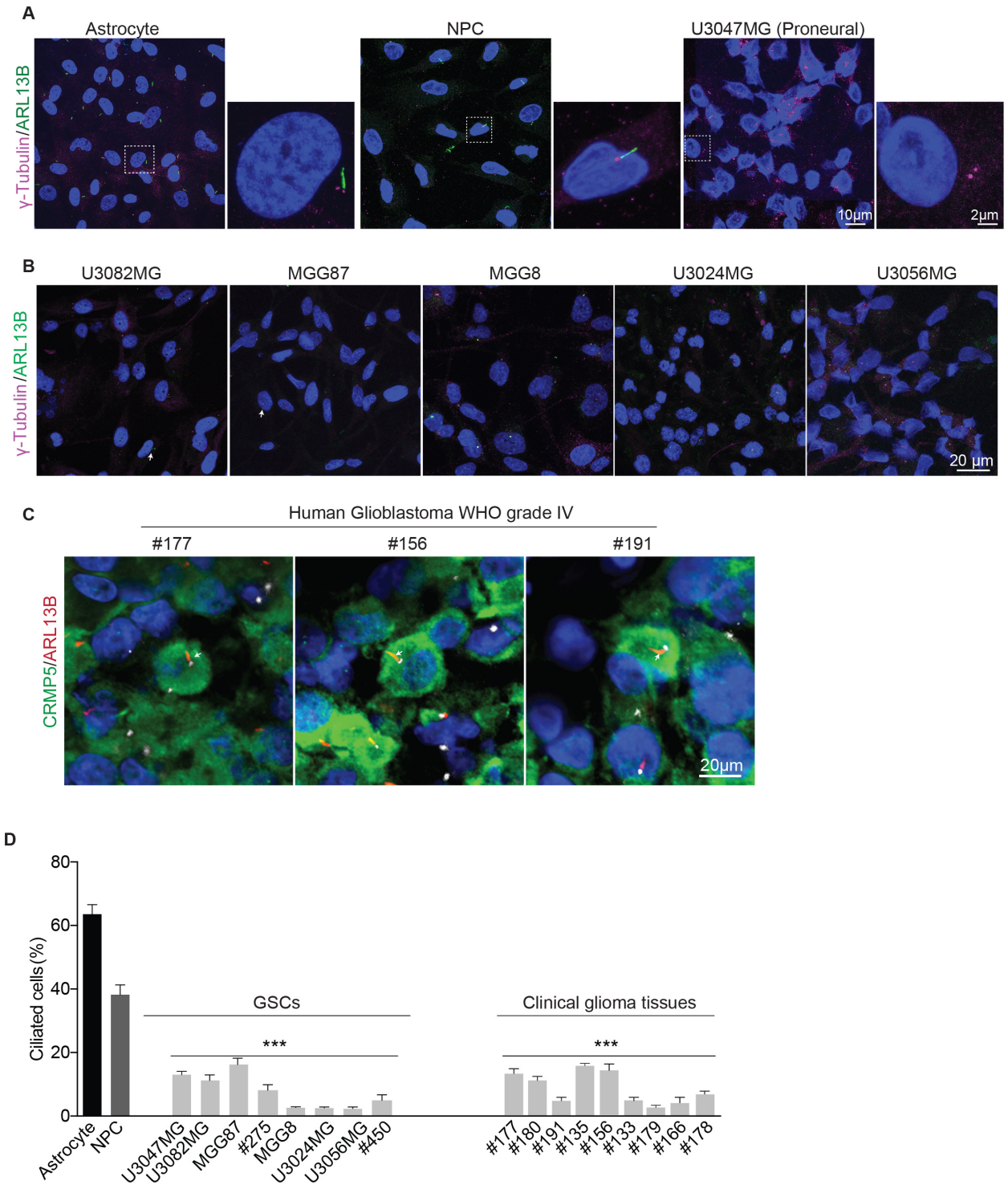


**Figure 3.1. Patient-derived GSCs exhibit suppressed ciliogenesis.**
**A.** Compared to iPSCs-derived astrocytes and NPCs, U3047MG, a representative proneural subtype GSC line exhibits suppressed ciliogenesis. ARL13B (green) labels cilia and γ-Tubulin (magenta) labels centrosomes. Scale bar, 10μm (overview), 2μm (inset). At least 500 cells were analyzed for each cell line from (n=4) independent experiments. **B.** Irrespective of various genetic backgrounds, tested GSCs (proneural, classical or mesenchymal) exhibit suppressed ciliogenesis. ARL13B is used to label cilia (green), and γ-Tubulin is used to label the centrosomes (basal bodies, magenta). Scale bar, 20 μm. **C.** Cilia occurrence in clinical tissues. Grade IV glioblastoma tissues mostly lack cilia (red, arrows). CRMP5 marks cancer cells in clinical tissues (green). **D.** The bar diagram quantifies frequencies of ciliated cells. Note that compared to astrocytes and NPCs, GSCs display an overall decrease in ciliation. Likewise, in clinical tissues, at least 9 independent glioblastoma grade IV tissues show an overall reduction in ciliation. Tumor cells were scored based on CRMP5 immunolabeling. At least

500 cells were analyzed in each cell line from three (n=3) independent experiments. One-way ANOVA, followed by Dunnett's multiple comparisons test ***P <0.0001. Error bars show +/- SEM.

Afterward, we performed the ultrastructural analysis of centrioles at an early stage of ciliogenesis, when the centriole anchors at the membrane, and serves as a basal body. The electron microscope (EM) results showed that compared to NPCs, cilium formation is suppressed at the early stages of ciliogenesis, specifically in U3047MG (proneural) **(Figure 3.2A)**. These results are in line with previously published data (Moser et al., 2014). Delayed cilia disassembly is associated with suppressing cell division via an extended $G_1$-S transition. In contrast, accelerated cilia disassembly or loss of cilia promoted cell proliferation (Jackson, 2011, Kim et al., 2015b, Li et al., 2011).
While ciliogenesis is suppressed in the various genetic backgrounds of GSCs, we anticipated that these GSCs could exhibit an increased cell proliferation. Therefore, astrocytes, NPCs, and GSCs were labeled with ethynyl-deoxyuridine (EdU). As expected, 24hrs after EdU pulse labeling, an increased cell number with incorporated EdU in NPCs compared to ciliated astrocytes were observed. Interestingly, the cell number of GSCs with incorporated EdU was also elevated and similar/comparable to NPCs **(Figure 3.2B).** Increased proliferation is coupled to the elevated rate of the cell cycle. Hence, to determine the cell cycle phase of GSCs, fluorescence ubiquitination cell-cycle indicator (FUCCI) was used. This method employs fluorescent probes, which enables the visualization of cell cycle progression. Following analyzes of the FUCCI experiment revealed that unlike astrocytes but similar to fast proliferating NPCs, only a small fraction of GSCs reside at $G_1/G_0$, a cell cycle stage of cilium assembly in healthy cells **(Figure 3.2C).** These data indicate that suppressed ciliogenesis in GSCs is associated with increased cell cycle progression.

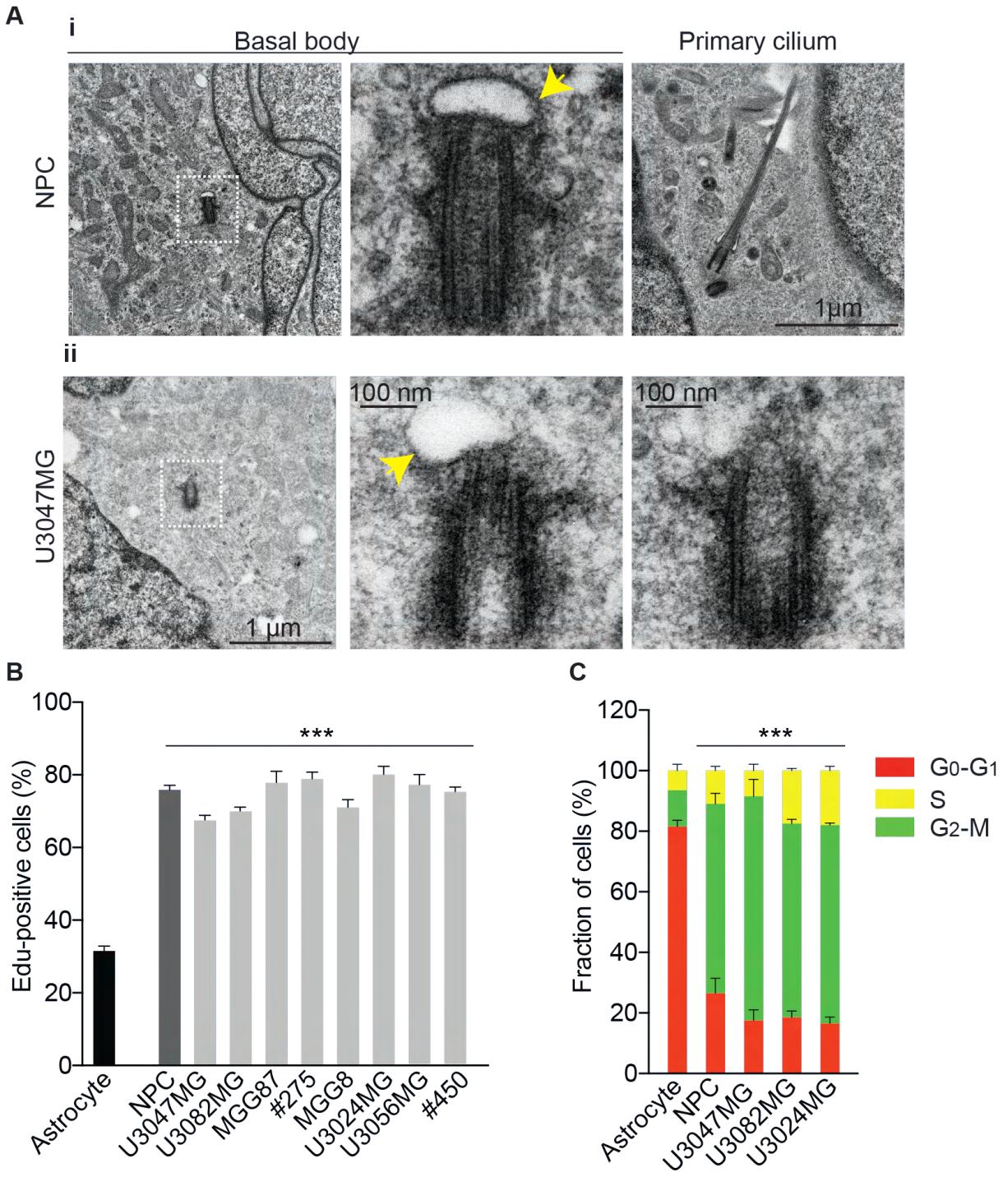


**Figure 3.2. Suppressed ciliogenesis promotes cell proliferation.**
**A.** Ultrastructural analysis of NPCs (top) compared to U3047MG cells (bottom). Note vesicle formation (yellow arrow). At least 15 independent centrioles were analyzed. Scale bar, 1µm (overview) and 100nm (inset). **B.** The bar diagram quantifies frequencies of EdU positive cells. Note that GSCs exhibit similar EdU profile of NPCs and exhibit an increased EdU incorporation compared to ciliated cycling astrocytes. At least 300 cells were analyzed in each cell line from (n=3) independent experiments. One-way ANOVA, followed by Dunnett's multiple comparisons test, ***P<0.001. Error bars show +/- SEM. **C.** The bar diagram quantifies cell cycle analysis by Fluorescence Ubiquitin Cell Cycle Indicator (FUCCI) tracing. Note that a significant fraction of GSCs and NPCs are retained at $G_2$-M (green). At least 100 cells were analyzed in each cell line from (n=4) independent experiments. Ordinary two-way ANOVA, followed by Tukey's multiple comparisons test, ***P <0.001. Error bars show +/- SEM.

## 3.2 GSCs have an elevated level of CDC that contains NEK2 and KIF24 as crucial components

Next, the aim was to investigate the molecular mechanism that suppressed ciliogenesis in GSCs. Because cilia formation is suppressed in GSCs at the early stages of ciliogenesis **(Figure 3.1)**, we speculated that CDC protein levels are elevated in this critical period to suppress ciliogenesis. Assuming that suppressed ciliogenesis in GSCs allows them to proliferate continuously escaping from the quiescence state $G_0$ (resting phase). This would aid in explaining the aggressive nature of GSCs.

Studies have shown that NEK2, a $S/G_2$ kinase, is elevated in cancer cells and plays a prominent role in cilia disassembly by activating its physiological substrate Kif24. This depolymerizing microtubule kinesin suppresses cilia formation (Kim et al., 2015b). To understand if NEK2 and KIF24 are part of the CDC complex co-immunoprecipitation was performed. Because CDC proteins are low abundant protein, the FLAG-tagged CPAP and FLAG-tagged NEK2 were used, which were stably expressed in HEK293 cells. By analyzing purified FLAG-tagged CPAP complexes, we identified that NEK2 co-purifies with CDCs' known component. Reciprocally, CDC components of Aurora-A, HDAC6, NDE1, OFD1, and CPAP co-purify with FLAG-tagged NEK2, which also included its substrate KIF24**.** Centrosome associated Outer dense fiber protein-2 (OFD-2) does not co-purify with CPAP, indicating the specificity of CPAP interaction with CDC components **(Figure 3.3A and B)**. Taken together, the co-immunoprecipitation performed in HEK293 confirms that NEK2 and KIF24 are components of the CDC.

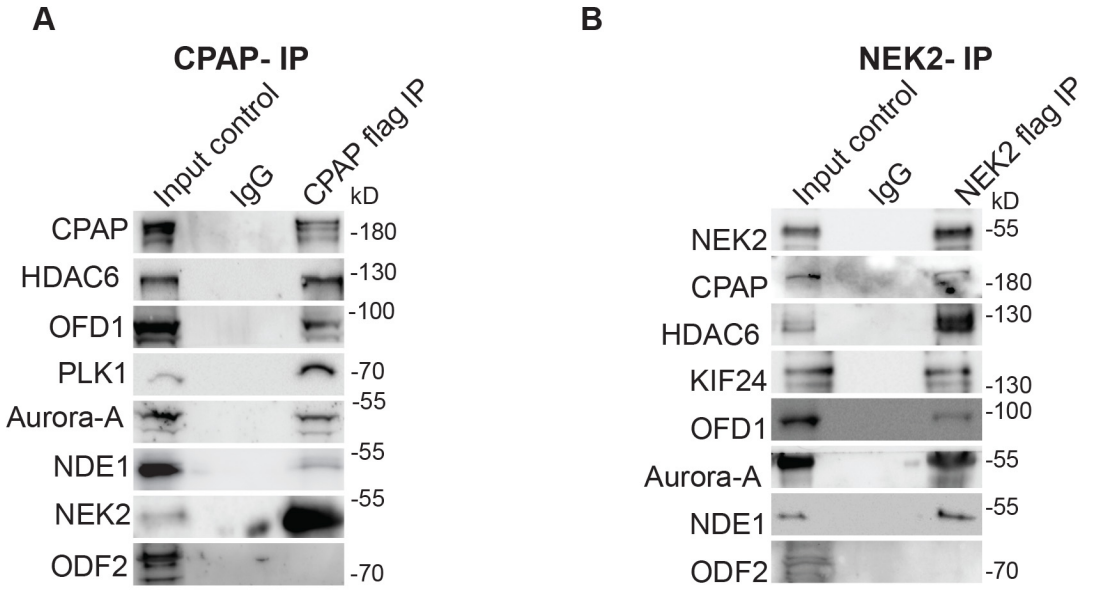


**Figure 3.3. NEK2 and KIF24 co-purify with CDC proteins.**
**A.** Immunopurification of CPAP complex from HEK293 cell extracts expressing CPAP-flag. NEK2 co-purifies with other components of CDC. Centrosome-associated Outer Dense Fiber protein-2 (OFD-2) does not co-purify with CPAP indicating the specificity of CPAP interaction with CDC components, including NEK2. IgG indicates negative control. **B.** Reciprocal immunopurification experiment. Immunopurification of NEK2 complex from HEK293 cell extracts expressing NEK2-flag. NEK2 co-purifies with other components of CDC, including KIF24. IgG indicates negative control.

However, this is an overexpression model. Therefore, to gain more insights about the CDC protein levels in GSCs, we performed a semi-quantitative Western blot analysis in patient-derived GSCs (U3047MG, U3082MG, MGG87) compared to control astrocytes. The finding from the results indicates that amounts of CDC protein extract overall increase in GSCs compared to ciliated astrocytes **(Figure 3.4A).** Additionally, immunostaining using specific antibodies against CDC (NDE1, OFD1, Aurora-A, and CPAP) further revealed that compared to NPCs, GSCs that have suppressed ciliogenesis recruit an enhanced level of CDC proteins at the basal body (ciliary base) **(Figure 3.4C).** Moreover, compared to NPCs, U3047MG cells displayed a significant increase in the immunoreactivity of KIF24 both in the cytoplasm and basal bodies **(Figure 3.4B).** Altogether data suggest that elevated levels of CDC proteins might be involved in the molecular mechanism that suppressed ciliogenesis and promotes the cell cycle progression in GSCs.

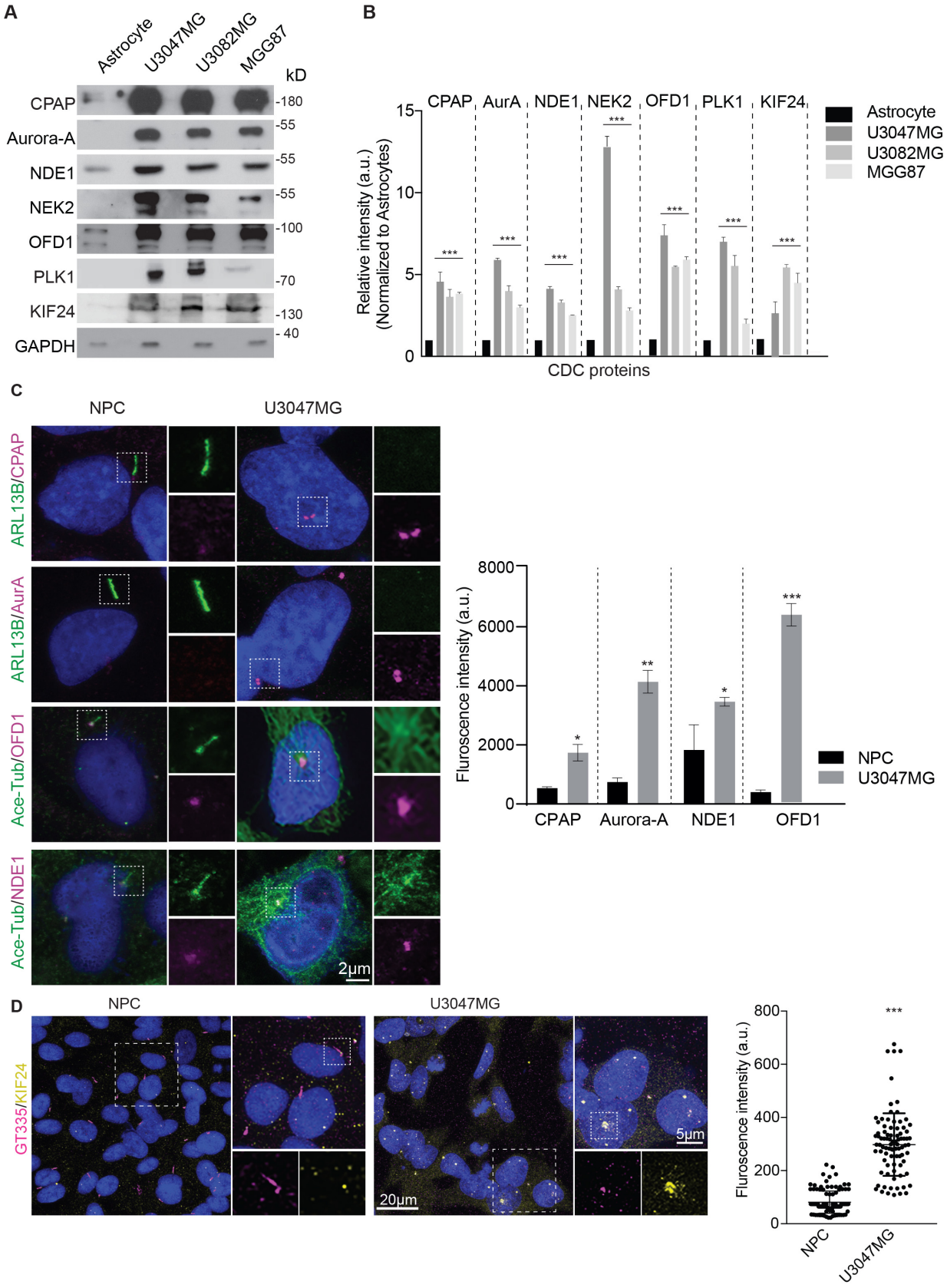


**Figure 3.4. GSCs have elevated levels of CDC components.**
**A.** Semi-quantitative Western blot exhibiting relative levels of tested CDC components between ciliated astrocytes and GSCs. An equivalent quantity of cell extracts was loaded. GSCs show an overall elevated level of CDC components. GAPDH was used as a loading control. **B.** The bar diagram quantifies the relative intensity of tested CDC components in ciliated astrocytes and GSCs. Western blots from three (n=3) independent experiments. Ordinary two-way ANOVA, followed by Sidak's multiple comparisons

test, ***P<0.001. Error bars show +/- SEM. **C**. Compared to NPCs, U3047MG exhibits an overall increased immunoreactivity to KIF24. Increased level of KIF24 is obviously visible in the cytoplasm and at ciliary bases. The bar diagram at right quantifies fluorescence intensity of KIF24. At least 200 cells were analyzed in each cell line from (n=4) independent experiments. Ordinary two-way ANOVA, followed multiple comparisons test, **P <0.001. Error bars show +/- SEM. **D**. Compared to NPCs, U3047MG cells recruit an enhanced level of CDC components to the ciliary base. Cilia are labeled either by ARL13B or acetylated α-tubulin (green). CDC components (red) were immunostained using antibodies specific to CPAP, Aurora-A, OFD1 and NDE1. Bar diagram at right quantifies fluorescence signal intensity. At least 200 were analyzed in each cell line from (n=4) independent experiments. Ordinary two-way ANOVA followed by Tukey's multiple comparisons test. ***P <0.001, **P <0.001, P <0.01. Error bars show +/- SEM. Scale bar 2 μm.

## 3.3 Depletion of CDC components induces cilia in GSCs

To investigate the potential mechanism to induce cilia in GSCs, we asked if targeting overexpressed CDC proteins is sufficient to induce ciliogenesis in GSCs. Therefore, shRNA-mediated depletion of selected CDC components (NEK2, HDAC6, and NDE1) in U3047MG cells was performed. Using western blot analysis depletion of targeted NEK2, HDAC6, and NDE1 proteins were confirmed. Surprisingly, according to the immunostaining of ARL13B (ciliary membrane marker), the depletion of all CDC components induced cilia in U3047MG cultures. However, the quantification analysis shows the highest increase in ciliation after NEK2 depletion **(Figure 3.5A-B)**. These data show that the depleting subset of CDC components in GSCs is sufficient to induce cilia.

Based on the shRNA-mediated CDC depletion experiments, NEK2 was the most promising candidate to restore ciliogenesis in GSCs **(Figure 3.5A and B).** Therefore, we targeted NEK2 in GSCs with different genetic backgrounds (proneural, mesenchymal, and classical). Of note is that NEK2 is a multifunctional protein. Hence, we decided to target only the catalytic part of the protein, which is implicated explicitly in cilia disassembly. We took advantage of the previously used plasmid carrying catalytically inactive NEK2 (NEK2-KD, NEK2-kinase-dead, in which catalytically active lysine is replaced with catalytically inactive arginine, NEK2-K37R) (Fry et al., 1995). It has been shown that mutated NEK2-K37R (NEK2-KD) cannot phosphorylate its physiological substrate KIF24, a kinesin that depolymerizes ciliary microtubule (Kim et al., 2015b).

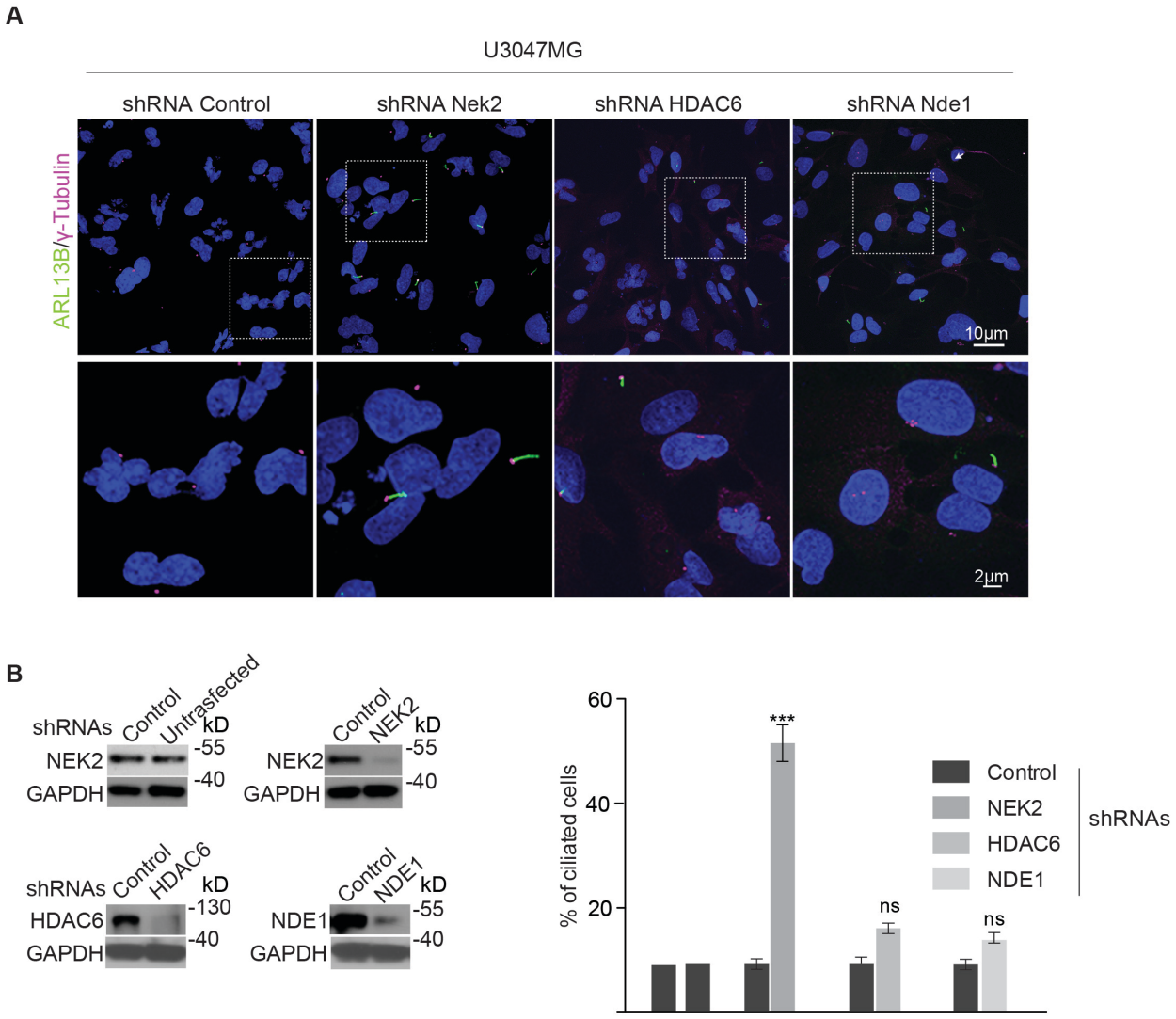


**Figure 3.5. Depletion of CDC components induce cilia in patient-derived GSC cell line.**
**A.** shRNA specifically targeting NEK2, HDAC6, and NDE1 depletes respective proteins and induces cilia in U3047MG cells. U3047MG is used as representative GSCs. ARL13B is applied to label cilia (green) and γ-Tubulin is used to label the centrosomes (basal bodies, magenta). Scale bar, 10 μm. Western blots below show shRNA-mediated depletion of specific CDC components. GAPDH is a loading control.
**B.** Bar diagram quantifies frequencies of ciliated cells in cultures treated with shRNA specific to CDC components. At least 200 cells were analyzed from (n=3) experiments. Ordinary two-way ANOVA followed by Sidak's multiple comparisons test. ***P <0.0001. Error bars show +/- SEM. 3.4 Overexpression of NEK2 kinase dead is sufficient restore cilia in GSCs.

Therefore, instead of depleting endogenous NEK2, a lentil-based inducible system was used to overexpress the catalytic inactive NEK2-KD in GSCs. Following several cloning steps, we generated a panel of GSC lines stably expressing doxycycline (DOX) inducing GFP-tagged NEK2-WT and NEK2-KD. Using this system, we revealed that upon 24 hrs. DOX induction, NEK2-KD expression, could induce cilia in proneural subtype GSCs (U3047MG, U3082MG, and MGG87), however not in classical (U3056MG) or mesenchymal subtypes (U3024MG) **(Figure 3.6 A and B**).

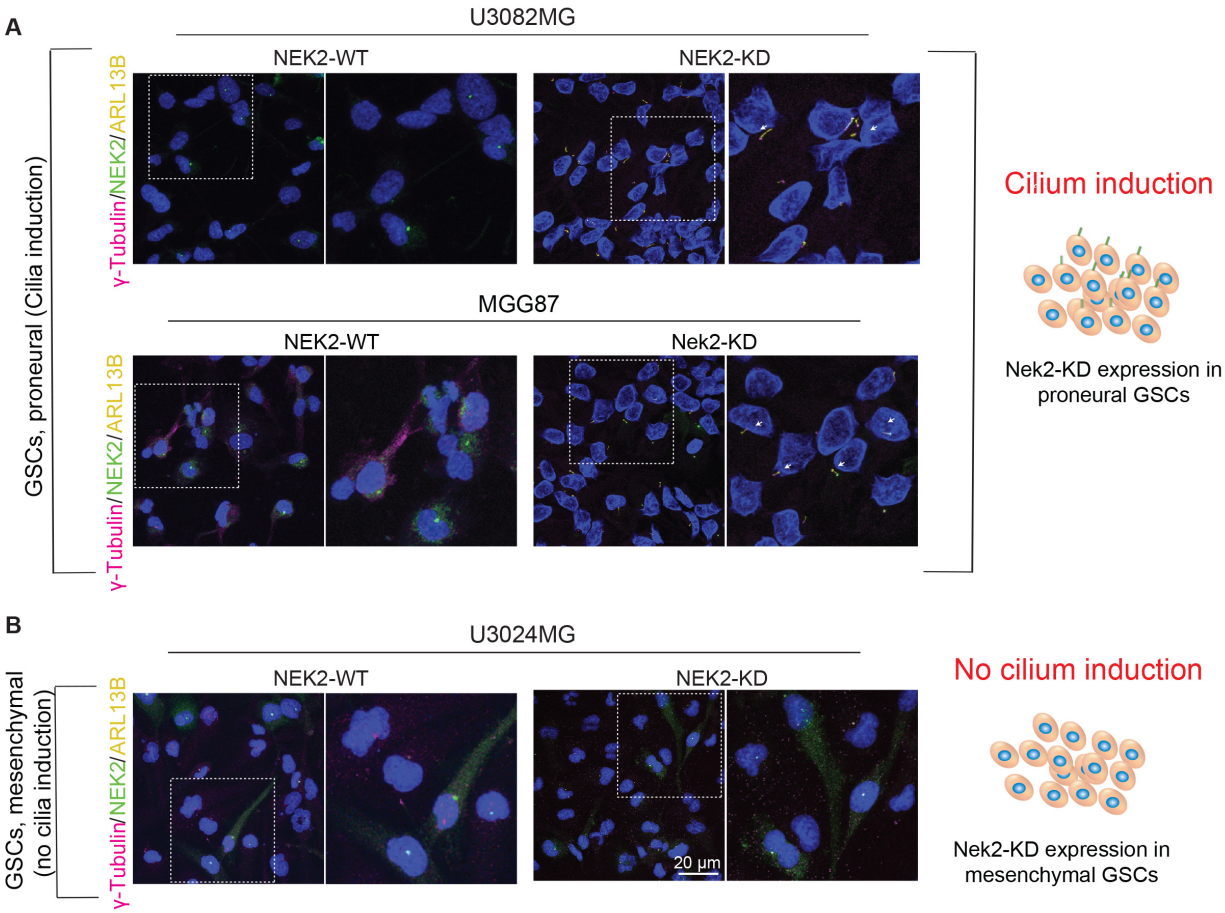


**Figure 3.6. Overexpression of NEK2-KD induce cilia in proneural subtype of GSCs.**
**A.** Catalytically inactive NEK2 kinase (NEK2-KD) overexpression could induce cilia in proneural subtype GSCs. **B.** In contrast, catalytically inactive NEK2 kinase (NEK2-KD) overexpression cannot induce cilia in mesenchymal subtype GSCs (U3024MG). ARL13B labels cilia (yellow), NEK2-WT and KD both target basal bodies (green), and γ-Tubulin labels the centrosomes (basal bodies, magenta). Scale bar, 20 μm.

Taken together, the data shed new light on the possible mechanism of cilia induction, suggesting that targeting CDC components can induce cilia in proneural subtype GSCs. To gain more insights into this mechanism, we studied the proneural GSCs in more detail.

Since cilia induction in GSCs was possible by overexpressing NEK2-KD (induced by DOX for 24 hrs), the percentage of ciliated cells was quantified, and then analyzed if this phenomenon is coupled to the cell cycle. First, all GSC lines stably expressing GFP-tagged NEK2-WT or NEK2-KD were treated with DOX for 24hrs and 72hrs and quantified the percentage of ciliated cells using ARL13B (ciliary membrane marker) **(Figure. 3.7A-C)**. The frequencies of ciliated GSCs did not vary significantly after 72hrs of DOX induction. Quantification analyzes demonstrate that NEK2-KD overexpression could significantly restore ciliogenesis in proneural subtype GSCs (U3047MG, U304782, MGG87, and #275) **(Figure 3.7C).** Moreover, cell proliferation analysis of ciliated U3047MG cells revealed that they proliferated significantly slower than non-ciliated cells as determined by EdU incorporation and Ki67 staining **(Figure 3.7E).** Overall, the data show that restoring ciliogenesis impairs GSCs proliferation.

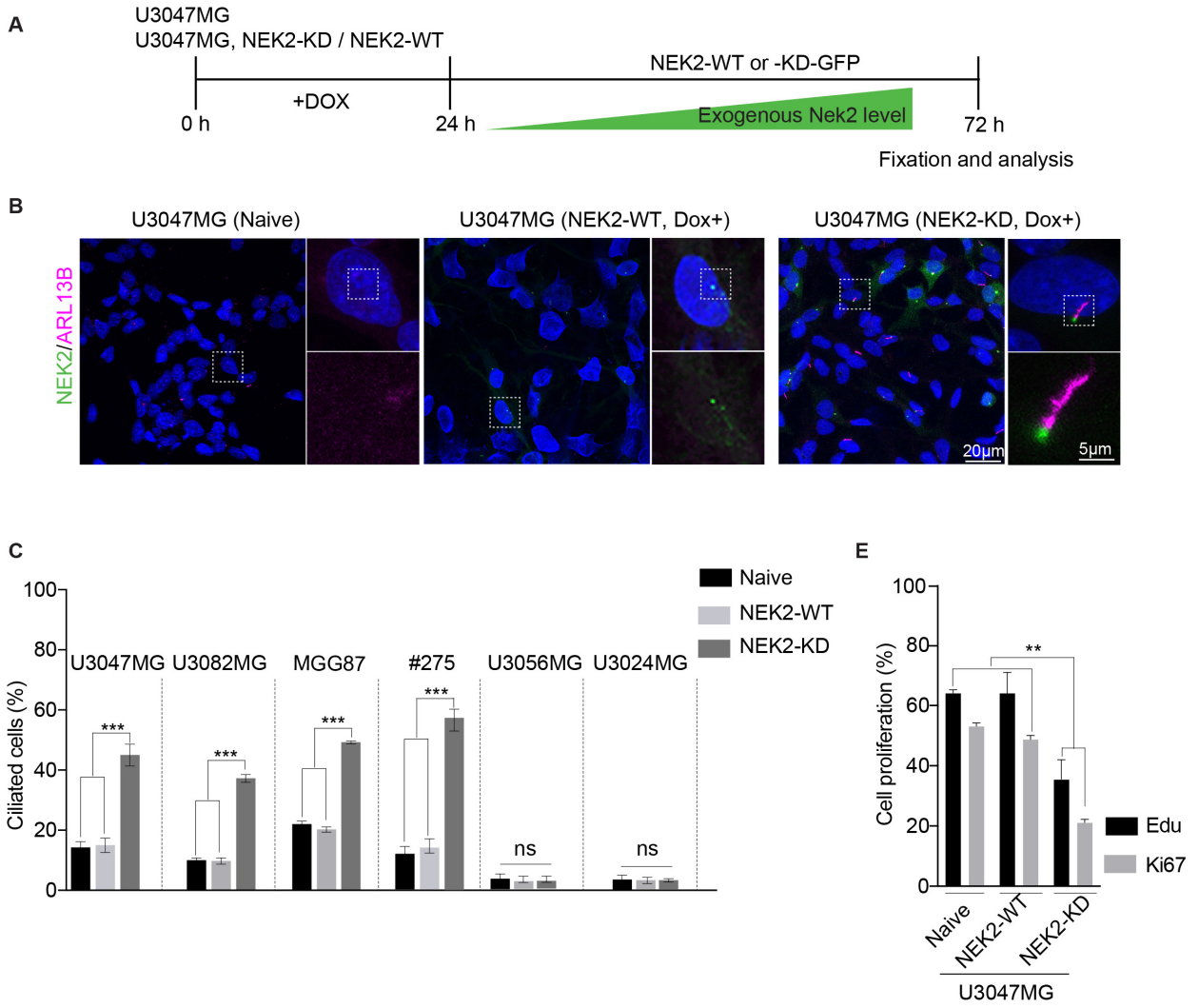


**Figure 3.7. Overexpression of NEK2-KD induces cilia and prevents cell proliferation.**
**A**. Experimental set up. Seeded GSCs were induced to express NEK2-WT and NEK2-KD (kinase dead, catalytically inactive), fixed and analyzed. **B**. Compared to U3047MG naïve or NEK2-WT expressing U3047MG, NEK2-KD expressing U3047MG displays cilia. NEK2 (green) labels centrosomes. ARL13B labels cilia (magenta). Scale bar, 20μm (overview), 5μm (Insert). n=4 independent experiments. **C**. Bar diagram quantifies frequencies of ciliated cells across different GSCs upon NEK2-KD expression. NEK2-KD could induce ciliogenesis in selective GSCs lines and not in mesenchymal (U3024MG) or classical (U3056MG) subtypes. At least 300 cells were analyzed in each cell line from (n=5) independent experiments. P values were obtained using ordinary two-way ANOVA, followed by Tukey's multiple comparisons test. ***P <0.0001. Error bars show +/- SEM. **D.** Cilium induction impairs proliferation rate of GSCs. Bar diagram quantifies cell proliferation profile of non-ciliated (naïve U3047MG, NEK2-WT expressing U3047MG) and ciliated GSCs (NEK2-KD expressing U3047MG) revealed by 48h EdU pulse chasing Ki67 immunoreactivity. At least 400 cells were analyzed in each cell line from (n=4) independent experiments. 2-way ANOVA, followed by Sidak's multiple comparisons test. **P <0.001. Error bars show +/- SEM.

Data demonstrate that ciliated U3047MG cells are majorly retained at $G_1/G_0$ **(Figure 3.2C)** prompted us to speculate that NEK2-KD-induced cilia are persistent, and thus cells presumably did not proceed to $G_2$-M transition. Thus cells presumably did not proceed to $G_2$-M transition (cell cycle re-entry). To test this hypothesis, DOX was withdrawn after day 3 of incubation, and GSCs were further cultured for a prolonged period of up to 10 days without DOX. Although NEK2 expression is unnoticeable at

day 10, the abundance of ciliated GSCs in Nek2-KD expressing cultures remain unchanged **(Figure 3.8B immunofluorescence staining left panel).** Concurrently, after DOX withdrawal, the cell proliferation did not continue in these GSCs **(Figure 3.8B bar diagram)**. These findings indicate that NEK2-KD-induced cilia are persistent and suggest that these GSCs do not re-enter the cell cycle**.** Overall, data show that catalytically inactive NEK2 is sufficient to induce ciliation persistently in proneural GSCs subtype.

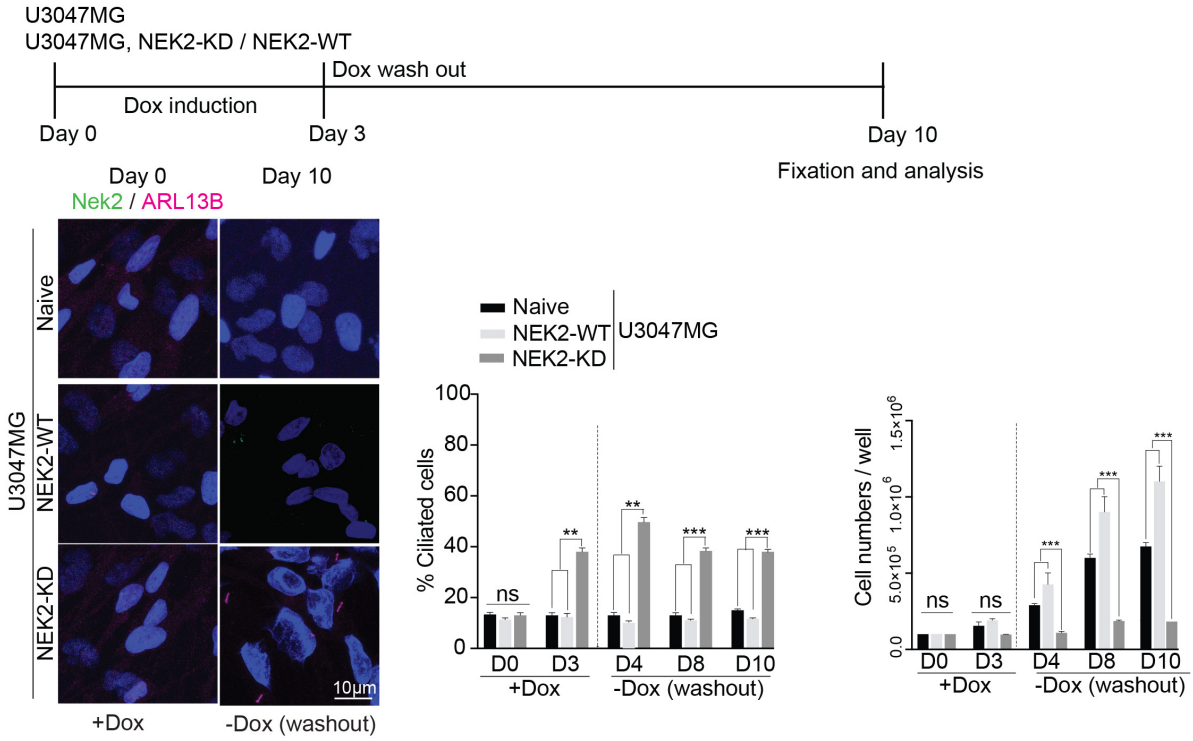


**Figure 3.8. Ciliogenesis is irreversibly induced in GSCs after NEK2-KD overexpression.** Experimental scheme of doxycycline induction and wash out experiment. NEK2-KD expressing GSCs still harbor primary cilia at day 10 even after removing doxycycline (Scale bar 10 µm). Bar diagram at right quantifies the fraction of ciliated cells and absolute cell numbers at various time points of doxycycline wash out. At least 1000 cells were analyzed in each cell line from (n=4) independent experiments. Ordinary two-way ANOVA, followed by Tukey's multiple comparisons test. ***P <0.001. Error bars show +/- SEM.

## 3.4 Ciliogenesis is associated with reduced recruitment of CDC

To understand plausible mechanisms of cilium induction, we analyzed the levels of CDC proteins before (U3047 naïve and NEK2-WT) and after cilium induction (U3047MG NEK2-KD). Since CDC proteins are downregulated in quiescence state (G1-G0) of the cell cycle, we analyzed protein levels before and after ciliation in GSCs. Western blot analysis of U3047MG cell extracts revealed an overall reduction in CDC protein levels after cilia induction (U3047MG NEK2-KD) **(Figure 3.9A).** Reasoning that this could be due to overall reduction in proliferation and retention of cells at $G_1$-$G_0$, prompting us to estimate the amount of individual CDC components recruitment to the basal bodies. Immunostaining using specific antibodies against CDC components (Aurora-A, CPAP, NDE1, and

OFD1) revealed that the recruitment of CDC components is drastically reduced in GSCs after cilium induction (U3047MG NEK2-KD) compared to healthy NPCs **(Figure 3.9B).**

Kif24 is a depolymerizing microtubule kinesin that localizes between the distal end of the basal body and the minus end of the ciliary microtubule (Kim et al., 2015b). Upon activation by Nek2, Kif24 readily stimulates ciliary microtubule depolymerization, possibly acting as a minus-end microtubule-depolymerizing factor. This orchestrated interplay of Nek2-Kif24 interaction ensures the suppressed ciliogenesis (Kim et al., 2015b). Therefore, we turned our investigation into the localization dynamics of Kif24 before and after cilium induction. To our surprise, we detected a mislocalization pattern of Kif24 in almost all of the ciliated U3047MG cells expressing Nek2-KD. Specifically, Kif24 was restricted to basal bodies and often absent at the minus end of ciliary microtubules **(Figure 3.9C-D).** Altogether, these results revealed that overexpression of the inactive catalytic domain of NEK2 (NEK2-KD) is sufficient to induce cilia in GSCs and to reduce CDC recruitment at the basal bodies. Surprisingly, upon cilium induction, the NEK2-KD is not able to localize its substrate KIF24 at the active site of the minus end ciliary microtubule. The data underlines an important role of the NEK2-KIF24 interaction for the proper cilium disassembly.

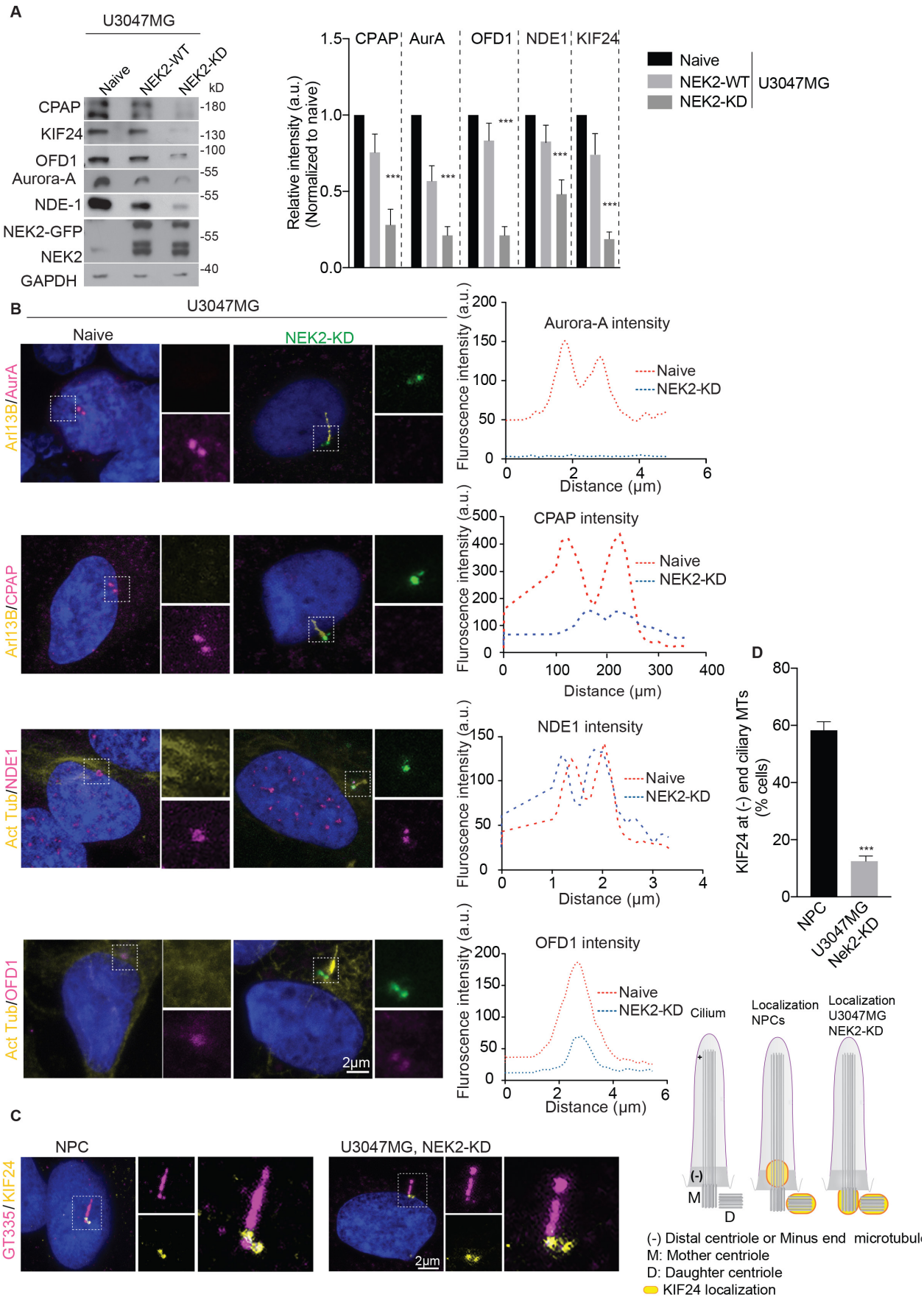


**Figure 3.9. Overexpression of NEK2-KD impairs CDC recruitment to the newly induced cilia in GSCs.**

**A**. Semi-quantitative Western blot exhibiting relative levels of CDC components before and after cilium induction in U3047MG cells. Cilium induction (NEK2-KD expressing U3047MG) is associated with a

reduction in overall CDC component levels. NEK2 antibody recognizes both endogenous and exogenous proteins. GAPDH was used as a loading control. The bar diagram at right quantifies the relative intensity of CDC components before and after cilium induction. Western blots from three (n=3) independent experiments. Ordinary two-way ANOVA, followed by Tukey's multiple comparisons test, ***P<0.001. Error bars show +/- SEM. **B.** Compared to non-ciliated U3047MG naïve, NEK2-KD expressing ciliated U3047MG cells recruit a reduced level of CDC components. Cilia are labeled either by ARL13B or acetylated α-tubulin (yellow). CDC components (magenta) were immunostained using antibodies specific to Aurora-A, CPAP, NDE1, and OFD1. NEK2-KD labels centrosomes at the base of cilia (green). Graphs at right display the distribution of fluorescence intensity of CDC components recruited to ciliary base before (red, naïve) and after (blue, NEK2-KD) cilium induction. At least 300 cells were analyzed in each cell line from (n=4) independent experiments. Scale bar 2 μm. **C.** KIF24 (yellow) localizes at distal centriole or minus end ciliary microtubule GT335 (magenta) in healthy NPCs. In contrast, KIF24 is restricted only to basal bodies in most of the NEK2-KD expressing ciliated U3047MG cells. Schematic at right depicts the KIF24 localization pattern before and after cilium induction. Imaging of KIF24 in U3047MG naïve cells is not shown as they have suppressed ciliogenesis. At least 200 cells were analyzed in each cell line from (n=4) independent experiments (Bar diagram below). Unpaired t-test. ***P<0.001. Error bars show +/- SEM. Scale bar 2 μm.
**D.** The bar diagram quantifies fractions of NPCs and ciliated U3047MG cells displaying normal localization pattern of KIF24 at the minus end ciliary microtubule. At least 300 cells were analyzed in each cell line from (n=4) independent experiments. Unpaired t-test, ***P <0.001. Error bars show +/- SEM.

## 3.5 Perturbing CDC recruitment can induce functional cilia in GSCs

To analyze if the induced ciliogenesis in GSC is structurally normal, we performed EM analysis of unciliated (U3047MG naïve) and ciliated (U3047MG NEK2-KD) cells. Ultrastructural analysis showed an elevated level of CDC components in unciliated (U3047MG naïve), is somewhat corroborated by the frequent presence of electron-dense satellite-like particles concentrated at the vicinities of basal bodies which we infrequently observed in ciliated cells (U3047MG NEK2-KD) **(Figure. 3.10A)**. The ultrastructure analysis revealed that newly induced cilia by NEK2-KD are structurally normal and comparable to healthy NPCs **(Figure 3.2Ai).**

The results arise the question if the newly induced cilia in GSCs, despite the typical structure, also have normal function. During cilia formation, axoneme elongation requires the amount of tubulin to enter cilium. This process is supported via the IFT cargo transport mechanism, which is used for cilia formation, maintenance, and function (Harris et al., 2018). Therefore, to functionally analyze newly induced cilia in GSCs, we analyzed immunofluorescence staining of the ciliary marker IFT88 and acetylated tubulin (Act Tub). Data reveals that ciliated GSCs (U3047MG NEK2-KD) were positive for both ciliary markers similar to healthy ciliated NPCs **(Figure 3.10B).** Overall the data suggest that newly induced cilia in GSCs might be functional.

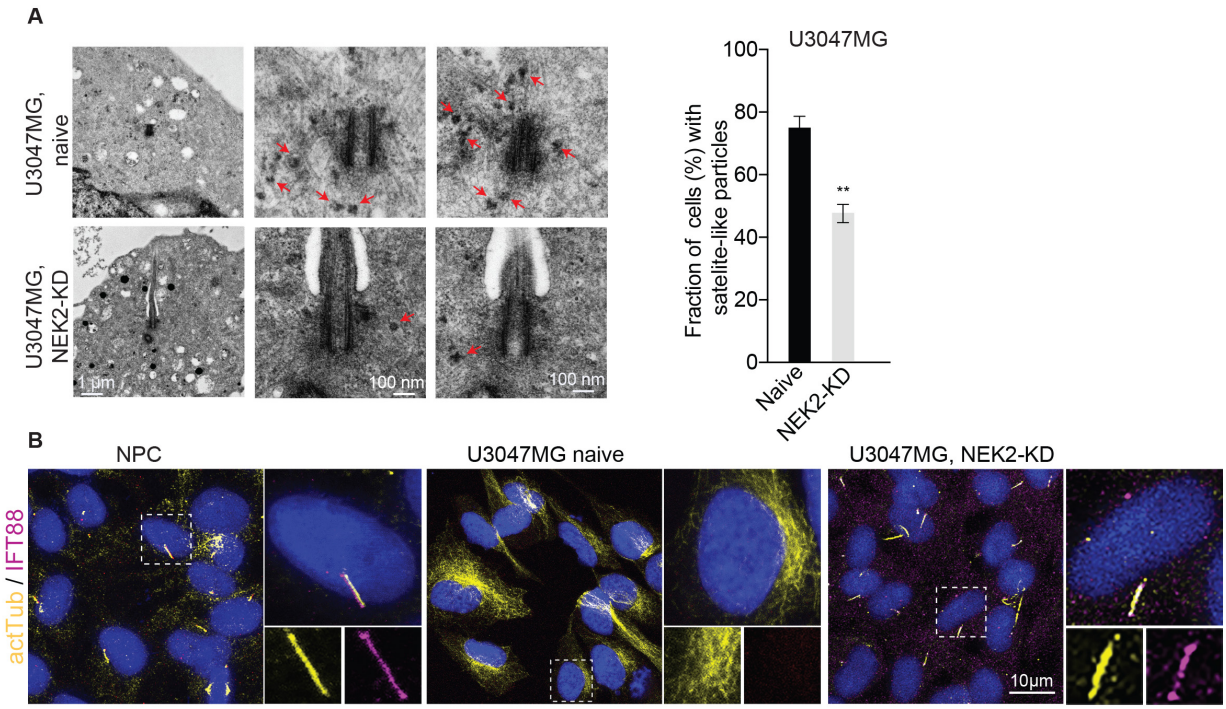


**Figure 3.10. Induced cilia in GSCs are structurally and functionally normal.**
**A**. Ultra-structural analysis of non-ciliated naïve U3047MG (top) compared to ciliated U3047MG cells (bottom). Numerous electron-dense satellite-like particles are prevalent (red arrow) in naïve U3047MG that are infrequently seen after cilium induction. The bar diagram at right quantifies it. At least 20 centrioles were analyzed. Scale bar 1 µm (low magnification) and 100nm (high magnification). Unpaired t-test. ***P<0.001. Error bars show +/- SEM. **B.** Just like healthy NPCs (left), newly induced cilia of U3047MG cells (right) display IFT88 particles (magenta). Cilia are labeled by acetylated α-tubulin (yellow). Naïve U3047MG cells do not display cilia nor IFT88 (middle). Both overview and magnified single cells are shown. Scale bar 10 µm. At least 500 cells were analyzed from (n=3) independent experiments.

However, the sole presence of ciliary markers does not reflect the functionality of newly induced cilia. Therefore, we also analyzed newly induced cilia to transduce Hh signaling because Hh signaling transduction acts through cilium (Bangs and Anderson, 2017). The overexpression of the catalytically inactive domain of NEK2 (U3047MG NEK2-KD) was induced with DOX for 48h, and the additionally stimulated with smoothened agonist (SAG) that activates SMO protein. SMO is an integral part of the Hh signaling pathway, which translocates from the plasma membrane to the cilium after activating the signaling (Bangs and Anderson, 2017). Upon SAG stimulation, the activated SMO relocated from basal body to the entire length of the cilium in healthy NPCs and newly induced cilium (U3047NEK2-KD) but not for unciliated cells (U3047MG naive) **(Figure 3.11)**. These results collectively reveal that perturbing CDC recruitment is sufficient to induce structurally and functionally normal cilia in GSCs.

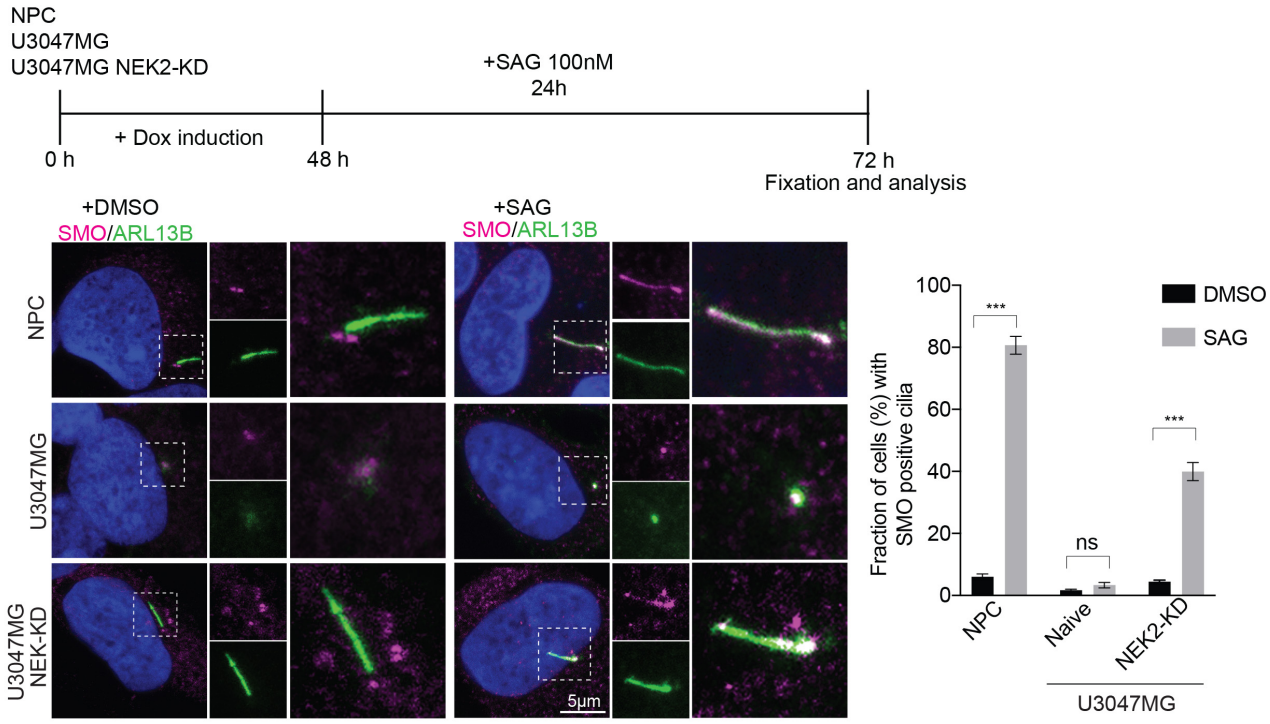


**Figure 3.11. Induced cilia in GSCs can transduce Hh signaling upon SAG activation.** Experimental set up of Shh signaling activation with SAG. In healthy NPCs, SMO (magenta) is restricted to basal bodies. Upon SAG addition, SMO translocates to primary cilium (top panel). Similar to healthy NPCs, U3047MG cells induced with cilia display SMO translocation to newly induced cilia (magenta, bottom panel). Cilia are labeled with ARL13B (green). Naïve U3047MG cells do not show cilia, and thus SMO is restricted to basal bodies (middle panel). Scale bar 5 µm. Bar diagram at right quantifies fractions of cells whose cilia respond to SAG activation. At least 200 cells were analyzed from (n=3) independent experiments. Ordinary two-way ANOVA followed by Sidak's multiple comparisons test ***P <0.0001. Error bars show +/- SEM.

## 3.6 Inducing ciliogenesis triggers GSCs differentiation

As cilia formation is coupled to the cell cycle in GSCs next, we asked the fate of the cells after ciliation. It has been shown that retarded cilium disassembly and extended $G_1$-S transition due to an inefficient CDC recruitment are sufficient to switch healthy NPCs from self-renewal to differentiation state (Gabriel et al., 2016). Therefore, we analyzed if proneural subtype GSCs induced with cilia (U3047MG NEK2-KD) could undergo differentiation. Using immunofluorescence staining, we analyzed neural stem cell markers such as NESTIN, PAX6 and SOX2 and differentiation markers such as TUJ1 (neuron marker) and GFAP, S100β (astrocyte marker) in GSCs before(U3047MG naïve and NEK2-WT) and after cilium induction(U3047MG NEK2-KD). Surprisingly, and in contrast to unciliated cells (U3047MG naïve, and NEK2-WT), the ciliated GSCs (U3047MG and U3082MG) expressing NEK2-KD exhibited significantly increased proportion of GFAP, S100β and TUJ1 positive cells, which are the identity markers of astrocytes and neurons **(Figure. 3.12A-B).** Importantly, the ciliated cells exhibited strongly reduced levels of specific neural and cancer stem cell markers such as NESTIN, PAX6, and SOX2, compared to the unciliated cells. However, none of these markers were detected in mesenchymal (U3024MG) and classical (U3056MG) subtype GSCs. Moreover, the

DOX-induced overexpression of NEK2-KD did not restore ciliogenesis in mesenchymal GSCs (U3024MG), suggesting that the differentiation process might be a cilia-dependent (**Figure 3.6B).**

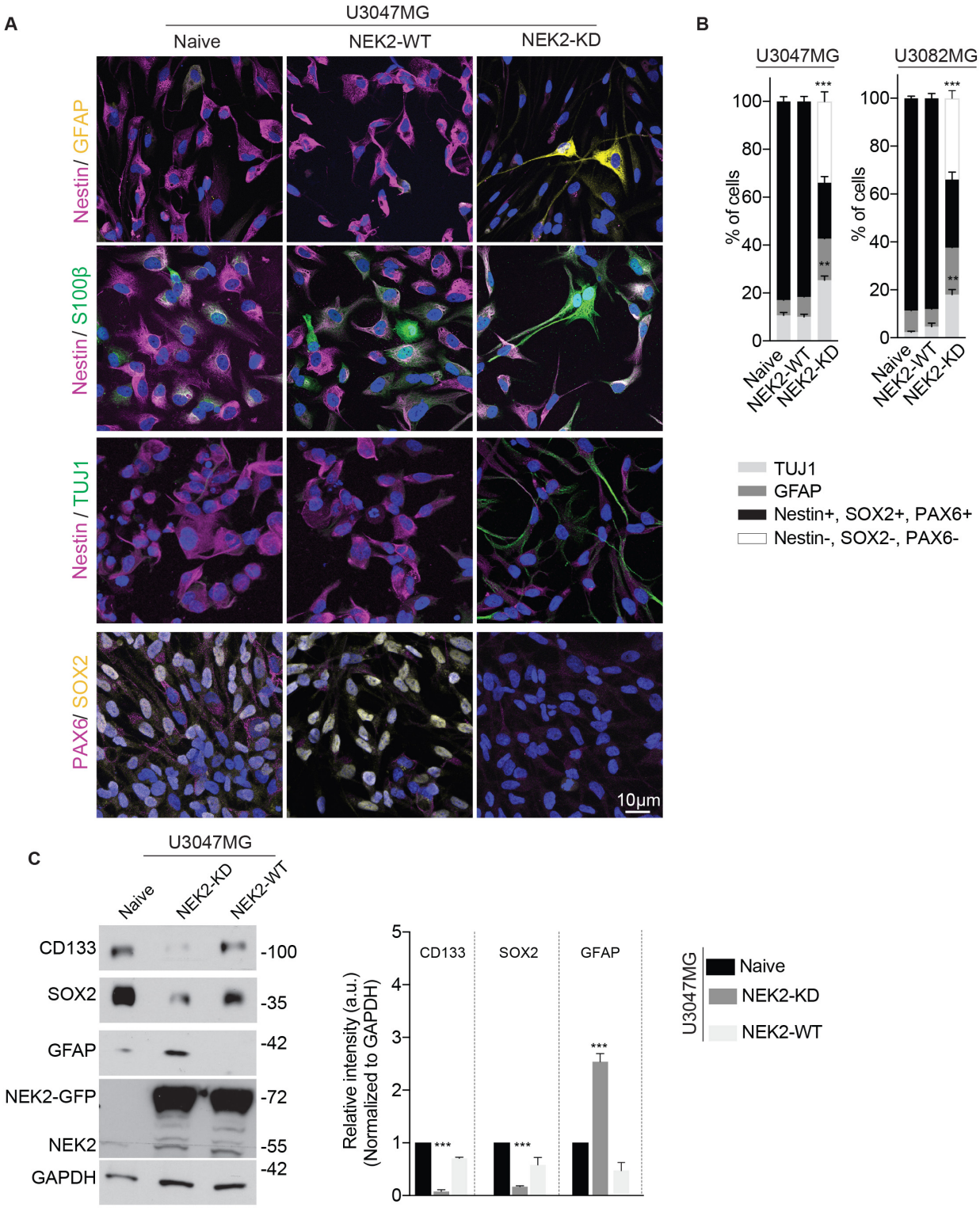


**Figure 3.12. Cilia induction trigger GSCs differentiation.**
**A.** Naïve or NEK2-WT expressing GSCs display neural stem cell marker Nestin (magenta), PAX6 (magenta), and SOX2 (yellow) but not differentiation markers of GFAP (yellow), S100β (green), and TUJ-1 (green) (left and middle panel). In contrast, upon cilium induction, GSCs are differentiated as specified by markers of GFAP, S100β, and TUJ1. Note that there is a drastic reduction in neural stem cell markers in NEK2-KD expressing cultures. Scale bar, 10 μm. **B.** Bar diagram at right quantifies fractions of GSCs (in percentages) positive for stemness (Nestin, SOX2, and PAX6) and differentiation (GFAP and TUJ1) markers. At least 200 cells were analyzed in each cell lines from (n=3) independent experiments. Ordinary two-way ANOVA followed by Tukey's multiple comparisons test ***P <0.0001, **P <0.001. Error bars

show +/- SEM. **C.** Western blot compares relative levels of stemness (CD133 and SOX2) and differentiation marker (GFAP) before and after cilium induction. GAPDH was used as a loading control. Bar diagram at right quantifies relative intensities of respective markers before and after cilium induction. Western blots from three (n=3) independent experiments. Ordinary two-way ANOVA followed by Tukey's multiple comparisons test, ***P<0.0001. Error bars show +/- SEM.

Additionally, we confirmed the results from the immunofluorescence and Western blot analysis of selected markers in GSC before and after cilia induction. The data show that upon DOX induction of NEK2-KD, the U3047MG NEK2-KD exhibits a significant reduction of the surface stem cell marker CD133 and nuclear stem cell marker SOX2. Most importantly, the cell displayed and an increased level of GFAP (astrocyte marker) **(Figure 3.12C)**. Collectively, data demonstrate that cilium controls the molecular switch between self-renew and differentiation state in GSCs.

## 3.7 GSCs differentiation is a cilium-dependent process

To further demonstrate that Nek2-KD induced GSCs differentiation is a cilium dependent process, we ablated cilia by depleting IFT88. Overexpression of IFT88 prevents $G_1$-S transition, whereas depletion of IFT88 causes cilium loss and promotes cell cycle progression (Robert et al., 2007, Loskutov et al., 2018). Thus, we used siRNA to deplete IFT88 and as a control scramble siRNA, which did not affect the IFT88 expression (control siRNA). First, we transfected U3047MG naïve and U3047MG NEK2-KD cells with the siRNA or control siRNA. 48hrs later, DOX was added to overexpress the NEK2-KD. Following an additional 48hrs (in total 96hrs), we analyzed IFT88 ciliary marker and co-stained with a marker for basal bodies and connecting cilia GT335 (Giessl et al., 2004) using immunofluorescence analysis. As expected, reduced levels of IFT88 and no colocalization of IFT88 with GT335 at the primary cilia were explicitly observed in siRNA-treated, but not in control siRNA-treated cells **(Figure 3.13).** Due to IFT88 depletion, the cells are unable to assemble cilia.

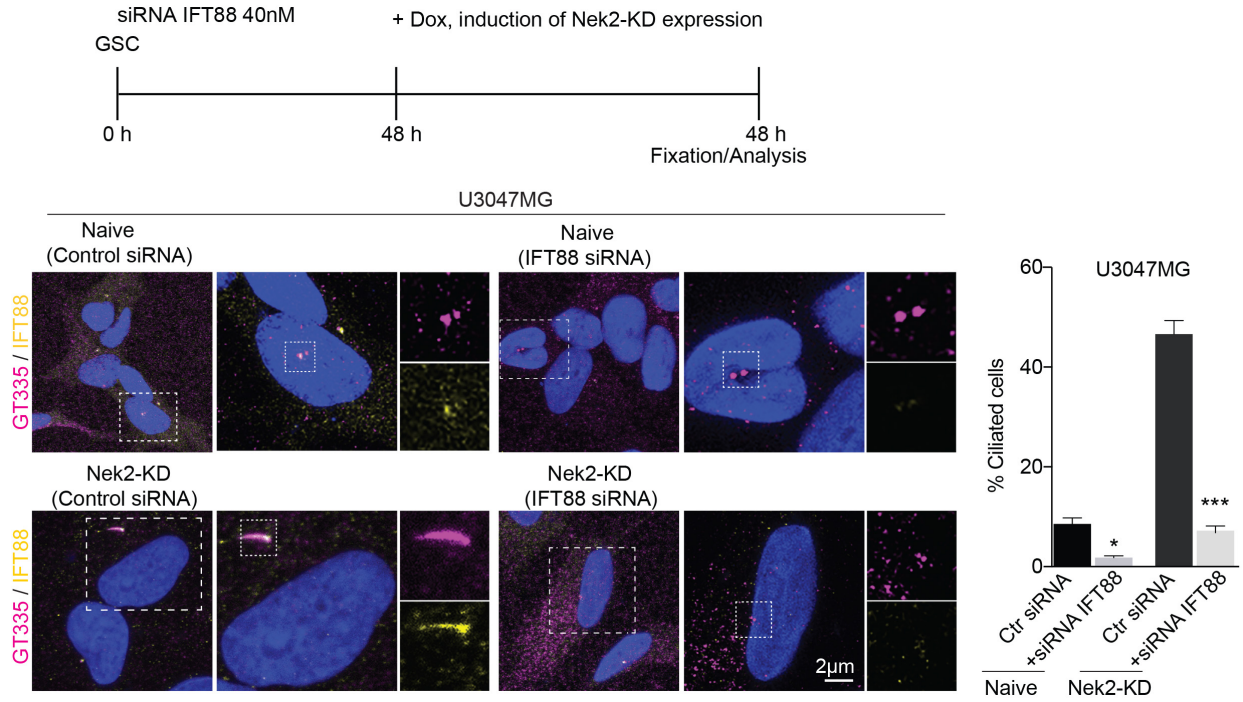


**Figure 3.13. Depletion of IFT88 prevents cilium assembly in GSC cell line.**
Experimental plan. NEK2-KD expression does not induce cilia in GSCs depleted of IFT88. Note NEK2-KD could induce cilia only in control siRNA-treated naïve GSCs cultures in which IFT88 immunoreactivity (yellow) is intact (left panel, both overview and magnified insets are shown). Cilia are labeled with glutamylated tubulin (magenta). In contrast, NEK2-KD does not induce cilia in IFT88 depleted cultures (right panel, both overview and magnified insets are shown). Note that IFT88 expression is lost. Scale bar 2 µm. Bar diagram at right quantifies frequencies of ciliated cells under various conditions tested. At least 300 cells were analyzed from (n=3) experiments. Ordinary one-way ANOVA followed by Tukey's multiple comparisons test. ***P <0.001. Error bars show +/- SEM.

We then tested whether NEK2-KD could still induce differentiation of U3047MG cultures unable to assemble cilia due to IFT88 siRNA treatment. Consequently, immunofluorescence analyzes of neural stem cell marker NESTIN and differentiation markers TUJ (neuron) and GFAP (astrocyte) were performed in GSCs after IFT88 depletion and NEK2-KD overexpression. Interestingly, NEK2-KD expression induced differentiation of GSCs into -GFAP and -TUJ1-positive cells in control siRNA-treated cultures but not in IFT88 siRNA-treated cultures **(Figure 3.14 and the table summarize the findings).** This data indicates that NEK2-KD induced differentiation process is cilia specific.

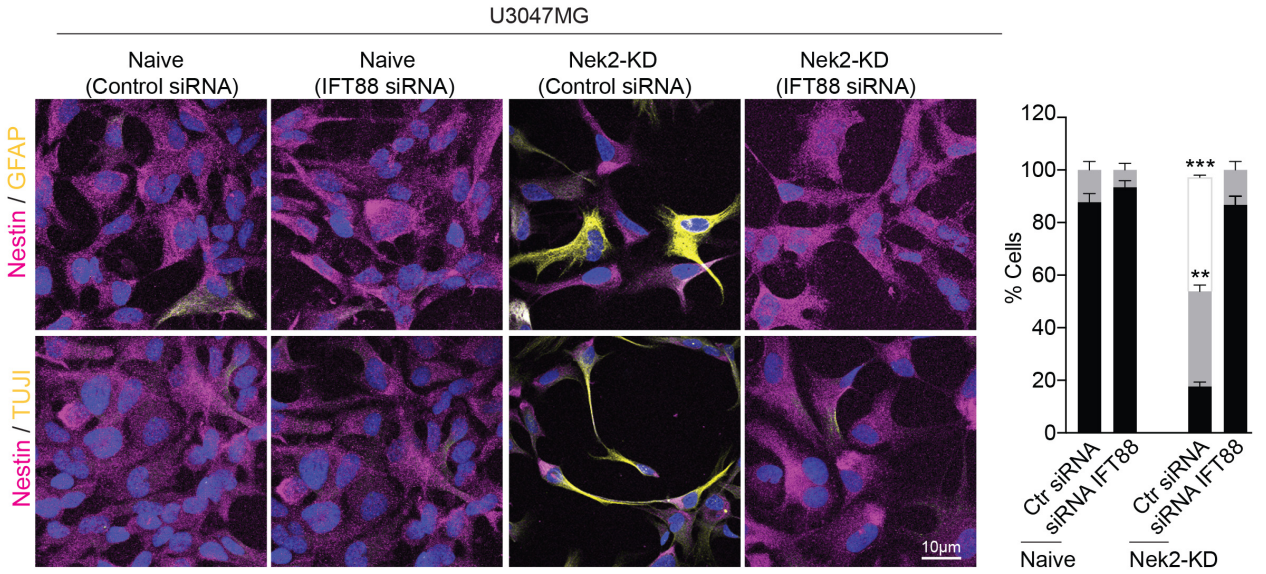


| U3047MG | Treatment | Cilia status | Differentiation (GFAP+ive, TUJ1+ive) |
|---|---|---|---|
| Naive | Control siRNA | Supressed | No |
| Naive | IFT88 siRNA | Supressed | No |
| Nek2-KD | Control siRNA | Induction | Yes |
| Nek2-KD | IFT88 siRNA | Supressed | No |

**Figure 3.14. NEK2-KD induced GSCs differentiation is cilium-dependent process.**
NEK2-KD expression triggers differentiation (GFAP and TUJ1-positive cells) only in control siRNA treated cells where NEK2-KD could induce cilia (refer to the previous experiment). Thus, NEK2-KD-mediated GSCs differentiation is cilium dependent. Note IFT88 depletion or control siRNA alone does not trigger GSCs differentiation (second and first panel from left). Except NEK2-KD expressing control siRNA-treated cultures, the rest of the cultures exhibit neural stem cell marker Nestin. Scale bar 10 µm. At least 100 cells were analyzed from (n=3) experiments. Ordinary two-way ANOVA followed by Tukey's multiple comparisons test. ***P <0.0001. Error bars show +/- SEM. The table below summarizes the experimental results.

## 3.8 PDGFR-α signaling is regulated through primary cilia

To dissect the mechanistic link between cilium induction and GSCs differentiation, the status of PDGFR-α signaling in U3047MG cells was analyzed. Proneural subtypes of GBMs have a strong correlation between PDGFR-α overexpression, amplification, and mutation (Verhaak et al., 2010). Furthermore, an increased level of PDGFR-α signaling positively correlates to the self-renewal property of GSCs, accelerated tumor onset, and increased tumor invasion (Clarke and Dirks, 2003). It has also been reported that cilia regulate PDGFR-α signaling in healthy cells (Schneider et al., 2005). Initially, the total protein levels were determined using western blot between different GSCs subtype. The data confirmed that PDGFR-α is overexpressed in proneural compare to mesenchymal and classical GSCs **(Figure 3.15A)**. Furthermore, to demonstrate that NEK2-KD-mediated cilium induction was prominent only in proneural subtype GSCs that overexpressed PDGFR-α, levels of proteins associated with PDGFR-α signaling pathway in ciliated and unciliated cells were analyzed. Western blot analysis revealed that in contrast to unciliated U3047MG (naïve and NEK-WT) cells, the ciliated cells (U3047MG NEK2-KD) display a drastically reduced level of PDGFR-α, which in turn

correlated to reduced levels of its downstream PDGFR-α signaling (e.g., AKT and c-MYC) **(Figure 3.15B).** This finding suggests that the newly induced cilia in U3047MG NEK2-KD cells can play a role in sequestering excessive PDGFR-α signaling.

Since the protein levels of PDGFR-α after cilium induction were drastically reduced, the localization of PDGFR-α after the cilium induction was examined. The immunofluorescent analysis was performed using PDGFR-α antibody and ARL13B (ciliary marker) in GSCs before (U3047MG naïve) and after cilium induction (U3047MG NEK2-KD). A confocal microscopy and super-resolution microscopy stimulated emission depletion (STED) revealed the localization of PDGFR-α, mainly in the newly induced cilium **(Figure 3.15 C-D)**. Importantly, naïve U3047MG cells that have suppressed ciliogenesis exhibited unspecific localization of PDGFR-α within the space of the nearly entire cell space suggesting that cilium induction switches PDGFR-α to be relocated to a newly induced cilium **(Figure 3.15 C)**.

Based on these findings, we reasoned that the upregulated PDGFR-α in GSCs is constitutively active in a ligand-independent manner, enabling them to continuously self-renew. To test this aspect, the dynamic localization of PDGFR-α at various time points upon its activation by its ligand PDGF-AA was imaged **(Figure 3.16)**. In control experiments that used healthy NPCs, we detected PDGFR-α signal in cilia 20 min after the ligand addition **(Figure 3.16A)**. In contrast, unciliated U3047MG cells always displayed excessive PDGFR-α localization in a ligand-independent manner **(Figure 3.16B)**. Strikingly, after cilium induction, U3047MG NEK2-KD cells displayed PDGFR-α dynamics similar to healthy NPCs, in which PDGFR-α is directed to a newly induced cilium **(Figure 3.16C).** In summary, these results elucidate the dominant effect of cilium induction in triggering differentiation of GSCs via resetting functional PDGFR-α signaling pathway.

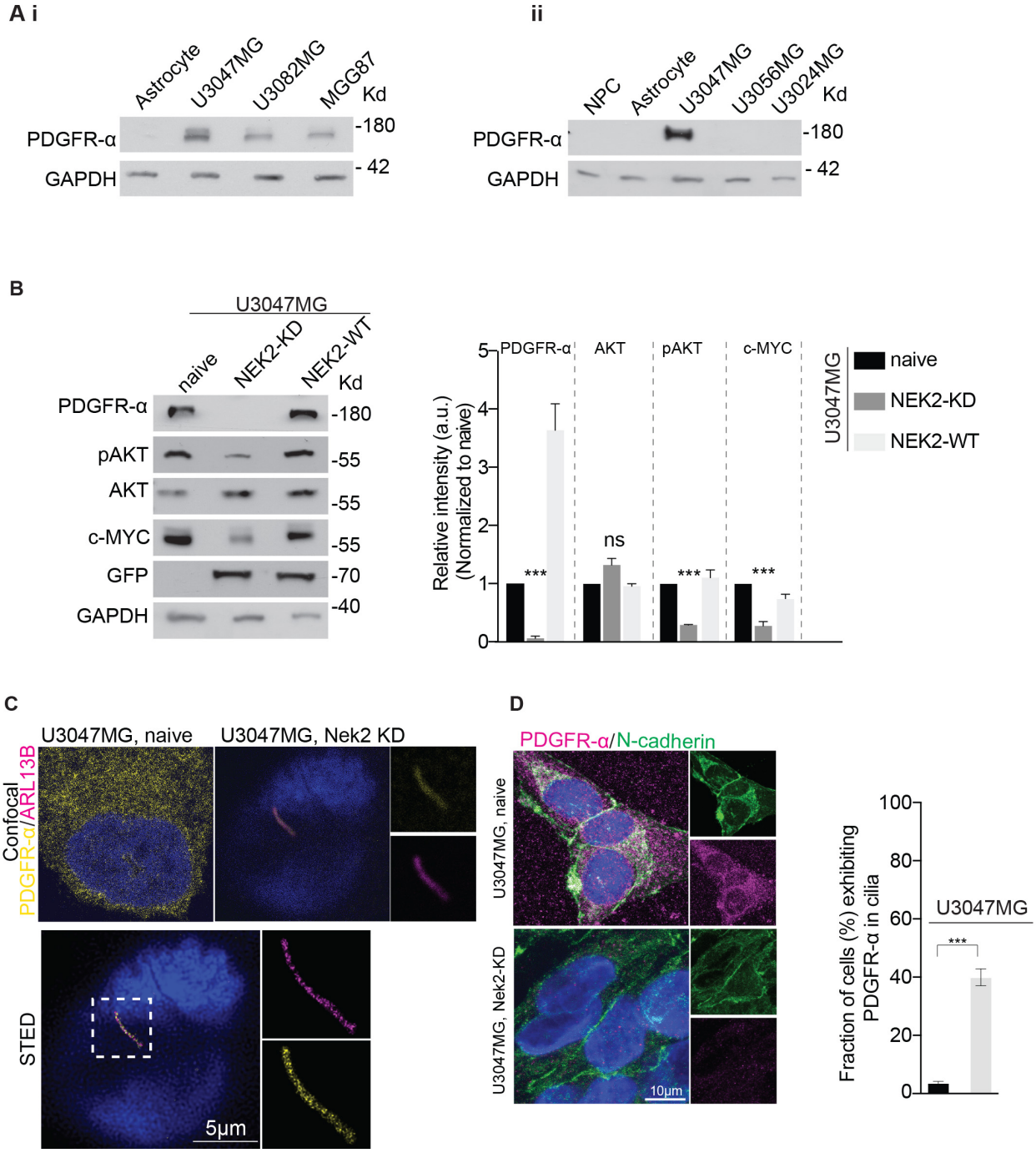


**Figure 3.15. Cilium induction relocates PDGFR-α to newly induced cilia.**
**A.** Proneural subtype GSCs (U3047MG, U3082MG, and MGG87) express higher levels of total PDGFR-α than ciliated astrocytes (i) or mesenchymal (U3024MG) and classical subtype (U3056MG) GSCs (ii). Equivalent quantities of cell extracts were loaded. **B.** Western blot compares relative levels total PDGFR-α and its downstream signaling effectors in GSCs before and after cilium induction. Note PDGFR-α level is drastically reduced after cilium induction (NEK2-KD expressing GSCs). Similarly, active AKT and c-MYC levels are also reduced. GAPDH was used as a loading control. Bar diagram at right quantifies relative levels of PDGFR-α and its downstream signaling effectors before and after cilium induction. Western blots from three (n=3) independent experiments. Ordinary two-way ANOVA, followed by Sidak's multiple comparisons test, ***P<0.001. Error bars show +/- SEM. **C-D.** Newly induced cilium sequesters PDGFR-α. Non-ciliated naïve U3047MG displays an all over distribution of PDGFR-α (yellow, left panel). Upon cilium induction, excessive PDGFR-α is directed to the newly induced cilium. Scale bar 5 μm. In panel (F), N-Cadherin marks plasma membrane (green) and PDGFR-α is in magenta. Scale bar 10 μm. Bar diagram at right quantifies frequencies of cells (in percentage) exhibiting PDGFR-α in the newly induced cilium. At least 200 cells were analyzed from (n=4) independent experiments. Unpaired t-test, ***P<0.001. Error bars show +/- SEM.

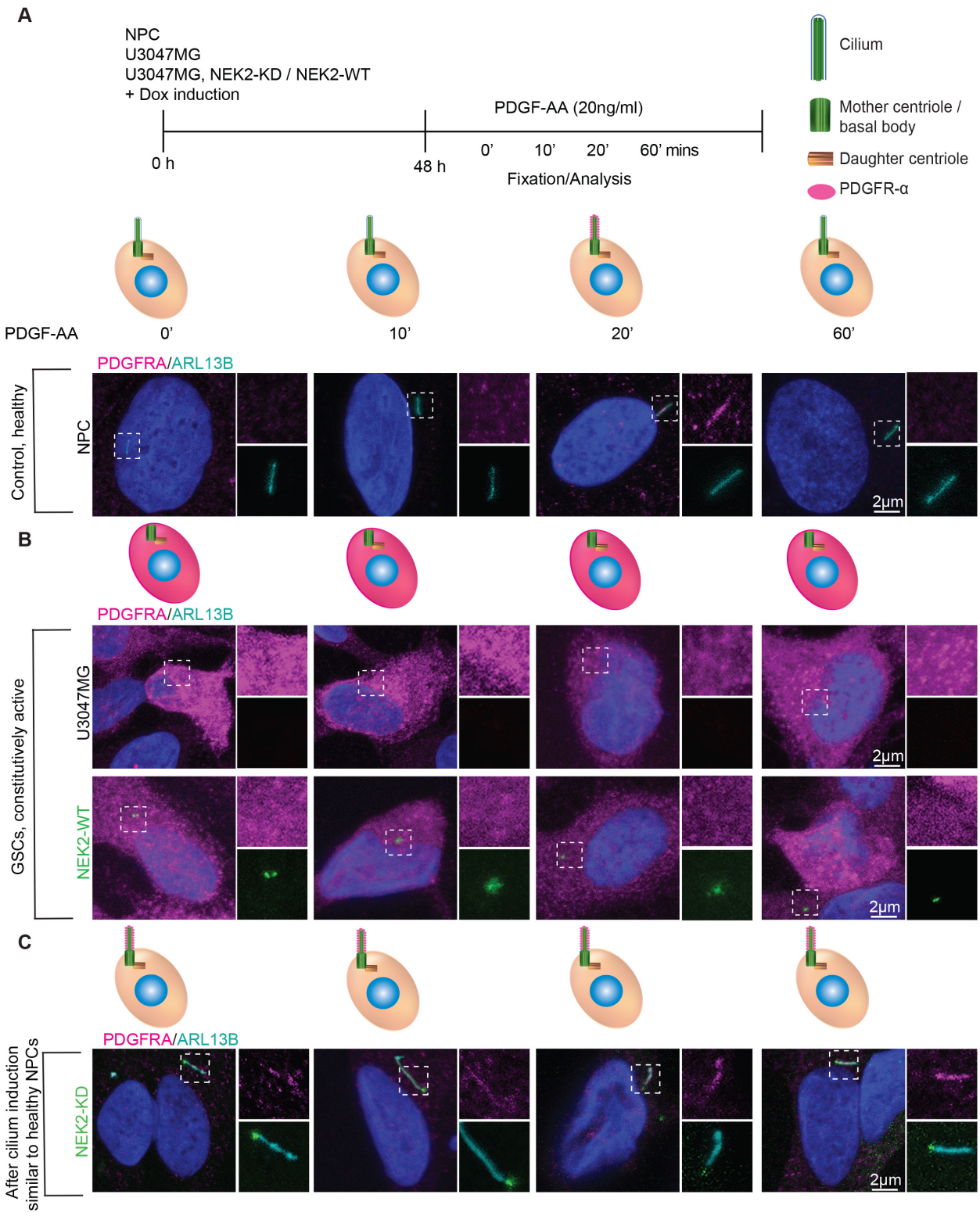


**Figure 3.16. PDGFR-α in proneural GSCs is constitutively active.**
**A.** Experimental plan. Top panel. In healthy NPCs, PDGFR-α is activated within 20 mins of PDGF-AA addition. Note that activated receptor localizes at the primary cilium. ARL13B labels cilia (cyan) and PDGFR-α is stained using specific antibodies (magenta). The cartoon is given to simplify the visualization of PDGFR-α dynamics. Scale bar 2 μm. At least 200 cells were analyzed from (n=3) experiments. **B.** Middle panel. Naïve or NEK2-WT (Green) expressing U3047MG cells exhibit strong PDGFR-α immunoreactivity (magenta) regardless of PDGF-AA addition, indicating that PDGFR-α in these cell types is constitutively active in a ligand-independent manner. NEK2-WT (green) labels centrosomes. The cartoon shows PDGFR-α distribution. Scale bar 2 μm. At least 100 cells were analyzed from (n=3) experiments. **C.** Bottom panel. NEK2-KD (green) expressing ciliated U3047MG cells behaves just like healthy NPCs and exhibits similar PDGFR-α dynamics upon ligand addition. A visibly apparent level of

PDGFR-α is directed to newly induced cilium at 60 mins of PDGF-AA addition. ARL13B labels cilia (cyan) and PDGFR-α is stained using specific antibodies (magenta). NEK2-WT (green) labels basal bodies. Cartoon simplifies the visualization of PDGFR-α dynamics. Scale bar 2 μm. At least 200 cells were analyzed from (n=3) experiments.

## 3.9 Global transcriptome analysis reveals differentiation toward neuronal lineage

To uncover the global impact of cilia induction in GSCs, the transcriptome of U3047MG cells before and after cilium induction was analyzed. More than 3000 differentially regulated genes were identified, among which 1651 were up and 1751 downregulated **(Figure. 3.17A).** Next, the differentially expressed genes were functionally annotated based on biological significance. Most of the differentially expressed genes were associated with biological processes involved in cell division, cell cycle, spindle organization, and brain development **(Figure 3.17B-C).** The upregulated included genes involved in ciliogenesis (e.g., *ARL13B, IFT88, IFT22, IFT57*), and neural differentiation (e.g., *TUBB3, GFAP*) (neuron). In contrast, the genes upregulated in the U3047MG NEK2-KD cells included genes involved in cilia disassembly (*KIF24, OFD1, NDE1, CENPJ; STIL, CCP110)* and cell cycle renewal (e.g., *MKI67, OLIG2, SOX10, PROM1*) **(Figure 3.17 D-E)**. The results further confirm that ciliated (U3047MG NEK2-KD) cells have a strong association with the pathways essential for neural differentiation. Overall, the results strongly suggest that NEK2-KD expressing in U3047MG cells induce ciliogenesis, whereas ciliated cells lose stemness and gain differentiation markers.

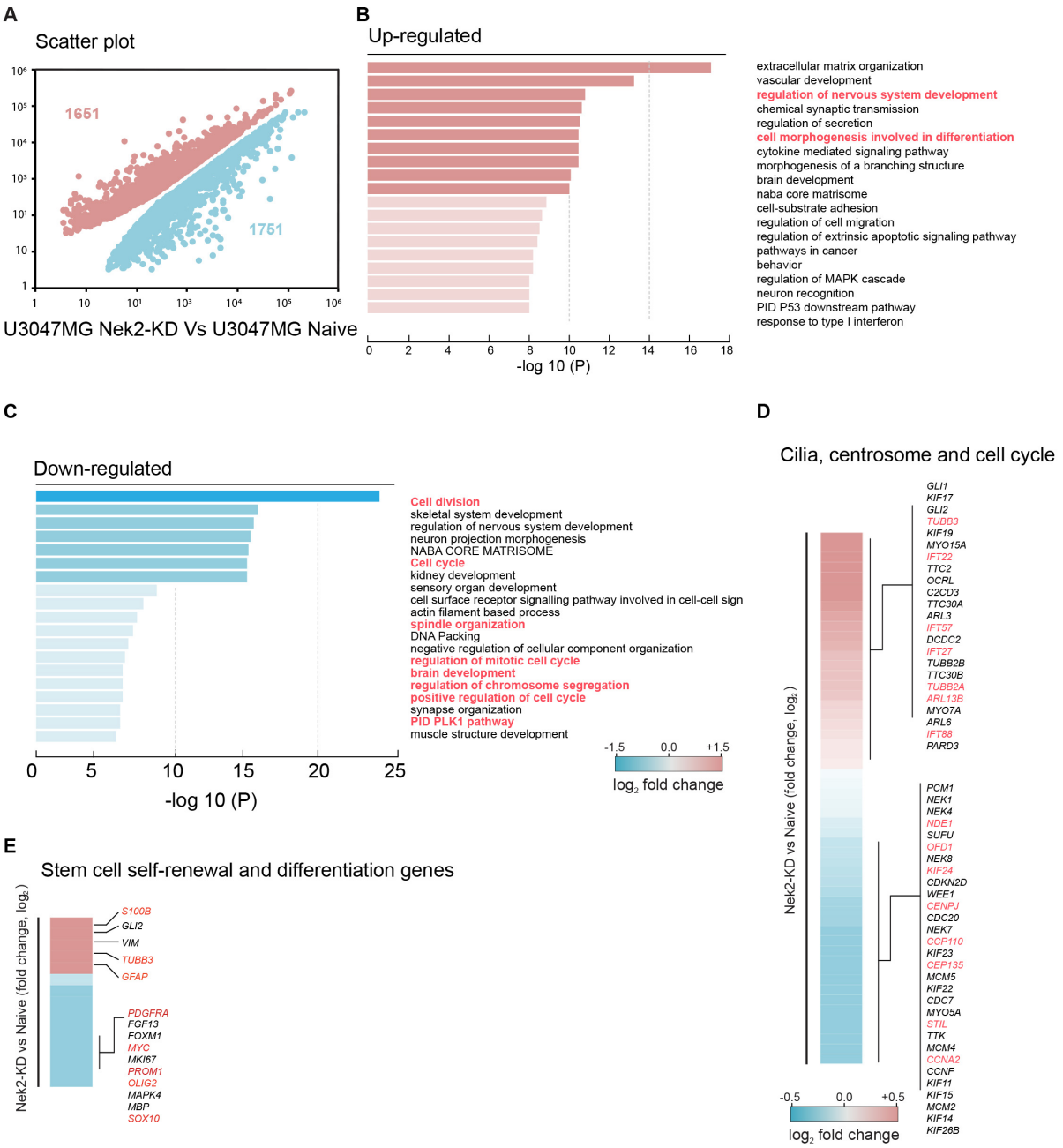


**Figure 3.17. NEK2-KD induces GSC expression profiles indicative of cilium-dependent cell differentiation.**

**A.** Scatter plot of changing gene expression levels (FPKM; >0.6 log2-fold change, FDR<0.01) in U3047MG naïve compared to ciliated GSCs U3047MG NEK2-KD cells. **B.** The top most enriched GO terms associated with the 1651 upregulated genes in NEK2-KD expressing U3047MG cells. Critical pathways related to cell cycle progression and differentiations are marked in red fonts. **C.** As in panel B, but for the 1751 downregulated genes in U3047MG NEK2-KD cells. Critical pathways related to cell cycle progression and differentiations are marked in red fonts. **D.** Log2-fold gene expression changes of genes associated with cilia, centrosome, and cell cycle regulation according to GSEA classification. **E.** As in panel **D**, but for genes associated with stem cell, self-renewal and cell differentiation. Selected genes related to stem cell and differentiation are marked in red fonts. Fold-change ±0.6 log2 adjusted P-value of <0.05. RNA sequencing analysis was performed and analyzed in Dr. Akis Papantonis lab.

## 3.10 Infiltration assay in 3D brain organoids

The current state-of-art to study GBM invasion behavior is based on injecting human GSCs into the mouse brain. However, this xenotransplantation approach does not fully recapitulate the GBM pathogenesis occurring in the human brain and limits the translation of basic GBM research to clinical application (Gopalakrishnan, 2019, Goranci-Buzhala et al., 2017, Linkous et al., 2019). The development of a suitable in vitro human model based on 3D brain organoids would provide a powerful model to study the invasive behavior of GSCs. Human brain organoids are powerful in vitro systems recapitulating many aspects of human brain development and functions, emerging as a 3D substrate to model GBM (Linkous et al., 2019, Ogawa et al., 2018), adapting our recently described protocol (Gabriel and Gopalakrishnan, 2017, Gabriel et al., 2016) and differentiated brain organoids from at least three independent hiPSCs lines (see methods section 5.6.3). Organoids exhibited typical cytoarchitectures such as ventricular zones and cortical plates, as shown before (Gabriel and Gopalakrishnan, 2017, Gabriel et al., 2016). Here, we demonstrated three different methods to assay GSCs invasion behavior in brain organoids; namely, **i)** Simultaneous co-culturing of GSCs during organoid differentiation **ii)** Supplementing GSCs as dispersed cells to organoids **iii)** Fusion of GSCs spheres to organoids.

### 3.10.1 Assay 1: co-culture iPSCs and GSCs

Taking advantage of having the GFP and RFP tagged iPSCs, we generated organoids that are more suitable to follow neurospheres formation and differentiation. First, we generated hybrid brain organoids by co-culturing 5000 GSCs with 35,000 iPSCs expressing a fluorescent reporter **(Figure. 3.18A)**. Co-cultured fluorescently tagged iPSCs were co-cultured together with primary U3047MG cells and with relapsed 275-BIS cells. Time-lapse imaging of these organoids at day-10, -20, and -30 revealed that in contrast to primary GSCs (U3047MG), the relapsed GSCs (275-BIS) progressively increased to grow. However, in later time points (day-20 onwards) when the organoid size increased, and tissue got denser, imaging of the organoids became problematic **(Figure. 3.18B, C)**.

To overcome this limitation and to quantitatively visualize the invasiveness of GSCs growth in organoids, the samples were fixed with PFA at indicated time points, and the EtOH-ECI-based tissue clearing method was optimized. The method rapidly clarified the organoids within 10-20 min that could further be subjected to microscopy analysis. Importantly, these clarified organoids enabled 3D imaging without disruption of their cytoarchitectures **(Figure. 3.19A, B)**. Quantification analysis demonstrates that the number of invasive protrusion and microtube length fail to grow in the later stages of development **(Figure 3.19 C-E).** The invasive protrusions and microtube networks are the known characteristics of invading GSCs into a host tissue (Osswald et al., 2015b). Strikingly, the invasive behavior of U3047MG with this protocol markedly differed from 275-BIS, which formed

distinct cell clusters exhibiting enhanced invasiveness, whereas, U3047MG grew as dispersed cells and stopped growing after day-10. Using this assay, we could study the early stage of the organoid development since, at later stage did not recapitulate GBM infiltration in the brain and the ability to form interconnected networks via tumor microtubes at day 30 (U3047MG and #275-BIS).

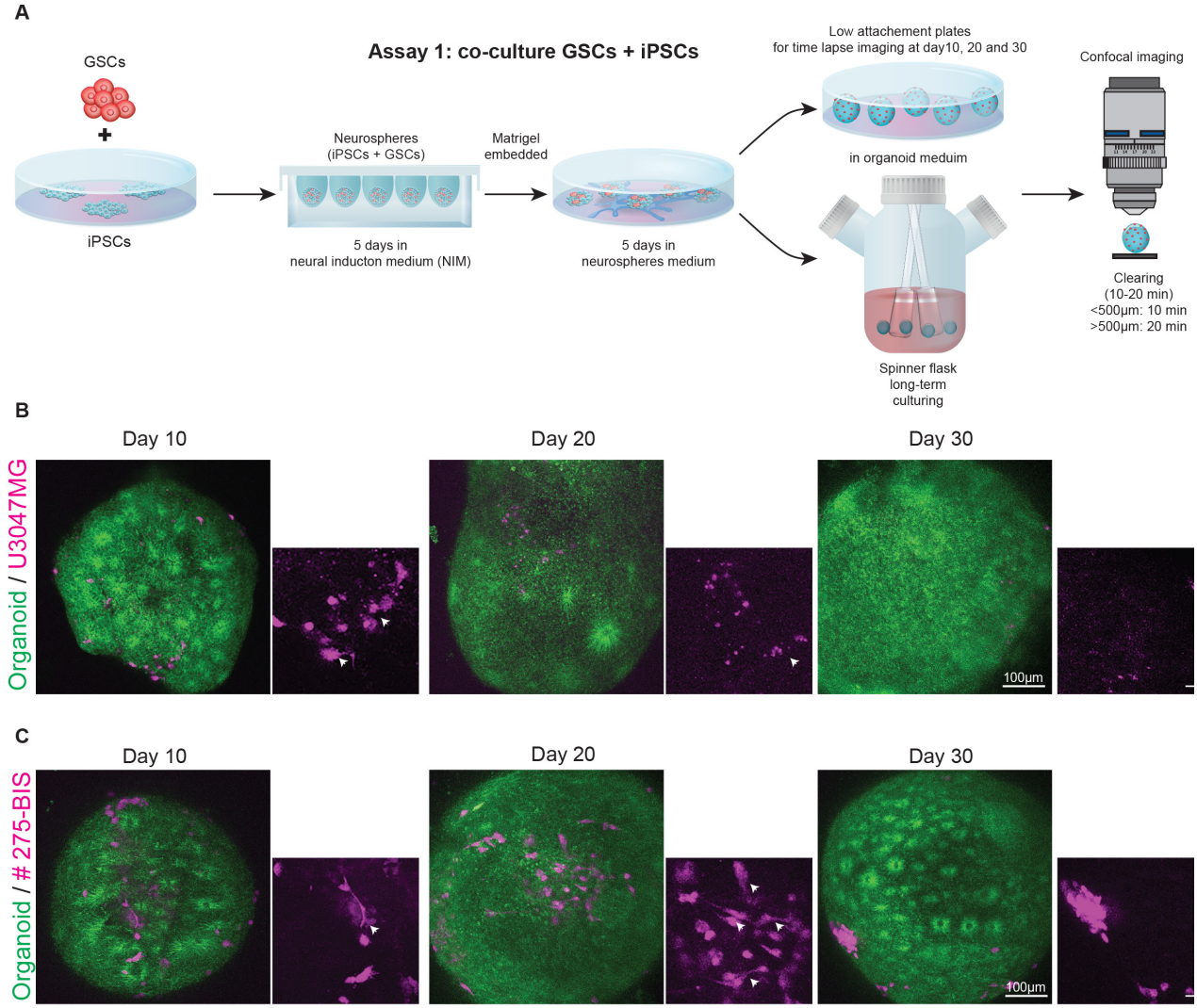


**Figure 3.18. Time-lapse confocal imaging of GSCs invasion in brain organoid using assay 1.** **A.** Schematic of experimental set up displaying step-by-step process from culturing iPSCs/GSCs until the imaging of hybrid organoids. Our optimized clearing condition clarifies tissues within 10 min (organoids smaller than 500 µm) to 20 min (organoids bigger than 500 µm). **B.** Time-lapse imaging of an organoid (green) cultured with U3047MG-mCherry (pseudo color magenta) at day 10, 20 and 30. Note that U3047MG cells grow as dispersed and stop growing after day10. Scale bar 100 µm. Representative image. At least 5 organoids from 3 different batches were tested. See Table 1 summarizing cell lines and organoids. **C.** Time-lapse imaging of an organoid (green) cultured with 275-BIS-GFP (pseudo color magenta) at day-10, -20 and -30. Unlike primary U3047MG, relapse 275-BIS cells grow as clusters and continue to expand with the formation of invasive protrusions (arrows). Note that GSCs are not visible in fully-grown organoids at day-30. Scale bar 100 µm. At least 9 organoids were analyzed from 3 different batches. **D.** Rapid tissue clearing and 3D imaging of organoids (green) cultured with U3047MG-mCherry (red). GSCs grow with the formation of invasive protrusions (arrows) at day-10. Barely visible growth is observed at day-20 and -30. Scale bar 50 µm, insets 5 µm. At least 4 organoids were analyzed from 3 different batches.

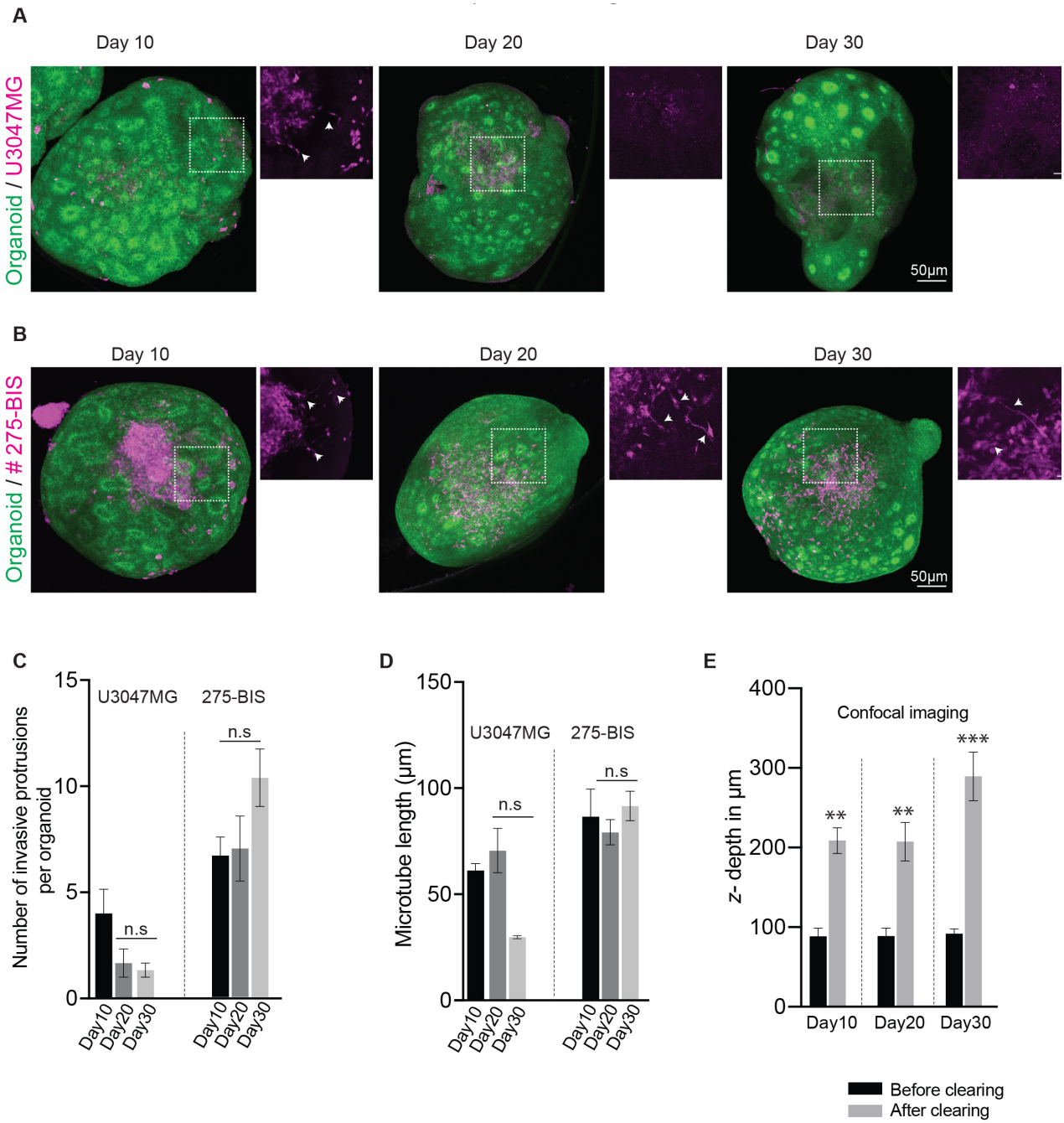


**Figure 3.19. Tissue cleared confocal imaging of GSCs invasion in brain organoid using assay 1.** **A.** Rapid tissue clearing and 3D imaging of organoids (green) cultured with U3047MG-mCherry (pseudo color magenta). GSCs grow with the formation of invasive protrusions (arrows) at day-10. Barely visible growth is observed at day-20 and -30. Scale bar 50 µm, insets 5 µm. At least 4 organoids were analyzed from 3 different batches. **B.** Tissue clearing and 3D imaging of organoids (green) cultured with 275-BIS-GFP (pseudo color magenta). GSCs progressively grow over time (from day-10 until day-30) with the formation of invasive protrusions and microtube networks (arrows). Scale bar 50 µm, insets 5 µm. At least 6 organoids were analyzed from 2 different batches. **C-E**. Bar graphs quantify of parameters of invasiveness such as the number of invasive protrusions and microtube lengths in tested GSCs lines. At least 80 microtubes were measured for each condition. Note that relapse 275-BIS cells display an overall increase in invasiveness. P values were obtained ed using two-way ANOVA, followed by Tukey's multiple comparisons test. n=3 batches, N=20 organoids per GSCs line n.s, not significant. Error bars show +/- SEM. **H.** Tissue clearing enhances the imaging depth of organoids. Note that relapse 275-BIS cells display progressive growth over time. n=3 batches, N=20 organoids were analyzed. P values were obtained using two-way ANOVA, followed by Sidak's multiple comparisons test. **p <0.001, ***p <0.0001. Error bars show +/- SEM. (This work was performed in collaboration with Dr. Arul Mariappan)

### 3.10.2 Assay 2: supplying GSCs to organoids

Since the first method could not recapitulate GBM infiltration at the later stages of brain organoid development, another invasion assay was developed aiming to study the attraction of GSCs toward organoids at the onset of the invasion. In this second assay condition, 5000 GSCs were applied at the vicinity of 10-day old organoids and imaged them at 1-day post-co-culture (dpc), 10 dpc, and 20 dpc after supplementing GSCs **(Figure 3.20A)**. Live and clarified tissue imaging revealed that within 24 hrs, both of the tested GSCs lines were attracted toward the periphery of organoids as a crescent-like structure that surrounded the organoid **(Figure 3.20B-C)**. At later time points, invading GSCs establish protrusion-like processes by which they extend their invasive fronts in the form of microtubes. These microtube-like structures target inner regions of the organoids **(Figure 3.21A, B)**.

This assay could distinguish the invasive behaviors of primary GSCs U3047MG and relapsed GSCs 275-BIS. The 275-BIS relapse line assembled into clusters of GSCs, which collectively invaded into organoids forming a tumor-like behavior. To analyze the infiltration of GSCs into brain organoid, the number of invasive protrusion and microtube length was quantified **(Figure 3.21A-B)**. These clusters release single cells, which form characteristic invasive protrusions and microtube networks, which grew up 150 μm in length establishing networks within GSCs **(Figure 3.21C-D)**. Importantly after the organoid clearing, the z-depth was increased and improved imaging of GSCs infiltration into brain organoid **(Figure 3.21E).** Collectively, establishing this assay offers an investigation of GBM biology in a host tissue equivalent to the early brain development stage.

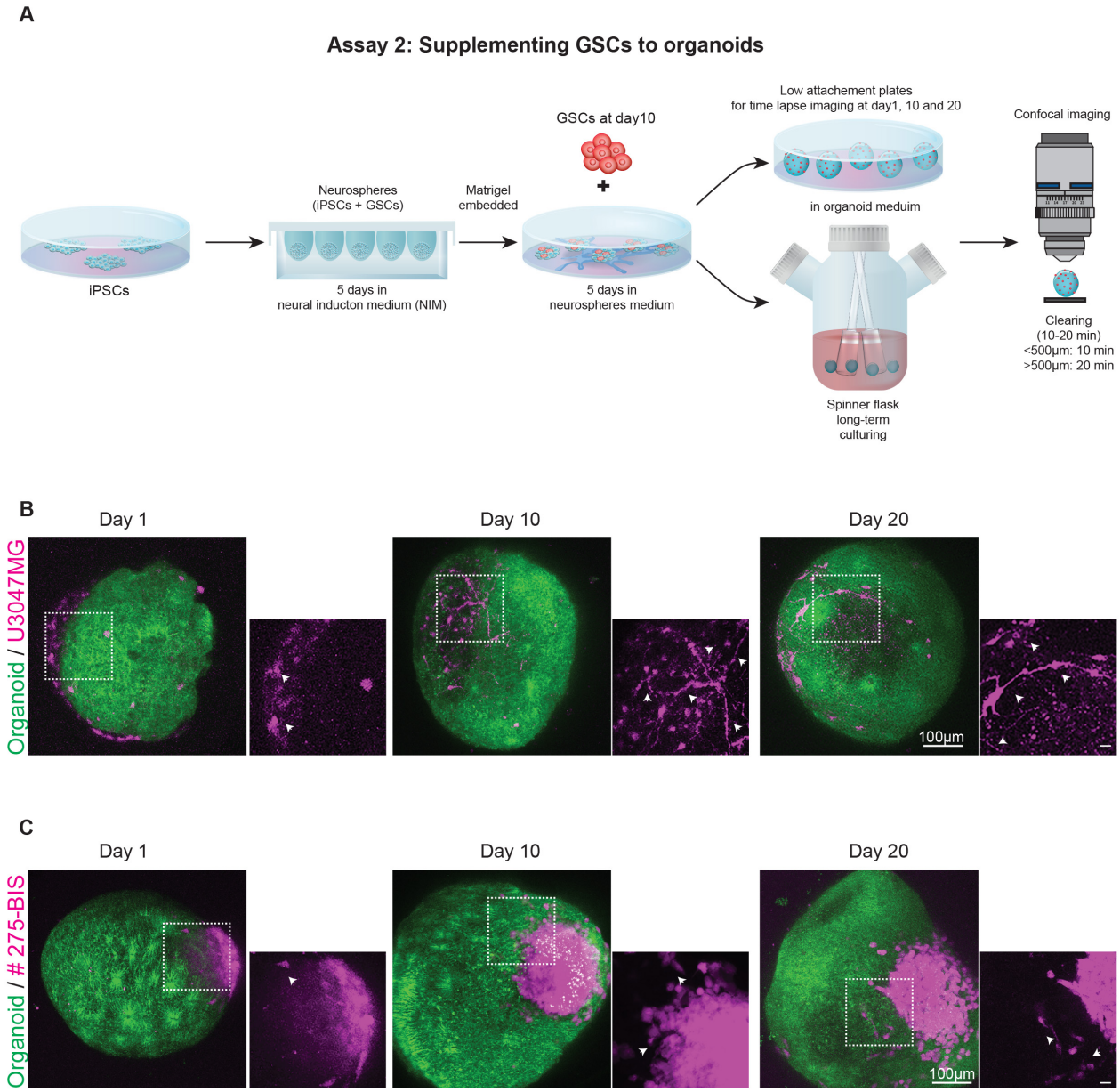


**Figure 3.20. Time-lapse confocal imaging of GSCs invasion in brain organoid using assay 2.** **A.** Schematic of experimental set up displaying step-by-step process from culturing iPSCs until the imaging of organoids with invading GSCs. **B.** Time-lapse imaging of an organoid (green) supplemented with U3047MG-mCherry (pseudo color magenta). Note that primary U3047MG cells attracted toward organoids forming a crescent-like organization within 24 hrs. In later time points of day-10 and -20, GSCs progressively invaded into the organoid forming invasive protrusions and microtube networks (arrows). Scale bar 100 µm. Representative image. At least 10 organoids were analyzed from 3 different batches. **C.** Time-lapse imaging of an organoid (pseudo color green) cultured with relapse 275-BIS-GFP cells (pseudo color magenta). Unlike U3047MG, 275-BIS cells distinctly grew as clusters and continued to expand within the organoids forming a tumor-like entity. Scale bar 100 µm. Representative image. At least 10 organoids were analyzed from 3 different batches.

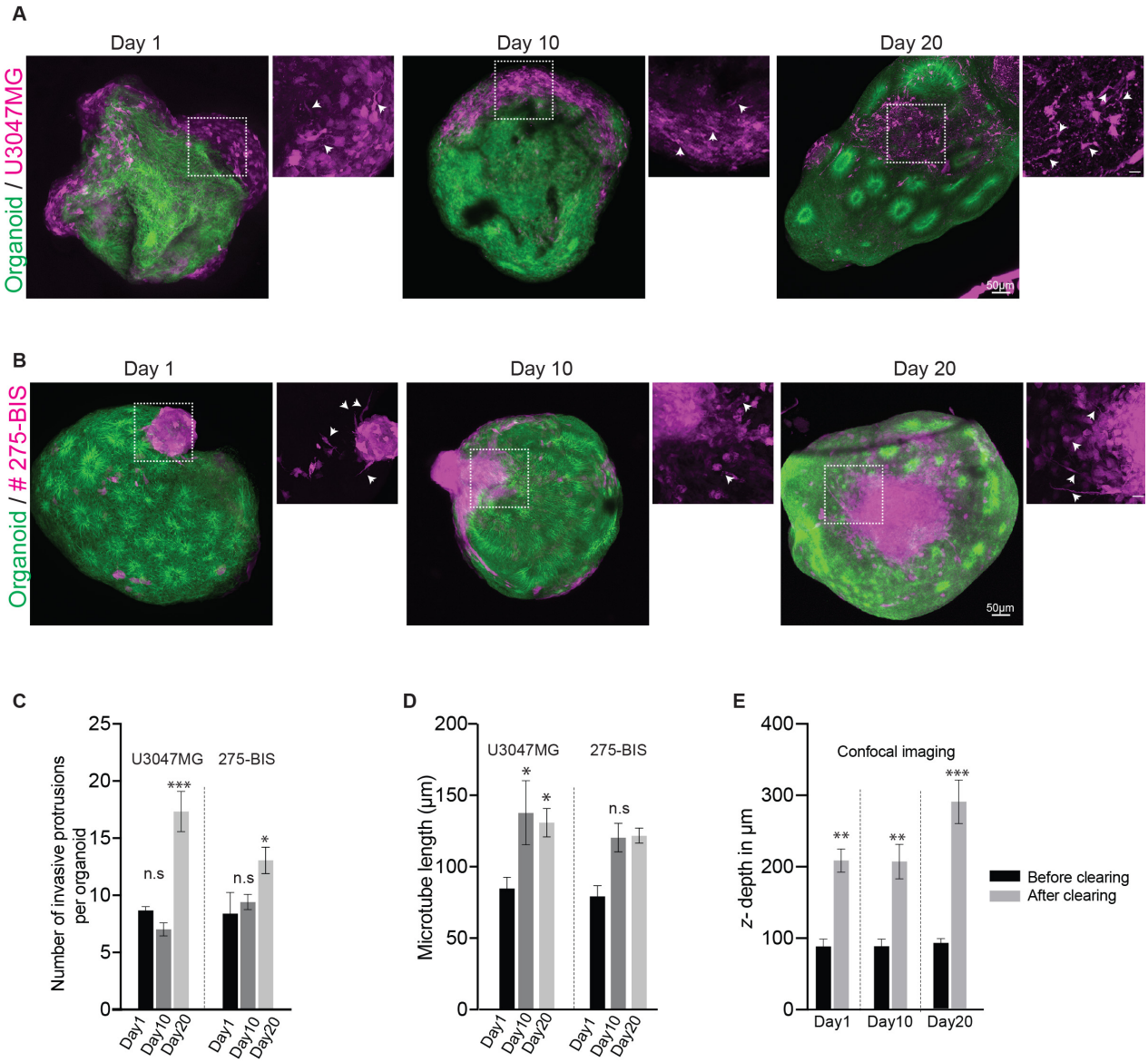


**Figure 3.21. Tissue cleared confocal imaging of GSCs invasion in brain organoid using assay 2.** **A.** Tissue clearing enhances the visualization of U3047MG-mCherry (pseudo color magenta) growth in organoids (green). GSCs grew with the formation of invasive protrusions (arrows) within 24 hrs. Note a crescent-like organization at the periphery of organoids, which then spreads into organoids as invasive protrusions and microtube networks (arrows) at later time points. Scale bar 50 µm, insets 5 µm. Representative image. At least 5 organoids were analyzed from 3 different batches. **B.** Tissue clearing and subsequent imaging of relapse 275-BIS-GFP cells (pseudo color magenta) within the organoids-RFP (pseudo color green). Note that relapse 275-BIS cells assemble into large clusters and then invade into the organoids forming a tumor-like entity. These clusters release single cells, which form characteristic invasive protrusions and microtube networks (arrows). Scale bar 50 µm, insets 5 µm. Representative image. At least 6 organoids were analyzed from 3 different batches. **C and D.** Bar graphs quantify the parameters of invasiveness. Note that 275-BIS distinctly differs from U3047MG displaying enhanced invasiveness. At least 50 microtubes were measured for each condition. n=3 batches, N=22 organoids per GSCs line were analyzed. P values were obtained using two-way ANOVA, followed by Tukey's multiple comparisons test. n.s, not significant. *p <0.01, ***p <0.0001. Error bars show +/- SEM. **H.** Tissue clearing enhances the imaging depth of organoids as imaged by a confocal microscope. Note the volume occupied by 275-BIS progressively increases over time. Data represent mean +/- SEM. n=3 batches, N=22 organoids. P values were obtained using two-way ANOVA, followed by Sidak's multiple comparisons test. **p <0.001, ***p <0.000. (This work was performed in collaboration with Dr. Arul Mariappan)

Both of the above methods offer an investigation of GBM biology in a host tissue that is equivalent to the early stage of brain development. However, GBM is primarily a disease of the elderly population. Therefore, we studied whether GSCs show tropism for mature brain organoids. As a first step, we ensured that these organoids contain cell types that express mature neuronal markers such as pre-synaptic protein Synapsin1 and MAP2 in a region-specific manner **Figure (3.22)**.

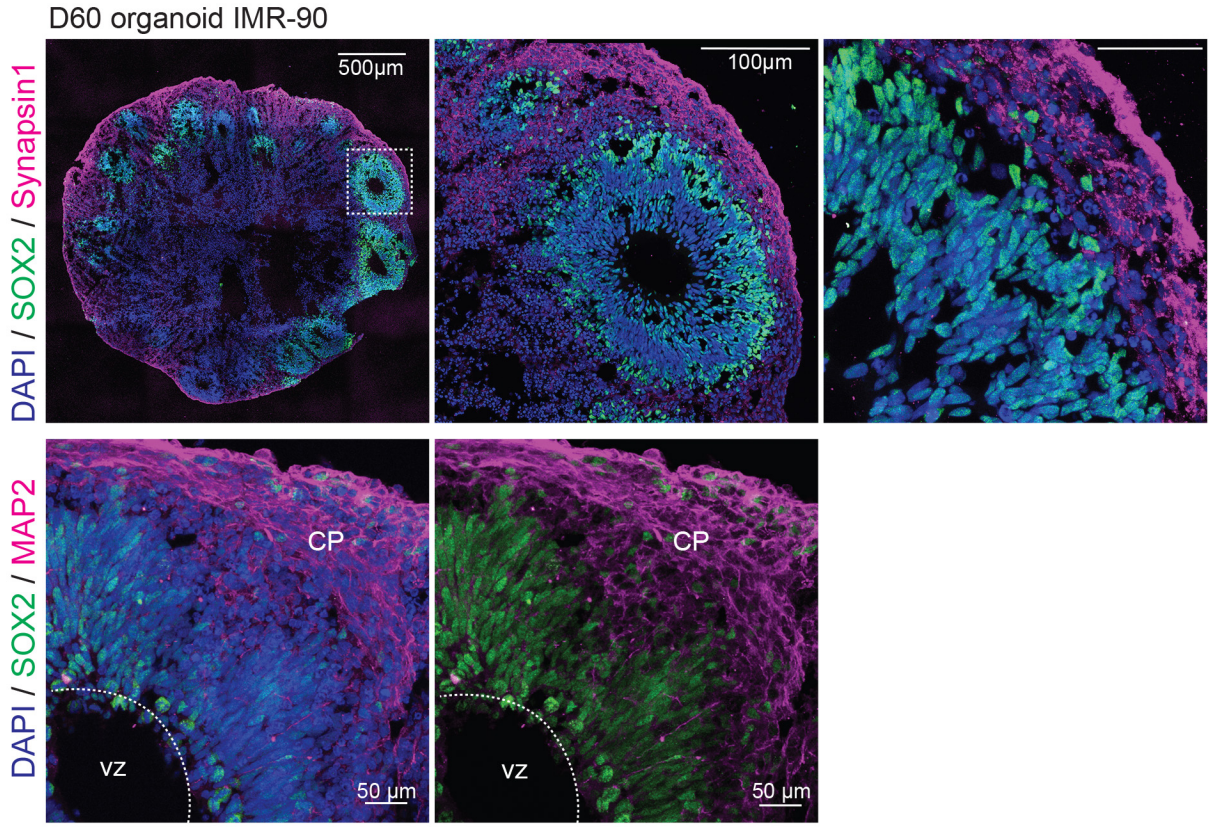


**Figure 3.22. iPSC-derived brain organoids express mature neural marker.**
Cryosection of 60-day-old organoids display mature markers such as Synapsin1 (magenta) and MAP2 (magenta) at the cortical plate (CP), a region basal to the ventricular zone (VZ), which was demarcated by SOX2 (green). Representative image. At least 20 organoids were analyzed from 3 batches. Scale bar 50 µm. (This work was performed in collaboration with Dr. Elke Gabriel)

### 3.10.3 Assay3: fusion of GSCs spheres with mature organoids

To allow the monitoring of the later stages of brain organoid development, we established the GSCs spheres assay. In assay 3, the GSCs cells are compactly packed (spheres) differently from assay 2, where the GSCs were dispersed as single cells**.** We combined 60-day-old organoids with GSCs spheres and incubated them for 24 hrs in low adherent “U” shaped wells. This process results in the formation of a fusion product that was named as GSCs-Organoids (GSCs spheres fused with organoids). GSCs-Organoids have been transferred into air diffusible plates that are amenable for applications such as time-lapse imaging and drug treatment **(Figure 3.23A).** Imaging of the samples revealed the onset of GSCs spheres integrating into organoids within 3 days **(Figure 3.23B-E).**

Interestingly, individual GSCs started to invade into organoids after seven days in day-20 organoids, whereas older organoid day-60 required only three days to incorporate into the brain organoids. Quantification analysis for integrating GSCs into immature and mature organoids revealed that both, primary GSC and relapsed GSCs integrate faster into mature organoids. Moreover, the GSCs were compact in spheres, indicating a profound tropism of GSCs to mature brain organoids **(Figure 3.23C-H).** In summary, all of the described assays unequivocally allow analyzing GSCs invasion and capable of distinguishing invasive patterns of primary and relapse GSCs. The described 3D invasive assays were able to show cell non-autonomous characteristics of GSCs such as interconnecting microtube networks and invasive processes. 3D organoids offer these unique opportunities for analyzing GSCs-host tissue interaction, which is not possible to model in 2D cultures.

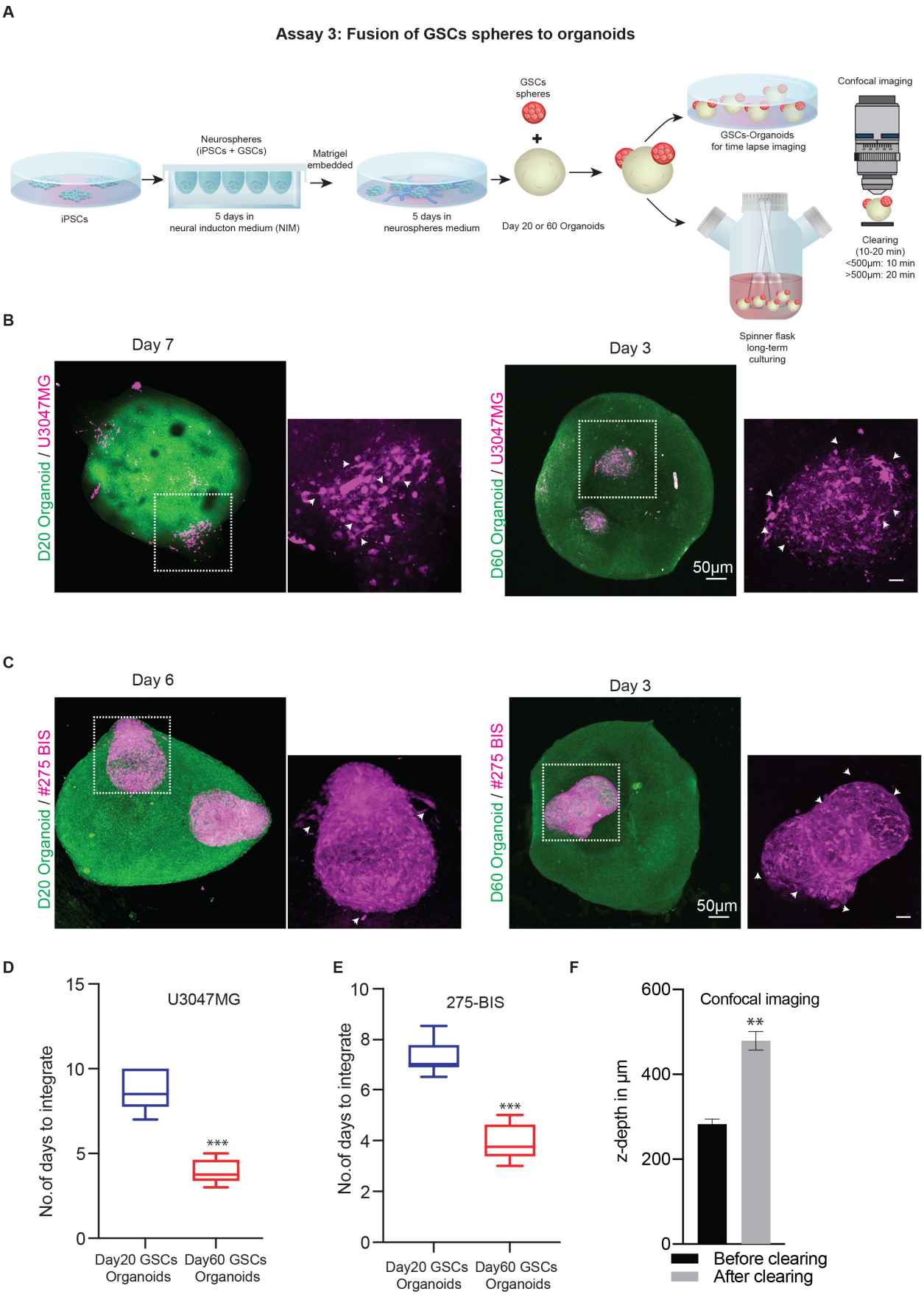


**Figure 3.23. Tissue cleared confocal imaging of fussed GSCs spheres to brain organoids using assay 3.**

**A.** Schematic of experimental set up displaying step-by-step process from culturing iPSCs until the imaging of GSCs-Organoids. **B.** Imaging of U3047MG-mCherry spheres (pseudo color magenta) fusing with 20-day and confocal stacks of 60-day-old organoid (green) to form GSCs-Organoid. Note that GSCs

spheres take 7 days to integrate in day-20 organoid versus day-60 organoid GSCs completed by day-3. Scale bar 50 µm. Representative image. At least 4 organoids were analyzed. **C.** Tissue clearing and 3D imaging of 275-BIS GFP (pseudo color magenta) GSCs-Organoids at day 20 and day 60 organoids. Note that GSCs spheres take 6 days to integrate in day-20 organoid versus day-60 organoid GSCs completes by day-3. The inset image shows that GSCs-sphere starts to release GSCs (arrows), which migrates into organoids forming protrusions and microtubes. Scale bar 100 µm, inset, 5µm. Representative image. At least 4 organoids were analyzed. **D.** Box plot depicting the time duration for GSCs spheres integration into the organoids. Mature organoids (day-60) integrate GSCs spheres faster than younger organoids (day-20). Blue box, integration to younger organoids (day-20). Red box, integration into mature organoids (day-60). n=3 batches, n=12 organoids per GSCs line were analyzed. P values were obtained ed using the unpaired t-test. ***p <0.0001. Error bars show +/- SEM. **E.** Box plot depicting the time duration for GSCs-sphere integration into the organoids. Mature organoids (day-60) integrate GSCs spheres faster than younger organoids (day-20). Blue box, integration to younger organoids (day-20). Red box, integration into mature organoids (day-60). n=3 batches, N=12 organoids per GSCs line were analyzed. P values were obtained ed using the unpaired t-test. ***p <0.0001. Error bars show +/- SEM. **F.** Tissue clearing enhances the microscopy imaging as revealed by at least two-fold increase in-depth coverage. n=3 batches, N=22 organoids. P values were obtained using the unpaired t-test. **p <0.001. Error bars show +/- SEM. (This work was performed in collaboration with Dr. Arul Mariappan).

## 3.11 Ciliated GSCs fail to invade into brain organoids

To analyze the impact of cilium induction in the cell fate of GSCs invasion, we used our recently optimized brain organoid-based GSCs invasion assay 2 supplementing GSCs as dispersed cells to organoids recapitulate the *in vivo* behavior of GSCs. To analyze and measure invasion of GSCs, we tagged GSCs with mCherry reporter. Furthermore, we performed GSCs invasion assay by seeding 1000 naïve and NEK2-KD expressing U3047MG cells at the vicinity of 10-day-old organoids. The organoids were generated from iPSCs expressing transgenic Tubulin-GFP reporter. After 24 hrs of seeding, we added DOX to induce NEK2-KD protein expression **(Figure. 3.24A).** Live imaging of the GSCs invasion into the brain organoid was followed at day-3. Time-lapse imaging of organoids at day-3 already revealed that U3047MG cells (pseudo color magenta) invaded into 3D organoids via establishing protrusion-like processes in the form of microtubes, known characteristics of invading GSCs into a host tissue **(Figure. 3.24B)** (Osswald et al., 2015b). In contrast, NEK2-KD expressing U3047MG cells failed to establish protrusion-like processes **(Figure 3.24B).**

To enhance the image quality and quantitatively determine the 3D invasion behavior of GSCs at the later time point of day-20, we utilized our rapid organoid clearing method **(see section method section 5.7.2 )**. Whereas naïve U3047MG cells extensively diffused and recapitulated GBM infiltration in the brain, Nek2-KD expressing cells failed to grow in brain organoids **(Figure 25A)**. As a result, in contrast to naïve, Nek2-KD expressing U3047MG cells exhibited as an impaired organoid invasion **(Figure 25B).**

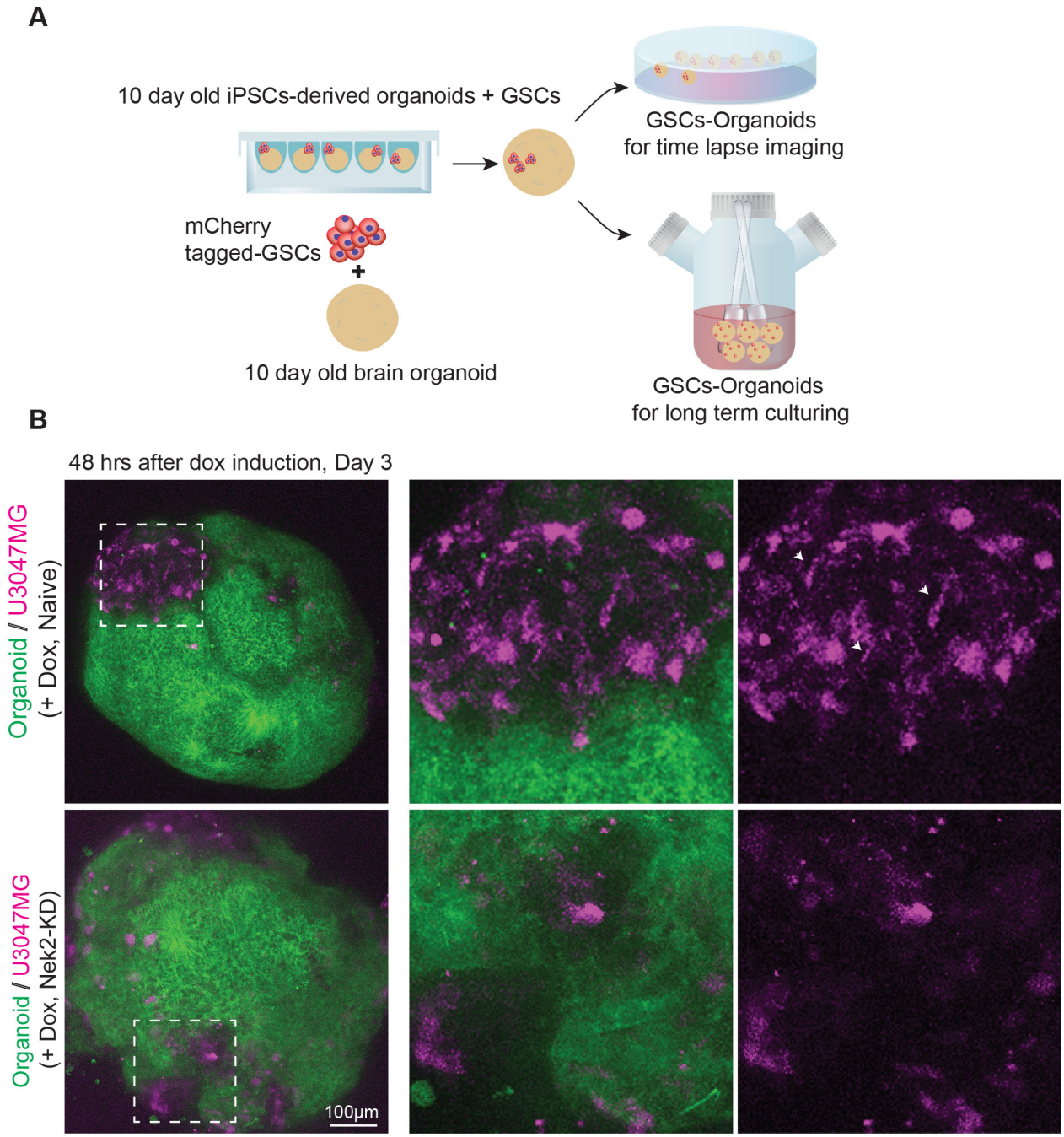


**Figure 3.24. Time-lapse confocal imaging shows that cilium induction prevents GSCs invasion into brain organoids.**

**A.** Experimental scheme showing the process of GSCs invasion assay. Co-culturing of labeled GSCs with 10-day-old brain organoids until imaging them. **B.** Imaging of live organoids (green) supplemented with U3047MG-mCherry (pseudo color magenta) 48-hrs after doxycycline induction. Note that U3047MG-mCherry cells progressively invade into the organoid forming invasive protrusions and microtube networks within 48-hrs (arrows, top panel). In contrast, NEK2-KD expressing U3047MG cells fail to assemble invasive protrusions and microtubes and thus fail to invade into the 3D organoid space (bottom panel). Scale bar 100 μm. Representative image. At least 20 organoids from 5 different batches are tested.

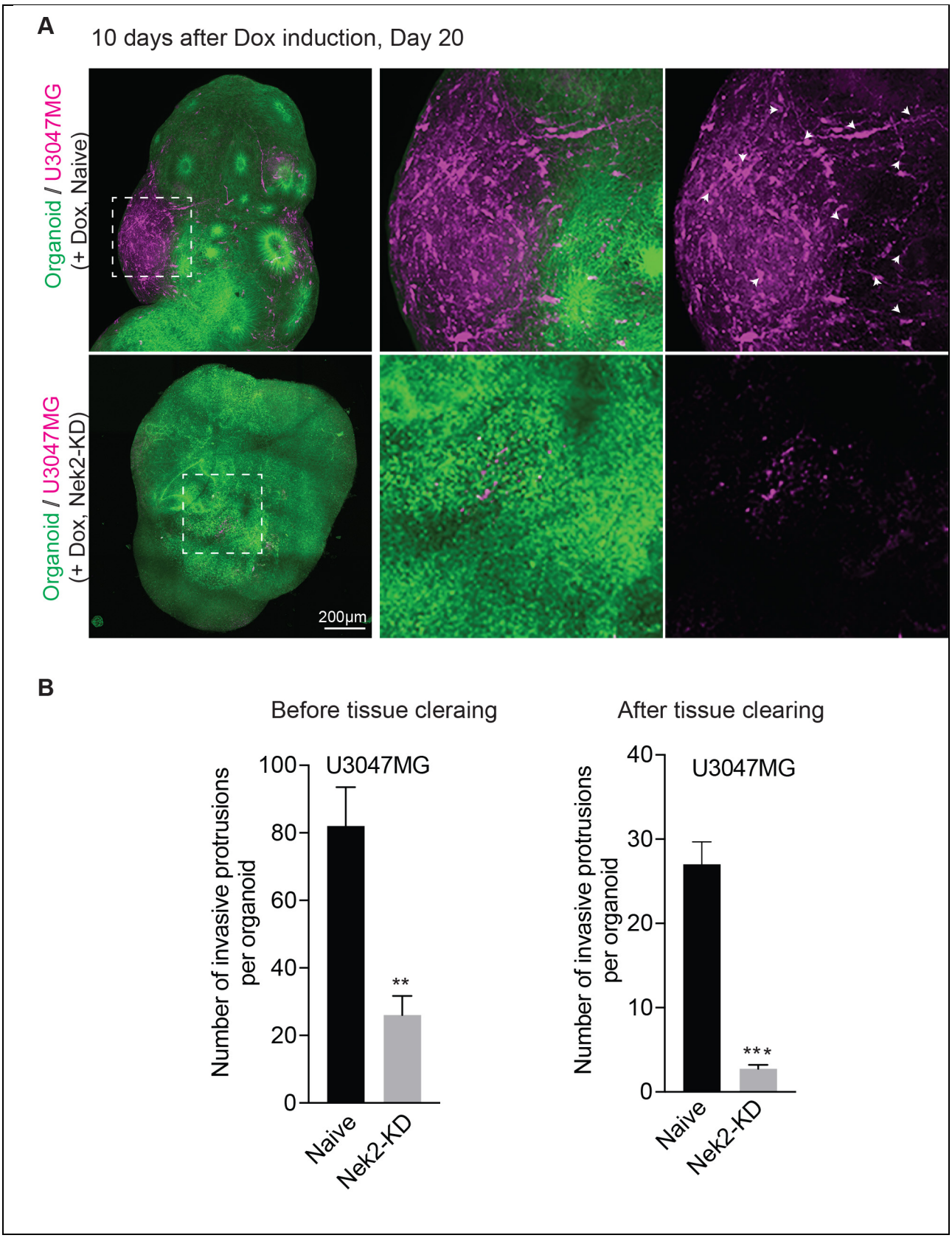


**Figure 3.25. Tissue cleared confocal imaging shows that cilium induction prevents GSCs invasion into brain organoids.**

**A.** Tissue cleared 3D imaging of the whole organoid after 20 days of GSCs invasion. Tissue clearing enhances the visualization of U3047MG-mCherry (pseudo-colored as magenta) growth into the organoids (green). Invading GSCs form protrusions and microtube networks (top panel). In contrast, NEK2-KD expressing U3047MG cells poorly grow within organoids, as evidenced by poor growth and less intensity (bottom panel). **B.** Bar graphs quantifies the parameters of invasiveness before and after cilium induction. At least 50 microtubes were measured. Bar graphs left quantifies the paraments before

tissue clearing and at the right after tissue clearing. Unpaired t-test, ***P<0.0001, **P <0.001. Error bars show +/- SEM.

## 3.12 Cilium induction triggers differentiation of GSCs within 3D organoids

Cilia formation switch GSCs from self-renewal to differentiation state, to analyze if the differentiation is a cause for invasion, we used 3D brain organoid system. Immunostaining of thin-sectioned brain organoid GSCs was performed to analyze the cell fate of GSCs before and after cilium induction. The same was observed in 2D analyzes in NEK2-KD expressing cells, but not naïve U3047MG cells were strongly positive for GFAP (astrocyte marker) **(Figure. 3.26A).**

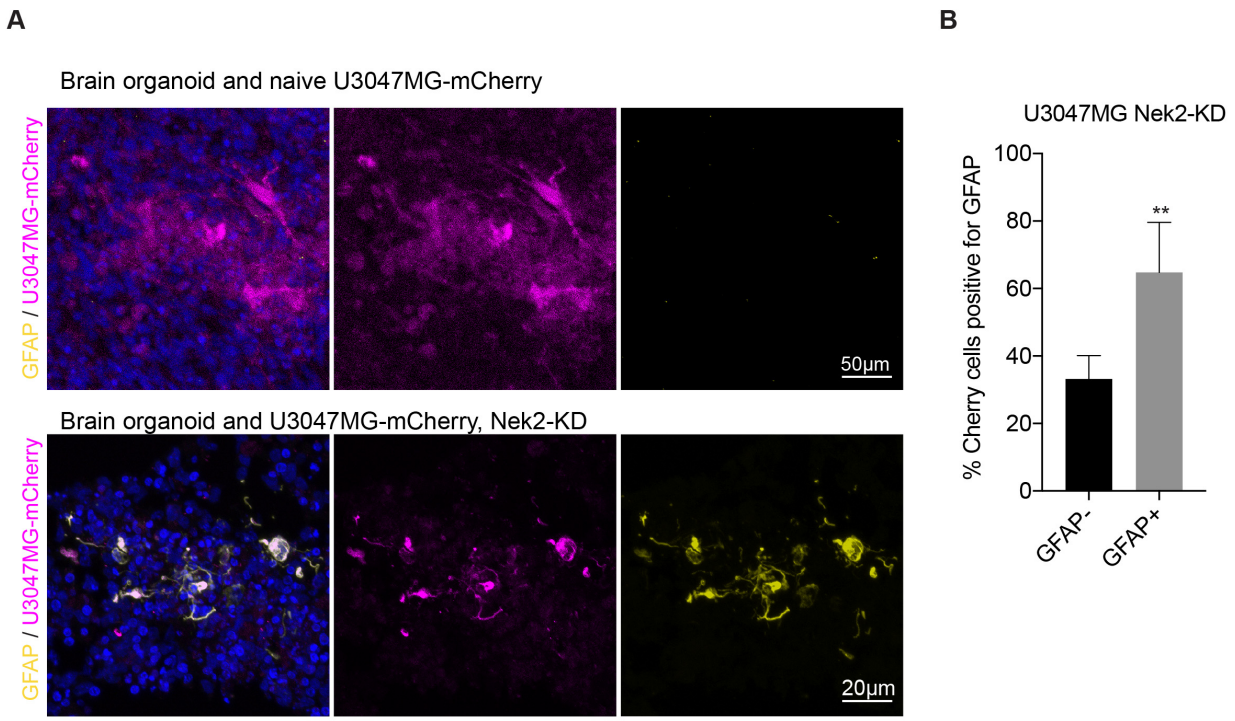


**Figure 3.26. Differentiated GSCs impairs invasion into brain organoids.**
**A.** Related to figure 3.15. Bright field images show that U3047MG-mCherry grows in 3D brain organoids. Upon NEK2-KD induction**,** U3047MG cells exhibit impaired growth. In these experiments, untagged iPSCs were used to generate brain organoids and imaged at day 20. Scale bar 200 µm. At least 20 organoids were analyzed from 5 different batches. **B.** Immunostaining of thin-sectioned organoid slices exhibit diffused growth of U3047MG-mCherry (pseudo color magenta). Note, U3047MG-mCherry cells do not differentiate to GFAP positive cells at this condition. Scale bar 50 µm. U3047MG-mCherry (magenta) cells undergo differentiation to GFAP positive cells (yellow) upon NEK2-KD induction. Note U3047MG-mCherry (pseudo color magenta) cells at this condition did not proliferate. Instead, they undergo differentiation as judged by their colocalization with GFAP (yellow). Graph at right quantifies GFAP-negative and GFAP–positive cells. Scale bar 20 µm. At least 100 cells were analyzed from 5 independent organoids. P values were obtained using the unpaired t-test. ***P <0.0001. Error bars show +/- SEM.

Moreover, quantification analyzes showed significant percentages of GFAP positive cells co-localize with Cherry-tagged (magenta pseudo color) ciliated cells (U3047MG NEK2-KD) **(Figure. 3.26B left bar diagram)**. These findings reveal that NEK2-KD expressing U3047MG cells underwent a

differentiation process identical to what was observed in our 2D experiments upon cilium induction. Together, our organoid-based invasion assay elucidates that NEK2-KD expression triggers the differentiation of GSCs within brain organoids impairing their invasion and migration.

In summary, we identify that irrespective of various background mutations, a panel of tested patient-derived GSCs exhibit suppressed ciliogenesis due to elevated CDC recruitment at the basal bodies. We then establish that suppressing CDC recruitment and altering their dynamic localization behavior at the basal body is sufficient to persistently induce cilium in a subset of GSCs that overexpress constitutively active receptor tyrosine kinase PDGFR-α. Upon cilium induction, PDGFR-α is sequestered to newly induced cilium from its original location with concomitant reduction of overall PDGFR-α levels. Inducing ciliogenesis triggers GSCs switching from self-renewal to differentiation state. Finally, GSCs induced with cilia failed to infiltrate into induced Pluripotent Stem Cells (iPSCs)-derived human brain organoids, which provide a near-native 3D environment of neural tissues for GSCs invasion.

# 4. Discussion

## 4.1 Glioma stem cells have suppressed ciliogenesis

Loss of primary cilia is commonly associated with multiple types of cancers, which have deregulated cell cycle progression, and altered cellular signaling, including glioblastoma tumors (Seeger-Nukpezah et al., 2013, Goranci-Buzhala et al., 2017, Moser et al., 2014, Fabbri et al., 2019, Seeley and Nachury, 2009). Despite these observations, the molecular mechanisms by which ciliogenesis is suppressed in glioma stem cells (GSCs) are still not well understood.

This thesis aimed to investigate the molecular mechanisms of cilia loss in patient-derived GSCs and identify molecular targets linked to primary cilia to control GCSs proliferation. Furthermore, the thesis also describes a novel method of analyzing GSCs invasion in human brain organoids. To determine at what degree ciliogenesis is suppressed in GBM, at least eight patient-derived GSCs (from tumors classified as proneural, mesenchymal, and classical) and nine different patient tissue biopsies were analyzed. Importantly, ciliogenesis was suppressed in both patient-derived GSCs and patient biopsies. These findings are in line with other studies, where suppressed ciliogenesis has been observed in a multitude of tumors, including breast cancer, prostate cancer, renal cell carcinoma, melanoma, and glioblastoma (Moser et al., 2009a, Moser et al., 2014, Seeger-Nukpezah et al., 2013, Yuan et al., 2010, Zingg et al., 2018).

Especially in the renal cell carcinomas (RCC), it has been shown that several ciliary genes are deregulated. More than 80% of RCCs harbors a mutation in the von Hippel-Lindau (*VHL*) tumor suppressor gene (Basten et al., 2013). Von Hippel-Lindau syndrome is an inherited autosomal-dominant disorder ($VHL^{+/-}$ heterozygotes). Patients with von Hippel-Lindau syndrome tend to develop multiple vascular tumors called hemangioblastomas, pheochromocytomas, and clear cell renal cell carcinomas (ccRCCs). Tumor development in patients with *VHL* syndrome is linked to inactivation or loss of remaining wild-type *VHL* allele in RCC (Lubensky et al., 1996, Mandriota et al., 2002). Protein VHL (pVHL) has been recognized as a multifunction protein mainly linked to tumor suppression (Frew and Krek, 2008). It has been shown that pVHL interacts and regulates microtubules dynamics, which is involved in the assembly and maintenance of primary cilia (Schermer et al., 2006, Thoma et al., 2010, Hergovich et al., 2003). The protein pVHL localizes to the cilia and controls ciliogenesis in kidney cells (Schermer et al., 2006). To control the ciliogenesis and signaling network, pVHL functions together with Glycogen synthase kinase-3 β (GSK3β) (Thoma et al., 2007), which is a protein kinase that regulates microtubule assembly, stability, and dynamics (Zhou and Snider, 2005). The depletion of pVHL fails to assemble cilia in kidney cells, whereas re-expression of pVHL restores ciliation in VHL-negative RCCs (Schermer et al., 2006). This finding suggests that the expression of pVHL is crucial for cilia assembly. Altogether, the data obtained in these studies support the finding that the defects in primary cilia assembly promote cell proliferation and tumor growth in a broad range of cancers.

## 4.2 Elevated levels of CDC complex suppress ciliogenesis in GSCs

Highly tumorigenic GSCs exhibit several similarities to NPCs: expression of neural stem cell markers, spheres assembly, and rapid self-renewal (Bhaduri et al., 2020, Rajakulendran et al., 2019). Identifying the molecular and regulatory features of GSCs strikingly different from NPCs will open up new avenues and unique strategies to selectively impair GSC's proliferation and invasion. Besides their similarities, NPCs and GSCs possibly differ in at least two aspects. First, cilium formation is suppressed at the early stages of ciliogenesis in patient-derived GSCs due to elevated levels of molecular players such as the CDC proteins that might trigger cilia disassembly. Second, GSCs are characterized by continuous self-renewal and suppressed capacity to neural differentiation (Park et al., 2017b, Rajakulendran et al., 2019). Delayed cilia disassembly triggers NPCs to exit the cell cycle ($G_1$-$G_0$), whereas accelerated cilia disassembly promotes NPCs proliferation (Li et al., 2011, Gabriel et al., 2016). Precise temporal cilia disassembly is essential for the switch between symmetric and asymmetric cell division essential for stem cell maintenance and tissue homeostasis (Calegari and Huttner, 2003, Lange et al., 2009, Li et al., 2011). This complex provide a novel cell cycle 'cilium checkpoint', that can control cell cycle progression in aberrant cells. It has been demonstrated that proteins that promote the cilium disassembly process are implicated in human diseases, particularly, cancer (Zhou et al., 2013, Xiang et al., 2017, Raab et al., 2018). These results led us to hypothesize that in hyper-proliferative patient-derived GSCs, the uncontrolled overexpression of CDC proteins could suppress cilium formation and facilitate chronic proliferation, a hallmark of GBM.

In this thesis, we demonstrate for the first time that GSCs have elevated levels of CDC proteins, highlighting the importance of these proteins in cancer. More interestingly, loss of cilia due to elevated levels of CDC components is in line with several other studies, in which some of the CDC proteins have been implicated in accelerated cilium disassembly and cilium loss. For example, Aurora-A, which is essential to initiate cilium disassembly (Pugacheva et al., 2007), is overexpressed in epithelial ovarian cancer cells (Do et al., 2014). The overexpression and recruitment of Aurora-A at the basal body (mother centriole) indicate that Aurora-A increases the rate of cilium disassembly while inhibiting the process of cilium formation (Egeberg et al., 2012). Moreover, Histone deacetylase, HDAC2 was identified to be overexpressed in pancreatic ductal adenocarcinoma cells. The inactivation of HDAC2 decreased Aurora-A expression, resulting in a cilium assembly (Kobayashi et al., 2017).

## 4.3 Targeting CDC complex is a potential mechanism to induce ciliogenesis in GSCs

The molecular interplay between CDC components recruitment and cilium disassembly remains elusive to this day, with no apparent studies carried out to test whether cilium reintroduction could be anti-tumorigenic, triggering differentiation of GSCs and/or impairing their invasion. Here we show, that depleting selected CDC proteins using shRNA (HDAC6, NEK2, and NDE1) was sufficient to

induce cilia in GSCs. Among these CDC components, depletion of NEK2 induced cilia significantly compared to the depletion of HDAC6 and NDE1. Since NEK2 is a multifunctional protein, implicated not only in ciliary disassembly but also critically important for centriole duplication (Jeong et al., 2007, Sonn et al., 2009, Boekhout and Wolthuis, 2015), we decided to target NEK2 also via an inducible NEK2-KD system carrying catalytically inactive NEK2. NEK2-KD (catalytically inactive, 'Kinase Dead') cannot phosphorylate its substrate KIF24, promoting cilia assembly. It has been previously shown that NEK2 phosphorylates KIF24 and negatively regulates ciliogenesis (Kim et al., 2015b). Hence, with NEK2, the CDC might contain an enzyme that can be activated to depolymerize the microtubule cytoskeleton of cilia. Furthermore, our idea is supported by a co-immunoprecipitation analysis that reveled the tight interaction of other CDC proteins with NEK2 and KIF24, which can promote cilia disassembly and cell cycle re-entry. Moreover, here we identify that overexpression of NEK2-KD failed to localize KIF24 to its active site at the minus end of ciliary microtubules in patient-derived GSCs. These findings prove a tight regulation of NEK2-KIF24 interaction as part of the CDC complex to promote cilium disassembly.

Together these results demonstrate that CDC is a novel regulator of ciliogenesis in patient-derived GSCs. The depletion of a Cyclin-dependent kinase 20 (CDK20 or CCRK) has also been shown to induce cilia in a small fraction of serum-starved GBM U251MG cells (Yang et al., 2013). It is noteworthy that, unlike GSCs, the commercially available U251MG cells were cultured in the presence of serum (Yang et al., 2013). It also remains unclear in Yang and colleagues' study whether the small fraction of ciliated cells observed is due to the depletion of kinase or serum starvation. It remains to be tested if the kinase CDK20 interacts with the other proteins of the CDC complex.

### 4.3.1 CDC proteins promote cell cycle progression in cancer cells

The finding that CDC proteins are deregulated in GSCs and control the cell cycle progression agrees with other studies. Proteins related to the CDC complex are upregulated in various cancer cells, leading to defective cilium assembly and cell cycle progression (Kim et al., 2015b). NEK2 overexpression has been reported to negatively regulate cilia formation, whereas depletion of kinase restores cilia and prevents cell proliferation in breast cancer cells (MCF10A, MCF10AT, MCF10DCIS.com, and MCF10CA1) (Kim et al., 2015b). Although MCF10A cells are non-malignant, they are immortal and hyperplastic and show increased levels of NEK2 (Neve et al., 2006, Yuan et al., 2010). Another CDC protein, HDAC6, is crucial for disassembling the ciliary axoneme. A recent study has shown that HDAC6 is upregulated in cholangiocarcinoma cancer and could be targeted using a pharmacological inhibitor (tubastatin-A), which induces cilia and prevents cell cycle proregression (Xiang et al., 2017).

More interestingly, apart from CDC component proteins, it has been shown that cancerous inhibitor of protein phosphatase 2A (CIP2A) is involved in cilium disassembly. CIP2A interacts directly with the oncogenic transcription factor c-MYC and prevents c-MYC proteolytic degradation (Junttila et al., 2007). CIP2A localizes at centrosomes. Increased recruitment of this protein at the basal body

promotes cilium disassembly through Aurora-A kinase-dependent mechanisms, whereas depletion enhances ciliation and ciliary length in RPE cells. Interestingly CIP2a depletion induces metabolic reprogramming independent of the cilium (Jeong et al., 2018). Since CIP2A is a tumor suppressor protein, it would be interesting to study if this protein expression level is increased in GSCs, which have suppressed ciliogenesis. Furthermore, CIP2A would be a potential candidate to investigate its interactions with CDC components further. Taken together, results from this thesis and work from others suggest that several proteins that regulate cilium disassembly are also upregulated in several cancer cells, resulting in suppressed ciliogenesis.

## 4.4 Newly induced cilia in GSCs are functional

We have demonstrated that upon induction of ciliogenesis by genetic manipulation, GSCs behave like NPCs, undergoing a spontaneous differentiation, suggesting that newly induced cilia are structurally and functionally normal. The presented results show that the newly induced cilia in GSCs are positive for IFT88 along the axoneme and can transduce the Hh signaling by relocating SMO along the cilium similar to control healthy NPC cells (Briscoe and Therond, 2013, Hassounah et al., 2012). Thus, we can conclude that GSCs are, in general, capable of forming a correct cilium, although ciliogenesis is not seen under malignant conditions. In astrocytes, the cilium is central hubs for Hh signaling, harboring Hh signaling key proteins, including SMO or PTCH1, and regulating cell survival under stress conditions (Yoshimura et al., 2011). Surprisingly, the cilium can mediate GBM proliferation through Hh signaling in GBM cells, but only in one of the three cell lines. This study suggests that GBM xenografts with GBM-S2 Kif3a disrupted cells increase GBM proliferation through Hh signaling compared to unmodified GBM-S2 cells *in vitro* and *in vivo*. This finding suggests that cilia could modulate GBM growth by Hh signaling, playing a dual role in GBM tumorigenesis (Hoang-Minh et al., 2016b). This finding might have more significant impact on the classical GBM subtype since the cell line used highly expressed several components of this pathway (Verhaak et al., 2010).

### 4.4.1 Dual role of cilia in brain tumors

Is the restoration of ciliogenesis a potential way to suppress tumorigenesis or tumor progression? Is it a general feature of cilia to block growth and proliferation? To elaborate cilia function and role in cancer, we will discuss the studies were it had been identified that cilia could have a dual role in cell cycle and tumorigenesis.

Medulloblastoma is the most common malignant brain tumor in children, initiating from the cerebral neural precursor cells (Louis et al., 2007). It is known that aberrant Hh signaling is one of the signaling pathways that drive medulloblastoma formation (Han et al., 2009, Haycraft et al., 2005, Liu et al., 2005). Mutations of upstream or downstream components of the Hh pathway in a pioneered

work have shown that the primary cilium plays a dual role in medulloblastoma formation. Strikingly, tumorigenesis is inhibited in a medulloblastoma mouse model, which has a loss of the cilium and constitutive active Smo expression, an upstream activator of Hh signaling (Han et al., 2009). In contrast, cilium loss was required for medulloblastoma growth driven by a constitutively active Gli2, a downstream transcription factor of Hh signaling. Thus, primary cilia can play a dual role in medulloblastoma, promoting, and inhibiting tumorigenesis (Han et al., 2009). The above results suggest that the Gli2-driven medulloblastoma formation requires the loss of the cilium for medulloblastoma development, which is opposite for Smo-driven medulloblastoma. One possible explanation for the opposite roles could be that primary cilium is required not only for Smo function but also for Gli3 repressor formation (Haycraft et al., 2005, Liu et al., 2005). The ciliary cargo IFT proteins are required for both Gli activator and repressor functions, and Gli proteins are insensitive to Hh ligand in the absence of IFT proteins. The Gli3 repressor was reduced Gli2-driven medulloblastoma mouse model, suggesting Gli3 could have an inhibitory effect in medulloblastoma growth.

Besides, the loss of primary cilium in a basal cell carcinoma mouse model driven by active Smo protects mice from tumorigenesis (Wong et al., 2009). In this context, disrupting Inturned (Intu), which is aberrantly elevated in the same mouse model, suppresses ciliogenesis and promotes basal cell carcinoma growth. Intu is crucial for IFT-a complex assembly during ciliogenesis (Yang et al., 2017). Together these data suggest that in some cases, the presence of primary cilium in tumor cells can mediate Hh signaling and promote tumor formation.

## 4.5 Cilium induction triggers GSCs to switch from a stemness to a differentiation state

The recruitment of CDC components (CPAP, Aurora-A, Nde1, and OFD1) to the ciliary base is associated with temporal cilia disassembly at the onset of cell cycle re-entry (Kim et al., 2015b, Kim et al., 2011, Gabriel et al., 2016, Tang et al., 2013, Pugacheva et al., 2007). Therefore, we asked whether targeting CDC proteins in patient-derived GSC would be sufficient to restore ciliogenesis and switch the cell fate. Recently, others and our laboratory have identified that primary cilia act as a molecular switch whose spatiotemporal dynamics decisively regulate NPCs self-renewal versus differentiation (Jackson, 2011, Gabriel et al., 2016). These results provide a conceptually novel ‘cilium checkpoint’ can be targeted to regulate stem cell fate. To address what happens to cell fate after cilium induction, differentiation markers (TUJ, GFAP, S100B) and stem cell proliferation markers (SOX2, PAX6, NESTIN) were analyzed by immunofluorescence and western blot analysis. Indeed, ciliated but not un-ciliated cells gained differentiation markers and lost neural and cancer stem cell markers.

Furthermore, RNA sequencing analysis supported the data. The majority of downregulated genes were associated with biological processes involved in cell division, cell cycle, and spindle

organization. Altogether, the results showed that re-inducing ciliogenesis in a subset of patient-derived GSCs triggered them to lose their stemness and switch to their differentiation programs.
Data demonstrates that cancer stem cells, which have aberrantly expressed PDGFR- α are sensitive to cilium induction, resulting in cell cycle exit, cilium formation, and differentiation-like cells. How cilium is induced in the aberrantly expressing PDGFR-α, subtype, and how the correlation of cilium with PDGFR-α is will be discussed below. Indeed, RNA sequencing analysis shows that *PDGFA* and oligodendrocyte progenitor genes (*OLIG2)* were downregulated upon cilium induction. Furthermore, we found downregulation of transcription factor *SOX9*, which is also involved in brain development and lineage specification. Notably, *SOX9* has been correlated with poor clinical outcome (Wen and Kesari, 2008). PDGFR-α overexpressing GSCs may harbor epigenetically regulated neurogenic and astrogenic features (Caren et al., 2015). Thus, restoring ciliogenesis could favor differentiation and loss of stemness. As an example, the transcription factor ASCL1 in proneural subtypes has been shown to unlock chromatin allowing new sites to activate differentiation programs (Caren et al., 2015). Although bulk RNA-sequencing approaches have been useful to support our functional analysis after cilium induction in GSCs, they provide limited insight into the actual heterogeneity of GBM tumors. GBM is a typical example of heterogeneous cancer; likewise, variation and molecular diversity are observed even within the same GBMs patient (Patel et al., 2014, Stommel et al., 2007). Therefore, single cells RNA sequencing would provide a much clearer picture of the genes affected before and after cilium induction in GSCs and might reveal the unknown epigenetic factors that could prevent cilium induction and differentiation in non-responding subtypes.

## 4.6 Cilium induction sequesters elevated level of PDGFR-α

This thesis data supports the notion that the cilium can be functionally restored in a subset of GSCs categorized as proneural subtypes expressing an elevated level of PDGFR-α. Restoring of the cilium first sequesters excessive PDGFR-α into newly induced cilia and resets aberrant PDGFR-α signaling. Importantly, cilium induction was efficient only in the patient-derived GSCs, which harbor PDGFR-α overexpression, belonging to the proneural subtype (Verhaak et al., 2010). Alterations in PDGFR signaling components and genes involved in oligodendrocyte development (*OLIG2, NKX2-2, and PDGF*) are observed to be hallmarks of the proneural signature in GBM, which accounts for approximately 30% of human gliomas (Brennan et al., 2009). Brain tumors derived from PDGFR-α displayed histologic features of oligodendroglioma. The gene products of both rearrangements showed constitutively elevated tyrosine kinase activity and transforming potential that can be reversed by PDGFR blockade (Ozawa et al., 2010).
Furthermore, PDGFR-α is regulated by CblE3 ubiquitin ligase. Upon PDGFR-AA ligand stimulation, the Cbl complex interacts with IFT20 and ubiquitinates PDGFR-α, resulting in the internalization of PDGFR-α. If primary cilium is lost upon depletion of IFT20, the Cbl complex is ubiquitinated and degraded, allowing overactivation of PDGFR-α at the plasma membrane (Schmid et al., 2018).

Notably, studies have shown that UBE3C, an E3 ubiquitin ligase, is highly expressed in glioma cells and tissues compared to adjacent healthy tissues. Clinically, the enhanced expression of UBE3C is correlated with poor patient survival and early disease recurrence (Low et al., 2012). This data suggests that the proneural GSCs that have suppressed ciliogenesis and overexpression of PDGFR-α might have an impaired Cbl E3 ubiquitin ligase that can prevent cilium formation and promote cell cycle progression. Moreover, it has been shown that downregulation of ubiquitin ligase in GBM cells induces cell differentiation and apoptosis (Low et al., 2012). Besides, drastic reductions in total PDGFR-$\alpha$ levels after cilium induction is a surprising phenomenon, suggesting that cilia could harbor proteasomal subunit components. Interestingly, at least three components of the 19S proteasomal subunits have been identified in mouse embryonic fibroblast cilia (Gerhardt et al., 2016). It is thus tempting to investigate if primary cilia of NPCs and GSCs harbor proteasomal subunits that can recognize PDGFR-α and critically regulate its amount and downstream signaling.

Additionally, activation of RTKs, such as EGFR, PDGFR-α, PDGFR-$\beta$ and FGFr1 by growth factors activates *in vitro* ubiquitin specific peptidase 8 (USP8) that deubiquitinates and stabilizes trichoplein and causes phosphorylation and activation of Aurora-A, resulting in the suppression of ciliogenesis (Kasahara et al., 2018). NDE1 also mediates the balance between ubiquitination and de-ubiquitination of trichoplein, a modulator of dynein activity localized at mother centriole and promoting cilium disassembly. Overexpression of NDE1 indirectly inhibits the ubiquitination of trichoplein by CRL3 KCTD17 (an E3 ligase component protein for trichoplein) and suppresses ciliogenesis. The serum-starved cell culture cells degrade NDE1 via the ubiquitin-proteasome system following the removal of trichoplein at the mother centriole, which promotes ciliogenesis (Inaba et al., 2016). Taken together, these data indicate that RTKs, ubiquitination complexes, and proteins that promote cilium disassembly (NDE1 and trichoplein and Aurora-A) seem to play a critical role in regulating ciliogenesis. Overall, in proneural GSCs, if ubiquitination mechanisms are upregulated, it might contribute to the overexpression of CDC proteins at the ciliary base, which in turn causes suppressed ciliogenesis and overexpression of PDGFR-$\alpha$.

## 4.7 Human brain organoid as a tool to study GSCs invasion assay

Cancer is not a cell-autonomous disease, thus requiring understanding cancer cells' biology and host cells, which are tightly connected, especially in GBM. GBM does not metastasize but infiltrates into brain epithelial tissue through diffused invasion and infiltration. Therefore, 2D cultures do not model the crucial cell-cell interactions process and tumor microenvironment. Mouse xenograft models address host-tumor cell interactions, but cannot recapitulate human brain development at the cellular and physiological level (Oberheim et al., 2009). The human brain's *in vitro* model is essential and provides useful insights into the many steps of GSCs invasion and progression. Recent advances in 3D cultures of human brain organoids allow us to study patient-specific GBMs ex vivo within a microenvironment similar to that in the human brain (Gabriel et al., 2016, Gabriel and

Gopalakrishnan, 2017). Therefore, we took advantage of using fluorescently labeled hiPSC and patient-derived GSCs, and we developed three assays to model human GSCs growth, invasion, and proliferation. Applying this strategy, we could measure invasive protrusions and microtube networks, well-known characteristics of invading GSCs into a host tissue (Osswald et al., 2015b).

**i)** Co-culturing of GSCs during organoid differentiation - the assay1, recapitulate GSCs behaviors to some extent in the early stage of development (day10 organoid) but failed to fully recapitulate it in the later stages (day20 and day30). Presumably, co-culturing GSCs with hiPSCs from the beginning of the organoid generation might change cell fate and does not further promote the growth of GSCs into brain organoid. Therefore the next assay aimed to study preference of GSCs for 10 day old organoids (supplementing GSCs as dispersed cells to organoids).

**ii)** Supplementing GSCs as dispersed cells to organoids – assay 2. GSCs are supplemented in the vicinity of organoids to recapitulate invasive growth and spontaneous formation of microtube protrusions in the organoids' inner side. Reports have shown that targeting a membrane protrusion in glioma, termed as "tumor microtubes" (TM), would be a potential biomarker for glioma patients. Interestingly, depleting the gap junction proteins Cx43 and GAP-43 inhibit TM formation and function. Using the assay 2, GSCs formed long membrane protrusions and TM structures within brain organoids. It will also be interesting to analyze whether invaded GSCs in brain organoids express these markers (Osswald et al., 2015a). Furthermore, as this model is grown *in vitro*, this enables a more manageable analysis of different manipulations and drug treatments, and allows precise control of physiological and environmental conditions.

**iii)**The fusion of GSCs spheres to organoids - assay 3. This data suggests that mature organoids can provide suitable microenvironmental determinants for GSCs growth. This aspect is consistent with the fact that neuronal activity generates mitogenic factors promoting glioma growth (Venkatesh et al., 2015, Venkatesh et al., 2017). Moreover, imaging GSC-organoids in 3D provided new opportunities to visualize structural morphology and host-tumor cell interaction in detail in the brain organoid environment. With the ECI-EtOH based clearing step, organoids can be rapidly tissue-cleared and imaged with enhanced fluorescence intensity and increasing z-depth penetration, allowing identifying more invasive protrusions.

Taken together, these three assay models provide the ability to successfully screen tumor cells in vitro for clinically active drugs and other interventions that have been extremely limited, particularly for GBM.

To study how the cilium induction effect GSCs invasion, the second assay was used. Live imaging at early invasion and confocal microscopy at later invasion periods showed that NEK2-KD-expressing-GSCs are not attracted to organoids than naïve GSCs. Interestingly, according to the expression of NEK2-KD, the subpopulation of cells that invade into the brain organoids are differentiated into astrocytes and cannot proliferate anymore. This data demonstrates that inducing ciliogenesis in subsets of patient-derived GSCs could trigger them to lose their stemness and switch

to their differentiation programs. As a result, GSCs with induced cilia failed to invade into 3D human brain organoids.

## 4.8 Future perspectives

Cilia loss has recently been recognized as a potentially important factor contributing to tumorigenesis and tumor growth (Zingg et al., 2018, Plotnikova et al., 2008, Seeger-Nukpezah et al., 2013). Even though the amount of molecular data is increasing, the underlying mechanisms for cilia loss remained poorly understood. In this dissertation, experiments substantiate that elevated CDC levels are implicated in suppressed ciliogenesis, at least in GSCs. Whether this is true for all other human cancer types is unclear and warrants for future investigation. Re-introducing ciliogenesis in GSCs has never been attempted before. Surprisingly, downregulating CDC is sufficient to induce ciliogenesis in a subset of patient-derived GSCs. It is tempting to test if re-introducing ciliogenesis is possible in other cancer cell types with suppressed ciliogenesis.

The observed elevated levels of CDC provide an opportunity to target the CDC components chemically. Ideally, it would be attractive to identify a chemical compound that can induce cilia in GSCs and trigger the cells to differentiate. The ideal lead compound will then serve as an alternative strategy to genetic manipulation (such as overexpressing NEK2-KD as performed in this work). Indeed, our laboratory has gained deep insights into CDCs' assembly mechanisms by purifying CPAP and its interacting components. Using high-throughput screening (HTS) will help to identify specific molecules that can induce ciliogenesis in GSCs using targets such as CPAP-CDC and NEK2-KIF24 interactions.

The current work has laid a foundation for such a chemical biology program. In particular, one of the attractive targets is the NEK2-KIF24 interaction that has been described in this dissertation. We await future experiments to establish a quantifiable interaction between Nek2-KIF24 and eventually use them to screen for compounds that can prevent NEK2-KIF24 interaction in cells.

Another intriguing aspect identified in this thesis is that cilium induction was possible only in the proneural subtype of GSCs that displayed an elevated level of PDGFR-α. This observation raises the question if cilium re-introduction depends on PDGFR-α status. It will be interesting to explore whether overexpressing PDGFR-α and Nek2-KD in other subtypes, can sensitize for cilium induction. This experiment may be particularly interesting in the mesenchymal subtype suggested evolving from proneural subtype (Ozawa et al., 2014).

Finally, given a pivotal role of cilia triggering GSCs from stemness to differentiation state, it has a broader impact in 3D brain organoids, which has recently received considerable attention as a human in vitro system to evaluate GSCs invasion and glioma-neuron interaction (Ogawa et al., 2018). It would be interesting to test if identified molecules, which prevent CPAP-CDC and NEK2-KIF24 interaction, could prevent GSCs invasion in brain organoids.

# 5. Material and Methods

## 5.1 Material

**Table 3. List of materials**

| | |
|---|---|
| (D)-Sucrose | Applichem, A4734 |
| 2-Mercaptoethanol, > 99% | Sigma-Aldrich, M6250 |
| 2-Propanol, molecular biology grade | Sigma-Aldrich, I9516 |
| Accutase | Life Technologies, A1110501 |
| Acetic Acid, Rotipuran 100% | Roth, 3738.3 |
| Acrylamide/ Bis acrylamide 30% | Sigma-Aldrich, A3574 |
| Agarose | Applichem, A8963 |
| Albumin from bovine serum | Sigma-Aldrich, A7906 |
| Ammonium persulfate | Applichem, A3583 |
| Ampicillin sodium salt | Applichem, A0839 |
| Antarctic Phosphatase | NEB, M0289S |
| Anti-Flag M2 Magnetic beads | Sigma-Aldrich, A2220 |
| B27 with Vitamin A | Gibco, 3582801 |
| B27 without Vitamin A | Gibco, 11500446 |
| bEGF | Peprotech, AF-100-15 |
| bFGF | Peprotech, 100-18B |
| Bradford reagent | Sigma-Aldrich, B6916 |
| BSA 10% | Sigma-Aldrich, |
| Chloroform | Sigma-Aldrich,C2432 |
| Click-iT™ EdU Alexa Fluor™ 594 Imaging kit | Life Technologies, C10339 |
| Complete EDTA free protease inhibitor cocktail tablets | Roche, 11844600 |
| D(+)-Glucose waterfree p. a. ACS | Roth, X997.2 |
| Deoxynucleotide solution mix | NEB, N0447S |
| Di-methyl sulfoxide, molecular biology grade > 99.9% | Sigma-Aldrich, D8418 |
| DMEM, high glucose, GlutaMAX™ supplement | Gibco, 61965059 |
| DMEM/ F12, GlutaMAX™ supplement | Gibco, 31331028 |
| DNA Gel Loading Dye (6X) | Thermo Fischer Scientific, R0611 |
| Dorsomorphin | Sigma, 5499 |
| Ethanol absolute, molecular biology grade | Applichem, A3678 |
| Ethyl cinnamate | Sigma, 112372-100G |
| FBS Good | PAN Biotech, #P30-19375 |
| Formaldehyde 37% p. A. | Sigma-Aldrich, F8775 |

| | |
|---|---|
| Gel Extraction Kit, peqGOLD | VWR Peqlab, 732-2777 |
| GeneRuler 1kb DNA Ladder | Fermentas, SM0311 |
| Glycerol, > 99% molecular biology grade | Sigma-Aldrich, G5516 |
| Glycine, molecular biology grade | Applichem, A1067 |
| Heparin | Stem Cell, 07980 |
| HEPES Buffer 1M | Sigma-Aldrich, H0887 |
| Hydrochloric acid 32% | Roth, X896.2 |
| Hygromycin B | InvivoGen, ant-hm-1 |
| Incidin Plus | Ecolab, 3011520 |
| Isopropanol | Carl Roth, 5752.3 |
| Kanamycin sulfate | Applichem, A1493 |
| L-Glutamin | Gibco, 25030081 |
| Laminin | Sigma, L2020 |
| LB-Agar | Roth, X964.1 |
| LB-Medium (Luria/ Miller) | Roth, X968.2 |
| Loading Dye Solution (6x) | Thermo Scientific, R0611 |
| Magnesium chloride solution (1M) | Applichem, A3888 |
| Matrigel Matrix | Corning, 356234 |
| MEM Non-Essential Amino Acids Solution | Gibco, 11140050 |
| Methanol, Rotipuran >99.9% ACS | Roth, 4627.5 |
| Mowiol 4-88 histology grade | Applichem, A9011 |
| MycoAlert Mycoplasma Detection Kit | Lonza, LT07418 |
| N2 Supplement (100x) | Gibco, 17502048 |
| Natriumhydrogencarbonate | Merck, 1.063.290.500 |
| Neurobasal-A Medium | Gibco, 10888022 |
| NeuroCult™ NS-A Basal Medium (Human) | Stem Cell, 05750 |
| NNNN tetramethyl ethylenediamine TEMED 99% | Sigma-Aldrich, T9281 |
| Non-fat dried milk powder | Applichem, A80830 |
| Non-silencing siRNA | Qiagen, 10272080 |
| On target plus human siRNA IFT88 | Smartpool, D |
| Opti-MEM | Invitrogen, 31985-047 |
| PageRuler Plus Prestained Ladder | Fermentas, 26620 |
| Paraformaldehyde | Roth, 0335 |
| PBS tablets | Gibco, 18912-014 |
| PDGF-AA | R&D system, AF-221-SP |
| Pen/Strep | Gibco, 15140122 |
| Penicillin, Streptomycin | Gibco, 15140122 |

| | |
|---|---|
| Phenylmethylsulfonyl Fluoride (PMSF) | Sigma- Aldrich, P7626-25G |
| Phusion® High-Fidelity DNA polymerase | New England Biolabs (NEB), M0530 |
| Plasmid Miniprep Kit I, peqGOLD | VWR Peqlab, 732-2780 |
| Poly-L-lysine | Culturex, 3438-100-01 |
| Poly-L-ornithine (PLO) | Sigma, P3655 |
| Potassium acetate | Merck, 4820.1000 |
| Potassium Chloride | Roth, 6781 |
| Primocin | InvivoGen, ant-pm-1 |
| RIPA lysis buffer system | Santa Cruz Biotechnology, sc-24948 |
| SAG | Tocris, 4366 |
| SB431542 | Selleckchem, S1067 |
| SDS molecular biology grade | Applichem, A2263 |
| Sodium acetate anhydrous p. A. | Applichem, A1522 |
| Sodium azide | Sigma-Aldrich, S8032 |
| Sodium carbonate | Roth, 8563 |
| Sodium chloride | Applichem, A1149 |
| Sodium dihydrogen phosphate dihydrate | Applichem, A3902 |
| Sodium hydroxide 1M | Applichem, A1432 |
| Sodium orthovanadate | Applichem, A2196 |
| Sodium pyruvate | Gibco, 11360-070 |
| Sodium sulfate anhydrous, molecular biology grade | Applichem, A3487 |
| Supersignal West Femto Chemiluminescent substrate | Thermo Scientific, #34095 |
| Supersignal West Pico Chemiluminescent substrate | Thermo Scientific, #34080 |
| SYBR Safe | Invitrogen S33102 |
| T4 DNA ligase | New England Biolabs (NEB), M0202 |
| Tissue-Tek O.C.T | Sakura, 4583 |
| TransIT-X2 Dynamic | Mirus, MR6003 |
| Tris Ultrapure | Applichem, A1086 |
| Triton-X-100, molecular biology grade | Applichem, A1388 |
| Trypsin-EDTA Solution | Sigma, T3924 |
| Tween20 | Caesar & Lorentz, 3472 |
| Y-27632 | Biozol, S1049 |

## 5.2 Instruments and Apparatus

| | |
|---|---|
| Biometra Thermal Cycler | Biometra, TOne |
| BIO-TEK plate reader | Bio-Tek |
| Docu pH-Meter | Sartorius |
| EPS 601 Power supply | GE Healthcare, 18-1130-02 |
| Gel Doc™ XR+ Gel Documentation system | Biorad, 1708195 |
| Mini-centrifuge MCF 2360 | LMS |
| Mini-PROTEAN Tetra Cell for Mini Precast Gels | BioRad, 165-8004 |
| Multitube block heater | VWR, 12621-104 |
| Nutating mixer | VWR, 82007-202 |
| Optima L-80 XP ultracentrifuge | Beckman Coulter Inc. |
| Rotator | Staurt, SB2 |
| SW 40 Ti Rotor, Swinging bucket, Titanium | Beckman Coulter Inc. |
| Vortex mixers | Labtech, LVM-202 |
| VWR VistaVision Stereo microscope | VWR, 82027-160 |
| X-ray film developer Curix 60 | Agfa Healthcare |

## 5.3 Cell lines

### ATCC cell lines

**Table 4. ATCC cell lines**

| Name | Organism | Cell type |
|---|---|---|
| HEK293 | *Homo sapiens*,human | Embryonic kidney |
| hTERT RPE-1 | *Homo sapiens*,human | Human retinal pigmented epithelium |

**Table 5. Human induced pluripotent stem cells**

| Name | Organism | Cell type |
|---|---|---|
| NPC | *Homo sapiens*,human | hiPSC-differentiated neural progenitor cells |
| Astrocyte | *Homo sapiens*,human | hiPSC-differentiated astrocyte |
| hiPSC IMR-90 | *Homo sapiens*,human | Reprogramed skin cells |
| hiPSC TUB A/B GFP | *Homo sapiens*,human | Reprogramed skin cells |
| hIPSC TUBA/B RFP | *Homo sapiens*,human | Reprogramed skin cells |

**Table 6. Patient-derived GSCs**

| Name | Organism | Cell type | Subtypes |
|---|---|---|---|
| U3047MG | *Homo sapiens*, human | GBM, brain | Proneural |
| U3033MG | *Homo sapiens*, human | GBM, brain | Proneural |
| U3082MG | *Homo sapiens*, human | GBM, brain | Proneural |
| MGG87 | *Homo sapiens*, human | GBM, brain | Proneural |
| MGG8 | *Homo sapiens*, human | GBM, brain | Proneural |
| #275 | *Homo sapiens*, human | GBM, brain | Proneural |
| U3056MG | *Homo sapiens*, human | GBM, brain | Classical |
| U3024MG | *Homo sapiens*, human | GBM, brain | Mesenchymal |

**Table 7. Targeted GSC lines**

| Original name (naïve) | Targeting | Plasmid | Used Name |
|---|---|---|---|
| U3047MG | NEK2-WT | pLIX_403 NEK2-WT EGFP | U3047MG NEK2-WT |
| U3047MG | NEK2-KD | pLIX_403 NEK2-KD EGFP | U3047MG NEK2-KD |
| U3082MG | NEK2-WT | pLIX_403 NEK2-WT EGFP | U3082MG NEK2-WT |
| U3082MG | NEK2-KD | pLIX_403 NEK2-KD EGFP | U3082MG NEK2-KD |
| MGG87 | NEK2-WT | pLIX_403 NEK2-WT EGFP | MGG87 NEK2-WT |
| MGG87 | NEK2-KD | pLIX_403 NEK2-KD EGFP | MGG87 NEK2-KD |
| #275 | NEK2-WT | pLIX_403 NEK2-WT EGFP | #275 NEK2-WT |
| #275 | NEK2-KD | pLIX_403 NEK2-KD EGFP | #275 NEK2-KD |
| U3056MG | NEK2-WT | pLIX_403 NEK2-WT EGFP | U3056MG NEK2-WT |
| U3056MG | NEK2-KD | pLIX_403 NEK2-KD EGFP | U3056MG NEK2-KD |
| U3024MG | NEK2-WT | pLIX_403 NEK2-WT EGFP | U3024MG NEK2-WT |
| U3024MG | NEK2-KD | pLIX_403 NEK2-KD EGFP | U3024MG NEK2-KD |
| MGG87 | NEK2-WT | pLIX_403 NEK2-WT EGFP | MGG87 NEK2-WT |
| MGG87 | NEK2-KD | pLIX_403 NEK2-KD EGFP | MGG87 NEK2-KD |

## 5.4 Antibodies

**Table 8. Primary antibodies**

| Antibody/clone | dilution | Company/ source |
|---|---|---|
| Acetylated tubulin, mouse | 1:500 (IF) | Sigma-Aldrich, T7451 |
| AKT, rabbit | 1:10000 (WB) | Cell signalling, 9272 |
| ARL13B, rabbit | 1:200 (IF) | Proteintech, 17711-1-AP |
| Aurora-A, mouse | 1:50 (IF), 1:1000 (WB) | Cell Signaling, #12100 |
| c-MYC, rabbit | 1:1000 (WB) | Abcam, ab32072 |
| CD133, mouse | 1:20 (IF), 1:100 (WB) | DSHB, HB#7 |
| CD15, mouse | 1:20 (IF), 1:100 (WB) | DSHB, MC-480 |
| CD44, mouse | 1:50 (IF) | DSHB; H4C4 |
| CPAP, mouse | 1:20 (IF) | Hybridoma, C44 |
| GAPDH, mouse | 1:10000 (WB) | Proteintech, 60004-I-Ig |
| GFAP, rabbit | 1:200 (IF) | Cell signaling, D1F4Q |
| GT335 | 1:1000 (IF) | Adipogen, AG-20B-0020-C100 |
| IFT88 | 1:500 (IF) | Proteintech, 13967-1-AP |
| Ki-67, mouse | 1:50(IF) | DSHB, 3E6 |

| | | |
|---|---|---|
| KIF24, rabbit | 1:200 (IF), 1:1000 (WB) | Gift from Prof. Brian Dynlacht |
| MAP2 | 1:200 (IF) | Proteintech, 17490-1-AP |
| N-cadherin, rabbit | 1:500 (IF) | Abcam, ab18203 |
| NDE1, rabbit | 1:100(IF), 1:1000(WB9 | Proteintech, 10233-1-AP |
| NEK2, mouse | 1:200 (IF), 1:1000 (WB) | BD Bioscience, 610593 |
| NESTIN, mouse | 1:100 (IF) | Novus Biological, 4D11, |
| ODF2, rabbit | 1:1000 (WB) | Proteintech,12058-1-AP |
| OFD1, rabbit | 1:100 (IF), 1:500 (WB) | Gift from Prof. Jeremy Reiter |
| PAX6, mouse | 1: 50 (IF) | DSHB, Iowa University |
| PDGFR-$\alpha$, mouse | 1:100 (IF), 1:500 (WB) | SantaCruz, sc-398206 |
| Phospho-AKT, rabbit | 1:10000 (WB) | Cell signalling, |
| S100$\beta$ | 1:1000 (IF) | Abcam, ab52642 |
| SOX2, rabbit | 1:200 (IF) | Millipore, AB5603 |
| Synapsin1 | 1:200 (IF) | Cell Signalling, 5297S |
| TUJ1, rabbit | 1:500 (IF) | Sigma, T2200 |
| $\alpha$-FLAG, mouse | 1:5000 (WB) | Sigma-Aldrich, F1804 |
| $\alpha$-tubulin, mouse | 1:3000 (WB) | Sigma, DM1A |

**Table 9. Secondary antibodies**

| Antibody | Dilution | Company/ source |
|---|---|---|
| Donkey anti-Rabbit IgG (H+L) Highly Cross-Adsorbed Secondary Antibody, Alexa Fluor 488 | 1:1000 (IF) | Invitrogen, A-21206 |
| Donkey anti-Rabbit IgG (H+L) Highly Cross-Adsorbed, Secondary Antibody, Alexa Fluor 594 | 1:1000 (IF) | Invitrogen, A-21207 |
| Donkey anti-Rabbit IgG (H+L) Highly Cross-Adsorbed Secondary Antibody, Alexa Fluor 647 | 1:1000 (IF) | Invitrogen, A-31573 |
| Goat anti-Mouse IgG (H+L) Cross-Adsorbed Secondary Antibody, Alexa Fluor 488 | 1:1000 (IF) | Invitrogen, A-11001 |
| Goat anti-Mouse IgG (H+L) Highly Cross-Adsorbed Secondary Antibody, Alexa Fluor 594 | 1:1000 (IF) | Invitrogen, A-11032 |
| Goat anti-Mouse IgG (H+L) Cross-Adsorbed Secondary Antibody, Alexa Fluor 647 | 1:1000 (IF) | Invitrogen, A-21235 |
| Donkey anti-Rat IgG (H+L) Highly Cross-Adsorbed Secondary Antibody, Alexa Fluor 594 | 1:1000 (IF) | Invitrogen, A-21209 |
| Goat anti-Rat IgG (H+L) Cross-Adsorbed Secondary Antibody, Alexa Fluor 647 | 1:1000 (IF) | Invitrogen, A-21247 |
| Goat anti-Mouse IgG (H+L) Secondary Antibody, HRP | 1:5000 (WB) | Thermo Fisher Scientific, 31430 |
| Goat anti-Rabbit IgG (H+L) Secondary Antibody, HRP | 1:5000 (WB) | Invitrogen, 31466 |
| Goat anti-Rat IgG (H+L) Secondary Antibody, HRP | 1:5000 (WB) | Thermo Fisher Scientific, 31470 |

## 5.5 Solutions and mixtures

**Table 10. Buffers**

| |
|---|
| **BRB80 (1X)** |
| 80 mM K-Pipes (pH 6.8) |
| 1 mM MgCl2 |
| 1 mM Na2EGTA |
| **Homogenization buffer** |
| BRB80(1x) |
| 100 mM NaCl |
| 14% Sucrose |
| 1 mM PMSF |
| 1 mM Sodium Orthovanadate1 Protease Inhibitor Cocktail tablet (per 30 mL) |
| **100 mM PMSF (stock solution)** |
| Dissolve in isopropanol, store at -20 °C in the dark. Must be heated to 37 °C to redissolve after storage |
| **10X DNA gel loading dye (CSH Protocols)** |
| 3.9 ml glycerol<br>500 µl 10% (w/v) SDS<br>200 µl 0.5 M EDTA<br>0.025 g bromophenol blue<br>0.025 g xylene cyanol<br>Bring to 10 ml total volume with H2O. |
| **PBS** |
| 145 mM NaCl<br>7.5 mM $Na_2HPO_4$ 2.5 mM $NaH_2PO_4$ pH adjusted to 7.4 |
| **PBST** |
| PBS<br>0.1% Triton-X |

## 5.6 Molecular biology

NEK2WT and NEK2KD (K32R) were subcloned from pLVX 3xflag plasmid into an inducible lentiviral vector pLIX_403 containing the hPGK promoter and in-frame with C-terminal GFP. The pLVX 3xflag NEK2-WT and pLVX 3xflagNEK2-KD were generously provided Daynlacht lab (Kim et al.,2015)

### 5.6.1 Polymerase chain reaction (PCR)

DNA fragments used for cloning were amplified from cDNA or plasmid using Phusion High -Fidelity DNA polymerase (NEB, M0530) as follows:

Phusion PCR reaction mix:

| | |
|---|---|
| 5x Phusion GC buffer | 10 µl |
| 10mM dNTPs | 1µl |
| 10µM Forward primer | 2,5µl |
| 10µM Reverse primer | 2,5µl |
| Template DNA | 50-250ng |
| Phusion DNA Polymerase | 0,5µl |
| Nuclease -free $H_2O$ | up to 50µl |

Phusion PCR thermocycling conditions:

| STEP | TEMPERATURE | TIME |
|---|---|---|
| 1. Initial denaturation | 98 ºC | 5 mins |
| 2. 35 cycles: | | |
| a. Denaturation | 98 ºC | 10 s |
| b. Annealing | 60 ºC | 30 s |
| c. Elongation | 72 ºC | 30 s per kb |
| 3. Final extension | 72 ºC | 10 mins |
| 4. Hold | 4 ºC | |

**Table 11. List of oligonucleotide sequences used for cloning.**

| | |
|---|---|
| Primers used for cloning NEK2 into pEGFP_N1 | Forward primer: CCGCTCGAGATGCCTTCCCGGGCTGAGG |
| | Reverse primer: ATAAGAATGCGGCCGCTAAACTATTTACTTGTACAGCTCGTCCA |
| Primers used for cloning the NEK2 GFP into pENTR1a | Forward primer: CGACGCGTCGATGCCTTCCCGGGCTGAG |
| | Reverse primer: ATAAGAATGCGGCCGCTAAACTATTTACTTGTACAGCTCGTCCA |
| Primers used for cloning CPAP into pSin GFP | Forward primer: CGGGATCCCGGGATGGTGAGCAAGGGCGAGGAGCTG |
| | Reverse primer: CGACGCGTCAGCTCCGTGTCCATTAGCACATTAC |

### 5.6.2 Gel electrophoresis

The DNA fragments obtained by PCR were separated using 1% agarose gel 1xTAE buffer stained with SYBER Safe (Invitrogen). In brief, DNA product was mixed with 6X loading dye (Thermo Fischer Scientific), Gene ruler 1kb Plus was used as a reference ladder for DNA separation. Gel electrophoresis was carried out at the 120V for 45 min; bands were visualized using the Gel DocTM XR+ Gel Documentation system (Biorad). The separated DNA bands were cut from the agarose gel and further processed using the Gel Extraction Kit from Peqlab (peqGOLD) following manufacturers' instructions.

### 5.6.3 Restriction digest

New England Biolabs (NEB) restriction enzymes were used following the manufacturer's instructions for the restriction digest of DNA at specific sites.

### 5.6.4 Ligation

T4 DNA Ligase (NEB, M0202) was used to perform ligation, following the manufacturer's instructions. A molar range 1:3 vector vs. insert was used for the ligations.

## 5.7 2D cell culture

### 5.7.1 Culturing and maintenance of patient-derived GSCs

Patient-derived GSCs (U3047MG, U3033MG, U3082MG, U3024MG, U3056MG #275) as previously described (Xie et al., 2015) (Marziali et al., 2017) were cultured in Neurocult NS-A basal medium (STEMCELL technologies, 05750), 10 % BSA (STEMCELL technologies), L-Glutamin (Gibco, 25030081), Heparin (STEMCELL technologies), B27 without vitamin A (Gibco), N2 (Gibco, A1370701), 20ng/ml EGF (Peprotech), 20ng/ml bFGF (Peprotech). Cells were maintained at 37°C, and 5% CO2 on Poly-L Ornithine (Sigma) and Laminin (Sigma) coated plates. GSCs were cultured in stem cell medium as described above and analyzed for expression of stem cell markers such as SOX2, PAX6, and NESTIN for the absence of differentiation markers such as TUJ and GFAP. To study PDGFR-α signaling cells were stimulated with 20 ng/ml PDGF-AA ligand (R&D Systems) for 10–60 min for Western blot and immunofluorescence analysis. To study Hh signaling the agonist SAG (Tocris) 100nM was used, cells were fixed after 24h and analyzed for the downstream signaling molecules.

Prof. Dr. Karin Forsberg-Nilsson provided us most of the patient-derived GBM cells (U3024MG, U3056MG, U3047MG, U3082MG, U3033MG), acquired from the Human Glioblastoma Cell Culture resource (www.hgcc.se) at the Department of Immunology, Genetics, and Pathology, Uppsala University, Sweden. Dr. Hiroaki Wakimoto provided us with GSC cells MGG87, MGG8, from Massachusetts General Hospital. Prof. Dr. Roberto Pallini provided us GSC cells #450 and #275 from Universita` Cattolica del Sacro Cuore, Rome, Italy. All patients provided written informed consent to the study according to research proposals approved by the Institutional Ethics Committee of Fondazione Policlinico Gemelli, ID 2253 of Universita` Cattolica del Sacro Cuore, Rome, Italy UCSC (Prot. 4720/17).

### 5.7.2 Lentiviral production and transduction of target cells

Constitutive overexpression of mCherry U3047MG lentiviral vectors was prepared using pSicoR-Ef1a-mCh-Puro (Addgene, #31845), inducible pLix 603 NEK2-KD EGFP, pLix 603 NEK2-KD EGFP. The lentiviral shRNA constructs pLKO.1-puro of CDC components (NDE1, OFD1, HDAC, NEK2) were kindly gifted by Dr.Rajalingam. The cloned vectors were packed into lentivirus using second-generation packaging plasmids (pPMD, Addgene, #12259 and pPAX, Addgene, #12260). Briefly, target vectors and packaging plasmids were transfected into HEK293TS cells using calcium chloride. After 16 h, the medium was changed, and the virus was collected after 8 h. The freshly collected virus was used to transduce target cells in a 1:1 ratio for 72–96 h.

To generate GSCs lines stably expressing inducible NEK2-WT and NEK-KD, was used pLIX 603 lenti inducible gateway cloning vector (Addgene, #31845). The target cells were transduced with lentivirus containing pLIX-NEK2-WT and pLIX-NEK2-KD and selected with Puromycin (InvivoGen). For the expression of transgene, all the stable cell lines generated under inducible promoter were

induced with 2-5 µg/ml of doxycycline (Sigma) for 24–96 h. Prof. Roberto Pallini kindly provided GSCs cell line #275 green fluorescent protein (GFP).

### 5.7.3 Culturing and maintenance of human iPSC culture

At least three different human iPSCs were used in this study, namely, mEGFP (AICS-0012), mRFP (AICS-0031) TUBA1B, and IMR90 (Wicell). Cells were plated on Matrigel (Corning) coated culture dishes for 1h at 37°C with 5% CO2 using mTeSR1 medium (STEMCELL technologies). Cultures were routinely tested for mycoplasma contamination using MycoAlert Kit (Lonza). Cells were dissociated into small aggregates with ReLeSR (STEMCELL technologies) every 5-7 days and split into 1:5 fresh Matrigel-coated dishes.

### 5.7.4 Derivation of neural progenitor cells (NPCs) from iPSCs

For the generation of NPCs, the protocol from STEMCELL technologies was used. In brief, mycoplasma free iPSCs were cultured and analyzed for appropriate stem cell morphology. Once freshly split iPSCs (48h) reached 80% confluence, cells were disassociated into single cells using Accutase (Sigma-Aldrich, A6964) for 5 min at 37°C. To start the neural differentiation, 45.000 iPSCs cells were seeded in Spheroid v-bottom 96-well microplates (Costar,) growing with neural induction medium (NIM, STEMCELL technologies, 05835) containing 10µM ROCK inhibitor Y-27632 (Biozol) for 24h. Medium for neurospheres was changed partly every day for 5 days. On day 5, 32 neurospheres were plated in 35mm dish coated with Poly-L Ornithine (Sigma) and Laminin (Sigma) using NIM medium for another 7 days, the medium was replaced on alternate days. Neural rosettes were selected using Neural rosette selection reagent (STEMCELL technologies), and further plated into a coated plate (as above) using neural progenitor maintenance medium (STEMCELL technologies). After 5 days in neural maintenance medium, the cells were stained for neural stem cell markers such as NESTIN, SOX2, and PAX6. To prevent spontaneous differentiation, NPCs were maintained up to passage 6.

### 5.7.5 Astrocyte generation from neural progenitor cells

For the generation of astrocytes derived from NPCs, the modified protocol was used for NPC generation (Shi et al., 2012). In brief, mycoplasma free iPSCs were seeded in a Matrigel-coated dish. To start NPCs generation in 2D, iPSCs cells were grown till they reached 100% confluency. Optimized neural induction medium was used 1:1 mixture of DMEM/F12 and Neurobasal, 1:200 N2 supplement (Gibco), 1:100 B27 supplement without vitamin A (Thermo Fisher Scientific), 50µl 2-mercaptoethanol, 5µg/ml Insulin (Sigma), 1:100 L-Glutamin (Gibco), and 1:100 MEM-NEAA (Gibco), the medium supplemented with two SMAD pathway inhibitors 2,5 µM dorsomorphin (Sigma) and, 10µM SB431542 (Selleckchem) to drive differentiation of iPSCs to neural lineage.

The neural induction medium was changed every day, and cells were monitored for the morphological changes during the differentiation time between 8-10 days after plating. When the neuroepithelium sheet was properly formed, cells were split in aggregates of 300 to 500 cells using Dispase 1mg/ml for 30-45 min at 37°C.

Aggregates were seeded into 6 cm coated PLO and Laminin plate with neural induction medium supplemented with 20ng/ml bFGF (Peprotech) and 10µM Rock inhibitor. FGF2 is used to promote the expansion of NSCs but does not block neural differentiation. The medium was changed the next day with a neural maintenance medium. Change medium next day with neural maintenance medium. The sizes of the passaged cell aggregates influence the cell fate of the primitive neuroepithelium. If the cell clumps are smaller in size, only fewer cortical stem and progenitor cells are generated. Low passage NPCs are used to start astrocyte differentiation. Ensure that NPCs are spit 24h before and confluency is 100% when we change medium to astrocyte differentiation: Neurobasal phenol-free (Gibco), IGF1 20ng/ml (Peprotech), Heregulin 10ng/ml (Peprotech) CNTF 10ng/ml, Glutamax 1x (Gibco), B27 without vitamin A 1x (Gibco), Primocin 100µg/ml (InvivoGen).

The astrocyte differentiation medium was changed every day until we observed morphology change. After 15 days, cells were split and analyzed for NESTIN and CD44 intermediate astrocyte marker. Until 80 % of the cells expressed GFAP and S100β,98 the cells where maintain in the astrocyte differentiation medium. For the astrocyte maintenance, astrocyte growing medium was used up to passage 5 when astrocytes get terminated. Astrocyte growing medium: 1:1 mixture of DMEM/F12(Gibco) and Neurobasal (Gibco), EGF 5ng/ml (Peprotech), B27 without vitamin A 1x (Gibco), N2 (Gibco), Primocin 100µg/ml (InvivoGen).

### 5.7.6 Small interfering (si)RNA transfection

Synthetic siRNA oligonucleotides were obtained from SMARTPool Dharmacon. Cells U3047MG and U3047MG NEK2-KD (+DOX 48h) (1×106) were transfected with 40 nM siRNA targeting IFT88 or with a scrambled sequence (negative control siRNA) for 72 h using TransIT-X2 Dynamic (Mirus) according to manufactures instructions. The knockdown efficiency of IFT88 siRNA was assessed using western blot analysis and immunofluorescence staining for IFT88. Negative control siRNA (Qiagen) was used as a scramble siRNA.

### 5.7.7 Immuno-staining and light microscopy analysis of 2D cells

**Fixation with Methanol**:
After removing the medium from the cells, cells were washed once washed in PBS, then cold Methanol (-20 °C) was added and incubated at -20 °C for 10 min. The methanol was then aspirated, and cold PBS was added to the fixed cells until further use.

**Fixation with 4 % PFA**:

Briefly, the medium was aspirated from the cells, and the cells were washed with prewarmed PBS. Prewarmed, 4% PFA was used to fic the cells at 37°C for 10 min. The fixative was then removed, and the cells were once again washed with PBS and stored at 4°C until further use.

**Blocking**:

Blocking solution 0,5% Fish gelatin was added and incubated for one hour at RT.

**Primary antibodies**:

The primary antibody was prepared in the blocking solution. Cells were incubated for one hour at RT or overnight with the primary antibody. Cells were washed 3x with a blocking solution for 5 min at RT.

**Secondary antibody:**

The secondary antibody was prepared in the blocking solution. Cells were incubated for one hour at RT.

**Mounting:**

After the final wash with a blocking solution, the cells were washed once with water to remove any salt and proteins. The coverslips were then partially dried. For coverslips mounting, 8µl Mowiol® was applied onto the slide, followed by placement of the coverslip upside down on top of it. Stored at 4 °C until imaging. Confocal images were collected using a Leica SP8 scanning confocal microscope. Fiji, Adobe Photoshop, and Illustrator were further used to process the images.

## 5.8 3D cell culture

### 5.8.1 Establishment of different assay conditions to model patient-derived GSCs in brain organoids

#### 5.8.1.1 Assay 1: Simultaneous co-culturing of GSCs with differentiating brain organoid differentiation

Brain organoids were generated as previously demonstrated with slight modifications (Gabriel and Gopalakrishnan, 2017, Gabriel et al., 2017, Gabriel et al., 2016). In brief, mycoplasma free iPSCs were cultured and checked for appropriate stem cell morphology. Once iPSCs reached 80% confluency cells were disassociated into single cells using Accutase (Sigma-Aldrich) for 5 min at 37°C. For this assay condition, we homogeneously mixed 35.000 iPSCs with 5000 GSCs in CellCarrier Spheroid ULA 96-well microplates (PerkinElmer) with the use of neural induction medium (NIM, STEMCELL technologies) containing 10µM ROCK inhibitor Y-27632 (Biozol) for 24h. 100µl of the mix was suspended into cell suspension was given into each well of ULA 96 well U-bottom and incubated at 37°C in 5% $CO_2$. This process helps in the formation of neurospheres, and the medium is changed once every day for the next 5 days.

Neurospheres were embedded in droplet of Matrigel (Corning, 356234) using an organoid-embedding sheet (STEMCELL technologies, 08579). Droplets were solidified at 37°C and were

grown 4 days without agitation in neurosphere medium containing a 1:1 mixture of DMEM/F12 and Neurobasal, 1:200 N2 supplement (Thermo Fisher Scientific), 1:100 B27 supplement without vitamin A (Thermo Fisher Scientific), 50µl 2-mercaptoethanol, Insulin (Sigma), 1:100 L-Glutamin (Gibco), and 1:100 MEM-NEAA (Gibco). After 4 days, neurospheres were transferred to a spinner flask containing brain organoid medium which is essentially neurosphere medium supplemented with two SMAD pathway inhibitors 2,5 µM dorsomorphin (Sigma,) and 25 µm SB431542 (Selleckchem). We name these organoids as hybrid organoids, as described in the results. Hybrid organoids were taken at day 10 and cultured in air diffusing low adherent plates (Lumox, Sarstedt). This set up allows the growth of organoids for a prolonged period of time, allowing us to image the same organoids at day 20 and 30. Imaging conditions are described at the respective section scheme **(Figure 3.12A)**. Except for the selected organoids for time-lapse imaging, the remaining organoids were cultured in spinner flasks for up to day-30 for endpoint analysis. From this batch of spinner flask organoids, organoids were selected for tissue clearing and 3D imaging at day-10, day-20, and day-30.

#### 5.8.1.2 Assay 2: Supplementing GSCs as dispersed cells to organoids

For this assay, brain organoids were generated as described above without co-culturing with GSCs. 10-day old organoids were shifted to 35 mm air diffusing low adherent plate Lumox dish (Sarstedt), and 1000 GSCs were provided at the vicinity of the organoids as depicted in the experimental scheme **(Figure. 3.13A).** After 24h, organoids were subjected to live imaging to analyze. GSCs invasion in a time-lapse manner at day-1, day-10, and day-20. The organoids that were no needed for the time-lapse imaging were transferred into spinner flasks for endpoint analysis at day 30. Organoids were selected for tissue clearing and 3D imaging on day-1, day-10, and day- 20 after GSCs invasion.

#### 5.8.1.3 Assay3: Fusion of GSCs spheres to organoids

Brain organoids used in this assay condition were generated as described above. Initiating fusion product (GSCs-Organoids), first GSCs spheres were established by seeding 5000 GSCs in low adherent “U” shaped microwells (ULA 96 well plate). GSCs spheres were added to either 20-day or 60-day organoids in low adherent “U” shaped microwells **(Figure 3.14 A)**. The resulting fusion product (GSCs-Organoids) was used to mimic conditions similar to tumor microenvironment or drug treatments. To mimic tumor microenvironment, we provided 100 nM recombinant human Neuroglin3/NLGN3 (R&Dsystems, 9069-NL). For drug testing, GSCs-organoid were subjected to ADAM10 inhibitor GI254023X (Sigma, SML0789) at a final concertation 100 nM.

### 5.8.2 Whole organoid tissue clearing

Tissue clearing was essentially performed based on the previously described method adapting additional modifications and optimizations (Klingberg et al, 2017). In brief, organoids were fixed in 4%PFA (Merck Millipore) for 30 min. Organoids were dehydrated sequentially in graded ethanol

(EtOH) series of 30% EtOH (vol/vol), 50% EtOH (vol/vol), 75% EtOH (vol/vol) and 100% EtOH (vol/vol) (each step for up to 5-10 min at 4°C in a gently shaking 2ml tube depending on the size of organoids) and subsequent tissue clearing was performed with Ethyl cinnamate (ECI; Sigma-Aldrich) for approximately 10-20 min at room temperature depending on the size of organoids. Clarified organoids were then placed into coverslip bottom µ-slides (Ibidi) and stored at 4°C until imaging.

### 5.8.3 Immunofluorescence microscopy and time-lapse imaging of organoids

For time-lapse imaging, organoids were grown in 35 mm air diffusing low adherent plate Lumox dish (Sarstedt), with low autofluorescence and high light transmission properties. Alternatively, we also used µ-Slide angiogenesis slides (Ibidi) for imaging live organoids. Images were acquired at different time points using Leica SP8 laser scanning confocal microscope equipped with 405, 488, 552 and 638nm diode lasers, a hybrid GaAsP detector, two confocal PMT SP detector, a HC PL APO 20x/0.75 CS2 plan apochromatic objective, and a HC PL APO 63x1.40 OIL CS2 plan apochromatic objective. Images were captured using the 20X air objective. The resulting 8-bit image files were imported into Fiji (ImageJ 1.52i) and maximum intensity projected. Finally, the TIFF files from Fiji were processed using Photoshop (Adobe CC 2018), and Adobe Illustrator (Adobe CC 2018).
Tissue cleared organoids were imaged using Zeiss LSM 880 Airyscan confocal microscope equipped with laser lines 405, 488, 561, and 633 nm, a GaAsP detector, two PMT detectors Plan-Neoflaur 10x/0.3, and Plan-Apochromat 20x/0.8 M27 objectives. The tissue organoids were placed in ECI in 35 mm air diffusing or µ-Slide angiogenesis slides while imaging. 3D image stacks were acquired for representative organoids. The interval between the stacks was kept 2-3 µm apart, depending on the size of the organoids. The captured image files were imported into Fiji. The files were further processed using Image J, Adobe photoshop CC 2018, and Adobe Illustrator CC 2018. The z-stack movies were prepared using Fiji. Image-based quantifications were performed manually using Fiji.
Super-resolution microscopy was performed on a 3D dimensional structured illumination microscope ELYRA PS.1 equipped with an alpha Plan-Fluar 100x/1.45 M27 oil-immersion objective, 405, 488 and 561nm laser lines, an EM-CCD camera with a maximum resolution of 1004x1004. SR-SIM images were processed using ZEN software (2.3, SP1, black, 64bit, release version 14.0.0.0; ZEISS, Oberkochen, Germany) for 3D reconstruction and deconvolution.

### 5.8.4 Organoid Immunostaining

Organoids were fixed with 4% paraformaldehyde (PFA, Merck Millipore) for 30 mins. Fixed organoids were then dehydrated in 30% sucrose overnight at 4 °C. Dehydrated organoids were added in the OCT compound and frozen for the sectioning at -20 °C. The sections were cut using a microtome. Cryosections were washed with PBS to remove excess OCT compound and blocked in 0,5% fish gelatin 0.1% Triton X-100 diluted in PBS for 1 h at room temperature. The sections were then

incubated overnight at 4 °C with primary antibodies diluted in blocking solution. The following primary antibodies were used for immunostaining: anti-MAP2 (rabbit, 1:200, Proteintech, 17490-1-AP), and anti-Synapsin1 (D12G5) (1:200, rabbit, Cell Signalling), and anti-GFAP (Cell signaling). Cryosections were incubated with secondary antibodies (goat-anti mouse Alexa 488 or 647; donkey anti-rabbit Alexa 488, 594 or 647) diluted in ablocking solution 1h at room temperature.

## 5.9 Biochemistry

### 5.9.1 Protein concentration

Protein concentration was measured using Bradford assay. To generate a standard curve absorbance at 595 nm series dilution of BSA protein was prepared (BSA solutions of concentrations 0, 0.25, 0.50, 0.75, 1.00, 1.25, 1.50, and 2.00 mg/ mL). In the 96 well plates, 1 μL of protein sample was added to which 99 μL of Bradford reagent (Sigma-Aldrich) was added. The plate was shaken for 30 s, and incubated for 10 minutes at RT, after which the absorbance at 595 nm was measured using a BIO-TEK plate reader. Protein concentrations were calculated using the standard curve.

### 5.9.2 Denaturing SDS-polyacrylamide gel electrophoresis (SDS-PAGE) and western blot

The electrophoretic gel separation of proteins was performed under denaturing conditions in the presence of SDS in a non-continuous gel system, which consisted of a 5 % stacking gel and 10 or 12 % resolving gel. According to their molecular size, the proteins are separated based on their similar mass/charge ratios during electrophoresis. The separation is possible since the negatively charged detergent SDS is complex with the proteins, their charge superimposed, resulting in a uniform negative charge. The protein samples were prepared with the SDS sample buffer (4X) for 10 min at 98 °C. As a reference, the pre-stained Gene Ruler from Thermofisher was used. 20 µg of protein per well was loaded on the well. The samples were allowed to run at 100 V for 10 min until it reached the resolving gel. Then the gel was run at 180 V until the ladder extended through the whole gel.

The separated proteins were transferred from the gel to a nitrocellulose membrane applying the wet transfer method using 20 % methanol at 135 V for 1 hour 15 min.

Once the transfer was complete, the membrane was soaked into 5 % milk in TRIS/HCl based buffer (TBS) for a minimum of 30 min at RT. The membrane was then washed six times with $ddH_20$ followed by TBS with 0.1 % Tween 20 (TBST) and incubated with primary antibodies overnight at 4 °C. The next morning the membrane rewashed with $ddH_20$ and TBST before incubating for one hour with the appropriate HRP-conjugated secondary antibody (1:5000 dilution). The membrane was developed using an ECL detection solution from Thermo scientific. To visualize the proteins, a conventional X-Ray film developing technique was used.

### 5.9.3 FLAG-immunoprecipitation (FLAG-IP)

Flag coted beads (Sigma Aldrich) were incubated with high-speed lysate (HSL) for 3h at 4°C. The lysates were prepared using HEK293T cells stable expressing pSIN CPAP-WT 3xflag and pLenti NEK2-WT 3xflag lysed with 1x BRB80 buffer (extract buffer) as described previously (Gopalakrishnan et al., 2011). After incubation, the beads were washed 3x times with extract buffer and washed 2x with high-salt buffer containing 500 mM salt, and final wash with buffer containing 100 mM NaCl, the samples were eluted by boiling them in 2x Laemmli buffer at 98°C. The beads were analyzed by western blotting for the CPAP and NEK2-complexes.

## 5.10 RNA sequencing and analysis

U3047MG (before ciliation) cells and U3047-NEK2-KD (after ciliation) cells were collected and washed. Total RNA was isolated and DNase-treated using the DirectZol RNA kit (Zymo Research). Approximately 2 µg of total RNA was used to subselect poly(A)$^+$ transcripts and generate strand-specific cDNA libraries (TrueSeq kit; Illumina).
Poly(A)-enriched RNA was prepared and sequenced on a HiSeq4000 platform (Illumina; strand-specific) to >35x106 reads per sample. Reads were quality assessed and mapped to hg19 using STAR (Dobin et al., 2013), followed by quantification of unique exon counts using featureCounts (Liao et al., 2014). Counts were further normalized via the RUVs function of RUVseq (Risso et al., 2014) to estimate factors of unwanted variation using those genes in the replicates for which the covariates of interest remain constant and correct for unwanted variation before differential gene expression was estimated using DESeq2 (Love et al., 2014). Genes with an FDR <0.01 and an absolute (log2) fold-change of >0.6 were deemed differentially-expressed and listed in the RNA sequencing table (Appendix). RNA sequencing analysis was performed and analyzed in Dr. Akis Papantoni's lab.

## 5.11 Statistical analysis

Data were analyzes statistically using GraphPad Prism 7 for Mac OS X (Version 7.0e, September 5, 2018). Data are presented as mean ± SEM The following tests were used to obtain P values: two-way ANOVA, followed by Sidak's multiple comparisons test or Tukey's multiple comparisons test or unpaired t-test or Dunnett's multiple comparisons test. n.s, indicates no significance, *P <0.01, **P <0.001, ***P <0.0001.

# References


ALBERTS, B., JOHNSON, A., LEWIS, J., WALTER, P., RAFF, M., and ROBERTOS, K. 2002. Molecular Biology of the Cell 4th Edition, *Garland Science*.

Alcantara D, O'Driscoll M (2014) Congenital microcephaly. American journal of medical genetics Part C, Seminars in medical genetics

Avidor-Reiss T, Gopalakrishnan J (2012) Building a centriole. Current opinion in cell biology

Bazzi H, Anderson KV (2014) Acentriolar mitosis activates a p53-dependent apoptosis pathway in the mouse embryo. Proceedings of the National Academy of Sciences of the United States of America 111: E1491-1500

Chang C, Ortiz K, Ansari A, Gershwin ME (2016) The Zika outbreak of the 21st century. Journal of autoimmunity 68: 1-13

Driggers RW, Ho CY, Korhonen EM, Kuivanen S, Jaaskelainen AJ, Smura T, Rosenberg A, Hill DA, DeBiasi RL, Vezina G, Timofeev J, Rodriguez FJ, Levanov L, Razak J, Iyengar P, Hennenfent A, Kennedy R, Lanciotti R, du Plessis A, Vapalahti O (2016) Zika Virus Infection with Prolonged Maternal Viremia and Fetal Brain Abnormalities. The New England journal of medicine

Gabriel E, Gopalakrishnan J (2017) Generation of iPSC-derived Human Brain Organoids to Model Early Neurodevelopmental Disorders. Journal of visualized experiments : JoVE

Gabriel E, Ramani A, Karow U, Gottardo M, Natarajan K, Gooi LM, Goranci-Buzhala G, Krut O, Peters F, Nikolic M, Kuivanen S, Korhonen E, Smura T, Vapalahti O, Papantonis A, Schmidt-Chanasit J, Riparbelli M, Callaini G, Kronke M, Utermohlen O, Gopalakrishnan J (2017) Recent Zika Virus Isolates Induce Premature Differentiation of Neural Progenitors in Human Brain Organoids. Cell stem cell

Gabriel E, Wason A, Ramani A, Gooi LM, Keller P, Pozniakovsky A, Poser I, Noack F, Telugu NS, Calegari F, Saric T, Hescheler J, Hyman AA, Gottardo M, Callaini G, Alkuraya FS, Gopalakrishnan J (2016a) CPAP promotes timely cilium disassembly to maintain neural progenitor pool. The EMBO journal 35: 803-819

Gabriel E, Wason A, Ramani A, Gooi LM, Keller P, Pozniakovsky A, Poser I, Noack F, Telugu NS, Calegari F, Saric T, Hescheler J, Hyman AA, Gottardo M, Callaini G, Alkuraya FS, Gopalakrishnan J (2016b) CPAP promotes timely cilium disassembly to maintain neural progenitor pool. The EMBO journal

Gabriel Eea CPAP promotes timely cilium disassembly to maintain neural progenitor pool. Under review in EMBO Journal

Garcez PP, Diaz-Alonso J, Crespo-Enriquez I, Castro D, Bell D, Guillemot F (2015) Cenpj/CPAP regulates progenitor divisions and neuronal migration in the cerebral cortex downstream of Ascl1. Nature communications 6: 6474

Gopalakrishnan J, Frederick Chim YC, Ha A, Basiri ML, Lerit DA, Rusan NM, Avidor-Reiss T (2012) Tubulin nucleotide status controls Sas-4-dependent pericentriolar material recruitment. Nature cell biology 14: 865-873

Gopalakrishnan J, Mennella V, Blachon S, Zhai B, Smith AH, Megraw TL, Nicastro D, Gygi SP, Agard DA, Avidor-Reiss T (2011) Sas-4 provides a scaffold for cytoplasmic complexes and tethers them in a centrosome. Nature communications 2: 359

Gotz M, Huttner WB (2005) The cell biology of neurogenesis. Nature reviews Molecular cell biology 6: 777-788

Insolera R, Bazzi H, Shao W, Anderson KV, Shi SH (2014) Cortical neurogenesis in the absence of centrioles. Nature neuroscience 17: 1528-1535

Lancaster MA, Renner M, Martin CA, Wenzel D, Bicknell LS, Hurles ME, Homfray T, Penninger JM, Jackson AP, Knoblich JA (2013) Cerebral organoids model human brain development and microcephaly. Nature 501: 373-379

Majora M, Sondenheimer K, Knechten M, Uthe I, Esser C, Schiavi A, Ventura N, Krutmann J (2018) HDAC inhibition improves autophagic and lysosomal function to prevent loss of subcutaneous fat in a mouse model of Cockayne syndrome. Science translational medicine 10

Mariani J, Coppola G, Zhang P, Abyzov A, Provini L, Tomasini L, Amenduni M, Szekely A, Palejev D, Wilson M, Gerstein M, Grigorenko EL, Chawarska K, Pelphrey KA, Howe JR, Vaccarino FM (2015) FOXG1-Dependent Dysregulation of GABA/Glutamate Neuron Differentiation in Autism Spectrum Disorders. Cell 162: 375-390

Mohammadi-Asl J, Hajjari M, Tahmasebi Birgani M, Riahi K, Nasiri H, Kollaee A (2018) Exome sequencing revealed a novel deletion in the ERCC8 gene in an Iranian family with Cockayne syndrome. Annals of human genetics 82: 304-308

Pyo JH, Park JS, Na HJ, Jeon HJ, Lee SH, Kim JG, Park SY, Jin YW, Kim YS, Yoo MA (2014) Functional modification of Drosophila intestinal stem cells by ionizing radiation. Radiation research 181: 376-386

Rakic P (1995) A small step for the cell, a giant leap for mankind: a hypothesis of neocortical expansion during evolution. Trends in neurosciences 18: 383-388

Shimada M, Matsuzaki F, Kato A, Kobayashi J, Matsumoto T, Komatsu K (2016) Induction of Excess Centrosomes in Neural Progenitor Cells during the Development of Radiation-Induced Microcephaly. PloS one 11: e0158236

Tsunekawa Y, Kikkawa T, Osumi N (2014) Asymmetric inheritance of Cyclin D2 maintains proliferative neural stem/progenitor cells: a critical event in brain development and evolution. Development, growth & differentiation 56: 349-357

Wollnik B A common mechanism for microcephaly. Nature genetics 42: 923-924

Zheng X, Gooi LM, Wason A, Gabriel E, Mehrjardi NZ, Yang Q, Zhang X, Debec A, Basiri ML, Avidor-Reiss T, Pozniakovsky A, Poser I, Saric T, Hyman AA, Li H, Gopalakrishnan J (2014) Conserved TCP domain of Sas-4/CPAP is essential for pericentriolar material tethering during centrosome biogenesis. Proceedings of the National Academy of Sciences of the United States of America 111: E354-363

Zheng X, Ramani A, Soni K, Gottardo M, Zheng S, Ming Gooi L, Li W, Feng S, Mariappan A, Wason A, Widlund P, Pozniakovsky A, Poser I, Deng H, Ou G, Riparbelli M, Giuliano C, Hyman AA, Sattler M, Gopalakrishnan J, Li H (2016) Molecular basis for CPAP-tubulin interaction in controlling centriolar and ciliary length. Nature communications 7: 11874

.

ALKURAYA, F. S., CAI, X., EMERY, C., MOCHIDA, G. H., AL-DOSARI, M. S., FELIE, J. M., HILL, R. S., BARRY, B. J., PARTLOW, J. N., GASCON, G. G., KENTAB, A., JAN, M., SHAHEEN, R., FENG, Y. & WALSH, C. A. 2011. Human mutations in NDE1 cause extreme microcephaly with lissencephaly [corrected]. *Am J Hum Genet,* 88**,** 536-47.

ANDRAE, J., GALLINI, R. & BETSHOLTZ, C. 2008. Role of platelet-derived growth factors in physiology and medicine. *Genes Dev,* 22**,** 1276-312.

AVIDOR-REISS, T. & GOPALAKRISHNAN, J. 2012. Building a centriole. *Curr Opin Cell Biol*.

AVIDOR-REISS, T. & GOPALAKRISHNAN, J. 2013. Cell Cycle Regulation of the Centrosome and Cilium. *Drug Discov Today Dis Mech,* 10**,** e119-e124.

BADANO, J. L., MITSUMA, N., BEALES, P. L. & KATSANIS, N. 2006. The ciliopathies: an emerging class of human genetic disorders. *Annu Rev Genomics Hum Genet,* 7**,** 125-48.

BALE, A. E. 2002. Hedgehog signaling and human disease. *Annu Rev Genomics Hum Genet,* 3**,** 47-65.

BANGS, F. & ANDERSON, K. V. 2017. Primary Cilia and Mammalian Hedgehog Signaling. *Cold Spring Harb Perspect Biol,* 9.

BASTEN, S. G., WILLEKERS, S., VERMAAT, J. S., SLAATS, G. G., VOEST, E. E., VAN DIEST, P. J. & GILES, R. H. 2013. Reduced cilia frequencies in human renal cell carcinomas versus neighboring parenchymal tissue. *Cilia,* 2**,** 2.

BAUDOIN, J. P., VIOU, L., LAUNAY, P. S., LUCCARDINI, C., ESPESO GIL, S., KIYASOVA, V., IRINOPOULOU, T., ALVAREZ, C., RIO, J. P., BOUDIER, T., LECHAIRE, J. P., KESSARIS, N., SPASSKY, N. & METIN, C. 2012. Tangentially migrating neurons assemble a primary cilium that promotes their reorientation to the cortical plate. *Neuron,* 76**,** 1108-22.

BAY, S. N., LONG, A. B. & CASPARY, T. 2018. Disruption of the ciliary GTPase Arl13b suppresses Sonic hedgehog overactivation and inhibits medulloblastoma formation. *Proc Natl Acad Sci U S A,* 115**,** 1570-1575.

BHADURI, A., DI LULLO, E., JUNG, D., MULLER, S., CROUCH, E. E., ESPINOSA, C. S., OZAWA, T., ALVARADO, B., SPATAZZA, J., CADWELL, C. R., WILKINS, G., VELMESHEV, D., LIU, S. J., MALATESTA, M., ANDREWS, M. G., MOSTAJO-RADJI, M. A., HUANG, E. J., NOWAKOWSKI, T. J., LIM, D. A., DIAZ, A., RALEIGH, D. R. & KRIEGSTEIN, A. R. 2020. Outer Radial Glia-like Cancer Stem Cells Contribute to Heterogeneity of Glioblastoma. *Cell Stem Cell,* 26**,** 48-63 e6.

BOEKHOUT, M. & WOLTHUIS, R. 2015. Nek2A destruction marks APC/C activation at the prophase-to-prometaphase transition by spindle-checkpoint-restricted Cdc20. *J Cell Sci,* 128**,** 1639-53.

BRENNAN, C., MOMOTA, H., HAMBARDZUMYAN, D., OZAWA, T., TANDON, A., PEDRAZA, A. & HOLLAND, E. 2009. Glioblastoma subclasses can be defined by activity among signal transduction pathways and associated genomic alterations. *PLoS One,* 4**,** e7752.

BREUNIG, J. J., SARKISIAN, M. R., ARELLANO, J. I., MOROZOV, Y. M., AYOUB, A. E., SOJITRA, S., WANG, B., FLAVELL, R. A., RAKIC, P. & TOWN, T. 2008. Primary cilia regulate hippocampal neurogenesis by mediating sonic hedgehog signaling. *Proc Natl Acad Sci U S A,* 105**,** 13127-32.

BRISCOE, J. & THEROND, P. P. 2013. The mechanisms of Hedgehog signalling and its roles in development and disease. *Nat Rev Mol Cell Biol,* 14**,** 416-29.

CAJANEK, L. & NIGG, E. A. 2014. Cep164 triggers ciliogenesis by recruiting Tau tubulin kinase 2 to the mother centriole. *Proc Natl Acad Sci U S A,* 111**,** E2841-50.

CALEGARI, F. & HUTTNER, W. B. 2003. An inhibition of cyclin-dependent kinases that lengthens, but does not arrest, neuroepithelial cell cycle induces premature neurogenesis. *J Cell Sci,* 116**,** 4947-55.

CAMARGO ORTEGA, G., FALK, S., JOHANSSON, P. A., PEYRE, E., BROIX, L., SAHU, S. K., HIRST, W., SCHLICHTHAERLE, T., DE JUAN ROMERO, C., DRAGANOVA, K., VINOPAL, S., CHINNAPPA, K., GAVRANOVIC, A., KARAKAYA, T., STEININGER, T., MERL-PHAM, J., FEEDERLE, R., SHAO, W., SHI, S. H., HAUCK, S. M., JUNGMANN, R., BRADKE, F., BORRELL, V., GEERLOF, A., REBER, S., TIWARI, V. K., HUTTNER, W. B., WILSCH-BRAUNINGER, M., NGUYEN, L. & GOTZ, M. 2019. The centrosome protein AKNA regulates neurogenesis via microtubule organization. *Nature,* 567**,** 113-117.

CAPPELLO, P., BLASER, H., GORRINI, C., LIN, D. C., ELIA, A. J., WAKEHAM, A., HAIDER, S., BOUTROS, P. C., MASON, J. M., MILLER, N. A., YOUNGSON, B., DONE, S. J. & MAK, T.

W. 2014. Role of Nek2 on centrosome duplication and aneuploidy in breast cancer cells. *Oncogene,* 33**,** 2375-84.
CAREN, H., STRICKER, S. H., BULSTRODE, H., GAGRICA, S., JOHNSTONE, E., BARTLETT, T. E., FEBER, A., WILSON, G., TESCHENDORFF, A. E., BERTONE, P., BECK, S. & POLLARD, S. M. 2015. Glioblastoma Stem Cells Respond to Differentiation Cues but Fail to Undergo Commitment and Terminal Cell-Cycle Arrest. *Stem Cell Reports,* 5**,** 829-842.
CARVALHO-SANTOS, Z., AZIMZADEH, J., PEREIRA-LEAL, J. B. & BETTENCOURT-DIAS, M. 2011. Evolution: Tracing the origins of centrioles, cilia, and flagella. *J Cell Biol,* 194**,** 165-75.
CHEFETZ, I., HOLMBERG, J. C., ALVERO, A. B., VISINTIN, I. & MOR, G. 2011. Inhibition of Aurora-A kinase induces cell cycle arrest in epithelial ovarian cancer stem cells by affecting NFkB pathway. *Cell Cycle,* 10**,** 2206-14.
CHEN, J. L., CHANG, C. H. & TSAI, J. W. 2019. Gli2 Rescues Delays in Brain Development Induced by Kif3a Dysfunction. *Cereb Cortex,* 29**,** 751-764.
CHIZHIKOV, V. V., DAVENPORT, J., ZHANG, Q., SHIH, E. K., CABELLO, O. A., FUCHS, J. L., YODER, B. K. & MILLEN, K. J. 2007. Cilia proteins control cerebellar morphogenesis by promoting expansion of the granule progenitor pool. *J Neurosci,* 27**,** 9780-9.
CHRISTENSEN, S. T., CLEMENT, C. A., SATIR, P. & PEDERSEN, L. B. 2012. Primary cilia and coordination of receptor tyrosine kinase (RTK) signalling. *J Pathol,* 226**,** 172-84.
CHRISTENSEN, S. T., MORTHORST, S. K., MOGENSEN, J. B. & PEDERSEN, L. B. 2017. Primary Cilia and Coordination of Receptor Tyrosine Kinase (RTK) and Transforming Growth Factor beta (TGF-beta) Signaling. *Cold Spring Harb Perspect Biol,* 9.
CHRISTENSEN, S. T., PEDERSEN, S. F., SATIR, P., VELAND, I. R. & SCHNEIDER, L. 2008. The primary cilium coordinates signaling pathways in cell cycle control and migration during development and tissue repair. *Curr Top Dev Biol,* 85**,** 261-301.
CLARKE, I. D. & DIRKS, P. B. 2003. A human brain tumor-derived PDGFR-alpha deletion mutant is transforming. *Oncogene,* 22**,** 722-33.
CORLESS, C. L., BARNETT, C. M. & HEINRICH, M. C. 2011. Gastrointestinal stromal tumours: origin and molecular oncology. *Nat Rev Cancer,* 11**,** 865-78.
CORMIER, A., CLEMENT, M. J., KNOSSOW, M., LACHKAR, S., SAVARIN, P., TOMA, F., SOBEL, A., GIGANT, B. & CURMI, P. A. 2009. The PN2-3 domain of centrosomal P4.1-associated protein implements a novel mechanism for tubulin sequestration. *J Biol Chem,* 284**,** 6909-17.
DERE, R., PERKINS, A. L., BAWA-KHALFE, T., JONASCH, D. & WALKER, C. L. 2015. beta-catenin links von Hippel-Lindau to aurora kinase A and loss of primary cilia in renal cell carcinoma. *J Am Soc Nephrol,* 26**,** 553-64.
DING, X. F., ZHOU, J., HU, Q. Y., LIU, S. C. & CHEN, G. 2015. The tumor suppressor pVHL down-regulates never-in-mitosis A-related kinase 8 via hypoxia-inducible factors to maintain cilia in human renal cancer cells. *J Biol Chem,* 290**,** 1389-94.
DO, T. V., XIAO, F., BICKEL, L. E., KLEIN-SZANTO, A. J., PATHAK, H. B., HUA, X., HOWE, C., O'BRIEN, S. W., MAGLATY, M., ECSEDY, J. A., LITWIN, S., GOLEMIS, E. A., SCHILDER, R. J., GODWIN, A. K. & CONNOLLY, D. C. 2014. Aurora kinase A mediates epithelial ovarian cancer cell migration and adhesion. *Oncogene,* 33**,** 539-49.
DOBIN, A., DAVIS, C. A., SCHLESINGER, F., DRENKOW, J., ZALESKI, C., JHA, S., BATUT, P., CHAISSON, M. & GINGERAS, T. R. 2013. STAR: ultrafast universal RNA-seq aligner. *Bioinformatics,* 29**,** 15-21.
EGEBERG, D. L., LETHAN, M., MANGUSO, R., SCHNEIDER, L., AWAN, A., JORGENSEN, T. S., BYSKOV, A. G., PEDERSEN, L. B. & CHRISTENSEN, S. T. 2012. Primary cilia and aberrant cell signaling in epithelial ovarian cancer. *Cilia,* 1**,** 15.
EMOTO, K., MASUGI, Y., YAMAZAKI, K., EFFENDI, K., TSUJIKAWA, H., TANABE, M., KITAGAWA, Y. & SAKAMOTO, M. 2014. Presence of primary cilia in cancer cells correlates with prognosis of pancreatic ductal adenocarcinoma. *Hum Pathol,* 45**,** 817-25.
EZRATTY, E. J., STOKES, N., CHAI, S., SHAH, A. S., WILLIAMS, S. E. & FUCHS, E. 2011. A role for the primary cilium in Notch signaling and epidermal differentiation during skin development. *Cell,* 145**,** 1129-41.
FABBRI, L., BOST, F. & MAZURE, N. M. 2019. Primary Cilium in Cancer Hallmarks. *Int J Mol Sci,* 20.
FANG, Y. & ZHANG, X. 2016. Targeting NEK2 as a promising therapeutic approach for cancer treatment. *Cell Cycle,* 15**,** 895-907.

FARINA, F., GAILLARD, J., GUERIN, C., COUTE, Y., SILLIBOURNE, J., BLANCHOIN, L. & THERY, M. 2016. The centrosome is an actin-organizing centre. *Nat Cell Biol,* 18**,** 65-75.
FLIEGAUF, M., BENZING, T. & OMRAN, H. 2007. When cilia go bad: cilia defects and ciliopathies. *Nat Rev Mol Cell Biol,* 8**,** 880-93.
FREDRIKSSON, L., LI, H. & ERIKSSON, U. 2004. The PDGF family: four gene products form five dimeric isoforms. *Cytokine Growth Factor Rev,* 15**,** 197-204.
FRY, A. M., SCHULTZ, S. J., BARTEK, J. & NIGG, E. A. 1995. Substrate specificity and cell cycle regulation of the Nek2 protein kinase, a potential human homolog of the mitotic regulator NIMA of Aspergillus nidulans. *J Biol Chem,* 270**,** 12899-905.
FU, W., ASP, P., CANTER, B. & DYNLACHT, B. D. 2014. Primary cilia control hedgehog signaling during muscle differentiation and are deregulated in rhabdomyosarcoma. *Proc Natl Acad Sci U S A,* 111**,** 9151-6.
GABRIEL, E. & GOPALAKRISHNAN, J. 2017. Generation of iPSC-derived Human Brain Organoids to Model Early Neurodevelopmental Disorders. *J Vis Exp*.
GABRIEL, E., RAMANI, A., KAROW, U., GOTTARDO, M., NATARAJAN, K., GOOI, L. M., GORANCI-BUZHALA, G., KRUT, O., PETERS, F., NIKOLIC, M., KUIVANEN, S., KORHONEN, E., SMURA, T., VAPALAHTI, O., PAPANTONIS, A., SCHMIDT-CHANASIT, J., RIPARBELLI, M., CALLAINI, G., KRONKE, M., UTERMOHLEN, O. & GOPALAKRISHNAN, J. 2017. Recent Zika Virus Isolates Induce Premature Differentiation of Neural Progenitors in Human Brain Organoids. *Cell Stem Cell*.
GABRIEL, E., WASON, A., RAMANI, A., GOOI, L. M., KELLER, P., POZNIAKOVSKY, A., POSER, I., NOACK, F., TELUGU, N. S., CALEGARI, F., SARIC, T., HESCHELER, J., HYMAN, A. A., GOTTARDO, M., CALLAINI, G., ALKURAYA, F. S. & GOPALAKRISHNAN, J. 2016. CPAP promotes timely cilium disassembly to maintain neural progenitor pool. *EMBO J,* 35**,** 803-19.
GARCIA, G., 3RD, RALEIGH, D. R. & REITER, J. F. 2018. How the Ciliary Membrane Is Organized Inside-Out to Communicate Outside-In. *Curr Biol,* 28**,** R421-R434.
GARCIA-GONZALO, F. R., CORBIT, K. C., SIREROL-PIQUER, M. S., RAMASWAMI, G., OTTO, E. A., NORIEGA, T. R., SEOL, A. D., ROBINSON, J. F., BENNETT, C. L., JOSIFOVA, D. J., GARCIA-VERDUGO, J. M., KATSANIS, N., HILDEBRANDT, F. & REITER, J. F. 2011. A transition zone complex regulates mammalian ciliogenesis and ciliary membrane composition. *Nat Genet,* 43**,** 776-84.
GARCIA-GONZALO, F. R. & REITER, J. F. 2012. Scoring a backstage pass: mechanisms of ciliogenesis and ciliary access. *J Cell Biol,* 197**,** 697-709.
GERDES, J. M., DAVIS, E. E. & KATSANIS, N. 2009. The vertebrate primary cilium in development, homeostasis, and disease. *Cell,* 137**,** 32-45.
GERHARDT, C., LEU, T., LIER, J. M. & RUTHER, U. 2016. The cilia-regulated proteasome and its role in the development of ciliopathies and cancer. *Cilia,* 5**,** 14.
GIESSL, A., PULVERMULLER, A., TROJAN, P., PARK, J. H., CHOE, H. W., ERNST, O. P., HOFMANN, K. P. & WOLFRUM, U. 2004. Differential expression and interaction with the visual G-protein transducin of centrin isoforms in mammalian photoreceptor cells. *J Biol Chem,* 279**,** 51472-81.
GLADIOLA GORANCI-BUZHALA, E. G., ARULJOTHI MARIAPPAN AND JAY GOPALAKRISHNAN 2017. Losers of primary cilia gain the benefit of survival. *Cancer Discovery,* In press.
GOETZ, S. C. & ANDERSON, K. V. 2010. The primary cilium: a signalling centre during vertebrate development. *Nat Rev Genet,* 11**,** 331-44.
GOETZ, S. C., LIEM, K. F., JR. & ANDERSON, K. V. 2012. The spinocerebellar ataxia-associated gene Tau tubulin kinase 2 controls the initiation of ciliogenesis. *Cell,* 151**,** 847-858.
GOMEZ-LOPEZ, S., LERNER, R. G. & PETRITSCH, C. 2014. Asymmetric cell division of stem and progenitor cells during homeostasis and cancer. *Cell Mol Life Sci,* 71**,** 575-97.
GOPALAKRISHNAN, J. 2019. The Emergence of Stem Cell-Based Brain Organoids: Trends and Challenges. *Bioessays,* 41**,** e1900011.
GOPALAKRISHNAN, J., MENNELLA, V., BLACHON, S., ZHAI, B., SMITH, A. H., MEGRAW, T. L., NICASTRO, D., GYGI, S. P., AGARD, D. A. & AVIDOR-REISS, T. 2011. Sas-4 provides a scaffold for cytoplasmic complexes and tethers them in a centrosome. *Nat Commun,* 2**,** 359.
GORANCI-BUZHALA, G., GABRIEL, E., MARIAPPAN, A. & GOPALAKRISHNAN, J. 2017. Losers of Primary Cilia Gain the Benefit of Survival. *Cancer Discov,* 7**,** 1374-1375.

GRADILONE, S. A., PISARELLO, M. J. L. & LARUSSO, N. F. 2017. Primary Cilia in Tumor Biology: The Primary Cilium as a Therapeutic Target in Cholangiocarcinoma. *Curr Drug Targets,* 18**,** 958-963.

GRADILONE, S. A., RADTKE, B. N., BOGERT, P. S., HUANG, B. Q., GAJDOS, G. B. & LARUSSO, N. F. 2013. HDAC6 inhibition restores ciliary expression and decreases tumor growth. *Cancer Res,* 73**,** 2259-70.

GUEMEZ-GAMBOA, A., COUFAL, N. G. & GLEESON, J. G. 2014. Primary cilia in the developing and mature brain. *Neuron,* 82**,** 511-21.

HAN, Y. G., KIM, H. J., DLUGOSZ, A. A., ELLISON, D. W., GILBERTSON, R. J. & ALVAREZ-BUYLLA, A. 2009. Dual and opposing roles of primary cilia in medulloblastoma development. *Nat Med,* 15**,** 1062-5.

HANKS, S. K. & HUNTER, T. 1995. Protein kinases 6. The eukaryotic protein kinase superfamily: kinase (catalytic) domain structure and classification. *FASEB J,* 9**,** 576-96.

HASSOUNAH, N. B., BUNCH, T. A. & MCDERMOTT, K. M. 2012. Molecular pathways: the role of primary cilia in cancer progression and therapeutics with a focus on Hedgehog signaling. *Clin Cancer Res,* 18**,** 2429-35.

HAYCRAFT, C. J., BANIZS, B., AYDIN-SON, Y., ZHANG, Q., MICHAUD, E. J. & YODER, B. K. 2005. Gli2 and Gli3 localize to cilia and require the intraflagellar transport protein polaris for processing and function. *PLoS Genet,* 1**,** e53.

HAYWARD, D. G., CLARKE, R. B., FARAGHER, A. J., PILLAI, M. R., HAGAN, I. M. & FRY, A. M. 2004. The centrosomal kinase Nek2 displays elevated levels of protein expression in human breast cancer. *Cancer Res,* 64**,** 7370-6.

HELDIN, C. H. & WESTERMARK, B. 1999. Mechanism of action and in vivo role of platelet-derived growth factor. *Physiol Rev,* 79**,** 1283-316.

HERGOVICH, A., LISZTWAN, J., BARRY, R., BALLSCHMIETER, P. & KREK, W. 2003. Regulation of microtubule stability by the von Hippel-Lindau tumour suppressor protein pVHL. *Nat Cell Biol,* 5**,** 64-70.

HIROKAWA, N., TANAKA, Y., OKADA, Y. & TAKEDA, S. 2006. Nodal flow and the generation of left-right asymmetry. *Cell,* 125**,** 33-45.

HO, L., ALI, S. A., AL-JAZRAWE, M., KANDEL, R., WUNDER, J. S. & ALMAN, B. A. 2013. Primary cilia attenuate hedgehog signalling in neoplastic chondrocytes. *Oncogene,* 32**,** 5388-96.

HOANG-MINH, L. B., DELEYROLLE, L. P., NAKAMURA, N. S., PARKER, A. K., MARTUSCELLO, R. T., REYNOLDS, B. A. & SARKISIAN, M. R. 2016a. PCM1 Depletion Inhibits Glioblastoma Cell Ciliogenesis and Increases Cell Death and Sensitivity to Temozolomide. *Transl Oncol,* 9**,** 392-402.

HOANG-MINH, L. B., DELEYROLLE, L. P., SIEBZEHNRUBL, D., UGARTEMENDIA, G., FUTCH, H., GRIFFITH, B., BREUNIG, J. J., DE LEON, G., MITCHELL, D. A., SEMPLE-ROWLAND, S., REYNOLDS, B. A. & SARKISIAN, M. R. 2016b. Disruption of KIF3A in patient-derived glioblastoma cells: effects on ciliogenesis, hedgehog sensitivity, and tumorigenesis. *Oncotarget,* 7**,** 7029-43.

HSU, W. B., HUNG, L. Y., TANG, C. J., SU, C. L., CHANG, Y. & TANG, T. K. 2008. Functional characterization of the microtubule-binding and -destabilizing domains of CPAP and d-SAS-4. *Exp Cell Res,* 314**,** 2591-602.

HUANGFU, D., LIU, A., RAKEMAN, A. S., MURCIA, N. S., NISWANDER, L. & ANDERSON, K. V. 2003. Hedgehog signalling in the mouse requires intraflagellar transport proteins. *Nature,* 426**,** 83-7.

HUMKE, E. W., DORN, K. V., MILENKOVIC, L., SCOTT, M. P. & ROHATGI, R. 2010. The output of Hedgehog signaling is controlled by the dynamic association between Suppressor of Fused and the Gli proteins. *Genes Dev,* 24**,** 670-82.

INABA, H., GOTO, H., KASAHARA, K., KUMAMOTO, K., YONEMURA, S., INOKO, A., YAMANO, S., WANIBUCHI, H., HE, D., GOSHIMA, N., KIYONO, T., HIROTSUNE, S. & INAGAKI, M. 2016. Ndel1 suppresses ciliogenesis in proliferating cells by regulating the trichoplein-Aurora A pathway. *J Cell Biol,* 212**,** 409-23.

INOKO, A., MATSUYAMA, M., GOTO, H., OHMURO-MATSUYAMA, Y., HAYASHI, Y., ENOMOTO, M., IBI, M., URANO, T., YONEMURA, S., KIYONO, T., IZAWA, I. & INAGAKI, M. 2012. Trichoplein and Aurora A block aberrant primary cilia assembly in proliferating cells. *J Cell Biol,* 197**,** 391-405.

ISHIKAWA, H. & MARSHALL, W. F. 2011. Ciliogenesis: building the cell's antenna. *Nat Rev Mol Cell Biol,* 12**,** 222-34.
ISHIKAWA, H. & MARSHALL, W. F. 2017. Intraflagellar Transport and Ciliary Dynamics. *Cold Spring Harb Perspect Biol,* 9.
ISHIKAWA, H., THOMPSON, J., YATES, J. R., 3RD & MARSHALL, W. F. 2012. Proteomic analysis of mammalian primary cilia. *Curr Biol,* 22**,** 414-9.
IZAWA, I., GOTO, H., KASAHARA, K. & INAGAKI, M. 2015. Current topics of functional links between primary cilia and cell cycle. *Cilia,* 4**,** 12.
JACKSON, P. K. 2011. Do cilia put brakes on the cell cycle? *Nat Cell Biol,* 13**,** 340-2.
JACOB, F., SALINAS, R. D., ZHANG, D. Y., NGUYEN, P. T. T., SCHNOLL, J. G., WONG, S. Z. H., THOKALA, R., SHEIKH, S., SAXENA, D., PROKOP, S., LIU, D. A., QIAN, X., PETROV, D., LUCAS, T., CHEN, H. I., DORSEY, J. F., CHRISTIAN, K. M., BINDER, Z. A., NASRALLAH, M., BREM, S., O'ROURKE, D. M., MING, G. L. & SONG, H. 2020. A Patient-Derived Glioblastoma Organoid Model and Biobank Recapitulates Inter- and Intra-tumoral Heterogeneity. *Cell,* 180**,** 188-204 e22.
JENSEN, V. L. & LEROUX, M. R. 2017. Gates for soluble and membrane proteins, and two trafficking systems (IFT and LIFT), establish a dynamic ciliary signaling compartment. *Curr Opin Cell Biol,* 47**,** 83-91.
JEONG, A. L., KA, H. I., HAN, S., LEE, S., LEE, E. W., SOH, S. J., JOO, H. J., SUMIYASUREN, B., PARK, J. Y., LIM, J. S., PARK, J. H., LEE, M. S. & YANG, Y. 2018. Oncoprotein CIP2A promotes the disassembly of primary cilia and inhibits glycolytic metabolism. *EMBO Rep,* 19.
JEONG, Y., LEE, J., KIM, K., YOO, J. C. & RHEE, K. 2007. Characterization of NIP2/centrobin, a novel substrate of Nek2, and its potential role in microtubule stabilization. *J Cell Sci,* 120**,** 2106-16.
JOHNSON, D. R. & O'NEILL, B. P. 2012. Glioblastoma survival in the United States before and during the temozolomide era. *J Neurooncol,* 107**,** 359-64.
JUNTTILA, M. R., PUUSTINEN, P., NIEMELA, M., AHOLA, R., ARNOLD, H., BOTTZAUW, T., ALA-AHO, R., NIELSEN, C., IVASKA, J., TAYA, Y., LU, S. L., LIN, S., CHAN, E. K., WANG, X. J., GRENMAN, R., KAST, J., KALLUNKI, T., SEARS, R., KAHARI, V. M. & WESTERMARCK, J. 2007. CIP2A inhibits PP2A in human malignancies. *Cell,* 130**,** 51-62.
KASAHARA, K., AOKI, H., KIYONO, T., WANG, S., KAGIWADA, H., YUGE, M., TANAKA, T., NISHIMURA, Y., MIZOGUCHI, A., GOSHIMA, N. & INAGAKI, M. 2018. EGF receptor kinase suppresses ciliogenesis through activation of USP8 deubiquitinase. *Nat Commun,* 9**,** 758.
KIM, J., JO, H., HONG, H., KIM, M. H., KIM, J. M., LEE, J. K., HEO, W. D. & KIM, J. 2015a. Actin remodelling factors control ciliogenesis by regulating YAP/TAZ activity and vesicle trafficking. *Nat Commun,* 6**,** 6781.
KIM, S., LEE, K., CHOI, J. H., RINGSTAD, N. & DYNLACHT, B. D. 2015b. Nek2 activation of Kif24 ensures cilium disassembly during the cell cycle. *Nat Commun,* 6**,** 8087.
KIM, S., ZAGHLOUL, N. A., BUBENSHCHIKOVA, E., OH, E. C., RANKIN, S., KATSANIS, N., OBARA, T. & TSIOKAS, L. 2011. Nde1-mediated inhibition of ciliogenesis affects cell cycle re-entry. *Nat Cell Biol,* 13**,** 351-60.
KINZEL, D., BOLDT, K., DAVIS, E. E., BURTSCHER, I., TRUMBACH, D., DIPLAS, B., ATTIE-BITACH, T., WURST, W., KATSANIS, N., UEFFING, M. & LICKERT, H. 2010. Pitchfork regulates primary cilia disassembly and left-right asymmetry. *Dev Cell,* 19**,** 66-77.
KISHI, K., VAN VUGT, M. A., OKAMOTO, K., HAYASHI, Y. & YAFFE, M. B. 2009. Functional dynamics of Polo-like kinase 1 at the centrosome. *Mol Cell Biol,* 29**,** 3134-50.
KOBAYASHI, T. & DYNLACHT, B. D. 2011. Regulating the transition from centriole to basal body. *J Cell Biol,* 193**,** 435-44.
KOBAYASHI, T., KIM, S., LIN, Y. C., INOUE, T. & DYNLACHT, B. D. 2014. The CP110-interacting proteins Talpid3 and Cep290 play overlapping and distinct roles in cilia assembly. *J Cell Biol,* 204**,** 215-29.
KOBAYASHI, T., NAKAZONO, K., TOKUDA, M., MASHIMA, Y., DYNLACHT, B. D. & ITOH, H. 2017. HDAC2 promotes loss of primary cilia in pancreatic ductal adenocarcinoma. *EMBO Rep,* 18**,** 334-343.
KOBAYASHI, T., TSANG, W. Y., LI, J., LANE, W. & DYNLACHT, B. D. 2011. Centriolar kinesin Kif24 interacts with CP110 to remodel microtubules and regulate ciliogenesis. *Cell,* 145**,** 914-25.

KOHLI, P., HOHNE, M., JUNGST, C., BERTSCH, S., EBERT, L. K., SCHAUSS, A. C., BENZING, T., RINSCHEN, M. M. & SCHERMER, B. 2017. The ciliary membrane-associated proteome reveals actin-binding proteins as key components of cilia. *EMBO Rep,* 18**,** 1521-1535.

KUMAMOTO, N., GU, Y., WANG, J., JANOSCHKA, S., TAKEMARU, K., LEVINE, J. & GE, S. 2012. A role for primary cilia in glutamatergic synaptic integration of adult-born neurons. *Nat Neurosci,* 15**,** 399-405, S1.

LANGE, C., HUTTNER, W. B. & CALEGARI, F. 2009. Cdk4/cyclinD1 overexpression in neural stem cells shortens G1, delays neurogenesis, and promotes the generation and expansion of basal progenitors. *Cell Stem Cell,* 5**,** 320-31.

LATHIA, J. D., MACK, S. C., MULKEARNS-HUBERT, E. E., VALENTIM, C. L. & RICH, J. N. 2015. Cancer stem cells in glioblastoma. *Genes Dev,* 29**,** 1203-17.

LEE, K. & RHEE, K. 2011. PLK1 phosphorylation of pericentrin initiates centrosome maturation at the onset of mitosis. *J Cell Biol,* 195**,** 1093-101.

LEE, K. H., JOHMURA, Y., YU, L. R., PARK, J. E., GAO, Y., BANG, J. K., ZHOU, M., VEENSTRA, T. D., YEON KIM, B. & LEE, K. S. 2012. Identification of a novel Wnt5a-CK1varepsilon-Dvl2-Plk1-mediated primary cilia disassembly pathway. *EMBO J,* 31**,** 3104-17.

LEE, S. H., JOO, K., JUNG, E. J., HONG, H., SEO, J. & KIM, J. 2018. Export of membrane proteins from the Golgi complex to the primary cilium requires the kinesin motor, KIFC1. *FASEB J,* 32**,** 957-968.

LEPANTO, P., BADANO, J. L. & ZOLESSI, F. R. 2016. Neuron's little helper: The role of primary cilia in neurogenesis. *Neurogenesis (Austin),* 3**,** e1253363.

LI, A., SAITO, M., CHUANG, J. Z., TSENG, Y. Y., DEDESMA, C., TOMIZAWA, K., KAITSUKA, T. & SUNG, C. H. 2011. Ciliary transition zone activation of phosphorylated Tctex-1 controls ciliary resorption, S-phase entry and fate of neural progenitors. *Nat Cell Biol,* 13**,** 402-11.

LI, J., KIM, S., KOBAYASHI, T., LIANG, F. X., KORZENIEWSKI, N., DUENSING, S. & DYNLACHT, B. D. 2012. Neurl4, a novel daughter centriole protein, prevents formation of ectopic microtubule organizing centres. *EMBO Rep,* 13**,** 547-53.

LIAO, Y., SMYTH, G. K. & SHI, W. 2014. featureCounts: an efficient general purpose program for assigning sequence reads to genomic features. *Bioinformatics,* 30**,** 923-30.

LIN, Y. C., CHANG, C. W., HSU, W. B., TANG, C. J., LIN, Y. N., CHOU, E. J., WU, C. T. & TANG, T. K. 2013. Human microcephaly protein CEP135 binds to hSAS-6 and CPAP, and is required for centriole assembly. *EMBO J,* 32**,** 1141-54.

LINDEMANN, C. B. & LESICH, K. A. 2010. Flagellar and ciliary beating: the proven and the possible. *J Cell Sci,* 123**,** 519-28.

LINKOUS, A., BALAMATSIAS, D., SNUDERL, M., EDWARDS, L., MIYAGUCHI, K., MILNER, T., REICH, B., COHEN-GOULD, L., STORASKA, A., NAKAYAMA, Y., SCHENKEIN, E., SINGHANIA, R., CIRIGLIANO, S., MAGDELDIN, T., LIN, Y., NANJANGUD, G., CHADALAVADA, K., PISAPIA, D., LISTON, C. & FINE, H. A. 2019. Modeling Patient-Derived Glioblastoma with Cerebral Organoids. *Cell Rep,* 26**,** 3203-3211 e5.

LIU, A., WANG, B. & NISWANDER, L. A. 2005. Mouse intraflagellar transport proteins regulate both the activator and repressor functions of Gli transcription factors. *Development,* 132**,** 3103-11.

LOSKUTOV, Y. & PUGACHEVA, E. N. 2019. Targeting primary cilia - associated signaling in glioblastoma: guided approach for drug development. *Oncoscience,* 6**,** 289-290.

LOSKUTOV, Y. V., GRIFFIN, C. L., MARINAK, K. M., BOBKO, A., MARGARYAN, N. V., GELDENHUYS, W. J., SARKARIA, J. N. & PUGACHEVA, E. N. 2018. LPA signaling is regulated through the primary cilium: a novel target in glioblastoma. *Oncogene,* 37**,** 1457-1471.

LOUIS, D. N., OHGAKI, H., WIESTLER, O. D., CAVENEE, W. K., BURGER, P. C., JOUVET, A., SCHEITHAUER, B. W. & KLEIHUES, P. 2007. The 2007 WHO classification of tumours of the central nervous system. *Acta Neuropathol,* 114**,** 97-109.

LOVE, M. I., HUBER, W. & ANDERS, S. 2014. Moderated estimation of fold change and dispersion for RNA-seq data with DESeq2. *Genome Biol,* 15**,** 550.

LOW, J., BLOSSER, W., DOWLESS, M., RICCI-VITIANI, L., PALLINI, R., DE MARIA, R. & STANCATO, L. 2012. Knockdown of ubiquitin ligases in glioblastoma cancer stem cells leads to cell death and differentiation. *J Biomol Screen,* 17**,** 152-62.

LU, Q., INSINNA, C., OTT, C., STAUFFER, J., PINTADO, P. A., RAHAJENG, J., BAXA, U., WALIA, V., CUENCA, A., HWANG, Y. S., DAAR, I. O., LOPES, S., LIPPINCOTT-SCHWARTZ, J.,

JACKSON, P. K., CAPLAN, S. & WESTLAKE, C. J. 2015. Early steps in primary cilium assembly require EHD1/EHD3-dependent ciliary vesicle formation. *Nat Cell Biol,* 17**,** 228-240.

LUBENSKY, I. A., GNARRA, J. R., BERTHEAU, P., WALTHER, M. M., LINEHAN, W. M. & ZHUANG, Z. 1996. Allelic deletions of the VHL gene detected in multiple microscopic clear cell renal lesions in von Hippel-Lindau disease patients. *Am J Pathol,* 149**,** 2089-94.

MACHOLD, R., HAYASHI, S., RUTLIN, M., MUZUMDAR, M. D., NERY, S., CORBIN, J. G., GRITLI-LINDE, A., DELLOVADE, T., PORTER, J. A., RUBIN, L. L., DUDEK, H., MCMAHON, A. P. & FISHELL, G. 2003. Sonic hedgehog is required for progenitor cell maintenance in telencephalic stem cell niches. *Neuron,* 39**,** 937-50.

MAHJOUB, M. R., XIE, Z. & STEARNS, T. 2010. Cep120 is asymmetrically localized to the daughter centriole and is essential for centriole assembly. *J Cell Biol,* 191**,** 331-46.

MANDRIOTA, S. J., TURNER, K. J., DAVIES, D. R., MURRAY, P. G., MORGAN, N. V., SOWTER, H. M., WYKOFF, C. C., MAHER, E. R., HARRIS, A. L., RATCLIFFE, P. J. & MAXWELL, P. H. 2002. HIF activation identifies early lesions in VHL kidneys: evidence for site-specific tumor suppressor function in the nephron. *Cancer Cell,* 1**,** 459-68.

MARSHALL, W. F., QIN, H., RODRIGO BRENNI, M. & ROSENBAUM, J. L. 2005. Flagellar length control system: testing a simple model based on intraflagellar transport and turnover. *Mol Biol Cell,* 16**,** 270-8.

MARSHALL, W. F. & ROSENBAUM, J. L. 2001. Intraflagellar transport balances continuous turnover of outer doublet microtubules: implications for flagellar length control. *J Cell Biol,* 155**,** 405-14.

MARZIALI, G., BUCCARELLI, M., GIULIANI, A., ILARI, R., GRANDE, S., PALMA, A., D'ALESSANDRIS, Q. G., MARTINI, M., BIFFONI, M., PALLINI, R. & RICCI-VITIANI, L. 2017. A three-microRNA signature identifies two subtypes of glioblastoma patients with different clinical outcomes. *Mol Oncol,* 11**,** 1115-1129.

MATSUKADO, Y., MACCARTY, C. S. & KERNOHAN, J. W. 1961. The growth of glioblastoma multiforme (astrocytomas, grades 3 and 4) in neurosurgical practice. *J Neurosurg,* 18**,** 636-44.

MCMAHON, A. P., INGHAM, P. W. & TABIN, C. J. 2003. Developmental roles and clinical significance of hedgehog signaling. *Curr Top Dev Biol,* 53**,** 1-114.

MICHAUD, E. J. & YODER, B. K. 2006. The primary cilium in cell signaling and cancer. *Cancer Res,* 66**,** 6463-7.

MIYAMOTO, T., HOSOBA, K., OCHIAI, H., ROYBA, E., IZUMI, H., SAKUMA, T., YAMAMOTO, T., DYNLACHT, B. D. & MATSUURA, S. 2015. The Microtubule-Depolymerizing Activity of a Mitotic Kinesin Protein KIF2A Drives Primary Cilia Disassembly Coupled with Cell Proliferation. *Cell Rep,* 10**,** 664-673.

MOLLA-HERMAN, A., GHOSSOUB, R., BLISNICK, T., MEUNIER, A., SERRES, C., SILBERMANN, F., EMMERSON, C., ROMEO, K., BOURDONCLE, P., SCHMITT, A., SAUNIER, S., SPASSKY, N., BASTIN, P. & BENMERAH, A. 2010. The ciliary pocket: an endocytic membrane domain at the base of primary and motile cilia. *J Cell Sci,* 123**,** 1785-95.

MOSER, J. J., FRITZLER, M. J., OU, Y. & RATTNER, J. B. 2009a. The PCM-basal body/primary cilium coalition. *Semin Cell Dev Biol*.

MOSER, J. J., FRITZLER, M. J. & RATTNER, J. B. 2009b. Primary ciliogenesis defects are associated with human astrocytoma/glioblastoma cells. *BMC Cancer,* 9**,** 448.

MOSER, J. J., FRITZLER, M. J. & RATTNER, J. B. 2014. Ultrastructural characterization of primary cilia in pathologically characterized human glioblastoma multiforme (GBM) tumors. *BMC Clin Pathol,* 14**,** 40.

MOUTAL, A., HONNORAT, J., MASSOMA, P., DESORMEAUX, P., BERTRAND, C., MALLEVAL, C., WATRIN, C., CHOUNLAMOUNTRI, N., MAYEUR, M. E., BESANCON, R., NAUDET, N., MAGADOUX, L., KHANNA, R., DUCRAY, F., MEYRONET, D. & THOMASSET, N. 2015. CRMP5 Controls Glioblastoma Cell Proliferation and Survival through Notch-Dependent Signaling. *Cancer Res,* 75**,** 3519-28.

NACHURY, M. V., LOKTEV, A. V., ZHANG, Q., WESTLAKE, C. J., PERANEN, J., MERDES, A., SLUSARSKI, D. C., SCHELLER, R. H., BAZAN, J. F., SHEFFIELD, V. C. & JACKSON, P. K. 2007. A core complex of BBS proteins cooperates with the GTPase Rab8 to promote ciliary membrane biogenesis. *Cell,* 129**,** 1201-13.

NACHURY, M. V. & MICK, D. U. 2019. Establishing and regulating the composition of cilia for signal transduction. *Nat Rev Mol Cell Biol,* 20**,** 389-405.

NACHURY, M. V., SEELEY, E. S. & JIN, H. 2010. Trafficking to the ciliary membrane: how to get across the periciliary diffusion barrier? *Annu Rev Cell Dev Biol,* 26**,** 59-87.

NEVE, R. M., CHIN, K., FRIDLYAND, J., YEH, J., BAEHNER, F. L., FEVR, T., CLARK, L., BAYANI, N., COPPE, J. P., TONG, F., SPEED, T., SPELLMAN, P. T., DEVRIES, S., LAPUK, A., WANG, N. J., KUO, W. L., STILWELL, J. L., PINKEL, D., ALBERTSON, D. G., WALDMAN, F. M., MCCORMICK, F., DICKSON, R. B., JOHNSON, M. D., LIPPMAN, M., ETHIER, S., GAZDAR, A. & GRAY, J. W. 2006. A collection of breast cancer cell lines for the study of functionally distinct cancer subtypes. *Cancer Cell,* 10**,** 515-27.

NIGG, E. A. & RAFF, J. W. 2009. Centrioles, centrosomes, and cilia in health and disease. *Cell,* 139**,** 663-78.

NOBUTANI, K., SHIMONO, Y., YOSHIDA, M., MIZUTANI, K., MINAMI, A., KONO, S., MUKOHARA, T., YAMASAKI, T., ITOH, T., TAKAO, S., MINAMI, H., AZUMA, T. & TAKAI, Y. 2014. Absence of primary cilia in cell cycle-arrested human breast cancer cells. *Genes Cells,* 19**,** 141-52.

OBERHEIM, N. A., TAKANO, T., HAN, X., HE, W., LIN, J. H., WANG, F., XU, Q., WYATT, J. D., PILCHER, W., OJEMANN, J. G., RANSOM, B. R., GOLDMAN, S. A. & NEDERGAARD, M. 2009. Uniquely hominid features of adult human astrocytes. *J Neurosci,* 29**,** 3276-87.

OGAWA, J., PAO, G. M., SHOKHIREV, M. N. & VERMA, I. M. 2018. Glioblastoma Model Using Human Cerebral Organoids. *Cell Rep,* 23**,** 1220-1229.

OSSWALD, M., JUNG, E., SAHM, F., SOLECKI, G., VENKATARAMANI, V., BLAES, J., WEIL, S., HORSTMANN, H., WIESTLER, B., SYED, M., HUANG, L., RATLIFF, M., KARIMIAN JAZI, K., KURZ, F. T., SCHMENGER, T., LEMKE, D., GOMMEL, M., PAULI, M., LIAO, Y., HARING, P., PUSCH, S., HERL, V., STEINHAUSER, C., KRUNIC, D., JARAHIAN, M., MILETIC, H., BERGHOFF, A. S., GRIESBECK, O., KALAMAKIS, G., GARASCHUK, O., PREUSSER, M., WEISS, S., LIU, H., HEILAND, S., PLATTEN, M., HUBER, P. E., KUNER, T., VON DEIMLING, A., WICK, W. & WINKLER, F. 2015a. Brain tumour cells interconnect to a functional and resistant network. *Nature*.

OSSWALD, M., JUNG, E., SAHM, F., SOLECKI, G., VENKATARAMANI, V., BLAES, J., WEIL, S., HORSTMANN, H., WIESTLER, B., SYED, M., HUANG, L., RATLIFF, M., KARIMIAN JAZI, K., KURZ, F. T., SCHMENGER, T., LEMKE, D., GOMMEL, M., PAULI, M., LIAO, Y., HARING, P., PUSCH, S., HERL, V., STEINHAUSER, C., KRUNIC, D., JARAHIAN, M., MILETIC, H., BERGHOFF, A. S., GRIESBECK, O., KALAMAKIS, G., GARASCHUK, O., PREUSSER, M., WEISS, S., LIU, H., HEILAND, S., PLATTEN, M., HUBER, P. E., KUNER, T., VON DEIMLING, A., WICK, W. & WINKLER, F. 2015b. Brain tumour cells interconnect to a functional and resistant network. *Nature,* 528**,** 93-8.

OSTROM, Q. T., BAUCHET, L., DAVIS, F. G., DELTOUR, I., FISHER, J. L., LANGER, C. E., PEKMEZCI, M., SCHWARTZBAUM, J. A., TURNER, M. C., WALSH, K. M., WRENSCH, M. R. & BARNHOLTZ-SLOAN, J. S. 2014. The epidemiology of glioma in adults: a "state of the science" review. *Neuro Oncol,* 16**,** 896-913.

OZAWA, T., BRENNAN, C. W., WANG, L., SQUATRITO, M., SASAYAMA, T., NAKADA, M., HUSE, J. T., PEDRAZA, A., UTSUKI, S., YASUI, Y., TANDON, A., FOMCHENKO, E. I., OKA, H., LEVINE, R. L., FUJII, K., LADANYI, M. & HOLLAND, E. C. 2010. PDGFRA gene rearrangements are frequent genetic events in PDGFRA-amplified glioblastomas. *Genes Dev,* 24**,** 2205-18.

PAN, J., WANG, Q. & SNELL, W. J. 2004. An aurora kinase is essential for flagellar disassembly in Chlamydomonas. *Dev Cell,* 6**,** 445-51.

PARIDAEN, J. T., WILSCH-BRAUNINGER, M. & HUTTNER, W. B. 2013. Asymmetric inheritance of centrosome-associated primary cilium membrane directs ciliogenesis after cell division. *Cell,* 155**,** 333-44.

PARK, N. I., GUILHAMON, P., DESAI, K., MCADAM, R. F., LANGILLE, E., O'CONNOR, M., LAN, X., WHETSTONE, H., COUTINHO, F. J., VANNER, R. J., LING, E., PRINOS, P., LEE, L., SELVADURAI, H., ATWAL, G., KUSHIDA, M., CLARKE, I. D., VOISIN, V., CUSIMANO, M. D., BERNSTEIN, M., DAS, S., BADER, G., ARROWSMITH, C. H., ANGERS, S., HUANG, X., LUPIEN, M. & DIRKS, P. B. 2017. ASCL1 Reorganizes Chromatin to Direct Neuronal

Fate and Suppress Tumorigenicity of Glioblastoma Stem Cells. *Cell Stem Cell,* 21**,** 209-224 e7.
PATEL, A. P., TIROSH, I., TROMBETTA, J. J., SHALEK, A. K., GILLESPIE, S. M., WAKIMOTO, H., CAHILL, D. P., NAHED, B. V., CURRY, W. T., MARTUZA, R. L., LOUIS, D. N., ROZENBLATT-ROSEN, O., SUVA, M. L., REGEV, A. & BERNSTEIN, B. E. 2014. Single-cell RNA-seq highlights intratumoral heterogeneity in primary glioblastoma. *Science,* 344**,** 1396-401.
PAZOUR, G. J., AGRIN, N., LESZYK, J. & WITMAN, G. B. 2005. Proteomic analysis of a eukaryotic cilium. *J Cell Biol,* 170**,** 103-13.
PAZOUR, G. J., DICKERT, B. L., VUCICA, Y., SEELEY, E. S., ROSENBAUM, J. L., WITMAN, G. B. & COLE, D. G. 2000. Chlamydomonas IFT88 and its mouse homologue, polycystic kidney disease gene tg737, are required for assembly of cilia and flagella. *J Cell Biol,* 151**,** 709-18.
PEDERSEN, L. B., VELAND, I. R., SCHRODER, J. M. & CHRISTENSEN, S. T. 2008. Assembly of primary cilia. *Dev Dyn,* 237**,** 1993-2006.
PITAVAL, A., SENGER, F., LETORT, G., GIDROL, X., GUYON, L., SILLIBOURNE, J. & THERY, M. 2017. Microtubule stabilization drives 3D centrosome migration to initiate primary ciliogenesis. *J Cell Biol,* 216**,** 3713-3728.
PITAVAL, A., TSENG, Q., BORNENS, M. & THERY, M. 2010. Cell shape and contractility regulate ciliogenesis in cell cycle-arrested cells. *J Cell Biol,* 191**,** 303-12.
PLOTNIKOVA, O. V., GOLEMIS, E. A. & PUGACHEVA, E. N. 2008. Cell cycle-dependent ciliogenesis and cancer. *Cancer Res,* 68**,** 2058-61.
PUGACHEVA, E. N., JABLONSKI, S. A., HARTMAN, T. R., HENSKE, E. P. & GOLEMIS, E. A. 2007. HEF1-dependent Aurora A activation induces disassembly of the primary cilium. *Cell,* 129**,** 1351-63.
RAAB, M., SANHAJI, M., MATTHESS, Y., HORLIN, A., LORENZ, I., DOTSCH, C., HABBE, N., WAIDMANN, O., KURUNCI-CSACSKO, E., FIRESTEIN, R., BECKER, S. & STREBHARDT, K. 2018. PLK1 has tumor-suppressive potential in APC-truncated colon cancer cells. *Nat Commun,* 9**,** 1106.
RAJAKULENDRAN, N., ROWLAND, K. J., SELVADURAI, H. J., AHMADI, M., PARK, N. I., NAUMENKO, S., DOLMA, S., WARD, R. J., SO, M., LEE, L., MACLEOD, G., PASILIAO, C., BRANDON, C., CLARKE, I. D., CUSIMANO, M. D., BERNSTEIN, M., BATADA, N., ANGERS, S. & DIRKS, P. B. 2019. Wnt and Notch signaling govern self-renewal and differentiation in a subset of human glioblastoma stem cells. *Genes Dev,* 33**,** 498-510.
RAMANI, A., MARIAPPAN, A., GOTTARDO, M., MANDAD, S., URLAUB, H., AVIDOR-REISS, T., RIPARBELLI, M., CALLAINI, G., DEBEC, A., FEEDERLE, R. & GOPALAKRISHNAN, J. 2018. Plk1/Polo Phosphorylates Sas-4 at the Onset of Mitosis for an Efficient Recruitment of Pericentriolar Material to Centrosomes. *Cell Rep,* 25**,** 3618-3630 e6.
RAZUMILAVA, N., GRADILONE, S. A., SMOOT, R. L., MERTENS, J. C., BRONK, S. F., SIRICA, A. E. & GORES, G. J. 2014. Non-canonical Hedgehog signaling contributes to chemotaxis in cholangiocarcinoma. *J Hepatol,* 60**,** 599-605.
RICH, J. N. & EYLER, C. E. 2008. Cancer stem cells in brain tumor biology. *Cold Spring Harb Symp Quant Biol,* 73**,** 411-20.
RISSO, D., NGAI, J., SPEED, T. P. & DUDOIT, S. 2014. Normalization of RNA-seq data using factor analysis of control genes or samples. *Nat Biotechnol,* 32**,** 896-902.
ROBERT, A., MARGALL-DUCOS, G., GUIDOTTI, J. E., BREGERIE, O., CELATI, C., BRECHOT, C. & DESDOUETS, C. 2007. The intraflagellar transport component IFT88/polaris is a centrosomal protein regulating G1-S transition in non-ciliated cells. *J Cell Sci,* 120**,** 628-37.
ROHATGI, R., MILENKOVIC, L. & SCOTT, M. P. 2007. Patched1 regulates hedgehog signaling at the primary cilium. *Science,* 317**,** 372-6.
SANCHEZ, I. & DYNLACHT, B. D. 2016. Cilium assembly and disassembly. *Nat Cell Biol,* 18**,** 711-7.
SARKISIAN, M. R., SIEBZEHNRUBL, D., HOANG-MINH, L., DELEYROLLE, L., SILVER, D. J., SIEBZEHNRUBL, F. A., GUADIANA, S. M., SRIVINASAN, G., SEMPLE-ROWLAND, S., HARRISON, J. K., STEINDLER, D. A. & REYNOLDS, B. A. 2014. Detection of primary cilia in human glioblastoma. *J Neurooncol,* 117**,** 15-24.
SATIR, P. & CHRISTENSEN, S. T. 2007. Overview of structure and function of mammalian cilia. *Annu Rev Physiol,* 69**,** 377-400.

SATIR, P., GUERRA, C. & BELL, A. J. 2007. Evolution and persistence of the cilium. *Cell Motil Cytoskeleton,* 64**,** 906-13.
SATIR, P., PEDERSEN, L. B. & CHRISTENSEN, S. T. 2010. The primary cilium at a glance. *J Cell Sci,* 123**,** 499-503.
SCHERMER, B., GHENOIU, C., BARTRAM, M., MULLER, R. U., KOTSIS, F., HOHNE, M., KUHN, W., RAPKA, M., NITSCHKE, R., ZENTGRAF, H., FLIEGAUF, M., OMRAN, H., WALZ, G. & BENZING, T. 2006. The von Hippel-Lindau tumor suppressor protein controls ciliogenesis by orienting microtubule growth. *J Cell Biol,* 175**,** 547-54.
SCHMID, F. M., SCHOU, K. B., VILHELM, M. J., HOLM, M. S., BRESLIN, L., FARINELLI, P., LARSEN, L. A., ANDERSEN, J. S., PEDERSEN, L. B. & CHRISTENSEN, S. T. 2018. IFT20 modulates ciliary PDGFRalpha signaling by regulating the stability of Cbl E3 ubiquitin ligases. *J Cell Biol,* 217**,** 151-161.
SCHMIDT, K. N., KUHNS, S., NEUNER, A., HUB, B., ZENTGRAF, H. & PEREIRA, G. 2012. Cep164 mediates vesicular docking to the mother centriole during early steps of ciliogenesis. *J Cell Biol,* 199**,** 1083-101.
SCHNEIDER, L., CAMMER, M., LEHMAN, J., NIELSEN, S. K., GUERRA, C. F., VELAND, I. R., STOCK, C., HOFFMANN, E. K., YODER, B. K., SCHWAB, A., SATIR, P. & CHRISTENSEN, S. T. 2010. Directional cell migration and chemotaxis in wound healing response to PDGF-AA are coordinated by the primary cilium in fibroblasts. *Cell Physiol Biochem,* 25**,** 279-92.
SCHNEIDER, L., CLEMENT, C. A., TEILMANN, S. C., PAZOUR, G. J., HOFFMANN, E. K., SATIR, P. & CHRISTENSEN, S. T. 2005. PDGFRalphaalpha signaling is regulated through the primary cilium in fibroblasts. *Curr Biol,* 15**,** 1861-6.
SCHRAML, P., FREW, I. J., THOMA, C. R., BOYSEN, G., STRUCKMANN, K., KREK, W. & MOCH, H. 2009. Sporadic clear cell renal cell carcinoma but not the papillary type is characterized by severely reduced frequency of primary cilia. *Mod Pathol,* 22**,** 31-6.
SEEGER-NUKPEZAH, T., LITTLE, J. L., SERZHANOVA, V. & GOLEMIS, E. A. 2013. Cilia and cilia-associated proteins in cancer. *Drug Discov Today Dis Mech,* 10**,** e135-e142.
SEELEY, E. S., CARRIERE, C., GOETZE, T., LONGNECKER, D. S. & KORC, M. 2009. Pancreatic cancer and precursor pancreatic intraepithelial neoplasia lesions are devoid of primary cilia. *Cancer Res,* 69**,** 422-30.
SEELEY, E. S. & NACHURY, M. V. 2009. Constructing and deconstructing roles for the primary cilium in tissue architecture and cancer. *Methods Cell Biol,* 94**,** 299-313.
SHARMA, A., AHER, A., DYNES, N. J., FREY, D., KATRUKHA, E. A., JAUSSI, R., GRIGORIEV, I., CROISIER, M., KAMMERER, R. A., AKHMANOVA, A., GONCZY, P. & STEINMETZ, M. O. 2016. Centriolar CPAP/SAS-4 Imparts Slow Processive Microtubule Growth. *Dev Cell,* 37**,** 362-76.
SHARMA, N., KOSAN, Z. A., STALLWORTH, J. E., BERBARI, N. F. & YODER, B. K. 2011. Soluble levels of cytosolic tubulin regulate ciliary length control. *Mol Biol Cell,* 22**,** 806-16.
SHI, Y., KIRWAN, P. & LIVESEY, F. J. 2012. Directed differentiation of human pluripotent stem cells to cerebral cortex neurons and neural networks. *Nat Protoc,* 7**,** 1836-46.
SHITAMUKAI, A. & MATSUZAKI, F. 2012. Control of asymmetric cell division of mammalian neural progenitors. *Dev Growth Differ,* 54**,** 277-86.
SHPAK, M., GOLDBERG, M. M. & COWPERTHWAITE, M. C. 2014. Cilia gene expression patterns in cancer. *Cancer Genomics Proteomics,* 11**,** 13-24.
SIEBZEHNRUBL, F. A., SILVER, D. J., TUGERTIMUR, B., DELEYROLLE, L. P., SIEBZEHNRUBL, D., SARKISIAN, M. R., DEVERS, K. G., YACHNIS, A. T., KUPPER, M. D., NEAL, D., NABILSI, N. H., KLADDE, M. P., SUSLOV, O., BRABLETZ, S., BRABLETZ, T., REYNOLDS, B. A. & STEINDLER, D. A. 2013. The ZEB1 pathway links glioblastoma initiation, invasion and chemoresistance. *EMBO Mol Med,* 5**,** 1196-212.
SINGLA, V., ROMAGUERA-ROS, M., GARCIA-VERDUGO, J. M. & REITER, J. F. 2010. Ofd1, a human disease gene, regulates the length and distal structure of centrioles. *Dev Cell,* 18**,** 410-24.
SONN, S., JEONG, Y. & RHEE, K. 2009. Nip2/centrobin may be a substrate of Nek2 that is required for proper spindle assembly during mitosis in early mouse embryos. *Mol Reprod Dev,* 76**,** 587-92.
SOROKIN 1968a.

SOROKIN, S. P. 1968b. Reconstructions of centriole formation and ciliogenesis in mammalian lungs. *J Cell Sci,* 3**,** 207-30.
SPALLUTO, C., WILSON, D. I. & HEARN, T. 2012. Nek2 localises to the distal portion of the mother centriole/basal body and is required for timely cilium disassembly at the G2/M transition. *Eur J Cell Biol,* 91**,** 675-86.
SPASSKY, N., HAN, Y. G., AGUILAR, A., STREHL, L., BESSE, L., LACLEF, C., ROS, M. R., GARCIA-VERDUGO, J. M. & ALVAREZ-BUYLLA, A. 2008. Primary cilia are required for cerebellar development and Shh-dependent expansion of progenitor pool. *Dev Biol,* 317**,** 246-59.
SPEKTOR, A., TSANG, W. Y., KHOO, D. & DYNLACHT, B. D. 2007. Cep97 and CP110 suppress a cilia assembly program. *Cell,* 130**,** 678-90.
STILES, C. D. & ROWITCH, D. H. 2008. Glioma stem cells: a midterm exam. *Neuron,* 58**,** 832-46.
STOMMEL, J. M., KIMMELMAN, A. C., YING, H., NABIOULLIN, R., PONUGOTI, A. H., WIEDEMEYER, R., STEGH, A. H., BRADNER, J. E., LIGON, K. L., BRENNAN, C., CHIN, L. & DEPINHO, R. A. 2007. Coactivation of receptor tyrosine kinases affects the response of tumor cells to targeted therapies. *Science,* 318**,** 287-90.
STUPP, R., MASON, W. P., VAN DEN BENT, M. J., WELLER, M., FISHER, B., TAPHOORN, M. J., BELANGER, K., BRANDES, A. A., MAROSI, C., BOGDAHN, U., CURSCHMANN, J., JANZER, R. C., LUDWIN, S. K., GORLIA, T., ALLGEIER, A., LACOMBE, D., CAIRNCROSS, J. G., EISENHAUER, E., MIRIMANOFF, R. O., EUROPEAN ORGANISATION FOR, R., TREATMENT OF CANCER BRAIN, T., RADIOTHERAPY, G. & NATIONAL CANCER INSTITUTE OF CANADA CLINICAL TRIALS, G. 2005. Radiotherapy plus concomitant and adjuvant temozolomide for glioblastoma. *N Engl J Med,* 352**,** 987-96.
SUNG, C. H. & LEROUX, M. R. 2013. The roles of evolutionarily conserved functional modules in cilia-related trafficking. *Nat Cell Biol,* 15**,** 1387-97.
TANAKA, S., LOUIS, D. N., CURRY, W. T., BATCHELOR, T. T. & DIETRICH, J. 2013. Diagnostic and therapeutic avenues for glioblastoma: no longer a dead end? *Nat Rev Clin Oncol,* 10**,** 14-26.
TANG, Z., LIN, M. G., STOWE, T. R., CHEN, S., ZHU, M., STEARNS, T., FRANCO, B. & ZHONG, Q. 2013. Autophagy promotes primary ciliogenesis by removing OFD1 from centriolar satellites. *Nature,* 502**,** 254-7.
TAYLOR, M. D., LIU, L., RAFFEL, C., HUI, C. C., MAINPRIZE, T. G., ZHANG, X., AGATEP, R., CHIAPPA, S., GAO, L., LOWRANCE, A., HAO, A., GOLDSTEIN, A. M., STAVROU, T., SCHERER, S. W., DURA, W. T., WAINWRIGHT, B., SQUIRE, J. A., RUTKA, J. T. & HOGG, D. 2002. Mutations in SUFU predispose to medulloblastoma. *Nat Genet,* 31**,** 306-10.
THOMA, C. R., FREW, I. J., HOERNER, C. R., MONTANI, M., MOCH, H. & KREK, W. 2007. pVHL and GSK3beta are components of a primary cilium-maintenance signalling network. *Nat Cell Biol,* 9**,** 588-95.
THOMA, C. R., MATOV, A., GUTBRODT, K. L., HOERNER, C. R., SMOLE, Z., KREK, W. & DANUSER, G. 2010. Quantitative image analysis identifies pVHL as a key regulator of microtubule dynamic instability. *J Cell Biol,* 190**,** 991-1003.
TSAI, J. J., HSU, W. B., LIU, J. H., CHANG, C. W. & TANG, T. K. 2019. CEP120 interacts with C2CD3 and Talpid3 and is required for centriole appendage assembly and ciliogenesis. *Sci Rep,* 9**,** 6037.
TUCKER, R. W., SCHER, C. D. & STILES, C. D. 1979. Centriole deciliation associated with the early response of 3T3 cells to growth factors but not to SV40. *Cell,* 18**,** 1065-72.
VENKATESH, H. S., JOHUNG, T. B., CARETTI, V., NOLL, A., TANG, Y., NAGARAJA, S., GIBSON, E. M., MOUNT, C. W., POLEPALLI, J., MITRA, S. S., WOO, P. J., MALENKA, R. C., VOGEL, H., BREDEL, M., MALLICK, P. & MONJE, M. 2015. Neuronal Activity Promotes Glioma Growth through Neuroligin-3 Secretion. *Cell,* 161**,** 803-16.
VENKATESH, H. S., TAM, L. T., WOO, P. J., LENNON, J., NAGARAJA, S., GILLESPIE, S. M., NI, J., DUVEAU, D. Y., MORRIS, P. J., ZHAO, J. J., THOMAS, C. J. & MONJE, M. 2017. Targeting neuronal activity-regulated neuroligin-3 dependency in high-grade glioma. *Nature,* 549**,** 533-537.
VERHAAK, R. G., HOADLEY, K. A., PURDOM, E., WANG, V., QI, Y., WILKERSON, M. D., MILLER, C. R., DING, L., GOLUB, T., MESIROV, J. P., ALEXE, G., LAWRENCE, M., O'KELLY, M., TAMAYO, P., WEIR, B. A., GABRIEL, S., WINCKLER, W., GUPTA, S., JAKKULA, L.,

FEILER, H. S., HODGSON, J. G., JAMES, C. D., SARKARIA, J. N., BRENNAN, C., KAHN, A., SPELLMAN, P. T., WILSON, R. K., SPEED, T. P., GRAY, J. W., MEYERSON, M., GETZ, G., PEROU, C. M., HAYES, D. N. & CANCER GENOME ATLAS RESEARCH, N. 2010. Integrated genomic analysis identifies clinically relevant subtypes of glioblastoma characterized by abnormalities in PDGFRA, IDH1, EGFR, and NF1. *Cancer Cell,* 17**,** 98-110.

VERTII, A., HUNG, H. F., HEHNLY, H. & DOXSEY, S. 2016. Human basal body basics. *Cilia,* 5**,** 13.

WALLINGFORD, J. B. & MITCHELL, B. 2011. Strange as it may seem: the many links between Wnt signaling, planar cell polarity, and cilia. *Genes Dev,* 25**,** 201-13.

WANG, G., CHEN, Q., ZHANG, X., ZHANG, B., ZHUO, X., LIU, J., JIANG, Q. & ZHANG, C. 2013a. PCM1 recruits Plk1 to the pericentriolar matrix to promote primary cilia disassembly before mitotic entry. *J Cell Sci,* 126**,** 1355-65.

WANG, L. & DYNLACHT, B. D. 2018. The regulation of cilium assembly and disassembly in development and disease. *Development,* 145.

WANG, L., FAILLER, M., FU, W. & DYNLACHT, B. D. 2018. A distal centriolar protein network controls organelle maturation and asymmetry. *Nat Commun,* 9**,** 3938.

WANG, W. J., TAY, H. G., SONI, R., PERUMAL, G. S., GOLL, M. G., MACALUSO, F. P., ASARA, J. M., AMACK, J. D. & TSOU, M. F. 2013b. CEP162 is an axoneme-recognition protein promoting ciliary transition zone assembly at the cilia base. *Nat Cell Biol,* 15**,** 591-601.

WATERS, A. M. & BEALES, P. L. 2011. Ciliopathies: an expanding disease spectrum. *Pediatr Nephrol,* 2*6***,** 1039-56.

WEICHERT, W., KRISTIANSEN, G., SCHMIDT, M., GEKELER, V., NOSKE, A., NIESPOREK, S., DIETEL, M. & DENKERT, C. 2005. Polo-like kinase 1 expression is a prognostic factor in human colon cancer. *World J Gastroenterol,* 11**,** 5644-50.

WEN, P. Y. & KESARI, S. 2008. Malignant gliomas in adults. *N Engl J Med,* 359**,** 492-507.

WEN, X., LAI, C. K., EVANGELISTA, M., HONGO, J. A., DE SAUVAGE, F. J. & SCALES, S. J. 2010. Kinetics of hedgehog-dependent full-length Gli3 accumulation in primary cilia and subsequent degradation. *Mol Cell Biol,* 30**,** 1910-22.

WESTLAKE, C. J., BAYE, L. M., NACHURY, M. V., WRIGHT, K. J., ERVIN, K. E., PHU, L., CHALOUNI, C., BECK, J. S., KIRKPATRICK, D. S., SLUSARSKI, D. C., SHEFFIELD, V. C., SCHELLER, R. H. & JACKSON, P. K. 2011. Primary cilia membrane assembly is initiated by Rab11 and transport protein particle II (TRAPPII) complex-dependent trafficking of Rabin8 to the centrosome. *Proc Natl Acad Sci U S A,* 108**,** 2759-64.

WIEGERING, A., DILDROP, R., KALFHUES, L., SPYCHALA, A., KUSCHEL, S., LIER, J. M., ZOBEL, T., DAHMEN, S., LEU, T., STRUCHTRUP, A., LEGENDRE, F., VESQUE, C., SCHNEIDER-MAUNOURY, S., SAUNIER, S., RUTHER, U. & GERHARDT, C. 2018. Cell type-specific regulation of ciliary transition zone assembly in vertebrates. *EMBO J,* 37.

WILLIAMS, C. L., LI, C., KIDA, K., INGLIS, P. N., MOHAN, S., SEMENEC, L., BIALAS, N. J., STUPAY, R. M., CHEN, N., BLACQUE, O. E., YODER, B. K. & LEROUX, M. R. 2011. MKS and NPHP modules cooperate to establish basal body/transition zone membrane associations and ciliary gate function during ciliogenesis. *J Cell Biol,* 192**,** 1023-41.

WONG, S. Y., SEOL, A. D., SO, P. L., ERMILOV, A. N., BICHAKJIAN, C. K., EPSTEIN, E. H., JR., DLUGOSZ, A. A. & REITER, J. F. 2009. Primary cilia can both mediate and suppress Hedgehog pathway-dependent tumorigenesis. *Nat Med,* 15**,** 1055-61.

WU, C. T., CHEN, H. Y. & TANG, T. K. 2018. Myosin-Va is required for preciliary vesicle transportation to the mother centriole during ciliogenesis. *Nat Cell Biol,* 20**,** 175-185.

XIANG, W., GUO, F., CHENG, W., ZHANG, J., HUANG, J., WANG, R., MA, Z. & XU, K. 2017. HDAC6 inhibition suppresses chondrosarcoma by restoring the expression of primary cilia. *Oncol Rep,* 38**,** 229-236.

XIE, Y., BERGSTROM, T., JIANG, Y., JOHANSSON, P., MARINESCU, V. D., LINDBERG, N., SEGERMAN, A., WICHER, G., NIKLASSON, M., BASKARAN, S., SREEDHARAN, S., EVERLIEN, I., KASTEMAR, M., HERMANSSON, A., ELFINEH, L., LIBARD, S., HOLLAND, E. C., HESSELAGER, G., ALAFUZOFF, I., WESTERMARK, B., NELANDER, S., FORSBERG-NILSSON, K. & UHRBOM, L. 2015. The Human Glioblastoma Cell Culture Resource: Validated Cell Models Representing All Molecular Subtypes. *EBioMedicine,* 2**,** 1351-63.

YANG, N., LEUNG, E. L., LIU, C., LI, L., EGUETHER, T., JUN YAO, X. J., JONES, E. C., NORRIS, D. A., LIU, A., CLARK, R. A., ROOP, D. R., PAZOUR, G. J., SHROYER, K. R. & CHEN, J.

2017. INTU is essential for oncogenic Hh signaling through regulating primary cilia formation in basal cell carcinoma. *Oncogene,* 36**,** 4997-5005.

YANG, T. T., CHONG, W. M., WANG, W. J., MAZO, G., TANOS, B., CHEN, Z., TRAN, T. M. N., CHEN, Y. D., WENG, R. R., HUANG, C. E., JANE, W. N., TSOU, M. B. & LIAO, J. C. 2018. Super-resolution architecture of mammalian centriole distal appendages reveals distinct blade and matrix functional components. *Nat Commun,* 9**,** 2023.

YANG, Y., ROINE, N. & MAKELA, T. P. 2013. CCRK depletion inhibits glioblastoma cell proliferation in a cilium-dependent manner. *EMBO Rep,* 14**,** 741-7.

YAO, M., LI, S., WU, X., DIAO, S., ZHANG, G., HE, H., BIAN, L. & LU, Y. 2018. Cellular origin of glioblastoma and its implication in precision therapy. *Cell Mol Immunol,* 15**,** 737-739.

YE, X., ZENG, H., NING, G., REITER, J. F. & LIU, A. 2014. C2cd3 is critical for centriolar distal appendage assembly and ciliary vesicle docking in mammals. *Proc Natl Acad Sci U S A,* 111**,** 2164-9.

YOSHIMURA, K., KAWATE, T. & TAKEDA, S. 2011. Signaling through the primary cilium affects glial cell survival under a stressed environment. *Glia,* 59**,** 333-44.

YUAN, K., FROLOVA, N., XIE, Y., WANG, D., COOK, L., KWON, Y. J., STEG, A. D., SERRA, R. & FROST, A. R. 2010. Primary cilia are decreased in breast cancer: analysis of a collection of human breast cancer cell lines and tissues. *J Histochem Cytochem,* 58**,** 857-70.

ZHANG, W., TAYLOR, S. P., NEVAREZ, L., LACHMAN, R. S., NICKERSON, D. A., BAMSHAD, M., UNIVERSITY OF WASHINGTON CENTER FOR MENDELIAN GENOMICS, C., KRAKOW, D. & COHN, D. H. 2016. IFT52 mutations destabilize anterograde complex assembly, disrupt ciliogenesis and result in short rib polydactyly syndrome. *Hum Mol Genet,* 25**,** 4012-4020.

ZHENG, X., GOOI, L. M., WASON, A., GABRIEL, E., MEHRJARDI, N. Z., YANG, Q., ZHANG, X., DEBEC, A., BASIRI, M. L., AVIDOR-REISS, T., POZNIAKOVSKY, A., POSER, I., SARIC, T., HYMAN, A. A., LI, H. & GOPALAKRISHNAN, J. 2014. Conserved TCP domain of Sas-4/CPAP is essential for pericentriolar material tethering during centrosome biogenesis. *Proc Natl Acad Sci U S A,* 111**,** E354-63.

ZHENG, X., RAMANI, A., SONI, K., GOTTARDO, M., ZHENG, S., MING GOOI, L., LI, W., FENG, S., MARIAPPAN, A., WASON, A., WIDLUND, P., POZNIAKOVSKY, A., POSER, I., DENG, H., OU, G., RIPARBELLI, M., GIULIANO, C., HYMAN, A. A., SATTLER, M., GOPALAKRISHNAN, J. & LI, H. 2016. Molecular basis for CPAP-tubulin interaction in controlling centriolar and ciliary length. *Nat Commun,* 7**,** 11874.

ZHOU, F. Q. & SNIDER, W. D. 2005. Cell biology. GSK-3beta and microtubule assembly in axons. *Science,* 308**,** 211-4.

ZHOU, W., YANG, Y., XIA, J., WANG, H., SALAMA, M. E., XIONG, W., XU, H., SHETTY, S., CHEN, T., ZENG, Z., SHI, L., ZANGARI, M., MILES, R., BEARSS, D., TRICOT, G. & ZHAN, F. 2013. NEK2 induces drug resistance mainly through activation of efflux drug pumps and is associated with poor prognosis in myeloma and other cancers. *Cancer Cell,* 23**,** 48-62.

ZINGG, D., DEBBACHE, J., PENA-HERNANDEZ, R., ANTUNES, A. T., SCHAEFER, S. M., CHENG, P. F., ZIMMERLI, D., HAEUSEL, J., CALCADA, R. R., TUNCER, E., ZHANG, Y., BOSSART, R., WONG, K. K., BASLER, K., DUMMER, R., SANTORO, R., LEVESQUE, M. P. & SOMMER, L. 2018. EZH2-Mediated Primary Cilium Deconstruction Drives Metastatic Melanoma Formation. *Cancer Cell,* 34**,** 69-84 e14.

ZOU, C., LI, J., BAI, Y., GUNNING, W. T., WAZER, D. E., BAND, V. & GAO, Q. 2005. Centrobin: a novel daughter centriole-associated protein that is required for centriole duplication. *J Cell Biol,* 171**,** 437-45.

# List of publications

1. **Goranci-Buzhala G**, Gabriel E, Mariappan A, **Gopalakrishnan J.** *Losers of Primary Cilia Gain the Benefit of survival.* **Cancer Discovery** 12, 1374-1375 **(2017).**
2. Gabriel E, Ramani A, Karow U, Gottardo M, Natarajan K, Gooi LM, **Goranci-Buzhala G**, Krut O, Peters F, Nikolic M, Kuivanen S, Korhonen E, Smura T, Vapalahti O, Papantonis A, Schmidt-Chanasit J, Riparbelli M, Callaini G, Krönke M, Utermöhlen O, Gopalakrishnan J. *Recent Zika virus isolates induce premature differentiation of neural progenitors in human brain organoids.* **Cell Stem Cell** 20, 1-10 **(2017).**
3. **Goranci-Buzhala G** [#], Mariappan A [#], Gabriel E, Ramani A, Ricci-Vitiani L, Buccarelli M, D'Alessandris QG, Pallini R, Gopalakrishnan J. *"Rapid and efficient assay of glioblastoma invasion in human brain organoids.* **Cell Reports** 10, 107738 **(2020)**
4. **Gladiola Goranci-Buzhala**, Aruljothi Mariappan, Lucia Ricci-Vitiani, Natasa Josipovic, Argyris Papantonis, Marco Gottardo, Giuliano Callaini, Krishnaraj Rajalingam, Brian Dynlacht, Kamyar Hadian, Roberto Pallini, Karin Forsberg-Nilsson, and Jay Gopalakrishnan* *Cilium induction triggers differentiation of glioma stem cells.* Under revision **Cell Stem Cell**

[#] These authors contributed equally to this work

# Curriculum vitae

Gladiola Goranci-Buzhala

gladiolagoranci@hotmail.com

**CURRENT POSITION**

**University of Cologne, Cologne, Germany** (From October 2015)

(Center for Molecular Medicine Cologne ) PhD student

**EDUCATION**

**University of Cologne, Cologne, Germany** (2012-2014)

MSc in Biological Science

**Hedmark University, Hamar, Norway** (2007-2008)

Exchange Student, two semesters

**University of Prishtina, Kosovo** (2004-2008)

BSc. Applied Biology

**WORK AND RESEARCH EXPERIENCE**

**University of Cologne, Germany** (From October 2015)
PhD Advisor: Prof. Jay Gopalakrishnan
Cilia induction by abrogating Nek2 function to inhibit proliferation and induce differentiation of glioma cells

- Characterization of patient-derived glioma stem cells
- Targeting cilia loss in glioma stem cells
- Reprograming human hiPSCs, neuronal differentiation
- Establishing a traceable in vitro cerebral organoid model to study the invasive behavior of glioma
- Screening for chemical compounds to target primary cilia in glioma cells

**University of Cologne**, **Germany** (2014-2015)
Research assistant; Advisor: Prof Carien Niessen
Characterizing if the p120 is required for desmosome assembly;
Identifying another essential binding partner implicated in desmosome formation.

**University of Cologne, Germany** (2013-2014)
Master's thesis research; Advisor: Prof. Carien Niessen
Classical cadherin mediated regulation of intercellular junction formation: role of endocytosis

- Is cadherin internalization required for desmosome assembly?
- Do reduced cadherin levels affect tight junctional stability in an EGFR dependent manner?

**University of Prishtina, Kosovo** (2004-2008)

Bachelor's thesis research

HP-SEC analyze of patatine modified by chemical and enzymatic treatment

**Hedmark University, Norway** (2007-2008)

Exchange Student, 2 semesters Methods in Biotechnology; Industrial Biotechnology ; Molecular Biology ; Environmental Chemistry; Thesis experimental lab work

## SKILLS AND TECHNIQUES

- Culturing, sub-culturing of primary cell types like mouse epithelial cells, human glioblastoma cells
- Culturing hiPSC cells and differentiated them to neural progenitor cells, astrocytes and neurons.
- Whole cell lysate preparation, protein estimation by BSA method, Western blot, Immunoprecipitation.
- Immunocytochemistry: fixation of cells, staining, and scanning for different protein targets
- Molecular Biology: PCR (Standard PCR), Cloning, DNA sequencing, TALEN.
- Microscopes: Leica LAS AF 32.0.9652, Leica Confocal TCS STED LAS AF 4.0, LEICA SP8 Confocal Olympus Fluoview FV 1000 Confocal
- Tools and Applications: Microsoft Office, Image J, Graph Pad Prism 5, Gentel, Adobe Photoshop, Adobe Illustrator, SerialClonar

## CERTIFICATES

| | |
|---|---|
| Effective Communication for Women in Science | 2014 |
| English for International Conferences and Projects | 2014 |
| General knowledge for killing lab animals | 2014 |
| Statistical Literacy workshop | 2015 |
| Scientific PowerPoint Presentation | 2016 |

## HONORS AND SCHOLARSHIPS

| | |
|---|---|
| Distinguished Student<br>Faculty of Mathematical and Natural Science; University of Prishtina | 2007 |
| Student Talk Prize; IPMM days University of Cologne | 2016 |
| Travel Grant; DAAD program IPaK | 2017 |
| The Best Poster Award; Graduated School for Biological Sciences CEWIS | 2017 |
| Student Talk Prize; IPMM days University of Cologne | 2019 |

# Acknowledgment

This thesis would not have been possible without the help and support of many people.
First and foremost, I would like to express my sincerest gratitude to my advisor, Prof. Dr. Jay Gopalakrishnan, for giving me the opportunity to join his lab and for making it possible for me to work on many amazing projects. I highly appreciate his excellent suggestions on my research and personal development and feel fortunate to have completed my thesis under his supervision.

I would also like to thank Prof. Dr. Bernhard Schermer and Prof. Dr. Mirka Uhlirova for agreeing to be part of my thesis committee. I have benefited greatly from numerous tutor meetings with both of them and from the valuable feedback that they gave on my thesis project.

This thesis would not have been possible without the financial support of the Graduate Program in Pharmacology and Experimental Therapeutics of the University of Cologne and Bayer AG. Special thanks to Dr. Marion Razowski, the scientific coordinator of the graduate school, for her ongoing support, from my enrollment to the program and throughout my Ph.D. studies. I would also like to thank the Interdisciplinary Program Molecular Medicine at the University of Cologne (IPMM) for offering many interesting courses, which have broadened my scientific knowledge and improved my soft skills.

I am particularly thankful to Arul Mariappan for his patience and academic advice. His motivation and focus have been a great source of inspiration for me; I have enjoyed working and spending time with him.

It has been a great experience to spend these years with the amazing colleagues of the CCB lab. They have always created a stimulating work environment where I had the chance to share my thoughts on scientific topics and beyond. I believe that while sharing the office and the lab space together, we have built lifelong friendships. In particular, I want to thank Prof. Jay for sharing his expertise on cloning and biochemistry, which have played a pivotal role in the success of my thesis project; Elke Gabriel for training me in cell culture, especially in iPSCs handling; Arul Mariappan for sharing his experience in confocal and light microscopy and helping me in writing and edit my thesis; Elke Gabriel for translating my PhD abstract into German; Marco Gottardo for performing electron microscopy experiments for my thesis project; Anand Ramani, Nazlican Altinsik, Afshin Iram, Erika Zernickel, for creating a positive and pleasant working atmosphere, both when the experiments went well or when they did not work out; my great master Abida Pranty and medical Stefanos Loizou students. Dr. Karthick Natarajan for helping me with iPSCs culturing in the beginning of Ph.D studies.

Especially I am thankful to my brother Shkamb for all the time he spent helping me to draw Illustrator figures for this thesis, and my brother Gramoz for motivating and supporting me throughout my Ph.D. studies, especially during the days when things did not go as smoothly as I wanted them.

I am deeply thankful to my friend Dr. Magdalena Laugsch for always being there for me and for helping me write up my thesis even during the last seconds before submission. I admire your positivity and the passion that you have for science.

I am indebted to the endless support and love that my family has given me during these years at the

Finally, I would like to express my deepest gratitude to my husband, Labi, who, even though he himself is far away from the biological community, has supported me all the way. He has always been understanding, even when I had to spend weekends in the lab, when I was stressing about experiments and writing or when at dinners I only talked about science. Your unconditional support has continuously encouraged me to chase my ambitions and has held my spirits high when things got tough. I love you!

I dedicate this thesis to my amazing son, MATIS, who is my hope and motivation to always work hard and keep going forward!

# Appendix

**Table 12. List of upregulated gene expression levels (FPKM; >0.6 log2-fold change, FDR<0.01) in U3047MG naïve), ciliated GSCs (U3047MG NEK2-KD) cells**

| Sr.No | Gene | Gene names | log2FoldChange | Pvalue |
|---|---|---|---|---|
| 1 | ENSG00000089169 | *RPH3A* | 7,223861578 | 0 |
| 2 | ENSG00000133048 | *CHI3L1* | 6,339190967 | 9,67773E-93 |
| 3 | ENSG00000128564 | *VGF* | 5,525096015 | 0 |
| 4 | ENSG00000205929 | *C21orf62* | 5,194185801 | 1,5444E-258 |
| 5 | ENSG00000118785 | *SPP1* | 5,121100364 | 0 |
| 6 | ENSG00000117152 | *RGS4* | 4,821116799 | 3,1756E-274 |
| 7 | ENSG00000137033 | *IL33* | 4,778551429 | 4,88101E-64 |
| 8 | ENSG00000198535 | *C2CD4A* | 4,774229985 | 1,7816E-106 |
| 9 | ENSG00000135333 | *EPHA7* | 4,706968939 | 1,25233E-35 |
| 10 | ENSG00000171951 | *SCG2* | 4,697727707 | 0 |
| 11 | ENSG00000131435 | *PDLIM4* | 4,696743102 | 0 |
| 12 | ENSG00000166741 | *NNMT* | 4,545095093 | 4,53178E-53 |
| 13 | ENSG00000104415 | *WISP1* | 4,509770205 | 2,3418E-122 |
| 14 | ENSG00000082293 | *COL19A1* | 4,486141497 | 1,6506E-133 |
| 15 | ENSG00000196277 | *GRM7* | 4,479967931 | 4,59502E-51 |
| 16 | ENSG00000141338 | *ABCA8* | 4,364939485 | 1,6757E-115 |
| 17 | ENSG00000134668 | *SPOCD1* | 4,248727317 | 2,16105E-69 |
| 18 | ENSG00000151702 | *FLI1* | 4,227320144 | 4,11244E-28 |
| 19 | ENSG00000110628 | *SLC22A18* | 4,215143269 | 7,3218E-107 |
| 20 | ENSG00000185100 | *ADSSL1* | 4,184900639 | 2,20037E-25 |
| 21 | ENSG00000113389 | *NPR3* | 4,170508184 | 6,92015E-24 |
| 22 | ENSG00000090339 | *ICAM1* | 4,11441223 | 6,60666E-59 |
| 23 | ENSG00000117450 | *PRDX1* | 4,054866331 | 2,1284E-122 |
| 24 | ENSG00000157502 | *MUM1L1* | 4,030025214 | 4,21031E-44 |
| 25 | ENSG00000187134 | *AKR1C1* | 3,967356734 | 3,63692E-39 |
| 26 | ENSG00000149571 | *KIRREL3* | 3,928424643 | 5,47705E-49 |
| 27 | ENSG00000133110 | *POSTN* | 3,924937515 | 0 |
| 28 | ENSG00000100985 | *MMP9* | 3,903527142 | 7,99339E-20 |
| 29 | ENSG00000174343 | *CHRNA9* | 3,792780426 | 4,34077E-45 |
| 30 | ENSG00000145623 | *OSMR* | 3,782542214 | 3,0083E-259 |
| 31 | ENSG00000106366 | *SERPINE1* | 3,778584563 | 0 |
| 32 | ENSG00000145934 | *TENM2* | 3,697660309 | 0 |
| 33 | ENSG00000099256 | *PRTFDC1* | 3,684017036 | 2,60113E-55 |
| 34 | ENSG00000159674 | *SPON2* | 3,673398094 | 2,80409E-20 |
| 35 | ENSG00000111335 | *OAS2* | 3,660119344 | 7,27973E-46 |
| 36 | ENSG00000150540 | *HNMT* | 3,610830552 | 1,1213E-101 |
| 37 | ENSG00000127920 | *GNG11* | 3,603513422 | 1,0247E-160 |
| 38 | ENSG00000163694 | *RBM47* | 3,601137026 | 1,27391E-83 |
| 39 | ENSG00000197977 | *ELOVL2* | 3,585950569 | 7,1426E-272 |
| 40 | ENSG00000197261 | *C6orf141* | 3,546218125 | 1,41805E-19 |
| 41 | ENSG00000198838 | *RYR3* | 3,502919887 | 1,84243E-81 |
| 42 | ENSG00000145920 | *CPLX2* | 3,494393476 | 3,33653E-16 |
| 43 | ENSG00000185070 | *FLRT2* | 3,486672256 | 4,27659E-15 |
| 44 | ENSG00000221818 | *EBF2* | 3,435902278 | 1,71336E-50 |
| 45 | ENSG00000120093 | *HOXB3* | 3,431377679 | 2,0446E-204 |
| 46 | ENSG00000169436 | *COL22A1* | 3,421834523 | 3,5461E-238 |
| 47 | ENSG00000115956 | *PLEK* | 3,3282404 | 1,2895E-12 |
| 48 | ENSG00000108771 | *DHX58* | 3,326767579 | 2,65968E-14 |
| 49 | ENSG00000130513 | *GDF15* | 3,323073359 | 1,0623E-115 |
| 50 | ENSG00000001036 | *FUCA2* | 3,318160106 | 2,66476E-82 |
| 51 | ENSG00000144481 | *TRPM8* | 3,310572222 | 6,3578E-255 |
| 52 | ENSG00000108602 | *ALDH3A1* | 3,305347043 | 6,59887E-29 |
| 53 | ENSG00000134986 | *NREP* | 3,304125719 | 4,1515E-163 |
| 54 | ENSG00000138759 | *FRAS1* | 3,283955549 | 5,3887E-135 |
| 55 | ENSG00000128641 | *MYO1B* | 3,263969903 | 2,75977E-22 |
| 56 | ENSG00000136352 | *NKX2-1* | 3,233413766 | 8,35362E-13 |
| 57 | ENSG00000196872 | *KIAA1211L* | 3,219745442 | 1,633E-111 |
| 58 | ENSG00000014914 | *MTMR11* | 3,191785532 | 4,9463E-146 |
| 59 | ENSG00000105376 | *ICAM5* | 3,182369125 | 9,0675E-110 |
| 60 | ENSG00000138821 | *SLC39A8* | 3,16868888 | 5,92701E-66 |
| 61 | ENSG00000107562 | *CXCL12* | 3,15565312 | 5,57521E-56 |
| 62 | ENSG00000118898 | *PPL* | 3,099618255 | 5,59797E-63 |
| 63 | ENSG00000157542 | *KCNJ6* | 3,07317783 | 8,8223E-24 |
| 64 | ENSG00000167157 | *PRRX2* | 3,0548022 | 2,45341E-18 |
| 65 | ENSG00000175899 | *A2M* | 3,052371268 | 0 |
| 66 | ENSG00000154734 | *ADAMTS1* | 3,051828092 | 1,7946E-208 |
| 67 | ENSG00000163661 | *PTX3* | 3,0498456 | 4,6877E-186 |
| 68 | ENSG00000095303 | *PTGS1* | 3,026697624 | 4,756E-100 |

| | | | | |
|---|---|---|---|---|
| 69 | ENSG00000135549 | *PKIB* | 3,012054632 | 3,3875E-260 |
| 70 | ENSG00000174791 | *RIN1* | 2,99922793 | 5,99016E-67 |
| 71 | ENSG00000113263 | *ITK* | 2,984377861 | 3,15066E-13 |
| 72 | ENSG00000149582 | *TMEM25* | 2,980403714 | 8,81278E-71 |
| 73 | ENSG00000124205 | *EDN3* | 2,978855229 | 3,63801E-09 |
| 74 | ENSG00000171658 | *NMRAL2P* | 2,97370674 | 1,64601E-10 |
| 75 | ENSG00000197921 | *HES5* | 2,963061095 | 2,23961E-24 |
| 76 | ENSG00000176697 | *BDNF* | 2,958458006 | 3,3059E-107 |
| 77 | ENSG00000180638 | *SLC47A2* | 2,951141178 | 3,05689E-22 |
| 78 | ENSG00000128165 | *ADM2* | 2,950014795 | 2,48628E-17 |
| 79 | ENSG00000204131 | *NHSL2* | 2,941277147 | 2,00109E-27 |
| 80 | ENSG00000196353 | *CPNE4* | 2,930843284 | 1,9898E-244 |
| 81 | ENSG00000108691 | *CCL2* | 2,928726749 | 5,36549E-13 |
| 82 | ENSG00000047648 | *ARHGAP6* | 2,903588008 | 1,5951E-166 |
| 83 | ENSG00000196878 | *LAMB3* | 2,900741475 | 2,64631E-68 |
| 84 | ENSG00000124145 | *SDC4* | 2,900077791 | 8,36492E-12 |
| 85 | ENSG00000256124 | *LINC01152* | 2,884868329 | 1,3833E-09 |
| 86 | ENSG00000064692 | *SNCAIP* | 2,884725022 | 8,44974E-42 |
| 87 | ENSG00000225217 | *HSPA7* | 2,874360754 | 5,25311E-22 |
| 88 | ENSG00000061337 | *LZTS1* | 2,87247717 | 0 |
| 89 | ENSG00000128285 | *MCHR1* | 2,87204445 | 1,32527E-56 |
| 90 | ENSG00000166482 | *MFAP4* | 2,858747309 | 3,45572E-74 |
| 91 | ENSG00000102024 | *PLS3* | 2,855342342 | 1,6081E-261 |
| 92 | ENSG00000211829 | *TRDC* | 2,843866122 | 3,78264E-10 |
| 93 | ENSG00000128849 | *CGNL1* | 2,83632936 | 1,83076E-97 |
| 94 | ENSG00000133083 | *DCLK1* | 2,830182604 | 4,17626E-77 |
| 95 | ENSG00000122861 | *PLAU* | 2,819575505 | 1,4303E-119 |
| 96 | ENSG00000139219 | *COL2A1* | 2,818155141 | 3,7493E-257 |
| 97 | ENSG00000141469 | *SLC14A1* | 2,81561976 | 3,88649E-39 |
| 98 | ENSG00000205090 | *TMEM240* | 2,815466558 | 1,52249E-11 |
| 99 | ENSG00000125931 | *CITED1* | 2,799709179 | 6,99787E-87 |
| 100 | ENSG00000113494 | *PRLR* | 2,788534459 | 7,64187E-11 |
| 101 | ENSG00000189184 | *PCDH18* | 2,786347851 | 5,10411E-44 |
| 102 | ENSG00000172020 | *GAP43* | 2,772473866 | 0 |
| 103 | ENSG00000174600 | *CMKLR1* | 2,758131131 | 8,16626E-30 |
| 104 | ENSG00000130429 | *ARPC1B* | 2,745934563 | 4,20651E-25 |
| 105 | ENSG00000089127 | *OAS1* | 2,740375413 | 2,067E-42 |
| 106 | ENSG00000056558 | *TRAF1* | 2,737347361 | 1,24275E-23 |
| 107 | ENSG00000138449 | *SLC40A1* | 2,736327389 | 1,41448E-54 |
| 108 | ENSG00000156265 | *MAP3K7CL* | 2,728226219 | 3,8955E-23 |
| 109 | ENSG00000129038 | *LOXL1* | 2,727903948 | 6,42557E-46 |
| 110 | ENSG00000175544 | *CABP4* | 2,72764762 | 1,10154E-08 |
| 111 | ENSG00000171189 | *GRIK1* | 2,725996361 | 1,85822E-96 |
| 112 | ENSG00000117650 | *NEK2* | 2,725159217 | 0 |
| 113 | ENSG00000127824 | *TUBA4A* | 2,720686367 | 1,6851E-116 |
| 114 | ENSG00000163191 | *S100A11* | 2,717204253 | 2,5602E-238 |
| 115 | ENSG00000063127 | *SLC6A16* | 2,716739173 | 6,92913E-21 |
| 116 | ENSG00000135744 | *AGT* | 2,712596076 | 2,7719E-208 |
| 117 | ENSG00000165905 | *LARGE2* | 2,712033136 | 1,4241E-08 |
| 118 | ENSG00000125851 | *PCSK2* | 2,711968198 | 6,79464E-12 |
| 119 | ENSG00000054356 | *PTPRN* | 2,706807965 | 1,66297E-73 |
| 120 | ENSG00000155760 | *FZD7* | 2,700584893 | 6,4574E-183 |
| 121 | ENSG00000110697 | *PITPNM1* | 2,696682041 | 2,21849E-19 |
| 122 | ENSG00000085871 | *MGST2* | 2,67692529 | 1,76517E-09 |
| 123 | ENSG00000182732 | *RGS6* | 2,67611169 | 9,5812E-104 |
| 124 | ENSG00000169116 | *PARM1* | 2,660961213 | 8,2045E-135 |
| 125 | ENSG00000265485 | *LINC01915* | 2,657997247 | 2,66301E-08 |
| 126 | ENSG00000011677 | *GABRA3* | 2,657862887 | 4,06767E-08 |
| 127 | ENSG00000196482 | *ESRRG* | 2,655662559 | 5,9347E-08 |
| 128 | ENSG00000102359 | *SRPX2* | 2,655114306 | 1,38499E-27 |
| 129 | ENSG00000181019 | *NQO1* | 2,617235178 | 1,0032E-243 |
| 130 | ENSG00000026559 | *KCNG1* | 2,61032574 | 2,25332E-20 |
| 131 | ENSG00000184574 | *LPAR5* | 2,596818284 | 2,39331E-09 |
| 132 | ENSG00000130775 | *THEMIS2* | 2,594899115 | 4,69952E-14 |
| 133 | ENSG00000168743 | *NPNT* | 2,59392634 | 2,3553E-17 |
| 134 | ENSG00000111087 | *GLI1* | 2,581733039 | 4,88935E-15 |
| 135 | ENSG00000244682 | *FCGR2C* | 2,580942516 | 9,81398E-15 |
| 136 | ENSG00000146674 | *IGFBP3* | 2,579656736 | 0 |
| 137 | ENSG00000213401 | *MAGEA12* | 2,555623736 | 1,32006E-06 |
| 138 | ENSG00000196139 | *AKR1C3* | 2,54964468 | 3,23108E-32 |
| 139 | ENSG00000229835 | *KHSRPP1* | 2,539513364 | 1,13556E-31 |
| 140 | ENSG00000198108 | *CHSY3* | 2,531834042 | 8,92562E-23 |
| 141 | ENSG00000172965 | *MIR4435-2HG* | 2,522790132 | 6,96488E-69 |
| 142 | ENSG00000158859 | *ADAMTS4* | 2,5140831 | 3,96972E-68 |
| 143 | ENSG00000120833 | *SOCS2* | 2,50777235 | 8,84414E-23 |
| 144 | ENSG00000170485 | *NPAS2* | 2,505815106 | 9,4841E-186 |
| 145 | ENSG00000075035 | *WSCD2* | 2,504603471 | 2,05004E-56 |
| 146 | ENSG00000140961 | *OSGIN1* | 2,503417179 | 6,92139E-73 |

| | | | | |
|---|---|---|---|---|
| 147 | ENSG00000127124 | *HIVEP3* | 2,500537977 | 3,04384E-72 |
| 148 | ENSG00000125869 | *LAMP5* | 2,496870117 | 1,0134E-124 |
| 149 | ENSG00000135457 | *TFCP2* | 2,477629929 | 1,69563E-25 |
| 150 | ENSG00000146648 | *EGFR* | 2,477075891 | 1,1354E-170 |
| 151 | ENSG00000128573 | *FOXP2* | 2,47523407 | 3,41086E-07 |
| 152 | ENSG00000188042 | *ARL4C* | 2,470667532 | 6,9564E-270 |
| 153 | ENSG00000257207 | *AC112229.3* | 2,467470418 | 6,31808E-08 |
| 154 | ENSG00000110492 | *MDK* | 2,46166455 | 1,19603E-36 |
| 155 | ENSG00000151388 | *ADAMTS12* | 2,457893709 | 2,80351E-78 |
| 156 | ENSG00000169499 | *PLEKHA2* | 2,446308978 | 1,7321E-118 |
| 157 | ENSG00000100097 | *LGALS1* | 2,441017358 | 0 |
| 158 | ENSG00000229298 | *TUBB8P1* | 2,440528359 | 3,14053E-12 |
| 159 | ENSG00000162374 | *ELAVL4* | 2,435182895 | 2,54685E-24 |
| 160 | ENSG00000142920 | *AZIN2* | 2,432704742 | 9,68336E-25 |
| 161 | ENSG00000179603 | *GRM8* | 2,431838306 | 6,90424E-10 |
| 162 | ENSG00000076344 | *RGS11* | 2,430412736 | 3,20123E-14 |
| 163 | ENSG00000008118 | *CAMK1G* | 2,429456283 | 3,35718E-09 |
| 164 | ENSG00000181649 | *PHLDA2* | 2,427687192 | 7,74967E-27 |
| 165 | ENSG00000133816 | *MICAL2* | 2,423930932 | 8,4885E-37 |
| 166 | ENSG00000074527 | *NTN4* | 2,422695517 | 3,52686E-08 |
| 167 | ENSG00000142627 | *EPHA2* | 2,411836358 | 1,62452E-67 |
| 168 | ENSG00000108846 | *ABCC3* | 2,38868819 | 1,05049E-24 |
| 169 | ENSG00000148344 | *PTGES* | 2,37905373 | 2,3257E-06 |
| 170 | ENSG00000143369 | *ECM1* | 2,377960149 | 2,97634E-37 |
| 171 | ENSG00000169220 | *RGS14* | 2,374527174 | 1,03603E-33 |
| 172 | ENSG00000060709 | *RIMBP2* | 2,369704175 | 2,39924E-20 |
| 173 | ENSG00000187867 | *PALM3* | 2,357447531 | 4,88808E-19 |
| 174 | ENSG00000246859 | *STARD4-AS1* | 2,353024638 | 5,2039E-17 |
| 175 | ENSG00000073150 | *PANX2* | 2,350697399 | 1,25938E-14 |
| 176 | ENSG00000147509 | *RGS20* | 2,349850149 | 6,54051E-25 |
| 177 | ENSG00000105639 | *JAK3* | 2,343814932 | 9,94586E-08 |
| 178 | ENSG00000100351 | *GRAP2* | 2,337453909 | 5,41042E-08 |
| 179 | ENSG00000141750 | *STAC2* | 2,331384607 | 9,73053E-24 |
| 180 | ENSG00000151023 | *ENKUR* | 2,329356333 | 2,35158E-19 |
| 181 | ENSG00000137752 | *CASP1* | 2,327205603 | 2,73818E-07 |
| 182 | ENSG00000184937 | *WT1* | 2,322076402 | 2,91155E-09 |
| 183 | ENSG00000110057 | *UNC93B1* | 2,318647109 | 8,44475E-41 |
| 184 | ENSG00000131378 | *RFTN1* | 2,318591236 | 3,47195E-65 |
| 185 | ENSG00000185885 | *IFITM1* | 2,31441695 | 1,35021E-12 |
| 186 | ENSG00000196542 | *SPTSSB* | 2,313539106 | 3,48557E-14 |
| 187 | ENSG00000163618 | *CADPS* | 2,308137433 | 2,06545E-10 |
| 188 | ENSG00000188523 | *CFAP77* | 2,299843404 | 5,96259E-09 |
| 189 | ENSG00000135363 | *LMO2* | 2,298225716 | 1,194E-129 |
| 190 | ENSG00000221866 | *PLXNA4* | 2,28153094 | 1,4782E-110 |
| 191 | ENSG00000158710 | *TAGLN2* | 2,280907136 | 4,9908E-159 |
| 192 | ENSG00000135077 | *HAVCR2* | 2,280101092 | 5,53831E-10 |
| 193 | ENSG00000196730 | *DAPK1* | 2,276348702 | 1,70904E-95 |
| 194 | ENSG00000160284 | *SPATC1L* | 2,275236621 | 1,48644E-36 |
| 195 | ENSG00000117114 | *ADGRL2* | 2,275060691 | 3,3421E-236 |
| 196 | ENSG00000161243 | *FBXO27* | 2,267811427 | 4,83232E-06 |
| 197 | ENSG00000120875 | *DUSP4* | 2,258775149 | 1,5381E-170 |
| 198 | ENSG00000147804 | *SLC39A4* | 2,254269459 | 7,43889E-18 |
| 199 | ENSG00000100336 | *APOL4* | 2,248529806 | 5,01494E-07 |
| 200 | ENSG00000130477 | *UNC13A* | 2,243440703 | 1,7155E-169 |
| 201 | ENSG00000160211 | *G6PD* | 2,235590068 | 1,6086E-246 |
| 202 | ENSG00000158246 | *FAM46B* | 2,22043465 | 9,34687E-27 |
| 203 | ENSG00000143333 | *RGS16* | 2,204605009 | 1,31743E-37 |
| 204 | ENSG00000137090 | *DMRT1* | 2,203813482 | 5,39616E-06 |
| 205 | ENSG00000162692 | *VCAM1* | 2,203538794 | 4,00647E-10 |
| 206 | ENSG00000081803 | *CADPS2* | 2,199346086 | 6,47097E-11 |
| 207 | ENSG00000130303 | *BST2* | 2,198406375 | 2,33417E-34 |
| 208 | ENSG00000204583 | *LRCOL1* | 2,195466105 | 2,97327E-09 |
| 209 | ENSG00000042286 | *AIFM2* | 2,188651641 | 6,28405E-21 |
| 210 | ENSG00000135324 | *MRAP2* | 2,183551404 | 1,48898E-46 |
| 211 | ENSG00000149295 | *DRD2* | 2,183075486 | 3,48239E-11 |
| 212 | ENSG00000197415 | *VEPH1* | 2,179210374 | 8,89709E-62 |
| 213 | ENSG00000117069 | *ST6GALNAC5* | 2,173198575 | 9,86473E-09 |
| 214 | ENSG00000167487 | *KLHL26* | 2,171591264 | 7,65426E-22 |
| 215 | ENSG00000059915 | *PSD* | 2,169829522 | 5,08749E-33 |
| 216 | ENSG00000175426 | *PCSK1* | 2,167230125 | 1,12458E-07 |
| 217 | ENSG00000154127 | *UBASH3B* | 2,162376461 | 8,9054E-202 |
| 218 | ENSG00000198865 | *CCDC152* | 2,16111847 | 3,14905E-18 |
| 219 | ENSG00000125531 | *FNDC11* | 2,160888912 | 2,24816E-05 |
| 220 | ENSG00000261801 | *LOXL1-AS1* | 2,159518797 | 1,31888E-05 |
| 221 | ENSG00000141524 | *TMC6* | 2,159083563 | 5,25305E-13 |
| 222 | ENSG00000182742 | *HOXB4* | 2,158318935 | 3,97087E-07 |
| 223 | ENSG00000146950 | *SHROOM2* | 2,145569156 | 1,9171E-171 |
| 224 | ENSG00000145703 | *IQGAP2* | 2,144702081 | 3,2946E-166 |

| | | | | |
|---|---|---|---|---|
| 225 | ENSG00000166750 | *SLFN5* | 2,143706974 | 1,92475E-51 |
| 226 | ENSG00000167011 | *NAT16* | 2,143312432 | 1,18983E-18 |
| 227 | ENSG00000249853 | *HS3ST5* | 2,142835853 | 8,74795E-07 |
| 228 | ENSG00000100433 | *KCNK10* | 2,142716528 | 1,74376E-21 |
| 229 | ENSG00000222041 | *CYTOR* | 2,14047033 | 3,07828E-28 |
| 230 | ENSG00000125398 | *SOX9* | 2,140236652 | 2,32E-290 |
| 231 | ENSG00000162595 | *DIRAS3* | 2,136520479 | 2,1599E-15 |
| 232 | ENSG00000223947 | *AC016738.1* | 2,134158527 | 2,7643E-09 |
| 233 | ENSG00000164251 | *F2RL1* | 2,129940751 | 4,51654E-22 |
| 234 | ENSG00000087116 | *ADAMTS2* | 2,129337023 | 7,05742E-08 |
| 235 | ENSG00000143786 | *CNIH3* | 2,127303387 | 1,6655E-112 |
| 236 | ENSG00000205683 | *DPF3* | 2,124466227 | 1,32188E-30 |
| 237 | ENSG00000132915 | *PDE6A* | 2,120179268 | 4,04357E-05 |
| 238 | ENSG00000117245 | *KIF17* | 2,120093006 | 1,45441E-07 |
| 239 | ENSG00000115461 | *IGFBP5* | 2,11809611 | 6,7762E-238 |
| 240 | ENSG00000184985 | *SORCS2* | 2,117957077 | 1,37477E-05 |
| 241 | ENSG00000164761 | *TNFRSF11B* | 2,116332079 | 2,51916E-16 |
| 242 | ENSG00000108448 | *TRIM16L* | 2,11370819 | 1,25363E-62 |
| 243 | ENSG00000266970 | *AC061992.1* | 2,109624879 | 6,11718E-06 |
| 244 | ENSG00000249992 | *TMEM158* | 2,109133412 | 4,2505E-204 |
| 245 | ENSG00000072210 | *ALDH3A2* | 2,101695763 | 3,1812E-267 |
| 246 | ENSG00000180801 | *ARSJ* | 2,098138562 | 1,62311E-75 |
| 247 | ENSG00000143473 | *KCNH1* | 2,082257273 | 9,38892E-12 |
| 248 | ENSG00000124839 | *RAB17* | 2,077238148 | 2,02607E-05 |
| 249 | ENSG00000099260 | *PALMD* | 2,068016514 | 1,54195E-08 |
| 250 | ENSG00000187260 | *WDR86* | 2,063651255 | 1,22849E-06 |
| 251 | ENSG00000185567 | *AHNAK2* | 2,055039681 | 2,79332E-41 |
| 252 | ENSG00000059804 | *SLC2A3* | 2,05430496 | 3,683E-138 |
| 253 | ENSG00000170290 | *SLN* | 2,04093409 | 6,13814E-05 |
| 254 | ENSG00000138823 | *MTTP* | 2,03012345 | 4,65882E-33 |
| 255 | ENSG00000176399 | *DMRTA1* | 2,028987244 | 1,25742E-18 |
| 256 | ENSG00000091986 | *CCDC80* | 2,027860847 | 2,3551E-214 |
| 257 | ENSG00000181291 | *TMEM132E* | 2,02758139 | 6,55861E-18 |
| 258 | ENSG00000155254 | *MARVELD1* | 2,023052101 | 1,51565E-29 |
| 259 | ENSG00000151136 | *BTBD11* | 2,022918666 | 2,91359E-09 |
| 260 | ENSG00000239552 | *HOXB-AS2* | 2,020764433 | 0,000102597 |
| 261 | ENSG00000261655 | *AC100803.2* | 2,018127011 | 0,000186187 |
| 262 | ENSG00000135074 | *ADAM19* | 2,010662068 | 5,395E-125 |
| 263 | ENSG00000133958 | *UNC79* | 2,002916193 | 5,78069E-24 |
| 264 | ENSG00000223414 | *LINC00473* | 2,001625175 | 8,2756E-05 |
| 265 | ENSG00000189171 | *S100A13* | 1,999428362 | 2,56782E-62 |
| 266 | ENSG00000184371 | *CSF1* | 1,994456852 | 4,69461E-92 |
| 267 | ENSG00000169245 | *CXCL10* | 1,994251332 | 0,000193765 |
| 268 | ENSG00000139410 | *SDSL* | 1,991679455 | 4,7165E-22 |
| 269 | ENSG00000147041 | *SYTL5* | 1,990267244 | 1,99955E-41 |
| 270 | ENSG00000174460 | *ZCCHC12* | 1,983962258 | 6,21322E-25 |
| 271 | ENSG00000226403 | *AL392089.1* | 1,981469679 | 8,97064E-16 |
| 272 | ENSG00000154736 | *ADAMTS5* | 1,968667397 | 9,65375E-05 |
| 273 | ENSG00000178033 | *FAM26E* | 1,96637833 | 7,75258E-06 |
| 274 | ENSG00000152137 | *HSPB8* | 1,963800459 | 4,09704E-10 |
| 275 | ENSG00000152954 | *NRSN1* | 1,962479697 | 1,61826E-11 |
| 276 | ENSG00000183323 | *CCDC125* | 1,962237035 | 3,69326E-06 |
| 277 | ENSG00000118257 | *NRP2* | 1,960429693 | 6,7865E-211 |
| 278 | ENSG00000234231 | *AC093616.1* | 1,955895995 | 7,06475E-10 |
| 279 | ENSG00000160712 | *IL6R* | 1,955873281 | 7,41449E-10 |
| 280 | ENSG00000162975 | *KCNF1* | 1,954920328 | 3,13489E-95 |
| 281 | ENSG00000137959 | *IFI44L* | 1,950705579 | 1,03516E-47 |
| 282 | ENSG00000197565 | *COL4A6* | 1,949729517 | 1,8059E-178 |
| 283 | ENSG00000178965 | *ERICH3* | 1,94902785 | 7,29516E-05 |
| 284 | ENSG00000197757 | *HOXC6* | 1,946325292 | 1,54218E-05 |
| 285 | ENSG00000019991 | *HGF* | 1,946115116 | 1,71232E-05 |
| 286 | ENSG00000142669 | *SH3BGRL3* | 1,945138395 | 5,8422E-89 |
| 287 | ENSG00000005884 | *ITGA3* | 1,944143187 | 1,9769E-149 |
| 288 | ENSG00000184524 | *CEND1* | 1,943029435 | 1,31037E-36 |
| 289 | ENSG00000110002 | *VWA5A* | 1,938486893 | 4,60091E-48 |
| 290 | ENSG00000156140 | *ADAMTS3* | 1,937598389 | 3,40213E-88 |
| 291 | ENSG00000165072 | *MAMDC2* | 1,929855722 | 1,81922E-06 |
| 292 | ENSG00000088882 | *CPXM1* | 1,92952266 | 3,9198E-134 |
| 293 | ENSG00000131477 | *RAMP2* | 1,928530045 | 1,54534E-12 |
| 294 | ENSG00000171227 | *TMEM37* | 1,926733201 | 5,94617E-06 |
| 295 | ENSG00000163803 | *PLB1* | 1,923988697 | 8,75746E-07 |
| 296 | ENSG00000172183 | *ISG20* | 1,923261917 | 7,41642E-08 |
| 297 | ENSG00000131080 | *EDA2R* | 1,923162326 | 2,1618E-08 |
| 298 | ENSG00000230314 | *ELOVL2-AS1* | 1,919618416 | 0,000315409 |
| 299 | ENSG00000135821 | *GLUL* | 1,911854852 | 6,1958E-305 |
| 300 | ENSG00000095752 | *IL11* | 1,906486624 | 4,25043E-06 |
| 301 | ENSG00000123496 | *IL13RA2* | 1,905993389 | 0,000186828 |
| 302 | ENSG00000188015 | *S100A3* | 1,905555795 | 5,67006E-05 |

| 303 | ENSG00000162804 | *SNED1* | 1,903217928 | 4,02474E-21 |
|---|---|---|---|---|
| 304 | ENSG00000159409 | *CELF3* | 1,903012803 | 3,02765E-15 |
| 305 | ENSG00000188916 | *FAM196A* | 1,901670964 | 2,5376E-133 |
| 306 | ENSG00000165507 | *C10orf10* | 1,900616346 | 1,21667E-07 |
| 307 | ENSG00000185924 | *RTN4RL1* | 1,900421389 | 7,91975E-10 |
| 308 | ENSG00000175832 | *ETV4* | 1,899758182 | 1,26924E-89 |
| 309 | ENSG00000204706 | *MAMDC2-AS1* | 1,893305876 | 2,54937E-09 |
| 310 | ENSG00000112981 | *NME5* | 1,888368183 | 1,32734E-11 |
| 311 | ENSG00000134531 | *EMP1* | 1,888090022 | 6,5514E-252 |
| 312 | ENSG00000122176 | *FMOD* | 1,885936019 | 0,000108145 |
| 313 | ENSG00000168679 | *SLC16A4* | 1,883964304 | 5,587E-27 |
| 314 | ENSG00000100968 | *NFATC4* | 1,883807871 | 0,00040304 |
| 315 | ENSG00000173404 | *INSM1* | 1,883643435 | 8,70669E-27 |
| 316 | ENSG00000039139 | *DNAH5* | 1,881164617 | 0,000370263 |
| 317 | ENSG00000129667 | *RHBDF2* | 1,880647608 | 0,000112086 |
| 318 | ENSG00000188153 | *COL4A5* | 1,880394548 | 4,0779E-204 |
| 319 | ENSG00000181773 | *GPR3* | 1,874854819 | 2,16899E-15 |
| 320 | ENSG00000196187 | *TMEM63A* | 1,873443008 | 4,06889E-71 |
| 321 | ENSG00000233384 | *AC096537.1* | 1,872159388 | 3,39967E-06 |
| 322 | ENSG00000128342 | *LIF* | 1,871558954 | 4,53661E-05 |
| 323 | ENSG00000104894 | *CD37* | 1,861921752 | 5,80204E-18 |
| 324 | ENSG00000138166 | *DUSP5* | 1,857505426 | 2,41568E-19 |
| 325 | ENSG00000176907 | *C8orf4* | 1,847111337 | 6,91862E-10 |
| 326 | ENSG00000250722 | *SELENOP* | 1,838098393 | 0,000129718 |
| 327 | ENSG00000100292 | *HMOX1* | 1,83651427 | 7,84472E-64 |
| 328 | ENSG00000186451 | *SPATA12* | 1,834786394 | 0,000131673 |
| 329 | ENSG00000185022 | *MAFF* | 1,833733843 | 1,40807E-19 |
| 330 | ENSG00000171812 | *COL8A2* | 1,826327338 | 1,95027E-07 |
| 331 | ENSG00000135519 | *KCNH3* | 1,824618025 | 1,65992E-34 |
| 332 | ENSG00000120915 | *EPHX2* | 1,823660828 | 2,58271E-07 |
| 333 | ENSG00000114737 | *CISH* | 1,821827668 | 8,34877E-05 |
| 334 | ENSG00000149131 | *SERPING1* | 1,820383319 | 5,79782E-06 |
| 335 | ENSG00000170345 | *FOS* | 1,819528954 | 2,7877E-113 |
| 336 | ENSG00000126368 | *NR1D1* | 1,819204448 | 1,1014E-53 |
| 337 | ENSG00000174521 | *TTC9B* | 1,816979187 | 1,02391E-07 |
| 338 | ENSG00000100196 | *KDELR3* | 1,816734892 | 2,01467E-38 |
| 339 | ENSG00000181656 | *GPR88* | 1,816394827 | 9,00381E-05 |
| 340 | ENSG00000139132 | *FGD4* | 1,812322646 | 9,44302E-19 |
| 341 | ENSG00000153930 | *ANKFN1* | 1,811772595 | 1,62497E-07 |
| 342 | ENSG00000168528 | *SERINC2* | 1,810534377 | 5,03044E-69 |
| 343 | ENSG00000167767 | *KRT80* | 1,800283713 | 3,86133E-20 |
| 344 | ENSG00000174939 | *ASPHD1* | 1,79891926 | 1,49787E-22 |
| 345 | ENSG00000242732 | *RTL5* | 1,798879022 | 3,31041E-47 |
| 346 | ENSG00000064012 | *CASP8* | 1,797064753 | 1,52233E-19 |
| 347 | ENSG00000113361 | *CDH6* | 1,793854016 | 3,71511E-80 |
| 348 | ENSG00000163359 | *COL6A3* | 1,791021314 | 2,15608E-10 |
| 349 | ENSG00000116962 | *NID1* | 1,78695901 | 3,7193E-151 |
| 350 | ENSG00000235092 | *ID2-AS1* | 1,786885787 | 0,000141513 |
| 351 | ENSG00000168734 | *PKIG* | 1,786841357 | 1,4714E-111 |
| 352 | ENSG00000225649 | *AC064875.1* | 1,784786594 | 2,69114E-63 |
| 353 | ENSG00000042493 | *CAPG* | 1,784467914 | 9,5587E-06 |
| 354 | ENSG00000101955 | *SRPX* | 1,777730438 | 1,70093E-89 |
| 355 | ENSG00000260404 | *AC110079.1* | 1,776414959 | 6,20139E-07 |
| 356 | ENSG00000128536 | *CDHR3* | 1,776362021 | 4,9864E-05 |
| 357 | ENSG00000224854 | *CDKN2A-AS1* | 1,775583963 | 9,18774E-06 |
| 358 | ENSG00000188859 | *FAM78B* | 1,773211826 | 4,41086E-12 |
| 359 | ENSG00000196155 | *PLEKHG4* | 1,77208399 | 0,000844431 |
| 360 | ENSG00000111052 | *LIN7A* | 1,77131398 | 1,18207E-52 |
| 361 | ENSG00000067182 | *TNFRSF1A* | 1,770319291 | 6,3485E-123 |
| 362 | ENSG00000138798 | *EGF* | 1,770167041 | 1,22934E-17 |
| 363 | ENSG00000142494 | *SLC47A1* | 1,769655833 | 1,96971E-69 |
| 364 | ENSG00000108551 | *RASD1* | 1,768022988 | 0,000100629 |
| 365 | ENSG00000165434 | *PGM2L1* | 1,766051446 | 1,26934E-67 |
| 366 | ENSG00000112297 | *CRYBG1* | 1,763796653 | 0,000289023 |
| 367 | ENSG00000142089 | *IFITM3* | 1,762878001 | 5,8728E-11 |
| 368 | ENSG00000260027 | *HOXB7* | 1,759271714 | 0,000205877 |
| 369 | ENSG00000128016 | *ZFP36* | 1,752782553 | 4,72832E-46 |
| 370 | ENSG00000007866 | *TEAD3* | 1,752759669 | 3,55306E-23 |
| 371 | ENSG00000169418 | *NPR1* | 1,750229192 | 1,11926E-10 |
| 372 | ENSG00000203950 | *RTL8A* | 1,748949753 | 1,06189E-34 |
| 373 | ENSG00000074047 | *GLI2* | 1,748144277 | 6,07284E-22 |
| 374 | ENSG00000179094 | *PER1* | 1,747303797 | 9,00807E-32 |
| 375 | ENSG00000167107 | *ACSF2* | 1,745923189 | 1,16912E-23 |
| 376 | ENSG00000138771 | *SHROOM3* | 1,743019609 | 1,36776E-40 |
| 377 | ENSG00000026025 | *VIM* | 1,738954833 | 1,0143E-262 |
| 378 | ENSG00000139970 | *RTN1* | 1,738834472 | 2,8667E-112 |
| 379 | ENSG00000092054 | *MYH7* | 1,732572757 | 2,76339E-06 |
| 380 | ENSG00000111799 | *COL12A1* | 1,731175149 | 7,43731E-92 |

| | | | | |
|---|---|---|---|---|
| 381 | ENSG00000184557 | *SOCS3* | 1,730449761 | 2,15637E-51 |
| 382 | ENSG00000225783 | *MIAT* | 1,730401909 | 4,762E-157 |
| 383 | ENSG00000184584 | *TMEM173* | 1,727461751 | 4,65238E-20 |
| 384 | ENSG00000145390 | *USP53* | 1,72411106 | 1,85398E-29 |
| 385 | ENSG00000006327 | *TNFRSF12A* | 1,723958666 | 7,05148E-89 |
| 386 | ENSG00000107611 | *CUBN* | 1,716838313 | 2,63563E-10 |
| 387 | ENSG00000130600 | *H19* | 1,715716787 | 3,9198E-134 |
| 388 | ENSG00000184156 | *KCNQ3* | 1,714813208 | 0,000262917 |
| 389 | ENSG00000109861 | *CTSC* | 1,714739406 | 5,8906E-174 |
| 390 | ENSG00000090975 | *PITPNM2* | 1,714267979 | 7,55628E-36 |
| 391 | ENSG00000135480 | *KRT7* | 1,713543654 | 0,001628887 |
| 392 | ENSG00000145819 | *ARHGAP26* | 1,711799746 | 1,02592E-56 |
| 393 | ENSG00000166573 | *GALR1* | 1,711649886 | 0,000946633 |
| 394 | ENSG00000142102 | *PGGHG* | 1,711542609 | 3,32123E-34 |
| 395 | ENSG00000253676 | *TAGLN2P1* | 1,710105381 | 0,000682904 |
| 396 | ENSG00000182379 | *NXPH4* | 1,707852083 | 2,04201E-31 |
| 397 | ENSG00000175592 | *FOSL1* | 1,70023848 | 4,38639E-24 |
| 398 | ENSG00000019549 | *SNAI2* | 1,699447355 | 9,35082E-12 |
| 399 | ENSG00000138080 | *EMILIN1* | 1,699327095 | 1,77544E-08 |
| 400 | ENSG00000243364 | *EFNA4* | 1,694159964 | 2,68027E-09 |
| 401 | ENSG00000172159 | *FRMD3* | 1,690944539 | 6,67502E-21 |
| 402 | ENSG00000155511 | *GRIA1* | 1,689706236 | 1,6552E-154 |
| 403 | ENSG00000111344 | *RASAL1* | 1,685760657 | 0,001751376 |
| 404 | ENSG00000248905 | *FMN1* | 1,682910077 | 5,25865E-12 |
| 405 | ENSG00000168306 | *ACOX2* | 1,676836799 | 4,71177E-12 |
| 406 | ENSG00000160691 | *SHC1* | 1,674392397 | 6,08789E-85 |
| 407 | ENSG00000142549 | *IGLON5* | 1,670635009 | 2,75767E-16 |
| 408 | ENSG00000173805 | *HAP1* | 1,66831583 | 5,77997E-95 |
| 409 | ENSG00000202111 | *VTRNA1-2* | 1,664907385 | 0,000958311 |
| 410 | ENSG00000086967 | *MYBPC2* | 1,663286759 | 9,4093E-05 |
| 411 | ENSG00000205056 | *LINC02397* | 1,661546825 | 0,000443329 |
| 412 | ENSG00000179796 | *LRRC3B* | 1,66049044 | 0,001691551 |
| 413 | ENSG00000100342 | *APOL1* | 1,660359557 | 0,001326021 |
| 414 | ENSG00000018408 | *WWTR1* | 1,65946723 | 1,1764E-28 |
| 415 | ENSG00000229036 | *VDAC1P8* | 1,656721684 | 0,000778706 |
| 416 | ENSG00000132164 | *SLC6A11* | 1,649794459 | 0,002137859 |
| 417 | ENSG00000086717 | *PPEF1* | 1,647213058 | 0,000178509 |
| 418 | ENSG00000185518 | *SV2B* | 1,64666255 | 0,001387599 |
| 419 | ENSG00000174059 | *CD34* | 1,645553327 | 1,27142E-08 |
| 420 | ENSG00000167306 | *MYO5B* | 1,644785674 | 1,22712E-49 |
| 421 | ENSG00000184672 | *RALYL* | 1,641663503 | 0,001684393 |
| 422 | ENSG00000170439 | *METTL7B* | 1,6406892 | 2,5897E-110 |
| 423 | ENSG00000164403 | *SHROOM1* | 1,640645469 | 0,000376625 |
| 424 | ENSG00000144649 | *FAM198A* | 1,638230221 | 0,002759258 |
| 425 | ENSG00000203999 | *LINC01270* | 1,637404148 | 0,002965761 |
| 426 | ENSG00000132530 | *XAF1* | 1,636577506 | 0,002541417 |
| 427 | ENSG00000140873 | *ADAMTS18* | 1,633454955 | 0,000141105 |
| 428 | ENSG00000105355 | *PLIN3* | 1,631631756 | 4,18356E-91 |
| 429 | ENSG00000147889 | *CDKN2A* | 1,629828607 | 1,29384E-10 |
| 430 | ENSG00000177675 | *CD163L1* | 1,628770503 | 0,003087711 |
| 431 | ENSG00000197555 | *SIPA1L1* | 1,628125559 | 6,723E-110 |
| 432 | ENSG00000162976 | *PQLC3* | 1,627098143 | 3,79166E-32 |
| 433 | ENSG00000139278 | *GLIPR1* | 1,626732979 | 5,42176E-53 |
| 434 | ENSG00000180758 | *GPR157* | 1,625567603 | 0,000256034 |
| 435 | ENSG00000105642 | *KCNN1* | 1,62342242 | 0,002526026 |
| 436 | ENSG00000162981 | *FAM84A* | 1,623015732 | 3,59284E-28 |
| 437 | ENSG00000074370 | *ATP2A3* | 1,622696202 | 0,003668256 |
| 438 | ENSG00000166349 | *RAG1* | 1,6224717 | 1,79704E-05 |
| 439 | ENSG00000164946 | *FREM1* | 1,622289263 | 6,27713E-78 |
| 440 | ENSG00000110080 | *ST3GAL4* | 1,621434171 | 1,34847E-39 |
| 441 | ENSG00000238266 | *LINC00707* | 1,620735737 | 0,000797995 |
| 442 | ENSG00000131951 | *LRRC9* | 1,620564659 | 0,002096234 |
| 443 | ENSG00000197405 | *C5AR1* | 1,619724537 | 0,001473068 |
| 444 | ENSG00000149256 | *TENM4* | 1,615791837 | 4,44021E-45 |
| 445 | ENSG00000201185 | *RNA5SP202* | 1,613519412 | 0,003509824 |
| 446 | ENSG00000203780 | *FANK1* | 1,611199919 | 0,00044297 |
| 447 | ENSG00000138623 | *SEMA7A* | 1,61045608 | 2,7447E-28 |
| 448 | ENSG00000015592 | *STMN4* | 1,609454932 | 1,03839E-06 |
| 449 | ENSG00000081923 | *ATP8B1* | 1,608351104 | 2,07181E-06 |
| 450 | ENSG00000135697 | *BCO1* | 1,608179749 | 0,003864276 |
| 451 | ENSG00000136267 | *DGKB* | 1,60475564 | 7,84089E-09 |
| 452 | ENSG00000143669 | *LYST* | 1,603938324 | 1,55635E-57 |
| 453 | ENSG00000176956 | *LY6H* | 1,603334241 | 0,003472839 |
| 454 | ENSG00000162814 | *SPATA17* | 1,602453504 | 8,55689E-05 |
| 455 | ENSG00000197747 | *S100A10* | 1,601240535 | 5,1283E-105 |
| 456 | ENSG00000056998 | *GYG2* | 1,598150119 | 5,40097E-40 |
| 457 | ENSG00000138650 | *PCDH10* | 1,596386871 | 1,06151E-30 |
| 458 | ENSG00000189410 | *SH2D5* | 1,595166906 | 1,67785E-06 |

| | | | | |
|---|---|---|---|---|
| 459 | ENSG00000066248 | *NGEF* | 1,592482314 | 1,04353E-21 |
| 460 | ENSG00000163565 | *IFI16* | 1,588286143 | 9,95029E-87 |
| 461 | ENSG00000137691 | *C11orf70* | 1,587864359 | 3,85959E-10 |
| 462 | ENSG00000137872 | *SEMA6D* | 1,587640692 | 2,0955E-139 |
| 463 | ENSG00000067715 | *SYT1* | 1,586267734 | 5,00166E-11 |
| 464 | ENSG00000188643 | *S100A16* | 1,585292622 | 7,4778E-120 |
| 465 | ENSG00000095397 | *WHRN* | 1,584664359 | 1,08192E-42 |
| 466 | ENSG00000088340 | *FER1L4* | 1,583358546 | 0,003841234 |
| 467 | ENSG00000086544 | *ITPKC* | 1,582235459 | 9,632E-54 |
| 468 | ENSG00000137843 | *PAK6* | 1,581548489 | 0,0039284 |
| 469 | ENSG00000144191 | *CNGA3* | 1,58076713 | 9,87313E-08 |
| 470 | ENSG00000145248 | *SLC10A4* | 1,580232211 | 0,004829166 |
| 471 | ENSG00000158816 | *VWA5B1* | 1,580050213 | 0,00062381 |
| 472 | ENSG00000203799 | *CCDC162P* | 1,579619105 | 0,001023815 |
| 473 | ENSG00000166292 | *TMEM100* | 1,579556195 | 1,61826E-23 |
| 474 | ENSG00000254615 | *AC027031.2* | 1,579544331 | 7,9473E-44 |
| 475 | ENSG00000104267 | *CA2* | 1,574378558 | 5,76602E-29 |
| 476 | ENSG00000243964 | *RPL23AP65* | 1,574332257 | 2,89887E-06 |
| 477 | ENSG00000186960 | *LINC01551* | 1,567464039 | 0,001155312 |
| 478 | ENSG00000141013 | *GAS8* | 1,566868899 | 7,04167E-12 |
| 479 | ENSG00000177875 | *CCDC184* | 1,564123755 | 2,49482E-10 |
| 480 | ENSG00000111859 | *NEDD9* | 1,563717709 | 6,79173E-80 |
| 481 | ENSG00000197813 | *AC011450.1* | 1,563656871 | 1,84373E-05 |
| 482 | ENSG00000150873 | *C2orf50* | 1,563580488 | 0,000838014 |
| 483 | ENSG00000254560 | *BBOX1-AS1* | 1,561157716 | 0,003230342 |
| 484 | ENSG00000075275 | *CELSR1* | 1,560272781 | 3,87898E-70 |
| 485 | ENSG00000178773 | *CPNE7* | 1,559831723 | 0,005045592 |
| 486 | ENSG00000180720 | *CHRM4* | 1,557584091 | 4,82147E-05 |
| 487 | ENSG00000130540 | *SULT4A1* | 1,557481741 | 0,003552638 |
| 488 | ENSG00000139722 | *VPS37B* | 1,552462382 | 2,70551E-29 |
| 489 | ENSG00000171533 | *MAP6* | 1,54941873 | 7,97893E-46 |
| 490 | ENSG00000161638 | *ITGA5* | 1,546753269 | 7,39353E-41 |
| 491 | ENSG00000103740 | *ACSBG1* | 1,546524733 | 9,09727E-32 |
| 492 | ENSG00000136546 | *SCN7A* | 1,545494994 | 3,80381E-07 |
| 493 | ENSG00000154589 | *LY96* | 1,544685488 | 1,10817E-07 |
| 494 | ENSG00000162873 | *KLHDC8A* | 1,54425169 | 2,0256E-144 |
| 495 | ENSG00000131620 | *ANO1* | 1,540459591 | 0,004888982 |
| 496 | ENSG00000196968 | *FUT11* | 1,536245886 | 1,67382E-21 |
| 497 | ENSG00000171450 | *CDK5R2* | 1,534558835 | 0,000271981 |
| 498 | ENSG00000196502 | *SULT1A1* | 1,533086923 | 9,27486E-11 |
| 499 | ENSG00000141756 | *FKBP10* | 1,53093852 | 2,6276E-140 |
| 500 | ENSG00000101384 | *JAG1* | 1,530597565 | 8,9547E-125 |
| 501 | ENSG00000186732 | *MPPED1* | 1,529871101 | 0,005010252 |
| 502 | ENSG00000144857 | *BOC* | 1,529727961 | 4,7557E-101 |
| 503 | ENSG00000175868 | *CALCB* | 1,519556592 | 0,002359061 |
| 504 | ENSG00000196358 | *NTNG2* | 1,519180618 | 4,26221E-19 |
| 505 | ENSG00000181856 | *SLC2A4* | 1,519003195 | 2,09506E-06 |
| 506 | ENSG00000253368 | *TRNP1* | 1,518771623 | 8,44667E-24 |
| 507 | ENSG00000171811 | *CFAP46* | 1,516844769 | 0,000429094 |
| 508 | ENSG00000204052 | *LRRC73* | 1,516733905 | 9,54631E-05 |
| 509 | ENSG00000117525 | *F3* | 1,516312672 | 7,47404E-46 |
| 510 | ENSG00000168334 | *XIRP1* | 1,514769985 | 0,00280119 |
| 511 | ENSG00000075426 | *FOSL2* | 1,510708846 | 4,54659E-45 |
| 512 | ENSG00000186409 | *CCDC30* | 1,510681858 | 2,54611E-06 |
| 513 | ENSG00000145362 | *ANK2* | 1,509723114 | 1,93863E-92 |
| 514 | ENSG00000180875 | *GREM2* | 1,509615653 | 0,007479296 |
| 515 | ENSG00000013583 | *HEBP1* | 1,509576465 | 1,70437E-07 |
| 516 | ENSG00000144218 | *AFF3* | 1,508214842 | 2,06449E-08 |
| 517 | ENSG00000256576 | *LINC02361* | 1,500975264 | 0,000329835 |
| 518 | ENSG00000149257 | *SERPINH1* | 1,49889937 | 2,5954E-49 |
| 519 | ENSG00000100228 | *RAB36* | 1,498814345 | 1,09488E-27 |
| 520 | ENSG00000125089 | *SH3TC1* | 1,496437166 | 0,004465413 |
| 521 | ENSG00000106624 | *AEBP1* | 1,495058553 | 1,07128E-70 |
| 522 | ENSG00000244230 | *RN7SL151P* | 1,494134999 | 0,000992846 |
| 523 | ENSG00000261409 | *AL035425.3* | 1,493751851 | 0,00014375 |
| 524 | ENSG00000214402 | *LCNL1* | 1,491871613 | 0,001450824 |
| 525 | ENSG00000044524 | *EPHA3* | 1,491255777 | 1,013E-157 |
| 526 | ENSG00000146376 | *ARHGAP18* | 1,489040802 | 1,69618E-11 |
| 527 | ENSG00000164056 | *SPRY1* | 1,488793465 | 2,57712E-71 |
| 528 | ENSG00000108176 | *DNAJC12* | 1,48665556 | 3,76423E-05 |
| 529 | ENSG00000188766 | *SPRED3* | 1,485110508 | 3,00523E-09 |
| 530 | ENSG00000246985 | *SOCS2-AS1* | 1,485100224 | 0,006868457 |
| 531 | ENSG00000164749 | *HNF4G* | 1,484660395 | 2,05115E-07 |
| 532 | ENSG00000074181 | *NOTCH3* | 1,483787374 | 5,62644E-95 |
| 533 | ENSG00000158220 | *ESYT3* | 1,482992955 | 5,62533E-05 |
| 534 | ENSG00000152932 | *RAB3C* | 1,478305336 | 0,000166392 |
| 535 | ENSG00000157110 | *RBPMS* | 1,475923214 | 1,49034E-58 |
| 536 | ENSG00000147883 | *CDKN2B* | 1,474690024 | 1,23458E-83 |

| | | | | |
|---|---|---|---|---|
| 537 | ENSG00000074219 | *TEAD2* | 1,47442265 | 8,46946E-63 |
| 538 | ENSG00000185942 | *NKAIN3* | 1,473980533 | 0,002031041 |
| 539 | ENSG00000179761 | *PIPOX* | 1,469831225 | 1,70079E-16 |
| 540 | ENSG00000250993 | *AC020551.1* | 1,469757905 | 0,009460309 |
| 541 | ENSG00000127863 | *TNFRSF19* | 1,466312092 | 4,4545E-99 |
| 542 | ENSG00000272549 | *AL356123.2* | 1,465122249 | 0,000561725 |
| 543 | ENSG00000062716 | *VMP1* | 1,464193147 | 1,9411E-102 |
| 544 | ENSG00000179388 | *EGR3* | 1,46365661 | 3,31064E-20 |
| 545 | ENSG00000003249 | *DBNDD1* | 1,461711895 | 2,89912E-47 |
| 546 | ENSG00000089199 | *CHGB* | 1,458251965 | 3,23841E-08 |
| 547 | ENSG00000072694 | *FCGR2B* | 1,455621877 | 7,40117E-08 |
| 548 | ENSG00000101000 | *PROCR* | 1,453414779 | 0,002508371 |
| 549 | ENSG00000008056 | *SYN1* | 1,45320925 | 4,77159E-09 |
| 550 | ENSG00000144891 | *AGTR1* | 1,452643476 | 0,002690228 |
| 551 | ENSG00000144908 | *ALDH1L1* | 1,449486372 | 0,007920122 |
| 552 | ENSG00000113532 | *ST8SIA4* | 1,446231418 | 0,009178574 |
| 553 | ENSG00000185201 | *IFITM2* | 1,444980182 | 1,16097E-17 |
| 554 | ENSG00000130270 | *ATP8B3* | 1,438904345 | 0,003765156 |
| 555 | ENSG00000105672 | *ETV2* | 1,438193334 | 0,000676396 |
| 556 | ENSG00000162783 | *IER5* | 1,436875644 | 4,40915E-57 |
| 557 | ENSG00000189143 | *CLDN4* | 1,431990605 | 1,70929E-05 |
| 558 | ENSG00000173727 | *AP000769.1* | 1,430791782 | 0,011862275 |
| 559 | ENSG00000168765 | *GSTM4* | 1,430136499 | 2,85724E-14 |
| 560 | ENSG00000136379 | *ABHD17C* | 1,429955402 | 6,96915E-42 |
| 561 | ENSG00000120594 | *PLXDC2* | 1,429532307 | 5,23033E-27 |
| 562 | ENSG00000100092 | *SH3BP1* | 1,428660584 | 4,47699E-07 |
| 563 | ENSG00000134215 | *VAV3* | 1,428446393 | 2,95471E-31 |
| 564 | ENSG00000253549 | *CA3-AS1* | 1,428338832 | 0,00486848 |
| 565 | ENSG00000153237 | *CCDC148* | 1,426331378 | 0,000587656 |
| 566 | ENSG00000222009 | *BTBD19* | 1,42574637 | 4,31316E-12 |
| 567 | ENSG00000139679 | *LPAR6* | 1,425038241 | 9,28326E-10 |
| 568 | ENSG00000133124 | *IRS4* | 1,42342308 | 0,000450184 |
| 569 | ENSG00000237819 | *AC002454.1* | 1,421221838 | 4,00239E-08 |
| 570 | ENSG00000149292 | *TTC12* | 1,419822951 | 0,009659112 |
| 571 | ENSG00000089060 | *SLC8B1* | 1,418275809 | 1,04229E-15 |
| 572 | ENSG00000130702 | *LAMA5* | 1,416983488 | 1,23031E-84 |
| 573 | ENSG00000234409 | *CCDC188* | 1,411640707 | 1,33349E-12 |
| 574 | ENSG00000170909 | *OSCAR* | 1,408700754 | 0,004647071 |
| 575 | ENSG00000126790 | *L3HYPDH* | 1,407790031 | 2,44138E-31 |
| 576 | ENSG00000175505 | *CLCF1* | 1,40742855 | 0,003379289 |
| 577 | ENSG00000120738 | *EGR1* | 1,403330713 | 2,37231E-87 |
| 578 | ENSG00000116717 | *GADD45A* | 1,402911575 | 2,62355E-41 |
| 579 | ENSG00000124813 | *RUNX2* | 1,402070148 | 1,67059E-07 |
| 580 | ENSG00000141682 | *PMAIP1* | 1,398840875 | 4,15292E-30 |
| 581 | ENSG00000169855 | *ROBO1* | 1,397112023 | 3,6349E-124 |
| 582 | ENSG00000108511 | *HOXB6* | 1,395819598 | 3,83772E-11 |
| 583 | ENSG00000113448 | *PDE4D* | 1,394346878 | 6,22786E-12 |
| 584 | ENSG00000146555 | *SDK1* | 1,393193552 | 5,30756E-32 |
| 585 | ENSG00000116329 | *OPRD1* | 1,391933556 | 1,61043E-07 |
| 586 | ENSG00000157423 | *HYDIN* | 1,39146804 | 0,01462489 |
| 587 | ENSG00000142733 | *MAP3K6* | 1,39100476 | 1,20201E-33 |
| 588 | ENSG00000111885 | *MAN1A1* | 1,390814559 | 0,002888326 |
| 589 | ENSG00000153714 | *LURAP1L* | 1,388069596 | 0,001930512 |
| 590 | ENSG00000188674 | *C2orf80* | 1,386094868 | 2,54012E-23 |
| 591 | ENSG00000175471 | *MCTP1* | 1,385644439 | 1,7763E-23 |
| 592 | ENSG00000102900 | *NUP93* | 1,385303932 | 3,5208E-127 |
| 593 | ENSG00000254827 | *SLC22A18AS* | 1,38394074 | 0,01183388 |
| 594 | ENSG00000106484 | *MEST* | 1,381734031 | 1,94056E-91 |
| 595 | ENSG00000102265 | *TIMP1* | 1,380394276 | 1,7554E-102 |
| 596 | ENSG00000180447 | *GAS1* | 1,376383401 | 6,6379E-100 |
| 597 | ENSG00000186806 | *VSIG10L* | 1,37467177 | 1,17325E-15 |
| 598 | ENSG00000169744 | *LDB2* | 1,374615805 | 5,39347E-19 |
| 599 | ENSG00000164066 | *INTU* | 1,373363392 | 2,79162E-11 |
| 600 | ENSG00000130751 | *NPAS1* | 1,370991951 | 3,52191E-21 |
| 601 | ENSG00000176692 | *FOXC2* | 1,370371072 | 0,007855577 |
| 602 | ENSG00000181350 | *LRRC75A* | 1,370232613 | 1,27127E-15 |
| 603 | ENSG00000110446 | *SLC15A3* | 1,364809223 | 0,001329287 |
| 604 | ENSG00000123689 | *G0S2* | 1,358937424 | 0,015134996 |
| 605 | ENSG00000116117 | *PARD3B* | 1,357197193 | 3,78258E-26 |
| 606 | ENSG00000197291 | *RAMP2-AS1* | 1,357157956 | 0,000888093 |
| 607 | ENSG00000248161 | *AC098487.1* | 1,356943938 | 0,005239278 |
| 608 | ENSG00000129951 | *PLPPR3* | 1,356016468 | 0,001294431 |
| 609 | ENSG00000130055 | *GDPD2* | 1,354364387 | 3,67804E-14 |
| 610 | ENSG00000233396 | *LINC01719* | 1,353404881 | 0,002757155 |
| 611 | ENSG00000169213 | *RAB3B* | 1,35021232 | 1,79668E-41 |
| 612 | ENSG00000112139 | *MDGA1* | 1,349241692 | 2,03572E-20 |
| 613 | ENSG00000110675 | *ELMOD1* | 1,347000596 | 1,11155E-10 |
| 614 | ENSG00000148600 | *CDHR1* | 1,346962299 | 5,94106E-30 |

| | | | | |
|---|---|---|---|---|
| 615 | ENSG00000164330 | *EBF1* | 1,343930915 | 3,94338E-10 |
| 616 | ENSG00000172216 | *CEBPB* | 1,343087791 | 3,2236E-25 |
| 617 | ENSG00000185215 | *TNFAIP2* | 1,339742433 | 0,01184841 |
| 618 | ENSG00000255277 | *ABCC6P2* | 1,337762318 | 0,004243517 |
| 619 | ENSG00000002933 | *TMEM176A* | 1,336217776 | 0,012933365 |
| 620 | ENSG00000221890 | *NPTXR* | 1,332746336 | 2,0141E-62 |
| 621 | ENSG00000139209 | *SLC38A4* | 1,331654857 | 7,21822E-05 |
| 622 | ENSG00000266928 | *AC020905.1* | 1,331321525 | 0,015619296 |
| 623 | ENSG00000132357 | *CARD6* | 1,331276835 | 0,00460094 |
| 624 | ENSG00000170006 | *TMEM154* | 1,329346077 | 0,001202684 |
| 625 | ENSG00000118242 | *MREG* | 1,327887429 | 1,14478E-34 |
| 626 | ENSG00000172780 | *RAB43* | 1,32766673 | 0,010626758 |
| 627 | ENSG00000161381 | *PLXDC1* | 1,326239353 | 0,000143115 |
| 628 | ENSG00000259146 | *AC005476.2* | 1,325477275 | 0,008697164 |
| 629 | ENSG00000196754 | *S100A2* | 1,325098586 | 2,56602E-05 |
| 630 | ENSG00000234840 | *LINC01239* | 1,324563795 | 0,015748398 |
| 631 | ENSG00000127666 | *TICAM1* | 1,324477694 | 3,37615E-14 |
| 632 | ENSG00000122735 | *DNAI1* | 1,324067555 | 0,006515787 |
| 633 | ENSG00000148803 | *FUOM* | 1,324043279 | 0,004392907 |
| 634 | ENSG00000249751 | *ECSCR* | 1,319973921 | 0,021776079 |
| 635 | ENSG00000123609 | *NMI* | 1,317758585 | 2,62741E-08 |
| 636 | ENSG00000143819 | *EPHX1* | 1,315797245 | 2,98654E-73 |
| 637 | ENSG00000042832 | *TG* | 1,315409418 | 0,02185331 |
| 638 | ENSG00000168135 | *KCNJ4* | 1,312696694 | 0,000497594 |
| 639 | ENSG00000222000 | *AC092675.1* | 1,311431696 | 0,004529314 |
| 640 | ENSG00000257497 | *AC121761.1* | 1,311368392 | 0,016595978 |
| 641 | ENSG00000177606 | *JUN* | 1,310689051 | 1,4282E-111 |
| 642 | ENSG00000135439 | *AGAP2* | 1,309484528 | 6,61019E-29 |
| 643 | ENSG00000197646 | *PDCD1LG2* | 1,308910494 | 0,008990685 |
| 644 | ENSG00000152413 | *HOMER1* | 1,307468412 | 1,69767E-55 |
| 645 | ENSG00000087086 | *FTL* | 1,306064741 | 5,992E-105 |
| 646 | ENSG00000171223 | *JUNB* | 1,305951312 | 4,90331E-32 |
| 647 | ENSG00000231313 | *AC078875.1* | 1,305411816 | 1,28589E-16 |
| 648 | ENSG00000136158 | *SPRY2* | 1,305312408 | 5,32336E-74 |
| 649 | ENSG00000128606 | *LRRC17* | 1,301846863 | 9,62515E-15 |
| 650 | ENSG00000129159 | *KCNC1* | 1,30138047 | 2,07532E-27 |
| 651 | ENSG00000012124 | *CD22* | 1,300906782 | 0,023979788 |
| 652 | ENSG00000043462 | *LCP2* | 1,300491102 | 0,024239808 |
| 653 | ENSG00000166831 | *RBPMS2* | 1,300011249 | 1,48375E-07 |
| 654 | ENSG00000129422 | *MTUS1* | 1,299963073 | 5,73091E-37 |
| 655 | ENSG00000126106 | *TMEM53* | 1,29814761 | 2,70073E-15 |
| 656 | ENSG00000182871 | *COL18A1* | 1,297607886 | 4,66228E-49 |
| 657 | ENSG00000258711 | *AL358334.2* | 1,296649403 | 0,005993854 |
| 658 | ENSG00000103021 | *CCDC113* | 1,294518626 | 1,95959E-06 |
| 659 | ENSG00000167065 | *DUSP18* | 1,292633676 | 1,95967E-07 |
| 660 | ENSG00000214353 | *VAC14-AS1* | 1,290682112 | 0,000924244 |
| 661 | ENSG00000156515 | *HK1* | 1,29045174 | 1,02947E-61 |
| 662 | ENSG00000183971 | *NPW* | 1,286499506 | 0,008304326 |
| 663 | ENSG00000125355 | *TMEM255A* | 1,285137463 | 4,02618E-84 |
| 664 | ENSG00000166578 | *IQCD* | 1,28505286 | 0,00039034 |
| 665 | ENSG00000081853 | *PCDHGA2* | 1,283317957 | 0,000890633 |
| 666 | ENSG00000107282 | *APBA1* | 1,281355843 | 1,16503E-39 |
| 667 | ENSG00000184949 | *FAM227A* | 1,280396829 | 7,86529E-05 |
| 668 | ENSG00000110786 | *PTPN5* | 1,279667978 | 0,000774513 |
| 669 | ENSG00000221963 | *APOL6* | 1,27954049 | 2,61095E-23 |
| 670 | ENSG00000137573 | *SULF1* | 1,277509476 | 0,022070622 |
| 671 | ENSG00000091844 | *RGS17* | 1,275659826 | 4,03159E-42 |
| 672 | ENSG00000008196 | *TFAP2B* | 1,274434327 | 0,005746248 |
| 673 | ENSG00000134802 | *SLC43A3* | 1,273687245 | 6,60301E-06 |
| 674 | ENSG00000142408 | *CACNG8* | 1,272467022 | 1,13318E-27 |
| 675 | ENSG00000228031 | *AC078842.1* | 1,271883723 | 0,003785193 |
| 676 | ENSG00000215788 | *TNFRSF25* | 1,268796142 | 0,001548333 |
| 677 | ENSG00000196557 | *CACNA1H* | 1,267247445 | 1,21037E-10 |
| 678 | ENSG00000145349 | *CAMK2D* | 1,265198781 | 2,82683E-79 |
| 679 | ENSG00000082512 | *TRAF5* | 1,263618948 | 8,69368E-07 |
| 680 | ENSG00000007171 | *NOS2* | 1,262497367 | 0,014864935 |
| 681 | ENSG00000246334 | *PRR7-AS1* | 1,261343495 | 0,000192727 |
| 682 | ENSG00000118997 | *DNAH7* | 1,261132473 | 0,002297051 |
| 683 | ENSG00000187944 | *C2orf66* | 1,260645379 | 0,025402357 |
| 684 | ENSG00000138119 | *MYOF* | 1,259317607 | 1,45398E-34 |
| 685 | ENSG00000108797 | *CNTNAP1* | 1,258262192 | 1,50694E-63 |
| 686 | ENSG00000170801 | *HTRA3* | 1,258110823 | 0,027314 |
| 687 | ENSG00000132481 | *TRIM47* | 1,255225778 | 1,65245E-14 |
| 688 | ENSG00000175040 | *CHST2* | 1,255194869 | 2,10373E-37 |
| 689 | ENSG00000272341 | *AL137003.2* | 1,252719931 | 3,43889E-06 |
| 690 | ENSG00000113205 | *PCDHB3* | 1,252409957 | 1,1965E-06 |
| 691 | ENSG00000164038 | *SLC9B2* | 1,252051091 | 1,30232E-11 |
| 692 | ENSG00000132879 | *FBXO44* | 1,252010928 | 3,33384E-17 |

| | | | | |
|---|---|---|---|---|
| 693 | ENSG00000177432 | *NAP1L5* | 1,251416541 | 3,72523E-14 |
| 694 | ENSG00000043143 | *JADE2* | 1,249595307 | 1,1346E-24 |
| 695 | ENSG00000162426 | *SLC45A1* | 1,249508737 | 3,78416E-10 |
| 696 | ENSG00000171680 | *PLEKHG5* | 1,249058288 | 2,87664E-07 |
| 697 | ENSG00000163219 | *ARHGAP25* | 1,248767478 | 1,68741E-05 |
| 698 | ENSG00000225067 | *RPL23AP2* | 1,24738863 | 0,013061778 |
| 699 | ENSG00000179168 | *GGN* | 1,245983966 | 8,89136E-06 |
| 700 | ENSG00000116745 | *RPE65* | 1,243217155 | 1,77881E-36 |
| 701 | ENSG00000137727 | *ARHGAP20* | 1,242382603 | 2,11331E-43 |
| 702 | ENSG00000129474 | *AJUBA* | 1,241762209 | 2,16946E-18 |
| 703 | ENSG00000136840 | *ST6GALNAC4* | 1,241079227 | 3,19916E-22 |
| 704 | ENSG00000101222 | *SPEF1* | 1,239513346 | 0,018632157 |
| 705 | ENSG00000256234 | *AC022509.2* | 1,236467835 | 0,023668996 |
| 706 | ENSG00000137501 | *SYTL2* | 1,236380886 | 8,49261E-27 |
| 707 | ENSG00000085831 | *TTC39A* | 1,235478402 | 0,020139087 |
| 708 | ENSG00000170412 | *GPRC5C* | 1,235358183 | 0,020678692 |
| 709 | ENSG00000177283 | *FZD8* | 1,235007353 | 7,12751E-28 |
| 710 | ENSG00000139880 | *CDH24* | 1,231718104 | 1,93627E-31 |
| 711 | ENSG00000166448 | *TMEM130* | 1,231167611 | 9,89502E-06 |
| 712 | ENSG00000174804 | *FZD4* | 1,231162797 | 2,34575E-39 |
| 713 | ENSG00000198431 | *TXNRD1* | 1,229982037 | 2,92934E-87 |
| 714 | ENSG00000103888 | *CEMIP* | 1,226451047 | 2,1985E-29 |
| 715 | ENSG00000156113 | *KCNMA1* | 1,223523001 | 2,08339E-27 |
| 716 | ENSG00000119431 | *HDHD3* | 1,2221091 | 3,29853E-13 |
| 717 | ENSG00000135502 | *SLC26A10* | 1,219897866 | 0,005112921 |
| 718 | ENSG00000168062 | *BATF2* | 1,219719293 | 0,021419759 |
| 719 | ENSG00000104611 | *SH2D4A* | 1,217700616 | 9,27668E-06 |
| 720 | ENSG00000186854 | *TRABD2A* | 1,216799973 | 0,002655314 |
| 721 | ENSG00000080709 | *KCNN2* | 1,215866289 | 0,001027111 |
| 722 | ENSG00000169126 | *ARMC4* | 1,215036829 | 9,10317E-05 |
| 723 | ENSG00000258404 | *LINC02320* | 1,21354147 | 0,036659271 |
| 724 | ENSG00000011422 | *PLAUR* | 1,210256357 | 1,52799E-05 |
| 725 | ENSG00000223969 | *AC002456.1* | 1,209594134 | 0,00260881 |
| 726 | ENSG00000117425 | *PTCH2* | 1,206368262 | 7,32171E-06 |
| 727 | ENSG00000229644 | *NAMPTP1* | 1,203615078 | 8,14131E-10 |
| 728 | ENSG00000123810 | *B9D2* | 1,202296201 | 2,34805E-07 |
| 729 | ENSG00000187266 | *EPOR* | 1,200864662 | 1,14721E-09 |
| 730 | ENSG00000148935 | *GAS2* | 1,200582014 | 1,2114E-12 |
| 731 | ENSG00000198796 | *ALPK2* | 1,200001993 | 1,59277E-05 |
| 732 | ENSG00000205129 | *C4orf47* | 1,19952677 | 0,02697282 |
| 733 | ENSG00000034152 | *MAP2K3* | 1,199142699 | 2,46486E-24 |
| 734 | ENSG00000240498 | *CDKN2B-AS1* | 1,198265089 | 0,000103681 |
| 735 | ENSG00000146216 | *TTBK1* | 1,196726789 | 2,39846E-08 |
| 736 | ENSG00000143226 | *FCGR2A* | 1,196333405 | 1,07839E-13 |
| 737 | ENSG00000107554 | *DNMBP* | 1,196201286 | 3,12945E-35 |
| 738 | ENSG00000179071 | *CCDC89* | 1,191748874 | 0,021756187 |
| 739 | ENSG00000011105 | *TSPAN9* | 1,189928489 | 5,86047E-31 |
| 740 | ENSG00000129990 | *SYT5* | 1,188993106 | 0,008433475 |
| 741 | ENSG00000164220 | *F2RL2* | 1,188697603 | 0,03252831 |
| 742 | ENSG00000127418 | *FGFRL1* | 1,187963635 | 7,63811E-54 |
| 743 | ENSG00000150995 | *ITPR1* | 1,186313413 | 4,45167E-10 |
| 744 | ENSG00000135424 | *ITGA7* | 1,185505936 | 3,34395E-84 |
| 745 | ENSG00000228528 | *AC068057.1* | 1,184807615 | 0,01686229 |
| 746 | ENSG00000062524 | *LTK* | 1,184611908 | 0,039318932 |
| 747 | ENSG00000249061 | *AC109492.1* | 1,183124839 | 0,03124999 |
| 748 | ENSG00000168772 | *CXXC4* | 1,18285885 | 1,22882E-07 |
| 749 | ENSG00000113070 | *HBEGF* | 1,182676856 | 1,28652E-13 |
| 750 | ENSG00000188483 | *IER5L* | 1,182205584 | 8,71207E-36 |
| 751 | ENSG00000164023 | *SGMS2* | 1,181246651 | 0,000374884 |
| 752 | ENSG00000187678 | *SPRY4* | 1,180229838 | 4,63362E-86 |
| 753 | ENSG00000139318 | *DUSP6* | 1,178490892 | 1,29902E-64 |
| 754 | ENSG00000068831 | *RASGRP2* | 1,177994798 | 0,030768078 |
| 755 | ENSG00000148175 | *STOM* | 1,177628922 | 7,20859E-15 |
| 756 | ENSG00000186523 | *FAM86B1* | 1,177540387 | 0,016362477 |
| 757 | ENSG00000133687 | *TMTC1* | 1,177151765 | 1,05411E-34 |
| 758 | ENSG00000205517 | *RGL3* | 1,176001153 | 6,88313E-07 |
| 759 | ENSG00000251002 | *AC244502.1* | 1,174467732 | 0,02940066 |
| 760 | ENSG00000106546 | *AHR* | 1,174039536 | 0,045483664 |
| 761 | ENSG00000106038 | *EVX1* | 1,173049391 | 0,037092279 |
| 762 | ENSG00000160282 | *FTCD* | 1,173044241 | 0,040639211 |
| 763 | ENSG00000172346 | *CSDC2* | 1,172458488 | 0,028610909 |
| 764 | ENSG00000227533 | *SLC2A1-AS1* | 1,171951477 | 0,035444265 |
| 765 | ENSG00000105835 | *NAMPT* | 1,171885027 | 4,30747E-44 |
| 766 | ENSG00000145246 | *ATP10D* | 1,171729626 | 6,46173E-17 |
| 767 | ENSG00000126803 | *HSPA2* | 1,170051787 | 0,046524373 |
| 768 | ENSG00000185250 | *PPIL6* | 1,169545612 | 0,000120197 |
| 769 | ENSG00000185133 | *INPP5J* | 1,168185053 | 3,05998E-07 |
| 770 | ENSG00000115641 | *FHL2* | 1,165489431 | 1,5946E-09 |

| | | | | |
|---|---|---|---|---|
| 771 | ENSG00000111331 | *OAS3* | 1,164126869 | 1,0907E-55 |
| 772 | ENSG00000155495 | *MAGEC1* | 1,163472322 | 0,042611056 |
| 773 | ENSG00000121769 | *FABP3* | 1,15936355 | 1,13094E-09 |
| 774 | ENSG00000226608 | *FTLP3* | 1,157645496 | 8,41878E-11 |
| 775 | ENSG00000132470 | *ITGB4* | 1,157366865 | 2,15931E-06 |
| 776 | ENSG00000106025 | *TSPAN12* | 1,155427529 | 1,93201E-29 |
| 777 | ENSG00000258947 | *TUBB3* | 1,153750324 | 9,76244E-10 |
| 778 | ENSG00000104856 | *RELB* | 1,152941753 | 1,99738E-11 |
| 779 | ENSG00000102032 | *RENBP* | 1,15212822 | 1,42894E-05 |
| 780 | ENSG00000070808 | *CAMK2A* | 1,151944173 | 1,31211E-06 |
| 781 | ENSG00000143036 | *SLC44A3* | 1,150981128 | 0,014122767 |
| 782 | ENSG00000188051 | *TMEM221* | 1,15060009 | 0,000459638 |
| 783 | ENSG00000227502 | *LINC01268* | 1,150543407 | 9,41962E-16 |
| 784 | ENSG00000223652 | *AC106786.1* | 1,150416113 | 0,029740574 |
| 785 | ENSG00000185681 | *MORN5* | 1,149502022 | 0,039940661 |
| 786 | ENSG00000134871 | *COL4A2* | 1,149440988 | 2,77762E-18 |
| 787 | ENSG00000257594 | *GALNT4* | 1,149134767 | 0,03882595 |
| 788 | ENSG00000106565 | *TMEM176B* | 1,148901221 | 0,028493808 |
| 789 | ENSG00000233901 | *LINC01503* | 1,146669334 | 0,026677004 |
| 790 | ENSG00000103528 | *SYT17* | 1,146388035 | 2,85548E-43 |
| 791 | ENSG00000185245 | *GP1BA* | 1,145008799 | 0,007622852 |
| 792 | ENSG00000169764 | *UGP2* | 1,144776126 | 1,55957E-84 |
| 793 | ENSG00000174808 | *BTC* | 1,144773993 | 0,011904314 |
| 794 | ENSG00000124302 | *CHST8* | 1,144462793 | 9,25375E-08 |
| 795 | ENSG00000115107 | *STEAP3* | 1,144286816 | 2,594E-25 |
| 796 | ENSG00000183092 | *BEGAIN* | 1,143004757 | 1,70172E-23 |
| 797 | ENSG00000101098 | *RIMS4* | 1,141053279 | 7,65897E-50 |
| 798 | ENSG00000061455 | *PRDM6* | 1,140135747 | 0,00119557 |
| 799 | ENSG00000103876 | *FAH* | 1,139636445 | 2,73816E-09 |
| 800 | ENSG00000154153 | *RETREG1* | 1,137796183 | 1,40079E-25 |
| 801 | ENSG00000160111 | *CPAMD8* | 1,137671946 | 0,03233548 |
| 802 | ENSG00000157168 | *NRG1* | 1,137125597 | 2,5024E-14 |
| 803 | ENSG00000236714 | *LINC01844* | 1,136864019 | 0,017393868 |
| 804 | ENSG00000229743 | *LINC01159* | 1,134725884 | 0,009622265 |
| 805 | ENSG00000185274 | *WBSCR17* | 1,133505147 | 2,48606E-26 |
| 806 | ENSG00000164845 | *FAM86FP* | 1,129650455 | 0,022943083 |
| 807 | ENSG00000228412 | *AL022068.1* | 1,129395504 | 0,021652533 |
| 808 | ENSG00000066056 | *TIE1* | 1,128913964 | 0,046107548 |
| 809 | ENSG00000228065 | *LINC01515* | 1,128107299 | 0,002413385 |
| 810 | ENSG00000150967 | *ABCB9* | 1,127994647 | 5,20643E-13 |
| 811 | ENSG00000183828 | *NUDT14* | 1,127991649 | 2,26645E-09 |
| 812 | ENSG00000156453 | *PCDH1* | 1,125996293 | 6,63014E-41 |
| 813 | ENSG00000172985 | *SH3RF3* | 1,125974298 | 3,96496E-18 |
| 814 | ENSG00000165886 | *UBTD1* | 1,125342118 | 7,87584E-24 |
| 815 | ENSG00000117600 | *PLPPR4* | 1,123114718 | 0,00371653 |
| 816 | ENSG00000134107 | *BHLHE40* | 1,122010758 | 2,74824E-45 |
| 817 | ENSG00000175182 | *FAM131A* | 1,121794833 | 3,74725E-10 |
| 818 | ENSG00000196083 | *IL1RAP* | 1,121643562 | 2,05107E-49 |
| 819 | ENSG00000177181 | *RIMKLA* | 1,121632601 | 7,34048E-15 |
| 820 | ENSG00000139269 | *INHBE* | 1,121616035 | 0,000292237 |
| 821 | ENSG00000140104 | *C14orf79* | 1,120786747 | 1,80947E-15 |
| 822 | ENSG00000183831 | *ANKRD45* | 1,119287487 | 0,002903093 |
| 823 | ENSG00000139292 | *LGR5* | 1,115886589 | 1,17796E-38 |
| 824 | ENSG00000057657 | *PRDM1* | 1,112752351 | 0,014203629 |
| 825 | ENSG00000119681 | *LTBP2* | 1,112660478 | 7,37444E-07 |
| 826 | ENSG00000156345 | *CDK20* | 1,109989796 | 1,20625E-17 |
| 827 | ENSG00000250318 | *AC003072.1* | 1,109592625 | 0,017419203 |
| 828 | ENSG00000141505 | *ASGR1* | 1,10894071 | 0,00354953 |
| 829 | ENSG00000148832 | *PAOX* | 1,107615389 | 0,003871555 |
| 830 | ENSG00000123095 | *BHLHE41* | 1,107113383 | 2,60556E-12 |
| 831 | ENSG00000116285 | *ERRFI1* | 1,107022306 | 4,27054E-39 |
| 832 | ENSG00000242861 | *AL591895.1* | 1,106098251 | 0,021271642 |
| 833 | ENSG00000113594 | *LIFR* | 1,105805037 | 9,53744E-47 |
| 834 | ENSG00000123104 | *ITPR2* | 1,105316538 | 2,90829E-59 |
| 835 | ENSG00000104419 | *NDRG1* | 1,104782813 | 1,84478E-40 |
| 836 | ENSG00000255366 | *AC120036.5* | 1,103946151 | 0,025433525 |
| 837 | ENSG00000075539 | *FRYL* | 1,103938319 | 1,33411E-36 |
| 838 | ENSG00000184743 | *ATL3* | 1,103304825 | 2,13817E-16 |
| 839 | ENSG00000254489 | *AL136088.1* | 1,102911593 | 0,047736413 |
| 840 | ENSG00000171476 | *HOPX* | 1,101441332 | 2,04234E-15 |
| 841 | ENSG00000102271 | *KLHL4* | 1,100279609 | 1,30188E-20 |
| 842 | ENSG00000169019 | *COMMD8* | 1,099710133 | 5,36705E-08 |
| 843 | ENSG00000134874 | *DZIP1* | 1,099106515 | 2,86514E-27 |
| 844 | ENSG00000121900 | *TMEM54* | 1,098610396 | 1,31722E-14 |
| 845 | ENSG00000239697 | *TNFSF12* | 1,098589316 | 0,016772931 |
| 846 | ENSG00000270069 | *MIR222HG* | 1,09723375 | 3,82077E-05 |
| 847 | ENSG00000118432 | *CNR1* | 1,095314528 | 1,38038E-14 |
| 848 | ENSG00000105427 | *CNFN* | 1,095149091 | 0,034378007 |

| | | | | |
|---|---|---|---|---|
| 849 | ENSG00000168505 | *GBX2* | 1,092845344 | 9,20645E-05 |
| 850 | ENSG00000138400 | *MDH1B* | 1,092280021 | 0,00059814 |
| 851 | ENSG00000129003 | *VPS13C* | 1,09021024 | 7,55448E-58 |
| 852 | ENSG00000157193 | *LRP8* | 1,089245662 | 2,05897E-47 |
| 853 | ENSG00000105245 | *NUMBL* | 1,088282467 | 1,74062E-54 |
| 854 | ENSG00000151474 | *FRMD4A* | 1,087356198 | 1,04191E-08 |
| 855 | ENSG00000139263 | *LRIG3* | 1,087351095 | 1,78663E-12 |
| 856 | ENSG00000183114 | *FAM43B* | 1,08714601 | 8,18708E-05 |
| 857 | ENSG00000139178 | *C1RL* | 1,084990224 | 0,000100605 |
| 858 | ENSG00000234899 | *SOX9-AS1* | 1,084326411 | 3,0576E-06 |
| 859 | ENSG00000185634 | *SHC4* | 1,084070644 | 8,1421E-16 |
| 860 | ENSG00000161267 | *BDH1* | 1,083145138 | 0,004913108 |
| 861 | ENSG00000179292 | *TMEM151A* | 1,082637832 | 0,004355159 |
| 862 | ENSG00000100078 | *PLA2G3* | 1,080789435 | 5,54898E-20 |
| 863 | ENSG00000237797 | *AL161935.3* | 1,079119401 | 0,004373506 |
| 864 | ENSG00000224713 | *AC025165.1* | 1,078592476 | 0,046806463 |
| 865 | ENSG00000166171 | *DPCD* | 1,078477935 | 1,08087E-08 |
| 866 | ENSG00000155158 | *TTC39B* | 1,078272203 | 1,37367E-06 |
| 867 | ENSG00000232599 | *AL008707.1* | 1,077543718 | 0,00439801 |
| 868 | ENSG00000133937 | *GSC* | 1,077388574 | 3,61657E-07 |
| 869 | ENSG00000091136 | *LAMB1* | 1,076062974 | 5,24421E-64 |
| 870 | ENSG00000175264 | *CHST1* | 1,074421312 | 8,82248E-08 |
| 871 | ENSG00000131069 | *ACSS2* | 1,07320464 | 1,05064E-42 |
| 872 | ENSG00000179242 | *CDH4* | 1,072631992 | 1,06432E-06 |
| 873 | ENSG00000160867 | *FGFR4* | 1,072238013 | 3,41182E-05 |
| 874 | ENSG00000198003 | *CCDC151* | 1,071936387 | 0,001245925 |
| 875 | ENSG00000109171 | *SLAIN2* | 1,071764894 | 2,50104E-26 |
| 876 | ENSG00000118307 | *CASC1* | 1,071342569 | 0,035017873 |
| 877 | ENSG00000182718 | *ANXA2* | 1,069872313 | 7,45178E-12 |
| 878 | ENSG00000092850 | *TEKT2* | 1,068355964 | 0,0025474 |
| 879 | ENSG00000100036 | *SLC35E4* | 1,068195155 | 8,62282E-10 |
| 880 | ENSG00000227954 | *TARID* | 1,067877702 | 0,000144914 |
| 881 | ENSG00000129151 | *BBOX1* | 1,065938484 | 2,60556E-12 |
| 882 | ENSG00000123685 | *BATF3* | 1,063760792 | 1,19672E-07 |
| 883 | ENSG00000006071 | *ABCC8* | 1,062126996 | 4,45975E-13 |
| 884 | ENSG00000130164 | *LDLR* | 1,061127439 | 4,29267E-67 |
| 885 | ENSG00000148841 | *ITPRIP* | 1,05890121 | 7,92154E-14 |
| 886 | ENSG00000258754 | *LINC01579* | 1,058329128 | 0,013575469 |
| 887 | ENSG00000114654 | *EFCC1* | 1,058295886 | 0,037621767 |
| 888 | ENSG00000232699 | *BDH2P1* | 1,057840286 | 0,023172854 |
| 889 | ENSG00000002587 | *HS3ST1* | 1,057707203 | 2,54098E-14 |
| 890 | ENSG00000136160 | *EDNRB* | 1,056421983 | 3,50835E-40 |
| 891 | ENSG00000175104 | *TRAF6* | 1,055472779 | 1,06451E-22 |
| 892 | ENSG00000112319 | *EYA4* | 1,055301835 | 6,49599E-53 |
| 893 | ENSG00000075213 | *SEMA3A* | 1,053020735 | 8,2485E-41 |
| 894 | ENSG00000126217 | *MCF2L* | 1,052779099 | 2,51441E-32 |
| 895 | ENSG00000255823 | *MTRNR2L8* | 1,052490341 | 0,003544363 |
| 896 | ENSG00000112539 | *C6orf118* | 1,05241578 | 0,000790228 |
| 897 | ENSG00000080561 | *MID2* | 1,052064599 | 6,08077E-05 |
| 898 | ENSG00000131724 | *IL13RA1* | 1,051963976 | 4,63302E-42 |
| 899 | ENSG00000171940 | *ZNF217* | 1,05163115 | 3,25833E-31 |
| 900 | ENSG00000183036 | *PCP4* | 1,051069091 | 1,02551E-14 |
| 901 | ENSG00000148158 | *SNX30* | 1,048818166 | 3,99742E-26 |
| 902 | ENSG00000135272 | *MDFIC* | 1,048785784 | 0,008457234 |
| 903 | ENSG00000140464 | *PML* | 1,047840302 | 7,25193E-26 |
| 904 | ENSG00000145358 | *DDIT4L* | 1,046540362 | 0,015107409 |
| 905 | ENSG00000149927 | *DOC2A* | 1,046433239 | 0,001994923 |
| 906 | ENSG00000141519 | *CCDC40* | 1,045451931 | 2,39721E-06 |
| 907 | ENSG00000248712 | *CCDC153* | 1,04404137 | 0,021797452 |
| 908 | ENSG00000198400 | *NTRK1* | 1,0436732 | 0,035367061 |
| 909 | ENSG00000181619 | *GPR135* | 1,043484084 | 0,013878903 |
| 910 | ENSG00000135842 | *FAM129A* | 1,042721967 | 1,34543E-18 |
| 911 | ENSG00000124107 | *SLPI* | 1,040188826 | 0,044655118 |
| 912 | ENSG00000072274 | *TFRC* | 1,039925141 | 2,47158E-73 |
| 913 | ENSG00000102174 | *PHEX* | 1,039564251 | 0,001847424 |
| 914 | ENSG00000170775 | *GPR37* | 1,039270777 | 0,000241535 |
| 915 | ENSG00000271952 | *LINC01954* | 1,038554091 | 0,036618435 |
| 916 | ENSG00000185046 | *ANKS1B* | 1,037922103 | 6,27343E-19 |
| 917 | ENSG00000164692 | *COL1A2* | 1,037469004 | 0,044391329 |
| 918 | ENSG00000090013 | *BLVRB* | 1,037292135 | 4,43842E-20 |
| 919 | ENSG00000144583 | *MARCH4* | 1,036941336 | 0,000379667 |
| 920 | ENSG00000102349 | *KLF8* | 1,035798731 | 0,011624938 |
| 921 | ENSG00000177679 | *SRRM3* | 1,035741444 | 0,009097076 |
| 922 | ENSG00000261604 | *AC114947.2* | 1,035450906 | 3,66283E-06 |
| 923 | ENSG00000225518 | *LINC01703* | 1,032362797 | 0,048492412 |
| 924 | ENSG00000248593 | *DSTNP2* | 1,031361547 | 0,001614901 |
| 925 | ENSG00000080493 | *SLC4A4* | 1,025429578 | 1,15965E-57 |
| 926 | ENSG00000116729 | *WLS* | 1,024174694 | 4,28019E-68 |

| 927 | ENSG00000186976 | *EFCAB6* | 1,023905454 | 0,002347215 |
|---|---|---|---|---|
| 928 | ENSG00000134070 | *IRAK2* | 1,023210756 | 8,53185E-08 |
| 929 | ENSG00000092421 | *SEMA6A* | 1,023204217 | 5,00443E-53 |
| 930 | ENSG00000071242 | *RPS6KA2* | 1,022727673 | 9,49932E-68 |
| 931 | ENSG00000106772 | *PRUNE2* | 1,021776839 | 1,17729E-64 |
| 932 | ENSG00000196843 | *ARID5A* | 1,020951479 | 7,47182E-25 |
| 933 | ENSG00000154265 | *ABCA5* | 1,020213727 | 0,000210054 |
| 934 | ENSG00000259523 | *AC022613.2* | 1,019529858 | 0,032046607 |
| 935 | ENSG00000135404 | *CD63* | 1,019346011 | 1,27261E-66 |
| 936 | ENSG00000105281 | *SLC1A5* | 1,018897984 | 1,86937E-29 |
| 937 | ENSG00000185507 | *IRF7* | 1,018540623 | 2,6068E-07 |
| 938 | ENSG00000138036 | *DYNC2LI1* | 1,018194245 | 5,21854E-16 |
| 939 | ENSG00000109180 | *OCIAD1* | 1,017224512 | 3,43476E-46 |
| 940 | ENSG00000010404 | *IDS* | 1,017058337 | 1,11303E-59 |
| 941 | ENSG00000237289 | *CKMT1B* | 1,016801196 | 0,009905172 |
| 942 | ENSG00000154678 | *PDE1C* | 1,016036569 | 0,000731531 |
| 943 | ENSG00000133019 | *CHRM3* | 1,015211186 | 9,47567E-26 |
| 944 | ENSG00000179361 | *ARID3B* | 1,013257923 | 0,001294642 |
| 945 | ENSG00000240204 | *SMKR1* | 1,01268258 | 0,04644253 |
| 946 | ENSG00000153976 | *HS3ST3A1* | 1,011898778 | 0,000671602 |
| 947 | ENSG00000196975 | *ANXA4* | 1,010551053 | 2,47564E-12 |
| 948 | ENSG00000148848 | *ADAM12* | 1,010218396 | 0,013332983 |
| 949 | ENSG00000243646 | *IL10RB* | 1,009945557 | 7,65885E-12 |
| 950 | ENSG00000130779 | *CLIP1* | 1,006819884 | 4,70089E-32 |
| 951 | ENSG00000165695 | *AK8* | 1,005935434 | 0,012280778 |
| 952 | ENSG00000124762 | *CDKN1A* | 1,005595955 | 3,60706E-36 |
| 953 | ENSG00000115657 | *ABCB6* | 1,005552626 | 1,80629E-05 |
| 954 | ENSG00000108379 | *WNT3* | 1,005341957 | 2,8452E-05 |
| 955 | ENSG00000108883 | *EFTUD2* | 1,004817395 | 6,01433E-77 |
| 956 | ENSG00000273079 | *GRIN2B* | 1,004755593 | 3,51841E-12 |
| 957 | ENSG00000105499 | *PLA2G4C* | 1,004491677 | 3,55296E-08 |
| 958 | ENSG00000213928 | *IRF9* | 1,003376561 | 0,010950268 |
| 959 | ENSG00000244026 | *FAM86DP* | 1,002647404 | 1,52612E-08 |
| 960 | ENSG00000175874 | *CREG2* | 1,001897293 | 0,025529851 |
| 961 | ENSG00000111817 | *DSE* | 1,000409346 | 5,00792E-09 |
| 962 | ENSG00000151025 | *GPR158* | 0,997383718 | 7,89338E-12 |
| 963 | ENSG00000126010 | *GRPR* | 0,996519858 | 0,037992264 |
| 964 | ENSG00000175197 | *DDIT3* | 0,995236404 | 6,34108E-11 |
| 965 | ENSG00000153832 | *FBXO36* | 0,994511125 | 3,67305E-06 |
| 966 | ENSG00000008283 | *CYB561* | 0,992379788 | 4,05079E-05 |
| 967 | ENSG00000235587 | *GAPDHP65* | 0,992063972 | 0,010419878 |
| 968 | ENSG00000247157 | *LINC01252* | 0,991961291 | 0,012941646 |
| 969 | ENSG00000101004 | *NINL* | 0,989393401 | 0,034072272 |
| 970 | ENSG00000096093 | *EFHC1* | 0,988909584 | 5,41094E-28 |
| 971 | ENSG00000251669 | *FAM86EP* | 0,988156422 | 0,01601319 |
| 972 | ENSG00000254429 | *AP001972.1* | 0,988024206 | 0,032191018 |
| 973 | ENSG00000172893 | *DHCR7* | 0,987675136 | 5,8892E-62 |
| 974 | ENSG00000144136 | *SLC20A1* | 0,987665734 | 2,67519E-46 |
| 975 | ENSG00000235363 | *SNRPGP10* | 0,987182945 | 0,004642612 |
| 976 | ENSG00000101255 | *TRIB3* | 0,986845308 | 5,48513E-20 |
| 977 | ENSG00000237172 | *B3GNT9* | 0,986728872 | 0,000201583 |
| 978 | ENSG00000143469 | *SYT14* | 0,982481366 | 2,39628E-05 |
| 979 | ENSG00000140939 | *NOL3* | 0,982377355 | 1,29838E-11 |
| 980 | ENSG00000106070 | *GRB10* | 0,9797426 | 1,44044E-38 |
| 981 | ENSG00000167601 | *AXL* | 0,976892544 | 1,98018E-32 |
| 982 | ENSG00000123364 | *HOXC13* | 0,976014008 | 0,007980046 |
| 983 | ENSG00000171160 | *MORN4* | 0,975849163 | 1,73321E-12 |
| 984 | ENSG00000262001 | *DLGAP1-AS2* | 0,975163987 | 0,000430848 |
| 985 | ENSG00000142694 | *EVA1B* | 0,97399156 | 0,000472377 |
| 986 | ENSG00000132688 | *NES* | 0,9736663 | 2,32477E-59 |
| 987 | ENSG00000186594 | *MIR22HG* | 0,973393944 | 7,75424E-05 |
| 988 | ENSG00000152315 | *KCNK13* | 0,973205706 | 0,004612926 |
| 989 | ENSG00000107798 | *LIPA* | 0,973013032 | 1,90225E-36 |
| 990 | ENSG00000131187 | *F12* | 0,972642088 | 2,39856E-07 |
| 991 | ENSG00000175866 | *BAIAP2* | 0,972299011 | 1,44791E-32 |
| 992 | ENSG00000139668 | *WDFY2* | 0,971928462 | 2,45874E-15 |
| 993 | ENSG00000137198 | *GMPR* | 0,970563126 | 7,4215E-12 |
| 994 | ENSG00000075043 | *KCNQ2* | 0,969408087 | 1,18078E-34 |
| 995 | ENSG00000026508 | *CD44* | 0,968755202 | 4,69463E-49 |
| 996 | ENSG00000178401 | *DNAJC22* | 0,968417287 | 1,48637E-06 |
| 997 | ENSG00000110660 | *SLC35F2* | 0,968390846 | 1,87338E-13 |
| 998 | ENSG00000178445 | *GLDC* | 0,967908974 | 1,51382E-40 |
| 999 | ENSG00000100592 | *DAAM1* | 0,967862835 | 1,13174E-13 |
| 1000 | ENSG00000243232 | *PCDHAC2* | 0,967609771 | 0,000123575 |
| 1001 | ENSG00000155962 | *CLIC2* | 0,966859223 | 0,004319645 |
| 1002 | ENSG00000111640 | *GAPDH* | 0,96393555 | 8,41408E-82 |
| 1003 | ENSG00000127125 | *PPCS* | 0,96369258 | 0,001709851 |
| 1004 | ENSG00000079974 | *RABL2B* | 0,963110618 | 8,17875E-15 |

| | | | | |
|---|---|---|---|---|
| 1005 | ENSG00000109944 | *C11orf63* | 0,963084352 | 0,000295772 |
| 1006 | ENSG00000102034 | *ELF4* | 0,961552045 | 5,98013E-05 |
| 1007 | ENSG00000174938 | *SEZ6L2* | 0,961395278 | 1,83343E-31 |
| 1008 | ENSG00000027001 | *MIPEP* | 0,960819181 | 2,22992E-08 |
| 1009 | ENSG00000160345 | *C9orf116* | 0,959670594 | 2,73358E-05 |
| 1010 | ENSG00000254389 | *RHPN1-AS1* | 0,959552677 | 0,019143237 |
| 1011 | ENSG00000130511 | *SSBP4* | 0,958671112 | 3,87557E-27 |
| 1012 | ENSG00000086062 | *B4GALT1* | 0,958029626 | 1,07164E-08 |
| 1013 | ENSG00000155367 | *PPM1J* | 0,957876695 | 0,002278197 |
| 1014 | ENSG00000104998 | *IL27RA* | 0,957693311 | 1,01652E-15 |
| 1015 | ENSG00000163485 | *ADORA1* | 0,957222321 | 1,1873E-09 |
| 1016 | ENSG00000136830 | *FAM129B* | 0,953691872 | 5,22429E-51 |
| 1017 | ENSG00000260528 | *FAM157C* | 0,952401327 | 0,044235055 |
| 1018 | ENSG00000069535 | *MAOB* | 0,950763369 | 0,021228325 |
| 1019 | ENSG00000135406 | *PRPH* | 0,950715765 | 4,44915E-06 |
| 1020 | ENSG00000168038 | *ULK4* | 0,94873688 | 3,96943E-05 |
| 1021 | ENSG00000105464 | *GRIN2D* | 0,948272261 | 1,03097E-07 |
| 1022 | ENSG00000230910 | *AL391807.1* | 0,946711357 | 3,39476E-07 |
| 1023 | ENSG00000204956 | *PCDHGA1* | 0,946286979 | 0,013150366 |
| 1024 | ENSG00000112936 | *C7* | 0,945334095 | 0,002779646 |
| 1025 | ENSG00000129167 | *TPH1* | 0,945160529 | 0,049010263 |
| 1026 | ENSG00000120278 | *PLEKHG1* | 0,944729243 | 1,21315E-19 |
| 1027 | ENSG00000183853 | *KIRREL* | 0,943870652 | 1,20968E-37 |
| 1028 | ENSG00000087266 | *SH3BP2* | 0,943055361 | 1,44193E-17 |
| 1029 | ENSG00000167617 | *CDC42EP5* | 0,941454303 | 0,000391705 |
| 1030 | ENSG00000134574 | *DDB2* | 0,939637073 | 7,9784E-07 |
| 1031 | ENSG00000196141 | *SPATS2L* | 0,939509193 | 3,40927E-41 |
| 1032 | ENSG00000124942 | *AHNAK* | 0,937943191 | 2,69848E-08 |
| 1033 | ENSG00000147588 | *PMP2* | 0,9363369 | 1,67339E-68 |
| 1034 | ENSG00000166886 | *NAB2* | 0,935784455 | 1,31682E-37 |
| 1035 | ENSG00000163331 | *DAPL1* | 0,935444845 | 0,039940661 |
| 1036 | ENSG00000228672 | *PROB1* | 0,935065178 | 1,15255E-05 |
| 1037 | ENSG00000198756 | *COLGALT2* | 0,934625552 | 1,90182E-46 |
| 1038 | ENSG00000160716 | *CHRNB2* | 0,934190846 | 0,003551788 |
| 1039 | ENSG00000165175 | *MID1IP1* | 0,934099738 | 2,78679E-28 |
| 1040 | ENSG00000160963 | *COL26A1* | 0,933719148 | 0,002294093 |
| 1041 | ENSG00000089159 | *PXN* | 0,932928592 | 2,38394E-36 |
| 1042 | ENSG00000160789 | *LMNA* | 0,932414545 | 1,4979E-45 |
| 1043 | ENSG00000091592 | *NLRP1* | 0,93241288 | 1,85331E-37 |
| 1044 | ENSG00000114744 | *COMMD2* | 0,931237318 | 3,20688E-44 |
| 1045 | ENSG00000054392 | *HHAT* | 0,930537578 | 1,42436E-05 |
| 1046 | ENSG00000105974 | *CAV1* | 0,929695183 | 2,05827E-08 |
| 1047 | ENSG00000167552 | *TUBA1A* | 0,927751449 | 2,08423E-68 |
| 1048 | ENSG00000171621 | *SPSB1* | 0,927706839 | 5,25936E-08 |
| 1049 | ENSG00000102445 | *RUBCNL* | 0,927684421 | 0,00767248 |
| 1050 | ENSG00000173110 | *HSPA6* | 0,927415486 | 0,011117726 |
| 1051 | ENSG00000028137 | *TNFRSF1B* | 0,926917123 | 2,64537E-05 |
| 1052 | ENSG00000197467 | *COL13A1* | 0,926180221 | 0,028265849 |
| 1053 | ENSG00000235703 | *LINC00894* | 0,925393771 | 3,36144E-05 |
| 1054 | ENSG00000146966 | *DENND2A* | 0,925333822 | 6,79724E-29 |
| 1055 | ENSG00000171798 | *KNDC1* | 0,923169895 | 0,01381885 |
| 1056 | ENSG00000100218 | *RSPH14* | 0,922994187 | 0,049333988 |
| 1057 | ENSG00000205593 | *DENND6B* | 0,920089372 | 1,40783E-10 |
| 1058 | ENSG00000130176 | *CNN1* | 0,920023587 | 0,005284729 |
| 1059 | ENSG00000226564 | *FTH1P20* | 0,919901013 | 1,76753E-06 |
| 1060 | ENSG00000152076 | *CCDC74B* | 0,918667035 | 3,33688E-06 |
| 1061 | ENSG00000131095 | *GFAP* | 0,918173648 | 4,22989E-47 |
| 1062 | ENSG00000107960 | *STN1* | 0,91708114 | 7,54005E-05 |
| 1063 | ENSG00000162645 | *GBP2* | 0,915941636 | 0,008124791 |
| 1064 | ENSG00000152582 | *SPEF2* | 0,9158292 | 0,01686229 |
| 1065 | ENSG00000071051 | *NCK2* | 0,915802219 | 2,22787E-34 |
| 1066 | ENSG00000116774 | *OLFML3* | 0,91573931 | 4,62982E-07 |
| 1067 | ENSG00000066382 | *MPPED2* | 0,915120668 | 1,43274E-10 |
| 1068 | ENSG00000075142 | *SRI* | 0,914638798 | 2,83308E-48 |
| 1069 | ENSG00000160813 | *PPP1R35* | 0,914535272 | 0,040212539 |
| 1070 | ENSG00000131981 | *LGALS3* | 0,914265148 | 0,000155548 |
| 1071 | ENSG00000151835 | *SACS* | 0,914200179 | 7,51479E-31 |
| 1072 | ENSG00000198879 | *SFMBT2* | 0,911360878 | 3,16208E-12 |
| 1073 | ENSG00000162745 | *OLFML2B* | 0,910675544 | 1,78303E-06 |
| 1074 | ENSG00000043355 | *ZIC2* | 0,910018078 | 7,7952E-08 |
| 1075 | ENSG00000260641 | *AC114811.2* | 0,909599086 | 0,027314 |
| 1076 | ENSG00000124788 | *ATXN1* | 0,909401825 | 2,34682E-27 |
| 1077 | ENSG00000092607 | *TBX15* | 0,909259484 | 0,000113871 |
| 1078 | ENSG00000145730 | *PAM* | 0,908445788 | 6,71884E-40 |
| 1079 | ENSG00000108861 | *DUSP3* | 0,907625905 | 3,55134E-28 |
| 1080 | ENSG00000248590 | *GLDCP1* | 0,907052653 | 0,007416197 |
| 1081 | ENSG00000272944 | *AC079834.2* | 0,90629508 | 0,048085674 |
| 1082 | ENSG00000123094 | *RASSF8* | 0,906251925 | 3,33551E-24 |

| | | | | |
|---|---|---|---|---|
| 1083 | ENSG00000174151 | *CYB561D1* | 0,906065716 | 5,41467E-11 |
| 1084 | ENSG00000139083 | *ETV6* | 0,905817511 | 1,00864E-14 |
| 1085 | ENSG00000180806 | *HOXC9* | 0,905386739 | 0,001443171 |
| 1086 | ENSG00000272502 | *AC104958.2* | 0,904852565 | 0,006474245 |
| 1087 | ENSG00000228232 | *GAPDHP1* | 0,904112023 | 3,41328E-08 |
| 1088 | ENSG00000159216 | *RUNX1* | 0,90338771 | 1,69981E-24 |
| 1089 | ENSG00000100994 | *PYGB* | 0,901414113 | 3,91191E-52 |
| 1090 | ENSG00000171444 | *MCC* | 0,900811698 | 1,81876E-15 |
| 1091 | ENSG00000198467 | *TPM2* | 0,899677353 | 3,25186E-09 |
| 1092 | ENSG00000103742 | *IGDCC4* | 0,899323593 | 1,75554E-09 |
| 1093 | ENSG00000149091 | *DGKZ* | 0,898827733 | 4,30131E-27 |
| 1094 | ENSG00000182103 | *FAM181B* | 0,897303864 | 2,08789E-32 |
| 1095 | ENSG00000106976 | *DNM1* | 0,896534072 | 4,34049E-31 |
| 1096 | ENSG00000152953 | *STK32B* | 0,89645714 | 1,34884E-25 |
| 1097 | ENSG00000186654 | *PRR5* | 0,894828133 | 0,044533965 |
| 1098 | ENSG00000126458 | *RRAS* | 0,892790884 | 6,76619E-11 |
| 1099 | ENSG00000023909 | *GCLM* | 0,891691309 | 5,05089E-11 |
| 1100 | ENSG00000111696 | *NT5DC3* | 0,891011107 | 7,74887E-16 |
| 1101 | ENSG00000109323 | *MANBA* | 0,890156016 | 1,26793E-12 |
| 1102 | ENSG00000171877 | *FRMD5* | 0,889389269 | 1,72333E-33 |
| 1103 | ENSG00000071575 | *TRIB2* | 0,888635795 | 1,14528E-59 |
| 1104 | ENSG00000040608 | *RTN4R* | 0,888523052 | 5,34196E-17 |
| 1105 | ENSG00000139044 | *B4GALNT3* | 0,888051692 | 3,66664E-17 |
| 1106 | ENSG00000240771 | *ARHGEF25* | 0,887609103 | 1,59413E-07 |
| 1107 | ENSG00000168778 | *TCTN2* | 0,886981236 | 2,87245E-09 |
| 1108 | ENSG00000122756 | *CNTFR* | 0,886677018 | 1,10175E-08 |
| 1109 | ENSG00000034510 | *TMSB10* | 0,88596284 | 3,30457E-61 |
| 1110 | ENSG00000107954 | *NEURL1* | 0,8845071 | 0,045987736 |
| 1111 | ENSG00000171992 | *SYNPO* | 0,882685881 | 0,022578569 |
| 1112 | ENSG00000149591 | *TAGLN* | 0,882375531 | 1,83919E-05 |
| 1113 | ENSG00000041982 | *TNC* | 0,882256544 | 1,18207E-52 |
| 1114 | ENSG00000163513 | *TGFBR2* | 0,881294209 | 2,39046E-16 |
| 1115 | ENSG00000103599 | *IQCH* | 0,880938849 | 0,00344217 |
| 1116 | ENSG00000169908 | *TM4SF1* | 0,880744473 | 8,02497E-38 |
| 1117 | ENSG00000169756 | *LIMS1* | 0,880460416 | 9,10801E-25 |
| 1118 | ENSG00000130940 | *CASZ1* | 0,880373876 | 0,007209251 |
| 1119 | ENSG00000135722 | *FBXL8* | 0,880287409 | 0,021475158 |
| 1120 | ENSG00000091409 | *ITGA6* | 0,878586118 | 2,59448E-31 |
| 1121 | ENSG00000221926 | *TRIM16* | 0,877327004 | 4,88504E-10 |
| 1122 | ENSG00000090020 | *SLC9A1* | 0,877071714 | 3,09055E-12 |
| 1123 | ENSG00000105287 | *PRKD2* | 0,876495129 | 1,7383E-14 |
| 1124 | ENSG00000145687 | *SSBP2* | 0,875926321 | 4,31305E-27 |
| 1125 | ENSG00000135437 | *RDH5* | 0,875368379 | 0,006675177 |
| 1126 | ENSG00000086205 | *FOLH1* | 0,873960305 | 2,89012E-13 |
| 1127 | ENSG00000157985 | *AGAP1* | 0,872981343 | 4,37329E-38 |
| 1128 | ENSG00000163545 | *NUAK2* | 0,870624668 | 7,30842E-05 |
| 1129 | ENSG00000121743 | *GJA3* | 0,870468945 | 0,013918194 |
| 1130 | ENSG00000198855 | *FICD* | 0,869319303 | 5,6619E-08 |
| 1131 | ENSG00000187534 | *PRR13P5* | 0,868006651 | 0,001247733 |
| 1132 | ENSG00000151322 | *NPAS3* | 0,867518106 | 1,10851E-26 |
| 1133 | ENSG00000269028 | *MTRNR2L12* | 0,865789735 | 0,002009361 |
| 1134 | ENSG00000185482 | *STAC3* | 0,865337183 | 0,007229228 |
| 1135 | ENSG00000116525 | *TRIM62* | 0,864815272 | 2,60694E-10 |
| 1136 | ENSG00000100151 | *PICK1* | 0,863071259 | 0,027329743 |
| 1137 | ENSG00000141569 | *TRIM65* | 0,860835802 | 2,32534E-15 |
| 1138 | ENSG00000234975 | *FTH1P2* | 0,857817673 | 4,31297E-13 |
| 1139 | ENSG00000009694 | *TENM1* | 0,856933584 | 4,49556E-22 |
| 1140 | ENSG00000115756 | *HPCAL1* | 0,856930075 | 2,33467E-14 |
| 1141 | ENSG00000172915 | *NBEA* | 0,856901368 | 7,0802E-18 |
| 1142 | ENSG00000178498 | *DTX3* | 0,856300717 | 2,35806E-14 |
| 1143 | ENSG00000143195 | *ILDR2* | 0,854720091 | 3,69383E-28 |
| 1144 | ENSG00000135048 | *TMEM2* | 0,853737357 | 2,3856E-22 |
| 1145 | ENSG00000159167 | *STC1* | 0,853452085 | 4,10734E-20 |
| 1146 | ENSG00000203727 | *SAMD5* | 0,852639093 | 3,97926E-05 |
| 1147 | ENSG00000187498 | *COL4A1* | 0,852425535 | 5,76304E-50 |
| 1148 | ENSG00000124772 | *CPNE5* | 0,852026349 | 1,88351E-19 |
| 1149 | ENSG00000126453 | *BCL2L12* | 0,850835513 | 2,08906E-09 |
| 1150 | ENSG00000250510 | *GPR162* | 0,850508315 | 3,20309E-22 |
| 1151 | ENSG00000131759 | *RARA* | 0,850163277 | 4,07636E-15 |
| 1152 | ENSG00000010626 | *LRRC23* | 0,849845951 | 1,39706E-07 |
| 1153 | ENSG00000196361 | *ELAVL3* | 0,848837134 | 3,47364E-20 |
| 1154 | ENSG00000151917 | *BEND6* | 0,848318774 | 0,000127986 |
| 1155 | ENSG00000068079 | *IFI35* | 0,84670478 | 1,73102E-07 |
| 1156 | ENSG00000184489 | *PTP4A3* | 0,846121264 | 1,11753E-12 |
| 1157 | ENSG00000006047 | *YBX2* | 0,845105612 | 0,012227486 |
| 1158 | ENSG00000179104 | *TMTC2* | 0,844666174 | 2,72257E-12 |
| 1159 | ENSG00000128284 | *APOL3* | 0,84459708 | 0,011589449 |
| 1160 | ENSG00000146242 | *TPBG* | 0,844278481 | 1,0675E-13 |

| | | | | |
|---|---|---|---|---|
| 1161 | ENSG00000167565 | *SERTAD3* | 0,844036034 | 6,85558E-09 |
| 1162 | ENSG00000169242 | *EFNA1* | 0,843880459 | 3,20467E-17 |
| 1163 | ENSG00000177542 | *SLC25A22* | 0,843804957 | 1,26651E-13 |
| 1164 | ENSG00000131504 | *DIAPH1* | 0,843653657 | 2,64013E-42 |
| 1165 | ENSG00000142552 | *RCN3* | 0,843259734 | 0,025081555 |
| 1166 | ENSG00000205213 | *LGR4* | 0,842746211 | 2,25368E-27 |
| 1167 | ENSG00000139636 | *LMBR1L* | 0,842512549 | 5,90141E-14 |
| 1168 | ENSG00000125246 | *CLYBL* | 0,841851738 | 0,000253022 |
| 1169 | ENSG00000131019 | *ULBP3* | 0,841549613 | 0,007697725 |
| 1170 | ENSG00000117480 | *FAAH* | 0,840221075 | 0,018513933 |
| 1171 | ENSG00000104313 | *EYA1* | 0,838819653 | 3,51739E-16 |
| 1172 | ENSG00000123983 | *ACSL3* | 0,838138499 | 1,27959E-43 |
| 1173 | ENSG00000251661 | *AC136475.1* | 0,836921656 | 0,011775035 |
| 1174 | ENSG00000131848 | *ZSCAN5A* | 0,83621055 | 3,70406E-05 |
| 1175 | ENSG00000197208 | *SLC22A4* | 0,836133966 | 6,00316E-05 |
| 1176 | ENSG00000115520 | *COQ10B* | 0,834374911 | 6,2813E-11 |
| 1177 | ENSG00000177839 | *PCDHB9* | 0,834012328 | 4,43979E-07 |
| 1178 | ENSG00000164741 | *DLC1* | 0,833324522 | 1,09615E-13 |
| 1179 | ENSG00000107317 | *PTGDS* | 0,832931126 | 0,000434714 |
| 1180 | ENSG00000123700 | *KCNJ2* | 0,832799952 | 6,61425E-05 |
| 1181 | ENSG00000135047 | *CTSL* | 0,832737578 | 1,24116E-19 |
| 1182 | ENSG00000135472 | *FAIM2* | 0,832659206 | 2,32839E-14 |
| 1183 | ENSG00000075618 | *FSCN1* | 0,831684337 | 1,17756E-50 |
| 1184 | ENSG00000083067 | *TRPM3* | 0,831574182 | 6,19852E-28 |
| 1185 | ENSG00000068650 | *ATP11A* | 0,830476516 | 3,61489E-20 |
| 1186 | ENSG00000172062 | *SMN1* | 0,829543541 | 0,000275301 |
| 1187 | ENSG00000115556 | *PLCD4* | 0,8292012 | 2,55892E-09 |
| 1188 | ENSG00000170537 | *TMC7* | 0,827252716 | 5,73894E-06 |
| 1189 | ENSG00000181104 | *F2R* | 0,825524848 | 4,54163E-28 |
| 1190 | ENSG00000177469 | *CAVIN1* | 0,824880843 | 1,31465E-36 |
| 1191 | ENSG00000196569 | *LAMA2* | 0,824372318 | 0,009403267 |
| 1192 | ENSG00000149489 | *ROM1* | 0,823656441 | 2,50466E-05 |
| 1193 | ENSG00000198221 | *AFDN-AS1* | 0,82322223 | 0,024561192 |
| 1194 | ENSG00000105717 | *PBX4* | 0,819792195 | 0,002287475 |
| 1195 | ENSG00000197879 | *MYO1C* | 0,819269872 | 2,48734E-13 |
| 1196 | ENSG00000118292 | *C1orf54* | 0,819182799 | 8,7378E-06 |
| 1197 | ENSG00000135862 | *LAMC1* | 0,818342519 | 1,22152E-39 |
| 1198 | ENSG00000100429 | *HDAC10* | 0,818173219 | 0,017744043 |
| 1199 | ENSG00000116106 | *EPHA4* | 0,818086641 | 1,48978E-30 |
| 1200 | ENSG00000120306 | *CYSTM1* | 0,817389249 | 8,98795E-17 |
| 1201 | ENSG00000137494 | *ANKRD42* | 0,81695338 | 9,5587E-06 |
| 1202 | ENSG00000162992 | *NEUROD1* | 0,81680921 | 0,000680812 |
| 1203 | ENSG00000099625 | *CBARP* | 0,816627431 | 3,08024E-13 |
| 1204 | ENSG00000185015 | *CA13* | 0,813628849 | 0,009607591 |
| 1205 | ENSG00000177426 | *TGIF1* | 0,8119081 | 1,38053E-29 |
| 1206 | ENSG00000166275 | *BORCS7* | 0,811533198 | 1,71194E-06 |
| 1207 | ENSG00000229119 | *AC026403.1* | 0,810879227 | 6,19666E-05 |
| 1208 | ENSG00000260822 | *AC004656.1* | 0,81078121 | 3,57761E-10 |
| 1209 | ENSG00000178078 | *STAP2* | 0,810307842 | 0,008091903 |
| 1210 | ENSG00000219507 | *FTH1P8* | 0,809800188 | 1,21625E-11 |
| 1211 | ENSG00000124140 | *SLC12A5* | 0,809387452 | 0,005563903 |
| 1212 | ENSG00000115271 | *GCA* | 0,808574967 | 6,22973E-05 |
| 1213 | ENSG00000111145 | *ELK3* | 0,808552225 | 1,37359E-12 |
| 1214 | ENSG00000010295 | *IFFO1* | 0,808326943 | 8,5843E-18 |
| 1215 | ENSG00000153214 | *TMEM87B* | 0,808141444 | 1,8918E-07 |
| 1216 | ENSG00000111846 | *GCNT2* | 0,807980523 | 9,13973E-09 |
| 1217 | ENSG00000137266 | *SLC22A23* | 0,80724605 | 9,97199E-13 |
| 1218 | ENSG00000162545 | *CAMK2N1* | 0,807102407 | 8,18185E-16 |
| 1219 | ENSG00000159214 | *CCDC24* | 0,805957431 | 4,85853E-05 |
| 1220 | ENSG00000082438 | *COBLL1* | 0,804899027 | 1,51231E-06 |
| 1221 | ENSG00000144645 | *OSBPL10* | 0,804013637 | 2,94163E-11 |
| 1222 | ENSG00000136810 | *TXN* | 0,801962499 | 4,81023E-28 |
| 1223 | ENSG00000115310 | *RTN4* | 0,801936401 | 6,39604E-37 |
| 1224 | ENSG00000257698 | *AC084033.3* | 0,80183671 | 1,46315E-06 |
| 1225 | ENSG00000130653 | *PNPLA7* | 0,80166209 | 0,001451732 |
| 1226 | ENSG00000182463 | *TSHZ2* | 0,801237491 | 0,000680067 |
| 1227 | ENSG00000108018 | *SORCS1* | 0,801089792 | 1,06907E-10 |
| 1228 | ENSG00000177337 | *DLGAP1-AS1* | 0,800826094 | 0,001723913 |
| 1229 | ENSG00000103241 | *FOXF1* | 0,79739853 | 4,72961E-05 |
| 1230 | ENSG00000165959 | *CLMN* | 0,79664862 | 3,39026E-13 |
| 1231 | ENSG00000121966 | *CXCR4* | 0,795815239 | 0,013478287 |
| 1232 | ENSG00000130635 | *COL5A1* | 0,795775663 | 2,12564E-34 |
| 1233 | ENSG00000177098 | *SCN4B* | 0,7944504 | 3,37829E-06 |
| 1234 | ENSG00000173166 | *RAPH1* | 0,794060517 | 0,000443678 |
| 1235 | ENSG00000065308 | *TRAM2* | 0,794024251 | 1,31852E-28 |
| 1236 | ENSG00000100427 | *MLC1* | 0,793331311 | 4,45472E-48 |
| 1237 | ENSG00000100246 | *DNAL4* | 0,792992488 | 1,11476E-11 |
| 1238 | ENSG00000120885 | *CLU* | 0,792880887 | 1,49583E-46 |

| | | | | |
|---|---|---|---|---|
| 1239 | ENSG00000076067 | *RBMS2* | 0,791998457 | 1,01515E-08 |
| 1240 | ENSG00000163482 | *STK36* | 0,791975772 | 8,87908E-18 |
| 1241 | ENSG00000160145 | *KALRN* | 0,791465988 | 8,02418E-13 |
| 1242 | ENSG00000268364 | *SMC5-AS1* | 0,791423924 | 0,045907943 |
| 1243 | ENSG00000186007 | *LEMD1* | 0,790966557 | 0,015095951 |
| 1244 | ENSG00000178947 | *SMIM10L2A* | 0,790535235 | 0,002395618 |
| 1245 | ENSG00000204852 | *TCTN1* | 0,789947863 | 2,62506E-16 |
| 1246 | ENSG00000042317 | *SPATA7* | 0,788824939 | 1,23155E-06 |
| 1247 | ENSG00000137944 | *KYAT3* | 0,788605431 | 2,48222E-10 |
| 1248 | ENSG00000150773 | *PIH1D2* | 0,78843835 | 0,032697234 |
| 1249 | ENSG00000175938 | *ORAI3* | 0,78763167 | 0,018015579 |
| 1250 | ENSG00000269893 | *SNHG8* | 0,787341466 | 8,1991E-05 |
| 1251 | ENSG00000131398 | *KCNC3* | 0,787308433 | 0,000186939 |
| 1252 | ENSG00000052850 | *ALX4* | 0,787097688 | 0,007756447 |
| 1253 | ENSG00000204054 | *LINC00963* | 0,78663617 | 4,68339E-10 |
| 1254 | ENSG00000140525 | *FANCI* | 0,786612143 | 4,25279E-33 |
| 1255 | ENSG00000080298 | *RFX3* | 0,78634004 | 1,2017E-13 |
| 1256 | ENSG00000168610 | *STAT3* | 0,786234296 | 6,09306E-37 |
| 1257 | ENSG00000003989 | *SLC7A2* | 0,786123265 | 1,42266E-06 |
| 1258 | ENSG00000163040 | *CCDC74A* | 0,786121636 | 2,64979E-07 |
| 1259 | ENSG00000151746 | *BICD1* | 0,78572699 | 1,89306E-18 |
| 1260 | ENSG00000177697 | *CD151* | 0,785375017 | 1,49938E-36 |
| 1261 | ENSG00000119669 | *IRF2BPL* | 0,785353663 | 4,00054E-22 |
| 1262 | ENSG00000142173 | *COL6A2* | 0,785304729 | 1,78306E-29 |
| 1263 | ENSG00000135063 | *FAM189A2* | 0,784750803 | 0,003814921 |
| 1264 | ENSG00000066027 | *PPP2R5A* | 0,78418488 | 1,50571E-13 |
| 1265 | ENSG00000135144 | *DTX1* | 0,784002102 | 5,4039E-08 |
| 1266 | ENSG00000196914 | *ARHGEF12* | 0,783464775 | 3,74646E-28 |
| 1267 | ENSG00000051128 | *HOMER3* | 0,782390462 | 2,55667E-11 |
| 1268 | ENSG00000152767 | *FARP1* | 0,781256061 | 5,00094E-35 |
| 1269 | ENSG00000063660 | *GPC1* | 0,781227737 | 3,68108E-48 |
| 1270 | ENSG00000182957 | *SPATA13* | 0,780897367 | 1,01979E-14 |
| 1271 | ENSG00000255471 | *AP001528.2* | 0,780274689 | 0,040157525 |
| 1272 | ENSG00000188158 | *NHS* | 0,779618442 | 1,41324E-06 |
| 1273 | ENSG00000117298 | *ECE1* | 0,778730749 | 3,28826E-24 |
| 1274 | ENSG00000133678 | *TMEM254* | 0,777894939 | 4,08966E-10 |
| 1275 | ENSG00000122642 | *FKBP9* | 0,77712885 | 9,09105E-30 |
| 1276 | ENSG00000157796 | *WDR19* | 0,776923555 | 2,94989E-12 |
| 1277 | ENSG00000079156 | *OSBPL6* | 0,776631201 | 9,13833E-21 |
| 1278 | ENSG00000168785 | *TSPAN5* | 0,776525083 | 9,13239E-18 |
| 1279 | ENSG00000150938 | *CRIM1* | 0,776457708 | 5,10003E-23 |
| 1280 | ENSG00000196154 | *S100A4* | 0,775817996 | 0,001868798 |
| 1281 | ENSG00000122694 | *GLIPR2* | 0,775535607 | 3,43527E-19 |
| 1282 | ENSG00000249550 | *LINC01234* | 0,775372691 | 0,00187505 |
| 1283 | ENSG00000149115 | *TNKS1BP1* | 0,774531716 | 6,4595E-22 |
| 1284 | ENSG00000115425 | *PECR* | 0,773137442 | 4,24658E-06 |
| 1285 | ENSG00000115504 | *EHBP1* | 0,772756212 | 5,04453E-19 |
| 1286 | ENSG00000128833 | *MYO5C* | 0,772653344 | 2,31049E-09 |
| 1287 | ENSG00000237493 | *AC034102.1* | 0,771536075 | 0,00111908 |
| 1288 | ENSG00000106367 | *AP1S1* | 0,771511849 | 1,72651E-18 |
| 1289 | ENSG00000137936 | *BCAR3* | 0,771179454 | 0,000229297 |
| 1290 | ENSG00000095564 | *BTAF1* | 0,770653273 | 1,39179E-36 |
| 1291 | ENSG00000034677 | *RNF19A* | 0,770184871 | 4,80735E-28 |
| 1292 | ENSG00000144061 | *NPHP1* | 0,770156374 | 1,30141E-05 |
| 1293 | ENSG00000261559 | *FSCN1P1* | 0,768851245 | 0,001882627 |
| 1294 | ENSG00000072310 | *SREBF1* | 0,767766139 | 2,0099E-23 |
| 1295 | ENSG00000099330 | *OCEL1* | 0,766998541 | 4,40697E-06 |
| 1296 | ENSG00000153707 | *PTPRD* | 0,765608485 | 1,41834E-19 |
| 1297 | ENSG00000110619 | *CARS* | 0,765313868 | 1,73068E-20 |
| 1298 | ENSG00000197121 | *PGAP1* | 0,763677094 | 2,42989E-24 |
| 1299 | ENSG00000100889 | *PCK2* | 0,763377109 | 5,20119E-05 |
| 1300 | ENSG00000100564 | *PIGH* | 0,763285951 | 0,000145775 |
| 1301 | ENSG00000178662 | *CSRNP3* | 0,762714036 | 0,004234604 |
| 1302 | ENSG00000150893 | *FREM2* | 0,762559049 | 3,56774E-05 |
| 1303 | ENSG00000223745 | *CCDC18-AS1* | 0,761291745 | 5,54667E-07 |
| 1304 | ENSG00000187239 | *FNBP1* | 0,760743067 | 1,82933E-20 |
| 1305 | ENSG00000197324 | *LRP10* | 0,758294511 | 3,67056E-21 |
| 1306 | ENSG00000117016 | *RIMS3* | 0,757511126 | 3,32142E-08 |
| 1307 | ENSG00000197444 | *OGDHL* | 0,75615376 | 0,000397639 |
| 1308 | ENSG00000251562 | *MALAT1* | 0,756097743 | 5,1963E-34 |
| 1309 | ENSG00000149761 | *NUDT22* | 0,755766076 | 2,69483E-05 |
| 1310 | ENSG00000163251 | *FZD5* | 0,75447472 | 6,73338E-09 |
| 1311 | ENSG00000099204 | *ABLIM1* | 0,752333605 | 2,39917E-08 |
| 1312 | ENSG00000089123 | *TASP1* | 0,751927753 | 0,002657769 |
| 1313 | ENSG00000124216 | *SNAI1* | 0,751846588 | 0,001396858 |
| 1314 | ENSG00000167595 | *PROSER3* | 0,751817985 | 6,7729E-07 |
| 1315 | ENSG00000143891 | *GALM* | 0,751606816 | 0,006336398 |
| 1316 | ENSG00000197948 | *FCHSD1* | 0,751245364 | 0,00527693 |

| 1317 | ENSG00000114251 | *WNT5A* | 0,751203888 | 2,2047E-05 |
|---|---|---|---|---|
| 1318 | ENSG00000166153 | *DEPDC4* | 0,751191939 | 0,04480256 |
| 1319 | ENSG00000188735 | *TMEM120B* | 0,750913584 | 3,41739E-07 |
| 1320 | ENSG00000162772 | *ATF3* | 0,750888756 | 5,4431E-06 |
| 1321 | ENSG00000007516 | *BAIAP3* | 0,750327157 | 4,73267E-05 |
| 1322 | ENSG00000116885 | *OSCP1* | 0,749866219 | 0,000148238 |
| 1323 | ENSG00000166924 | *NYAP1* | 0,749787898 | 0,005121417 |
| 1324 | ENSG00000171914 | *TLN2* | 0,749596456 | 1,27748E-13 |
| 1325 | ENSG00000113555 | *PCDH12* | 0,749111147 | 0,02070334 |
| 1326 | ENSG00000249087 | *ZNF436-AS1* | 0,748810439 | 2,31095E-05 |
| 1327 | ENSG00000112972 | *HMGCS1* | 0,748722729 | 7,01978E-44 |
| 1328 | ENSG00000172380 | *GNG12* | 0,74865427 | 3,14333E-37 |
| 1329 | ENSG00000100647 | *SUSD6* | 0,748637416 | 8,95337E-13 |
| 1330 | ENSG00000106100 | *NOD1* | 0,748509909 | 4,8002E-05 |
| 1331 | ENSG00000130813 | *C19orf66* | 0,747815807 | 8,35745E-08 |
| 1332 | ENSG00000173221 | *GLRX* | 0,746331461 | 0,00355123 |
| 1333 | ENSG00000198586 | *TLK1* | 0,746165862 | 3,00685E-17 |
| 1334 | ENSG00000152763 | *WDR78* | 0,746139999 | 0,017309416 |
| 1335 | ENSG00000008300 | *CELSR3* | 0,745793293 | 9,67184E-20 |
| 1336 | ENSG00000174915 | *PTDSS2* | 0,744054726 | 1,73875E-14 |
| 1337 | ENSG00000239713 | *APOBEC3G* | 0,74334043 | 4,50283E-05 |
| 1338 | ENSG00000103942 | *HOMER2* | 0,74286973 | 1,27475E-07 |
| 1339 | ENSG00000107731 | *UNC5B* | 0,742240867 | 0,000317972 |
| 1340 | ENSG00000135362 | *PRR5L* | 0,742085279 | 1,08838E-07 |
| 1341 | ENSG00000228878 | *SEPT7-AS1* | 0,741802496 | 0,001528123 |
| 1342 | ENSG00000257704 | *INAFM1* | 0,741085501 | 0,000112356 |
| 1343 | ENSG00000088826 | *SMOX* | 0,741034426 | 8,69149E-14 |
| 1344 | ENSG00000196739 | *COL27A1* | 0,74096062 | 9,02591E-15 |
| 1345 | ENSG00000142082 | *SIRT3* | 0,740504342 | 2,63211E-10 |
| 1346 | ENSG00000159388 | *BTG2* | 0,740429668 | 7,91075E-26 |
| 1347 | ENSG00000069020 | *MAST4* | 0,739840292 | 0,000491082 |
| 1348 | ENSG00000112769 | *LAMA4* | 0,739406318 | 3,35682E-40 |
| 1349 | ENSG00000185033 | *SEMA4B* | 0,739025518 | 3,25484E-17 |
| 1350 | ENSG00000197558 | *SSPO* | 0,737819293 | 0,037396452 |
| 1351 | ENSG00000163001 | *CFAP36* | 0,737571068 | 1,14268E-13 |
| 1352 | ENSG00000068323 | *TFE3* | 0,737363908 | 5,54015E-22 |
| 1353 | ENSG00000133195 | *SLC39A11* | 0,736806879 | 1,09567E-05 |
| 1354 | ENSG00000163931 | *TKT* | 0,736086133 | 4,48635E-44 |
| 1355 | ENSG00000261934 | *PCDHGA9* | 0,735113988 | 0,008223539 |
| 1356 | ENSG00000073670 | *ADAM11* | 0,734915843 | 6,75282E-06 |
| 1357 | ENSG00000136002 | *ARHGEF4* | 0,734374171 | 2,84754E-14 |
| 1358 | ENSG00000015475 | *BID* | 0,73427975 | 9,64257E-19 |
| 1359 | ENSG00000269069 | *AC007842.1* | 0,734223131 | 0,031480098 |
| 1360 | ENSG00000124785 | *NRN1* | 0,733654499 | 5,36014E-21 |
| 1361 | ENSG00000125844 | *RRBP1* | 0,73364273 | 2,32749E-25 |
| 1362 | ENSG00000184319 | *RPL23AP82* | 0,733091491 | 1,19012E-05 |
| 1363 | ENSG00000120332 | *TNN* | 0,731898479 | 0,036670684 |
| 1364 | ENSG00000133627 | *ACTR3B* | 0,731033742 | 8,34683E-06 |
| 1365 | ENSG00000139190 | *VAMP1* | 0,73007229 | 1,88829E-09 |
| 1366 | ENSG00000157103 | *SLC6A1* | 0,729313126 | 1,29436E-05 |
| 1367 | ENSG00000158715 | *SLC45A3* | 0,729010049 | 0,04153032 |
| 1368 | ENSG00000116514 | *RNF19B* | 0,728873369 | 2,54476E-07 |
| 1369 | ENSG00000087842 | *PIR* | 0,728848426 | 2,38832E-20 |
| 1370 | ENSG00000198961 | *PJA2* | 0,728427577 | 5,91541E-36 |
| 1371 | ENSG00000168067 | *MAP4K2* | 0,728286063 | 5,49115E-07 |
| 1372 | ENSG00000172890 | *NADSYN1* | 0,728136483 | 6,79309E-17 |
| 1373 | ENSG00000243199 | *AC115223.1* | 0,727351818 | 4,21628E-05 |
| 1374 | ENSG00000182132 | *KCNIP1* | 0,726830701 | 1,69779E-06 |
| 1375 | ENSG00000179295 | *PTPN11* | 0,726744953 | 1,19582E-33 |
| 1376 | ENSG00000155980 | *KIF5A* | 0,725592178 | 3,2466E-16 |
| 1377 | ENSG00000157514 | *TSC22D3* | 0,725137391 | 7,36187E-05 |
| 1378 | ENSG00000178234 | *GALNT11* | 0,725051828 | 9,78603E-13 |
| 1379 | ENSG00000185483 | *ROR1* | 0,725013347 | 0,028629787 |
| 1380 | ENSG00000179304 | *FAM156B* | 0,724353989 | 0,007718719 |
| 1381 | ENSG00000220848 | *RPS18P9* | 0,724010712 | 0,023303445 |
| 1382 | ENSG00000124313 | *IQSEC2* | 0,723699521 | 1,24078E-05 |
| 1383 | ENSG00000171159 | *C9orf16* | 0,722700482 | 1,52233E-19 |
| 1384 | ENSG00000177694 | *NAALADL2* | 0,721203314 | 0,009907698 |
| 1385 | ENSG00000109339 | *MAPK10* | 0,719870307 | 2,83026E-05 |
| 1386 | ENSG00000224183 | *SDHDP6* | 0,719830297 | 0,01686923 |
| 1387 | ENSG00000159842 | *ABR* | 0,718834983 | 3,95543E-21 |
| 1388 | ENSG00000133639 | *BTG1* | 0,718104833 | 7,1925E-26 |
| 1389 | ENSG00000069399 | *BCL3* | 0,717896891 | 0,000277985 |
| 1390 | ENSG00000125510 | *OPRL1* | 0,71745478 | 0,04207008 |
| 1391 | ENSG00000180739 | *S1PR5* | 0,717336395 | 0,002264493 |
| 1392 | ENSG00000164953 | *TMEM67* | 0,71690431 | 5,29405E-05 |
| 1393 | ENSG00000119408 | *NEK6* | 0,715493466 | 2,40206E-30 |
| 1394 | ENSG00000106992 | *AK1* | 0,715321344 | 0,011387651 |

| | | | | |
|---|---|---|---|---|
| 1395 | ENSG00000136425 | *CIB2* | 0,714136494 | 1,0143E-06 |
| 1396 | ENSG00000109736 | *MFSD10* | 0,712488967 | 3,26554E-11 |
| 1397 | ENSG00000162004 | *CCDC78* | 0,712327476 | 3,24285E-05 |
| 1398 | ENSG00000091129 | *NRCAM* | 0,711912951 | 6,78256E-22 |
| 1399 | ENSG00000221968 | *FADS3* | 0,711738144 | 1,01302E-13 |
| 1400 | ENSG00000177640 | *CASC2* | 0,711260875 | 0,047900661 |
| 1401 | ENSG00000145715 | *RASA1* | 0,709119932 | 8,45815E-16 |
| 1402 | ENSG00000107819 | *SFXN3* | 0,708829386 | 1,17862E-13 |
| 1403 | ENSG00000184056 | *VPS33B* | 0,708484639 | 4,62982E-07 |
| 1404 | ENSG00000218418 | *AL591135.1* | 0,707975401 | 0,018373116 |
| 1405 | ENSG00000139192 | *TAPBPL* | 0,7077751 | 0,000263398 |
| 1406 | ENSG00000006118 | *TMEM132A* | 0,707149474 | 2,11691E-29 |
| 1407 | ENSG00000102007 | *PLP2* | 0,706180081 | 7,0043E-07 |
| 1408 | ENSG00000139645 | *ANKRD52* | 0,705758573 | 2,66637E-22 |
| 1409 | ENSG00000169641 | *LUZP1* | 0,705380136 | 1,56027E-14 |
| 1410 | ENSG00000176155 | *CCDC57* | 0,704766885 | 3,34206E-11 |
| 1411 | ENSG00000230383 | *AC009245.1* | 0,702909074 | 0,002959458 |
| 1412 | ENSG00000082146 | *STRADB* | 0,702470609 | 9,01907E-15 |
| 1413 | ENSG00000146001 | *PCDHB18P* | 0,701905239 | 0,000730588 |
| 1414 | ENSG00000130304 | *SLC27A1* | 0,700909908 | 3,28995E-25 |
| 1415 | ENSG00000196182 | *STK40* | 0,7006976 | 1,4708E-18 |
| 1416 | ENSG00000197586 | *ENTPD6* | 0,700550419 | 2,01005E-16 |
| 1417 | ENSG00000148339 | *SLC25A25* | 0,700444512 | 1,6591E-17 |
| 1418 | ENSG00000254682 | *AP002387.1* | 0,700339471 | 9,10317E-05 |
| 1419 | ENSG00000181754 | *AMIGO1* | 0,699840117 | 0,000231946 |
| 1420 | ENSG00000185386 | *MAPK11* | 0,699736364 | 3,35326E-13 |
| 1421 | ENSG00000100344 | *PNPLA3* | 0,699656098 | 4,2367E-06 |
| 1422 | ENSG00000116157 | *GPX7* | 0,699333001 | 0,010492928 |
| 1423 | ENSG00000118707 | *TGIF2* | 0,698651248 | 0,000203728 |
| 1424 | ENSG00000171055 | *FEZ2* | 0,698519917 | 6,70136E-15 |
| 1425 | ENSG00000177614 | *PGBD5* | 0,697719364 | 7,09067E-07 |
| 1426 | ENSG00000084710 | *EFR3B* | 0,697510101 | 3,53672E-07 |
| 1427 | ENSG00000173846 | *PLK3* | 0,696762353 | 0,00037398 |
| 1428 | ENSG00000013364 | *MVP* | 0,696519008 | 3,4013E-08 |
| 1429 | ENSG00000143801 | *PSEN2* | 0,696142598 | 3,56343E-05 |
| 1430 | ENSG00000117280 | *RAB29* | 0,694704085 | 4,08261E-11 |
| 1431 | ENSG00000140022 | *STON2* | 0,694164709 | 4,62881E-05 |
| 1432 | ENSG00000125520 | *SLC2A4RG* | 0,694159774 | 1,2114E-12 |
| 1433 | ENSG00000198435 | *NRARP* | 0,693716561 | 0,002959458 |
| 1434 | ENSG00000167778 | *SPRYD3* | 0,69343939 | 1,20509E-10 |
| 1435 | ENSG00000205352 | *PRR13* | 0,692915643 | 3,64798E-09 |
| 1436 | ENSG00000162542 | *TMCO4* | 0,69285514 | 0,048614427 |
| 1437 | ENSG00000168389 | *MFSD2A* | 0,692736899 | 0,001186613 |
| 1438 | ENSG00000185008 | *ROBO2* | 0,692160744 | 7,71176E-23 |
| 1439 | ENSG00000143061 | *IGSF3* | 0,692085762 | 3,96617E-17 |
| 1440 | ENSG00000116406 | *EDEM3* | 0,692068845 | 3,00138E-17 |
| 1441 | ENSG00000186815 | *TPCN1* | 0,692039744 | 2,57807E-07 |
| 1442 | ENSG00000128294 | *TPST2* | 0,692034174 | 1,23662E-11 |
| 1443 | ENSG00000100612 | *DHRS7* | 0,690446346 | 1,47966E-11 |
| 1444 | ENSG00000130589 | *HELZ2* | 0,690116525 | 6,59622E-10 |
| 1445 | ENSG00000269958 | *AL049840.4* | 0,689922903 | 0,000797995 |
| 1446 | ENSG00000099999 | *RNF215* | 0,689395145 | 4,22477E-09 |
| 1447 | ENSG00000182095 | *TNRC18* | 0,689382167 | 3,93637E-23 |
| 1448 | ENSG00000060138 | *YBX3* | 0,688841211 | 9,2238E-24 |
| 1449 | ENSG00000058799 | *YIPF1* | 0,688748637 | 4,89951E-08 |
| 1450 | ENSG00000161714 | *PLCD3* | 0,688552296 | 4,472E-19 |
| 1451 | ENSG00000024422 | *EHD2* | 0,687926801 | 1,06011E-24 |
| 1452 | ENSG00000173295 | *FAM86B3P* | 0,687765734 | 0,024007574 |
| 1453 | ENSG00000072110 | *ACTN1* | 0,686920499 | 6,70241E-18 |
| 1454 | ENSG00000174943 | *KCTD13* | 0,686001748 | 2,75358E-06 |
| 1455 | ENSG00000140853 | *NLRC5* | 0,685560316 | 1,01298E-06 |
| 1456 | ENSG00000185043 | *CIB1* | 0,684733112 | 8,08578E-11 |
| 1457 | ENSG00000026652 | *AGPAT4* | 0,684096712 | 1,53087E-17 |
| 1458 | ENSG00000143590 | *EFNA3* | 0,68107109 | 0,015861904 |
| 1459 | ENSG00000114423 | *CBLB* | 0,680877908 | 3,03455E-13 |
| 1460 | ENSG00000128394 | *APOBEC3F* | 0,680579971 | 0,008577461 |
| 1461 | ENSG00000168890 | *TMEM150A* | 0,680447778 | 0,000298977 |
| 1462 | ENSG00000134253 | *TRIM45* | 0,679989445 | 5,36267E-09 |
| 1463 | ENSG00000162433 | *AK4* | 0,679289183 | 7,81672E-10 |
| 1464 | ENSG00000131711 | *MAP1B* | 0,67913779 | 1,99228E-28 |
| 1465 | ENSG00000171552 | *BCL2L1* | 0,677933834 | 4,33328E-16 |
| 1466 | ENSG00000105643 | *ARRDC2* | 0,677688761 | 0,00103502 |
| 1467 | ENSG00000178607 | *ERN1* | 0,677196791 | 0,000164173 |
| 1468 | ENSG00000256185 | *AC055720.2* | 0,676906231 | 0,036898581 |
| 1469 | ENSG00000099250 | *NRP1* | 0,676725282 | 3,68679E-05 |
| 1470 | ENSG00000197019 | *SERTAD1* | 0,676015931 | 6,84058E-06 |
| 1471 | ENSG00000164442 | *CITED2* | 0,67498157 | 1,27029E-09 |
| 1472 | ENSG00000128683 | *GAD1* | 0,674964111 | 9,80956E-19 |

| | | | | |
|---|---|---|---|---|
| 1473 | ENSG00000163879 | *DNALI1* | 0,673765431 | 1,27883E-11 |
| 1474 | ENSG00000197077 | *KIAA1671* | 0,673276084 | 4,47553E-07 |
| 1475 | ENSG00000130475 | *FCHO1* | 0,672107225 | 0,001376291 |
| 1476 | ENSG00000173706 | *HEG1* | 0,671717338 | 1,3366E-10 |
| 1477 | ENSG00000104936 | *DMPK* | 0,671401453 | 2,28637E-14 |
| 1478 | ENSG00000120658 | *ENOX1* | 0,671186679 | 0,00099389 |
| 1479 | ENSG00000151176 | *PLBD2* | 0,670616761 | 2,42372E-09 |
| 1480 | ENSG00000162923 | *WDR26* | 0,670311564 | 4,86546E-22 |
| 1481 | ENSG00000146006 | *LRRTM2* | 0,670251174 | 3,5928E-09 |
| 1482 | ENSG00000162576 | *MXRA8* | 0,669794534 | 0,045350249 |
| 1483 | ENSG00000173812 | *EIF1* | 0,669500361 | 3,81931E-32 |
| 1484 | ENSG00000123992 | *DNPEP* | 0,669481359 | 3,5157E-14 |
| 1485 | ENSG00000203943 | *SAMD13* | 0,668918459 | 0,049246501 |
| 1486 | ENSG00000187164 | *SHTN1* | 0,668768008 | 3,29548E-11 |
| 1487 | ENSG00000173153 | *ESRRA* | 0,668310007 | 8,35745E-08 |
| 1488 | ENSG00000170145 | *SIK2* | 0,668168872 | 1,86586E-14 |
| 1489 | ENSG00000184640 | *SEPT9* | 0,667416146 | 1,19616E-34 |
| 1490 | ENSG00000173227 | *SYT12* | 0,667093438 | 6,01718E-05 |
| 1491 | ENSG00000169519 | *METTL15* | 0,66634741 | 2,01656E-05 |
| 1492 | ENSG00000119922 | *IFIT2* | 0,666329052 | 1,14684E-06 |
| 1493 | ENSG00000142657 | *PGD* | 0,66599907 | 1,66563E-32 |
| 1494 | ENSG00000100095 | *SEZ6L* | 0,665249736 | 2,62169E-26 |
| 1495 | ENSG00000005238 | *FAM214B* | 0,664815978 | 1,10888E-06 |
| 1496 | ENSG00000132535 | *DLG4* | 0,663877703 | 9,1459E-12 |
| 1497 | ENSG00000099957 | *P2RX6* | 0,662612582 | 1,77822E-05 |
| 1498 | ENSG00000169871 | *TRIM56* | 0,662287829 | 1,69779E-06 |
| 1499 | ENSG00000136444 | *RSAD1* | 0,661565092 | 1,83088E-11 |
| 1500 | ENSG00000165323 | *FAT3* | 0,661225197 | 4,2872E-17 |
| 1501 | ENSG00000099326 | *MZF1* | 0,661152234 | 2,25933E-11 |
| 1502 | ENSG00000049759 | *NEDD4L* | 0,661095522 | 4,902E-12 |
| 1503 | ENSG00000168310 | *IRF2* | 0,661031995 | 1,07153E-08 |
| 1504 | ENSG00000185880 | *TRIM69* | 0,660324525 | 2,10624E-11 |
| 1505 | ENSG00000023171 | *GRAMD1B* | 0,658907022 | 1,62833E-05 |
| 1506 | ENSG00000184792 | *OSBP2* | 0,658490698 | 3,82639E-05 |
| 1507 | ENSG00000225177 | *AL590617.2* | 0,657255394 | 0,001122531 |
| 1508 | ENSG00000110013 | *SIAE* | 0,654608221 | 6,79473E-10 |
| 1509 | ENSG00000182405 | *PGBD4* | 0,65410755 | 0,005193943 |
| 1510 | ENSG00000008277 | *ADAM22* | 0,653832496 | 6,47327E-15 |
| 1511 | ENSG00000143545 | *RAB13* | 0,653148129 | 3,64329E-21 |
| 1512 | ENSG00000166411 | *IDH3A* | 0,652827769 | 1,68628E-07 |
| 1513 | ENSG00000152894 | *PTPRK* | 0,652022809 | 2,7045E-16 |
| 1514 | ENSG00000183579 | *ZNRF3* | 0,651104949 | 6,89616E-11 |
| 1515 | ENSG00000088836 | *SLC4A11* | 0,650972111 | 0,00103468 |
| 1516 | ENSG00000050130 | *JKAMP* | 0,650901381 | 5,80206E-10 |
| 1517 | ENSG00000184216 | *IRAK1* | 0,650292492 | 2,42558E-23 |
| 1518 | ENSG00000126705 | *AHDC1* | 0,649972975 | 1,6314E-11 |
| 1519 | ENSG00000170448 | *NFXL1* | 0,649930887 | 7,37147E-05 |
| 1520 | ENSG00000182168 | *UNC5C* | 0,649577713 | 7,20573E-11 |
| 1521 | ENSG00000176845 | *METRNL* | 0,649505647 | 3,02126E-06 |
| 1522 | ENSG00000164951 | *PDP1* | 0,649484534 | 1,87553E-08 |
| 1523 | ENSG00000128581 | *IFT22* | 0,648632563 | 1,33332E-08 |
| 1524 | ENSG00000005379 | *TSPOAP1* | 0,64852545 | 0,040336062 |
| 1525 | ENSG00000049130 | *KITLG* | 0,648513411 | 0,000101102 |
| 1526 | ENSG00000137486 | *ARRB1* | 0,648367576 | 0,001307352 |
| 1527 | ENSG00000165338 | *HECTD2* | 0,648345151 | 5,52254E-07 |
| 1528 | ENSG00000240036 | *AC104563.1* | 0,646791223 | 0,004791575 |
| 1529 | ENSG00000120068 | *HOXB8* | 0,646648538 | 0,004248784 |
| 1530 | ENSG00000143641 | *GALNT2* | 0,646534028 | 3,26445E-22 |
| 1531 | ENSG00000184465 | *WDR27* | 0,64621893 | 2,53829E-09 |
| 1532 | ENSG00000155542 | *SETD9* | 0,645025495 | 0,000124073 |
| 1533 | ENSG00000176826 | *FKBP9P1* | 0,644344635 | 0,01916257 |
| 1534 | ENSG00000160172 | *FAM86C2P* | 0,644284926 | 0,016023147 |
| 1535 | ENSG00000131370 | *SH3BP5* | 0,644072157 | 0,018866879 |
| 1536 | ENSG00000121039 | *RDH10* | 0,64404941 | 5,29751E-05 |
| 1537 | ENSG00000125746 | *EML2* | 0,643592506 | 1,36628E-05 |
| 1538 | ENSG00000074416 | *MGLL* | 0,64308183 | 1,04004E-19 |
| 1539 | ENSG00000035687 | *ADSS* | 0,642841889 | 4,51788E-10 |
| 1540 | ENSG00000204634 | *TBC1D8* | 0,642520074 | 4,39637E-06 |
| 1541 | ENSG00000159208 | *CIART* | 0,640146538 | 1,27149E-05 |
| 1542 | ENSG00000167037 | *SGSM1* | 0,640047585 | 0,001029086 |
| 1543 | ENSG00000167733 | *HSD11B1L* | 0,639281716 | 7,09598E-06 |
| 1544 | ENSG00000185621 | *LMLN* | 0,638767063 | 2,90371E-05 |
| 1545 | ENSG00000143995 | *MEIS1* | 0,638761087 | 2,32851E-07 |
| 1546 | ENSG00000004660 | *CAMKK1* | 0,638543912 | 0,028499031 |
| 1547 | ENSG00000133135 | *RNF128* | 0,638400512 | 8,35425E-09 |
| 1548 | ENSG00000152495 | *CAMK4* | 0,637912374 | 0,017513699 |
| 1549 | ENSG00000104687 | *GSR* | 0,637814176 | 5,58027E-14 |
| 1550 | ENSG00000160446 | *ZDHHC12* | 0,637696603 | 2,37068E-06 |

| 1551 | ENSG00000168275 | *COA6* | 0,637669231 | 4,09782E-05 |
|---|---|---|---|---|
| 1552 | ENSG00000150977 | *RILPL2* | 0,637028536 | 0,000244679 |
| 1553 | ENSG00000179611 | *DGKZP1* | 0,636304712 | 0,000277616 |
| 1554 | ENSG00000133321 | *RARRES3* | 0,636171011 | 0,027299501 |
| 1555 | ENSG00000181004 | *BBS12* | 0,636108645 | 0,022516083 |
| 1556 | ENSG00000146776 | *ATXN7L1* | 0,63567838 | 0,007831875 |
| 1557 | ENSG00000102466 | *FGF14* | 0,635485304 | 0,002023282 |
| 1558 | ENSG00000255284 | *AP006621.3* | 0,635463104 | 0,016896682 |
| 1559 | ENSG00000006282 | *SPATA20* | 0,63432464 | 1,99669E-12 |
| 1560 | ENSG00000011028 | *MRC2* | 0,634043746 | 4,7165E-22 |
| 1561 | ENSG00000105855 | *ITGB8* | 0,633706702 | 4,69693E-19 |
| 1562 | ENSG00000124275 | *MTRR* | 0,633686923 | 1,42742E-11 |
| 1563 | ENSG00000003402 | *CFLAR* | 0,633251924 | 2,85486E-09 |
| 1564 | ENSG00000126777 | *KTN1* | 0,632802092 | 1,33468E-21 |
| 1565 | ENSG00000139146 | *FAM60A* | 0,632586491 | 2,51724E-09 |
| 1566 | ENSG00000084444 | *FAM234B* | 0,632324237 | 7,13533E-08 |
| 1567 | ENSG00000235750 | *KIAA0040* | 0,631946805 | 0,0004871 |
| 1568 | ENSG00000072195 | *SPEG* | 0,631738842 | 3,89047E-15 |
| 1569 | ENSG00000212694 | *LINC01089* | 0,631024268 | 0,003125776 |
| 1570 | ENSG00000233639 | *LINC01158* | 0,630901287 | 2,18028E-08 |
| 1571 | ENSG00000138411 | *HECW2* | 0,629734982 | 0,017552299 |
| 1572 | ENSG00000131873 | *CHSY1* | 0,628870881 | 1,7476E-12 |
| 1573 | ENSG00000174206 | *C12orf66* | 0,628754956 | 0,001520124 |
| 1574 | ENSG00000047230 | *CTPS2* | 0,627793674 | 1,86651E-07 |
| 1575 | ENSG00000161091 | *MFSD12* | 0,627779109 | 1,17281E-11 |
| 1576 | ENSG00000105696 | *TMEM59L* | 0,627728407 | 1,78888E-08 |
| 1577 | ENSG00000135926 | *TMBIM1* | 0,626672264 | 4,7171E-06 |
| 1578 | ENSG00000196236 | *XPNPEP3* | 0,626225131 | 2,5098E-08 |
| 1579 | ENSG00000157064 | *NMNAT2* | 0,625886955 | 0,03010122 |
| 1580 | ENSG00000229117 | *RPL41* | 0,625381957 | 1,10267E-16 |
| 1581 | ENSG00000189157 | *FAM47E* | 0,625214024 | 0,009207402 |
| 1582 | ENSG00000105953 | *OGDH* | 0,624799434 | 7,24369E-19 |
| 1583 | ENSG00000214455 | *RCN1P2* | 0,623777388 | 4,01827E-05 |
| 1584 | ENSG00000160991 | *ORAI2* | 0,622635971 | 2,92215E-13 |
| 1585 | ENSG00000025434 | *NR1H3* | 0,622494082 | 0,000386509 |
| 1586 | ENSG00000167371 | *PRRT2* | 0,621252867 | 2,15649E-06 |
| 1587 | ENSG00000099331 | *MYO9B* | 0,621113858 | 2,56429E-22 |
| 1588 | ENSG00000166986 | *MARS* | 0,620426657 | 3,36477E-21 |
| 1589 | ENSG00000235552 | *AP005202.1* | 0,620209683 | 1,31374E-11 |
| 1590 | ENSG00000163449 | *TMEM169* | 0,62008061 | 2,51403E-09 |
| 1591 | ENSG00000135452 | *TSPAN31* | 0,619998156 | 6,3016E-07 |
| 1592 | ENSG00000126456 | *IRF3* | 0,619129856 | 1,05598E-09 |
| 1593 | ENSG00000234741 | *GAS5* | 0,619016127 | 4,30455E-15 |
| 1594 | ENSG00000100211 | *CBY1* | 0,618890193 | 0,000498836 |
| 1595 | ENSG00000123600 | *METTL8* | 0,61804787 | 1,92926E-05 |
| 1596 | ENSG00000196411 | *EPHB4* | 0,617995897 | 6,81546E-11 |
| 1597 | ENSG00000105419 | *MEIS3* | 0,617912328 | 1,63516E-17 |
| 1598 | ENSG00000126391 | *FRMD8* | 0,617872697 | 5,244E-18 |
| 1599 | ENSG00000196839 | *ADA* | 0,617764063 | 1,78303E-06 |
| 1600 | ENSG00000131188 | *PRR7* | 0,616762509 | 5,89063E-05 |
| 1601 | ENSG00000229891 | *LINC01315* | 0,61674999 | 0,010960927 |
| 1602 | ENSG00000134324 | *LPIN1* | 0,616591619 | 4,10848E-16 |
| 1603 | ENSG00000130363 | *RSPH3* | 0,616101728 | 0,000451765 |
| 1604 | ENSG00000131408 | *NR1H2* | 0,615879209 | 4,78079E-14 |
| 1605 | ENSG00000106333 | *PCOLCE* | 0,615640498 | 0,029971824 |
| 1606 | ENSG00000107551 | *RASSF4* | 0,615355771 | 0,001819865 |
| 1607 | ENSG00000131015 | *ULBP2* | 0,615330692 | 0,036838424 |
| 1608 | ENSG00000182902 | *SLC25A18* | 0,61522657 | 0,020092527 |
| 1609 | ENSG00000135931 | *ARMC9* | 0,615141533 | 7,99946E-06 |
| 1610 | ENSG00000182154 | *MRPL41* | 0,61450482 | 9,76608E-05 |
| 1611 | ENSG00000101986 | *ABCD1* | 0,614065147 | 5,85679E-05 |
| 1612 | ENSG00000115183 | *TANC1* | 0,61388628 | 1,92431E-21 |
| 1613 | ENSG00000179912 | *R3HDM2* | 0,613480048 | 3,35736E-09 |
| 1614 | ENSG00000183150 | *GPR19* | 0,613448374 | 0,000647602 |
| 1615 | ENSG00000144791 | *LIMD1* | 0,613138594 | 1,04819E-07 |
| 1616 | ENSG00000164088 | *PPM1M* | 0,61295811 | 3,39503E-05 |
| 1617 | ENSG00000135414 | *GDF11* | 0,612802691 | 2,21687E-16 |
| 1618 | ENSG00000232389 | *AL583856.1* | 0,612778826 | 0,003157117 |
| 1619 | ENSG00000127838 | *PNKD* | 0,611406482 | 2,04296E-11 |
| 1620 | ENSG00000170581 | *STAT2* | 0,611247174 | 9,35796E-19 |
| 1621 | ENSG00000139289 | *PHLDA1* | 0,610642842 | 8,12041E-30 |
| 1622 | ENSG00000198920 | *KIAA0753* | 0,610329713 | 1,53147E-07 |
| 1623 | ENSG00000130023 | *ERMARD* | 0,609781975 | 0,000139672 |
| 1624 | ENSG00000153208 | *MERTK* | 0,609423137 | 3,67305E-06 |
| 1625 | ENSG00000235162 | *C12orf75* | 0,609216762 | 3,38163E-08 |
| 1626 | ENSG00000157881 | *PANK4* | 0,609119825 | 1,26415E-09 |
| 1627 | ENSG00000232533 | *AC093673.1* | 0,60908793 | 0,000585288 |
| 1628 | ENSG00000176454 | *LPCAT4* | 0,608970148 | 1,39048E-08 |

| | | | | |
|---|---|---|---|---|
| 1629 | ENSG00000119650 | *IFT43* | 0,608908818 | 0,000259173 |
| 1630 | ENSG00000205643 | *CDPF1* | 0,607888274 | 0,000157838 |
| 1631 | ENSG00000187815 | *ZFP69* | 0,607601572 | 0,006029625 |
| 1632 | ENSG00000121897 | *LIAS* | 0,606775945 | 0,013775979 |
| 1633 | ENSG00000104518 | *GSDMD* | 0,605751744 | 0,01974714 |
| 1634 | ENSG00000234608 | *MAPKAPK5-AS1* | 0,605218785 | 0,011624842 |
| 1635 | ENSG00000204685 | *STARD7-AS1* | 0,604955992 | 0,043926946 |
| 1636 | ENSG00000131697 | *NPHP4* | 0,604860227 | 3,79427E-06 |
| 1637 | ENSG00000134333 | *LDHA* | 0,604271283 | 1,47974E-24 |
| 1638 | ENSG00000145217 | *SLC26A1* | 0,604224053 | 0,020043752 |
| 1639 | ENSG00000027697 | *IFNGR1* | 0,604211244 | 8,82248E-08 |
| 1640 | ENSG00000087903 | *RFX2* | 0,603792708 | 2,32716E-06 |
| 1641 | ENSG00000143324 | *XPR1* | 0,603709787 | 1,18954E-11 |
| 1642 | ENSG00000219626 | *FAM228B* | 0,603697294 | 0,005896054 |
| 1643 | ENSG00000188010 | *MORN2* | 0,603513838 | 5,29221E-05 |
| 1644 | ENSG00000223825 | *DAZAP2P1* | 0,60225346 | 0,02940066 |
| 1645 | ENSG00000196656 | *AC004057.1* | 0,602010564 | 0,00017732 |
| 1646 | ENSG00000169439 | *SDC2* | 0,600632144 | 1,40526E-12 |
| 1647 | ENSG00000123815 | *COQ8B* | 0,600612718 | 2,0154E-14 |
| 1648 | ENSG00000136114 | *THSD1* | 0,600253813 | 2,29329E-08 |
| 1649 | ENSG00000099290 | *WASHC2A* | 0,600246592 | 0,002417098 |
| 1650 | ENSG00000106610 | *STAG3L4* | 0,60002213 | 0,007845417 |

Table 13. List of downregulated gene expression levels (FPKM; >0.6 log2-fold change, FDR<0.01) in U3047MG naïve), ciliated GSCs (U3047MG NEK2-KD) cells.

| Sr.No | Gene | Gene names | log2FoldChange | Pvalue |
|---|---|---|---|---|
| 1 | ENSG00000144230 | *GPR17* | -8,039437989 | 5,9258E-236 |
| 2 | ENSG00000078596 | *ITM2A* | -7,96985221 | 4,7233E-180 |
| 3 | ENSG00000114279 | *FGF12* | -7,520108233 | 3,2679E-274 |
| 4 | ENSG00000100146 | *SOX10* | -7,481328633 | 0 |
| 5 | ENSG00000146250 | *PRSS35* | -7,251321342 | 8,0122E-122 |
| 6 | ENSG00000148123 | *PLPPR1* | -7,246471645 | 1,221E-258 |
| 7 | ENSG00000175356 | *SCUBE2* | -6,780567363 | 5,8031E-232 |
| 8 | ENSG00000134121 | *CHL1* | -6,760962734 | 2,6302E-190 |
| 9 | ENSG00000158887 | *MPZ* | -6,40530121 | 0 |
| 10 | ENSG00000078725 | *BRINP1* | -6,357409534 | 2,2383E-274 |
| 11 | ENSG00000072163 | *LIMS2* | -5,83276228 | 1,0989E-183 |
| 12 | ENSG00000151892 | *GFRA1* | -5,794326359 | 6,3983E-152 |
| 13 | ENSG00000136574 | *GATA4* | -5,766016195 | 4,4439E-109 |
| 14 | ENSG00000163453 | *IGFBP7* | -5,505430534 | 1,8935E-220 |
| 15 | ENSG00000120675 | *DNAJC15* | -5,502092519 | 2,61697E-85 |
| 16 | ENSG00000132329 | *RAMP1* | -5,474184732 | 0 |
| 17 | ENSG00000126861 | *OMG* | -5,369447549 | 0 |
| 18 | ENSG00000134184 | *GSTM1* | -5,358941952 | 9,27724E-82 |
| 19 | ENSG00000018236 | *CNTN1* | -5,353850875 | 0 |
| 20 | ENSG00000112280 | *COL9A1* | -5,242521422 | 0 |
| 21 | ENSG00000128242 | *GAL3ST1* | -5,196959503 | 2,0198E-110 |
| 22 | ENSG00000227051 | *C14orf132* | -5,16133079 | 1,6299E-277 |
| 23 | ENSG00000130287 | *NCAN* | -5,145009178 | 0 |
| 24 | ENSG00000101203 | *COL20A1* | -5,065865942 | 0 |
| 25 | ENSG00000101695 | *RNF125* | -5,063432816 | 6,1807E-126 |
| 26 | ENSG00000101445 | *PPP1R16B* | -5,046959014 | 3,3882E-139 |
| 27 | ENSG00000180787 | *ZFP3* | -5,046714725 | 3,14294E-97 |
| 28 | ENSG00000164176 | *EDIL3* | -5,032304208 | 0 |
| 29 | ENSG00000170011 | *MYRIP* | -4,979734623 | 7,7539E-55 |
| 30 | ENSG00000102313 | *ITIH6* | -4,87405976 | 1,0008E-278 |
| 31 | ENSG00000197448 | *GSTK1* | -4,854588382 | 4,1445E-230 |
| 32 | ENSG00000110090 | *CPT1A* | -4,839770982 | 1,84526E-98 |
| 33 | ENSG00000197971 | *MBP* | -4,824502299 | 4,40892E-71 |
| 34 | ENSG00000122012 | *SV2C* | -4,798767138 | 4,58443E-39 |
| 35 | ENSG00000126860 | *EVI2A* | -4,787288789 | 6,07885E-39 |
| 36 | ENSG00000101311 | *FERMT1* | -4,768140717 | 0 |
| 37 | ENSG00000196218 | *RYR1* | -4,671503299 | 8,12621E-50 |
| 38 | ENSG00000248184 | *LINC02283* | -4,566857829 | 9,37288E-89 |
| 39 | ENSG00000107807 | *TLX1* | -4,563055892 | 7,34764E-30 |
| 40 | ENSG00000110455 | *ACCS* | -4,530826392 | 1,04738E-41 |
| 41 | ENSG00000172349 | *IL16* | -4,525882069 | 2,89912E-47 |
| 42 | ENSG00000157445 | *CACNA2D3* | -4,491087072 | 7,23341E-34 |
| 43 | ENSG00000168309 | *FAM107A* | -4,4783084 | 1,6717E-100 |
| 44 | ENSG00000166582 | *CENPV* | -4,468670495 | 0 |
| 45 | ENSG00000109220 | *CHIC2* | -4,430498686 | 0 |
| 46 | ENSG00000225127 | *LINC00237* | -4,332391656 | 7,11028E-24 |
| 47 | ENSG00000130762 | *ARHGEF16* | -4,28456177 | 1,28614E-51 |
| 48 | ENSG00000169129 | *AFAP1L2* | -4,232133669 | 8,9304E-130 |
| 49 | ENSG00000003137 | *CYP26B1* | -4,21351088 | 3,91067E-59 |
| 50 | ENSG00000106688 | *SLC1A1* | -4,188323627 | 0 |
| 51 | ENSG00000162670 | *BRINP3* | -4,130973686 | 1,28565E-94 |
| 52 | ENSG00000183715 | *OPCML* | -4,125076044 | 0 |
| 53 | ENSG00000187955 | *COL14A1* | -4,111903354 | 5,41695E-35 |
| 54 | ENSG00000261377 | *PDCD6IPP2* | -4,089150458 | 4,65122E-30 |
| 55 | ENSG00000137558 | *PI15* | -4,028665098 | 4,94074E-27 |
| 56 | ENSG00000134864 | *GGACT* | -4,026112875 | 2,22877E-22 |
| 57 | ENSG00000156535 | *CD109* | -3,997969818 | 2,54906E-92 |
| 58 | ENSG00000162998 | *FRZB* | -3,993243672 | 1,44022E-40 |
| 59 | ENSG00000228203 | *RNF144A-AS1* | -3,956922978 | 6,60208E-25 |
| 60 | ENSG00000112796 | *ENPP5* | -3,954005801 | 4,18772E-36 |
| 61 | ENSG00000171885 | *AQP4* | -3,951673155 | 0 |
| 62 | ENSG00000100441 | *KHNYN* | -3,948628567 | 1,01472E-64 |
| 63 | ENSG00000204241 | *AP000911.1* | -3,862532743 | 2,86878E-25 |
| 64 | ENSG00000165757 | *KIAA1462* | -3,814305302 | 2,2197E-195 |
| 65 | ENSG00000167755 | *KLK6* | -3,804063685 | 1,78517E-26 |
| 66 | ENSG00000166897 | *ELFN2* | -3,755315995 | 0 |
| 67 | ENSG00000144668 | *ITGA9* | -3,750649223 | 2,0864E-190 |
| 68 | ENSG00000109610 | *SOD3* | -3,727763894 | 2,13471E-77 |
| 69 | ENSG00000163864 | *NMNAT3* | -3,726838735 | 3,88943E-40 |
| 70 | ENSG00000143458 | *GABPB2* | -3,726373003 | 8,02551E-30 |
| 71 | ENSG00000225614 | *ZNF469* | -3,712103039 | 1,10545E-62 |
| 72 | ENSG00000187720 | *THSD4* | -3,656399494 | 1,04529E-40 |
| 73 | ENSG00000173210 | *ABLIM3* | -3,656370041 | 4,35282E-52 |

| | | | | |
|---|---|---|---|---|
| 74 | ENSG00000187902 | *SHISA7* | -3,650018774 | 5,60706E-33 |
| 75 | ENSG00000116833 | *NR5A2* | -3,647153064 | 4,352E-24 |
| 76 | ENSG00000170091 | *HMP19* | -3,616790489 | 1,80114E-34 |
| 77 | ENSG00000184961 | *RPL7AP49* | -3,616367323 | 8,57731E-27 |
| 78 | ENSG00000103316 | *CRYM* | -3,609870107 | 1,38527E-25 |
| 79 | ENSG00000113805 | *CNTN3* | -3,607247578 | 3,56628E-45 |
| 80 | ENSG00000255442 | *AC109635.5* | -3,566458006 | 1,1088E-25 |
| 81 | ENSG00000060718 | *COL11A1* | -3,534235195 | 0 |
| 82 | ENSG00000184785 | *SMIM10* | -3,520421068 | 2,10994E-16 |
| 83 | ENSG00000153902 | *LGI4* | -3,51232754 | 3,15534E-17 |
| 84 | ENSG00000171840 | *NINJ2* | -3,504266385 | 7,03623E-41 |
| 85 | ENSG00000103811 | *CTSH* | -3,489508845 | 5,69629E-62 |
| 86 | ENSG00000221946 | *FXYD7* | -3,4807093 | 5,42584E-18 |
| 87 | ENSG00000049540 | *ELN* | -3,479404015 | 0 |
| 88 | ENSG00000187398 | *LUZP2* | -3,47747786 | 1,1191E-112 |
| 89 | ENSG00000177570 | *SAMD12* | -3,47563295 | 3,50821E-14 |
| 90 | ENSG00000163235 | *TGFA* | -3,469717146 | 2,0147E-201 |
| 91 | ENSG00000186369 | *LINC00643* | -3,463405987 | 2,98305E-50 |
| 92 | ENSG00000077713 | *SLC25A43* | -3,453521637 | 5,8648E-29 |
| 93 | ENSG00000101204 | *CHRNA4* | -3,452433949 | 4,747E-24 |
| 94 | ENSG00000107249 | *GLIS3* | -3,448146504 | 3,8738E-102 |
| 95 | ENSG00000142449 | *FBN3* | -3,436752085 | 2,74944E-31 |
| 96 | ENSG00000117154 | *IGSF21* | -3,424787741 | 1,93201E-29 |
| 97 | ENSG00000204099 | *NEU4* | -3,406767899 | 1,42759E-71 |
| 98 | ENSG00000166091 | *CMTM5* | -3,399186869 | 9,3634E-176 |
| 99 | ENSG00000109107 | *ALDOC* | -3,397663819 | 1,7575E-233 |
| 100 | ENSG00000205730 | *ITPRIPL2* | -3,392936404 | 2,70296E-54 |
| 101 | ENSG00000174607 | *UGT8* | -3,388858157 | 4,7653E-151 |
| 102 | ENSG00000152049 | *KCNE4* | -3,323438153 | 3,22778E-21 |
| 103 | ENSG00000151364 | *KCTD14* | -3,315768216 | 1,47499E-25 |
| 104 | ENSG00000151876 | *FBXO4* | -3,313933989 | 1,44337E-19 |
| 105 | ENSG00000082684 | *SEMA5B* | -3,296303061 | 9,7142E-252 |
| 106 | ENSG00000197083 | *ZNF300P1* | -3,294065155 | 2,26565E-14 |
| 107 | ENSG00000203805 | *PLPP4* | -3,282412459 | 4,71634E-65 |
| 108 | ENSG00000204291 | *COL15A1* | -3,261996833 | 0 |
| 109 | ENSG00000211445 | *GPX3* | -3,241011427 | 1,13027E-54 |
| 110 | ENSG00000104833 | *TUBB4A* | -3,223666104 | 1,9254E-293 |
| 111 | ENSG00000104205 | *SGK3* | -3,223294935 | 8,05806E-66 |
| 112 | ENSG00000168214 | *RBPJ* | -3,21327966 | 0 |
| 113 | ENSG00000164932 | *CTHRC1* | -3,174625598 | 2,4676E-207 |
| 114 | ENSG00000181997 | *AQP7P2* | -3,155141307 | 6,51891E-15 |
| 115 | ENSG00000172936 | *MYD88* | -3,140966003 | 6,82149E-93 |
| 116 | ENSG00000254896 | *OPCML-IT1* | -3,135476322 | 2,13973E-15 |
| 117 | ENSG00000181458 | *TMEM45A* | -3,12715506 | 8,26785E-60 |
| 118 | ENSG00000115232 | *ITGA4* | -3,120489879 | 2,62741E-69 |
| 119 | ENSG00000178038 | *ALS2CL* | -3,10220772 | 2,18385E-16 |
| 120 | ENSG00000272462 | *U91328.2* | -3,090544325 | 2,45016E-13 |
| 121 | ENSG00000170745 | *KCNS3* | -3,070752405 | 4,90545E-62 |
| 122 | ENSG00000186088 | *GSAP* | -3,070263056 | 3,23258E-17 |
| 123 | ENSG00000116852 | *KIF21B* | -3,059259913 | 3,5696E-103 |
| 124 | ENSG00000158089 | *GALNT14* | -3,055748347 | 3,56663E-14 |
| 125 | ENSG00000145681 | *HAPLN1* | -3,051894425 | 0 |
| 126 | ENSG00000070182 | *SPTB* | -3,041465833 | 9,04188E-44 |
| 127 | ENSG00000173705 | *SUSD5* | -3,0385486 | 1,68157E-46 |
| 128 | ENSG00000107518 | *ATRNL1* | -3,011880544 | 1,6125E-99 |
| 129 | ENSG00000198682 | *PAPSS2* | -3,009755411 | 1,0734E-84 |
| 130 | ENSG00000198028 | *ZNF560* | -3,002373748 | 1,00478E-15 |
| 131 | ENSG00000065361 | *ERBB3* | -3,000898729 | 0 |
| 132 | ENSG00000263753 | *LINC00667* | -2,995983633 | 1,27023E-23 |
| 133 | ENSG00000145365 | *TIFA* | -2,977322923 | 8,08491E-13 |
| 134 | ENSG00000112559 | *MDFI* | -2,975891378 | 3,38344E-81 |
| 135 | ENSG00000197943 | *PLCG2* | -2,971905258 | 3,95597E-10 |
| 136 | ENSG00000262223 | *AC110285.1* | -2,96999267 | 1,27186E-24 |
| 137 | ENSG00000081479 | *LRP2* | -2,967887869 | 1,20666E-41 |
| 138 | ENSG00000174469 | *CNTNAP2* | -2,956436628 | 2,32802E-36 |
| 139 | ENSG00000158008 | *EXTL1* | -2,929240454 | 1,4451E-104 |
| 140 | ENSG00000072182 | *ASIC4* | -2,927041293 | 4,33488E-46 |
| 141 | ENSG00000173482 | *PTPRM* | -2,922669511 | 1,84213E-89 |
| 142 | ENSG00000118596 | *SLC16A7* | -2,881642161 | 3,81087E-11 |
| 143 | ENSG00000154856 | *APCDD1* | -2,87786193 | 1,7391E-274 |
| 144 | ENSG00000168542 | *COL3A1* | -2,872472173 | 1,83144E-21 |
| 145 | ENSG00000091490 | *SEL1L3* | -2,853646384 | 0 |
| 146 | ENSG00000231584 | *FAHD2CP* | -2,845244478 | 3,71431E-09 |
| 147 | ENSG00000135750 | *KCNK1* | -2,833835105 | 2,48714E-21 |
| 148 | ENSG00000103489 | *XYLT1* | -2,829782321 | 6,8017E-217 |
| 149 | ENSG00000169297 | *NR0B1* | -2,817496117 | 1,4468E-137 |
| 150 | ENSG00000176788 | *BASP1* | -2,805687461 | 5,87742E-22 |
| 151 | ENSG00000169031 | *COL4A3* | -2,788130103 | 5,19249E-11 |

| | | | | |
|---|---|---|---|---|
| 152 | ENSG00000187527 | *ATP13A5* | -2,77615307 | 2,58589E-11 |
| 153 | ENSG00000183960 | *KCNH8* | -2,759741876 | 4,90578E-35 |
| 154 | ENSG00000154764 | *WNT7A* | -2,75136343 | 8,28556E-18 |
| 155 | ENSG00000205809 | *KLRC2* | -2,748200139 | 9,34842E-15 |
| 156 | ENSG00000162849 | *KIF26B* | -2,746453132 | 2,43977E-79 |
| 157 | ENSG00000169891 | *REPS2* | -2,746075751 | 4,6043E-135 |
| 158 | ENSG00000123243 | *ITIH5* | -2,731733609 | 1,44115E-26 |
| 159 | ENSG00000119673 | *ACOT2* | -2,724595128 | 3,18627E-18 |
| 160 | ENSG00000245060 | *LINC00847* | -2,723045762 | 6,91699E-10 |
| 161 | ENSG00000058866 | *DGKG* | -2,718324513 | 7,56966E-51 |
| 162 | ENSG00000241186 | *TDGF1* | -2,710470671 | 2,41039E-08 |
| 163 | ENSG00000001561 | *ENPP4* | -2,706295338 | 9,21165E-63 |
| 164 | ENSG00000226479 | *TMEM185B* | -2,686865833 | 5,34697E-09 |
| 165 | ENSG00000164181 | *ELOVL7* | -2,676304226 | 9,48044E-15 |
| 166 | ENSG00000112309 | *B3GAT2* | -2,656519988 | 4,54246E-16 |
| 167 | ENSG00000243902 | *ELFN2* | -2,654502832 | 2,29357E-09 |
| 168 | ENSG00000187837 | *HIST1H1C* | -2,652474674 | 5,0082E-152 |
| 169 | ENSG00000106868 | *SUSD1* | -2,632982032 | 3,34973E-35 |
| 170 | ENSG00000198417 | *MT1F* | -2,630569348 | 2,41327E-10 |
| 171 | ENSG00000183549 | *ACSM5* | -2,628054183 | 8,89213E-08 |
| 172 | ENSG00000147257 | *GPC3* | -2,622129911 | 1,17051E-20 |
| 173 | ENSG00000171033 | *PKIA* | -2,61085775 | 2,3194E-101 |
| 174 | ENSG00000181585 | *TMIE* | -2,610246106 | 2,23713E-23 |
| 175 | ENSG00000172348 | *RCAN2* | -2,607007135 | 3,5027E-16 |
| 176 | ENSG00000189058 | *APOD* | -2,604236944 | 0 |
| 177 | ENSG00000183508 | *FAM46C* | -2,587830673 | 9,46421E-32 |
| 178 | ENSG00000157734 | *SNX22* | -2,579038603 | 8,3775E-257 |
| 179 | ENSG00000138613 | *APH1B* | -2,575541455 | 3,16359E-22 |
| 180 | ENSG00000112379 | *ARFGEF3* | -2,574819189 | 2,7957E-173 |
| 181 | ENSG00000255571 | *MIR9-3HG* | -2,569654949 | 4,34276E-33 |
| 182 | ENSG00000137809 | *ITGA11* | -2,55530653 | 2,55243E-41 |
| 183 | ENSG00000188452 | *CERKL* | -2,547277662 | 6,89564E-18 |
| 184 | ENSG00000120756 | *PLS1* | -2,545494977 | 1,21725E-29 |
| 185 | ENSG00000155974 | *GRIP1* | -2,544286728 | 1,49288E-12 |
| 186 | ENSG00000220785 | *MTMR9LP* | -2,53729554 | 2,85889E-52 |
| 187 | ENSG00000246273 | *SBF2-AS1* | -2,53530746 | 2,35396E-07 |
| 188 | ENSG00000081052 | *COL4A4* | -2,531305307 | 9,80378E-17 |
| 189 | ENSG00000154654 | *NCAM2* | -2,523774871 | 2,1098E-118 |
| 190 | ENSG00000130958 | *SLC35D2* | -2,522438191 | 1,09585E-10 |
| 191 | ENSG00000100399 | *CHADL* | -2,521352783 | 9,38359E-51 |
| 192 | ENSG00000158258 | *CLSTN2* | -2,518411457 | 2,10847E-28 |
| 193 | ENSG00000187123 | *LYPD6* | -2,511859417 | 6,13388E-94 |
| 194 | ENSG00000180818 | *HOXC10* | -2,501615403 | 2,54602E-07 |
| 195 | ENSG00000162552 | *WNT4* | -2,497343024 | 2,83342E-09 |
| 196 | ENSG00000196132 | *MYT1* | -2,496795052 | 9,1392E-123 |
| 197 | ENSG00000101605 | *MYOM1* | -2,496097632 | 1,97472E-12 |
| 198 | ENSG00000186466 | *AQP7P1* | -2,491554863 | 5,44795E-36 |
| 199 | ENSG00000145824 | *CXCL14* | -2,491281835 | 1,70763E-26 |
| 200 | ENSG00000153132 | *CLGN* | -2,490494023 | 8,3196E-44 |
| 201 | ENSG00000134853 | *PDGFRA* | -2,486863084 | 0 |
| 202 | ENSG00000123612 | *ACVR1C* | -2,482958065 | 1,19395E-06 |
| 203 | ENSG00000204624 | *DISP3* | -2,479922215 | 3,4784E-58 |
| 204 | ENSG00000072133 | *RPS6KA6* | -2,476969781 | 1,52441E-06 |
| 205 | ENSG00000176595 | *KBTBD11* | -2,474426009 | 1,38464E-54 |
| 206 | ENSG00000141639 | *MAPK4* | -2,472603933 | 2,01497E-95 |
| 207 | ENSG00000157766 | *ACAN* | -2,472005294 | 1,0455E-241 |
| 208 | ENSG00000136153 | *LMO7* | -2,468909448 | 7,30961E-59 |
| 209 | ENSG00000126005 | *MMP24-AS1* | -2,464672974 | 4,3375E-19 |
| 210 | ENSG00000101638 | *ST8SIA5* | -2,464647895 | 1,55698E-17 |
| 211 | ENSG00000231995 | *AL590399.4* | -2,462814105 | 2,38905E-21 |
| 212 | ENSG00000065609 | *SNAP91* | -2,46063687 | 1,66581E-13 |
| 213 | ENSG00000141431 | *ASXL3* | -2,45043073 | 1,38742E-12 |
| 214 | ENSG00000070214 | *SLC44A1* | -2,444318585 | 0 |
| 215 | ENSG00000255745 | *AC023796.1* | -2,442798115 | 1,66019E-07 |
| 216 | ENSG00000099810 | *MTAP* | -2,440239427 | 2,1234E-53 |
| 217 | ENSG00000118322 | *ATP10B* | -2,437980045 | 1,1054E-123 |
| 218 | ENSG00000136205 | *TNS3* | -2,424931227 | 2,7226E-193 |
| 219 | ENSG00000116985 | *BMP8B* | -2,419904428 | 7,94246E-36 |
| 220 | ENSG00000159871 | *LYPD5* | -2,418480788 | 1,16989E-12 |
| 221 | ENSG00000187135 | *VSTM2B* | -2,414193204 | 1,13244E-37 |
| 222 | ENSG00000053900 | *ANAPC4* | -2,409677163 | 3,6553E-157 |
| 223 | ENSG00000248485 | *PCP4L1* | -2,406000669 | 9,80226E-09 |
| 224 | ENSG00000082482 | *KCNK2* | -2,404323754 | 7,85592E-25 |
| 225 | ENSG00000183117 | *CSMD1* | -2,402058726 | 1,00365E-08 |
| 226 | ENSG00000168481 | *LGI3* | -2,397541205 | 8,08813E-24 |
| 227 | ENSG00000187994 | *RINL* | -2,396914365 | 3,44908E-17 |
| 228 | ENSG00000103089 | *FA2H* | -2,395623171 | 2,51669E-29 |
| 229 | ENSG00000165078 | *CPA6* | -2,393229827 | 3,49682E-06 |

| | | | | |
|---|---|---|---|---|
| 230 | ENSG00000253250 | *C8orf88* | -2,380790003 | 8,85368E-07 |
| 231 | ENSG00000124920 | *MYRF* | -2,375582634 | 4,8573E-156 |
| 232 | ENSG00000183196 | *CHST6* | -2,363669971 | 2,9403E-25 |
| 233 | ENSG00000002746 | *HECW1* | -2,362475868 | 2,5884E-14 |
| 234 | ENSG00000244752 | *CRYBB2* | -2,362258021 | 1,19304E-06 |
| 235 | ENSG00000237457 | *LINC01351* | -2,361164937 | 7,92316E-08 |
| 236 | ENSG00000150244 | *TRIM48* | -2,356047829 | 2,57674E-07 |
| 237 | ENSG00000197594 | *ENPP1* | -2,350432443 | 7,97893E-46 |
| 238 | ENSG00000264186 | *SNRPCP4* | -2,348411686 | 1,96923E-06 |
| 239 | ENSG00000184613 | *NELL2* | -2,347103137 | 8,30228E-13 |
| 240 | ENSG00000168675 | *LDLRAD4* | -2,344531036 | 1,36509E-48 |
| 241 | ENSG00000131668 | *BARX1* | -2,335833408 | 2,0424E-23 |
| 242 | ENSG00000077063 | *CTTNBP2* | -2,32845408 | 2,8166E-111 |
| 243 | ENSG00000187546 | *AGMO* | -2,327366305 | 4,16903E-09 |
| 244 | ENSG00000165966 | *PDZRN4* | -2,322767878 | 7,83787E-09 |
| 245 | ENSG00000178026 | *LRRC75B* | -2,322178069 | 5,68768E-11 |
| 246 | ENSG00000120696 | *KBTBD7* | -2,318234951 | 1,12284E-31 |
| 247 | ENSG00000250317 | *SMIM20* | -2,31624485 | 3,5471E-151 |
| 248 | ENSG00000018625 | *ATP1A2* | -2,311245568 | 1,76301E-73 |
| 249 | ENSG00000178538 | *CA8* | -2,308381171 | 1,52337E-46 |
| 250 | ENSG00000150551 | *LYPD1* | -2,301814574 | 3,18797E-37 |
| 251 | ENSG00000038210 | *PI4K2B* | -2,295939698 | 4,2378E-173 |
| 252 | ENSG00000115896 | *PLCL1* | -2,290898413 | 6,56618E-09 |
| 253 | ENSG00000188620 | *HMX3* | -2,281201517 | 5,72472E-07 |
| 254 | ENSG00000188906 | *LRRK2* | -2,276041119 | 2,5254E-274 |
| 255 | ENSG00000249799 | *SNRPCP13* | -2,27498194 | 1,67144E-05 |
| 256 | ENSG00000198331 | *HYLS1* | -2,272227113 | 1,84717E-06 |
| 257 | ENSG00000101542 | *CDH20* | -2,265242722 | 1,73823E-14 |
| 258 | ENSG00000138670 | *RASGEF1B* | -2,264647132 | 4,26798E-18 |
| 259 | ENSG00000164659 | *KIAA1324L* | -2,262598673 | 1,97169E-11 |
| 260 | ENSG00000169071 | *ROR2* | -2,260816392 | 1,2196E-09 |
| 261 | ENSG00000167034 | *NKX3-1* | -2,252403982 | 5,88821E-22 |
| 262 | ENSG00000119283 | *TRIM67* | -2,251908388 | 1,10346E-08 |
| 263 | ENSG00000128709 | *HOXD9* | -2,247473001 | 2,6293E-23 |
| 264 | ENSG00000126947 | *ARMCX1* | -2,246993452 | 3,53478E-17 |
| 265 | ENSG00000146197 | *SCUBE3* | -2,246766383 | 5,35507E-85 |
| 266 | ENSG00000158373 | *HIST1H2BD* | -2,246383855 | 8,47359E-18 |
| 267 | ENSG00000116544 | *DLGAP3* | -2,244984561 | 2,01423E-14 |
| 268 | ENSG00000137968 | *SLC44A5* | -2,242606279 | 2,56105E-42 |
| 269 | ENSG00000125820 | *NKX2-2* | -2,242202164 | 1,05843E-94 |
| 270 | ENSG00000131196 | *NFATC1* | -2,23599072 | 5,48545E-74 |
| 271 | ENSG00000136297 | *MMD2* | -2,226540772 | 1,6867E-11 |
| 272 | ENSG00000177932 | *ZNF354C* | -2,219892159 | 1,23752E-11 |
| 273 | ENSG00000153234 | *NR4A2* | -2,218675793 | 5,57295E-37 |
| 274 | ENSG00000151376 | *ME3* | -2,217032538 | 2,71913E-35 |
| 275 | ENSG00000170965 | *PLAC1* | -2,211930654 | 2,19762E-08 |
| 276 | ENSG00000261786 | *AC006058.1* | -2,211574325 | 1,7215E-122 |
| 277 | ENSG00000162755 | *KLHDC9* | -2,20598151 | 2,21216E-05 |
| 278 | ENSG00000168228 | *ZCCHC4* | -2,205570379 | 7,0499E-66 |
| 279 | ENSG00000151692 | *RNF144A* | -2,198961472 | 1,9915E-268 |
| 280 | ENSG00000050030 | *KIAA2022* | -2,197742281 | 3,9896E-34 |
| 281 | ENSG00000223749 | *MIR503HG* | -2,191073811 | 1,71457E-75 |
| 282 | ENSG00000266709 | *AC005224.4* | -2,188779648 | 2,74257E-06 |
| 283 | ENSG00000164122 | *ASB5* | -2,17081651 | 2,98807E-05 |
| 284 | ENSG00000064787 | *BCAS1* | -2,169857078 | 3,10409E-06 |
| 285 | ENSG00000124657 | *OR2B6* | -2,165487977 | 2,10915E-05 |
| 286 | ENSG00000198597 | *ZNF536* | -2,159128426 | 5,25832E-05 |
| 287 | ENSG00000168453 | *HR* | -2,15440813 | 1,3778E-103 |
| 288 | ENSG00000154175 | *ABI3BP* | -2,151254814 | 3,43121E-13 |
| 289 | ENSG00000238113 | *LINC01410* | -2,150277063 | 2,14564E-05 |
| 290 | ENSG00000225968 | *ELFN1* | -2,145629498 | 2,00458E-20 |
| 291 | ENSG00000158406 | *HIST1H4H* | -2,129255276 | 3,85016E-11 |
| 292 | ENSG00000089041 | *P2RX7* | -2,12739205 | 2,0153E-242 |
| 293 | ENSG00000132199 | *ENOSF1* | -2,125916076 | 7,56134E-31 |
| 294 | ENSG00000134716 | *CYP2J2* | -2,122872981 | 2,27053E-14 |
| 295 | ENSG00000170624 | *SGCD* | -2,121261942 | 7,16552E-81 |
| 296 | ENSG00000264515 | *AC011474.1* | -2,116773946 | 1,5796E-06 |
| 297 | ENSG00000183780 | *SLC35F3* | -2,115808523 | 1,03071E-07 |
| 298 | ENSG00000168539 | *CHRM1* | -2,107403907 | 8,18146E-15 |
| 299 | ENSG00000091513 | *TF* | -2,104757521 | 3,02137E-29 |
| 300 | ENSG00000164007 | *CLDN19* | -2,103745853 | 7,77045E-05 |
| 301 | ENSG00000169840 | *GSX1* | -2,103455405 | 6,54775E-15 |
| 302 | ENSG00000136237 | *RAPGEF5* | -2,103089442 | 5,31013E-11 |
| 303 | ENSG00000134996 | *OSTF1* | -2,099747743 | 5,63217E-19 |
| 304 | ENSG00000013016 | *EHD3* | -2,094198585 | 2,597E-148 |
| 305 | ENSG00000251350 | *LINC02475* | -2,090389521 | 6,04657E-05 |
| 306 | ENSG00000141655 | *TNFRSF11A* | -2,087693427 | 8,13906E-05 |
| 307 | ENSG00000119698 | *PPP4R4* | -2,085831072 | 5,41073E-07 |

| | | | | |
|---|---|---|---|---|
| 308 | ENSG00000164241 | *C5orf63* | -2,075822062 | 3,30475E-06 |
| 309 | ENSG00000169181 | *GSG1L* | -2,07031411 | 1,22089E-10 |
| 310 | ENSG00000249577 | *AC010424.1* | -2,068958376 | 2,02106E-05 |
| 311 | ENSG00000152402 | *GUCY1A2* | -2,068848122 | 4,01952E-30 |
| 312 | ENSG00000100628 | *ASB2* | -2,068279131 | 7,80666E-07 |
| 313 | ENSG00000184347 | *SLIT3* | -2,059081067 | 2,42549E-06 |
| 314 | ENSG00000183018 | *SPNS2* | -2,056677421 | 6,11472E-10 |
| 315 | ENSG00000224272 | *AC131097.3* | -2,054337819 | 2,975E-09 |
| 316 | ENSG00000221887 | *HMSD* | -2,054328008 | 4,50983E-08 |
| 317 | ENSG00000272079 | *AC004233.3* | -2,052490854 | 8,41716E-06 |
| 318 | ENSG00000261195 | *AC027130.1* | -2,05108171 | 2,79021E-05 |
| 319 | ENSG00000102760 | *RGCC* | -2,050926899 | 3,21455E-21 |
| 320 | ENSG00000137801 | *THBS1* | -2,04384977 | 1,70905E-23 |
| 321 | ENSG00000235098 | *ANKRD65* | -2,036601791 | 3,88222E-12 |
| 322 | ENSG00000198732 | *SMOC1* | -2,034991756 | 1,9915E-268 |
| 323 | ENSG00000144339 | *TMEFF2* | -2,034507047 | 3,54879E-28 |
| 324 | ENSG00000169783 | *LINGO1* | -2,033298924 | 1,1276E-153 |
| 325 | ENSG00000114480 | *GBE1* | -2,032887097 | 4,78954E-36 |
| 326 | ENSG00000240005 | *AC106047.1* | -2,018194667 | 4,45992E-07 |
| 327 | ENSG00000148219 | *ASTN2* | -2,008827636 | 7,34165E-67 |
| 328 | ENSG00000187210 | *GCNT1* | -2,004434994 | 2,24081E-06 |
| 329 | ENSG00000186684 | *CYP27C1* | -2,003500648 | 5,17557E-13 |
| 330 | ENSG00000259985 | *AC017100.1* | -1,999963932 | 3,52542E-16 |
| 331 | ENSG00000265194 | *AL359922.2* | -1,996610383 | 2,61996E-05 |
| 332 | ENSG00000184905 | *TCEAL2* | -1,99107011 | 0,000158639 |
| 333 | ENSG00000106733 | *NMRK1* | -1,991043007 | 3,43487E-13 |
| 334 | ENSG00000067798 | *NAV3* | -1,989412433 | 4,67746E-06 |
| 335 | ENSG00000104332 | *SFRP1* | -1,987309168 | 3,6304E-152 |
| 336 | ENSG00000115239 | *ASB3* | -1,978191705 | 2,13568E-11 |
| 337 | ENSG00000160801 | *PTH1R* | -1,970374196 | 6,34104E-10 |
| 338 | ENSG00000123388 | *HOXC11* | -1,969374497 | 4,85391E-06 |
| 339 | ENSG00000124635 | *HIST1H2BJ* | -1,969175771 | 2,07585E-07 |
| 340 | ENSG00000140332 | *TLE3* | -1,968159499 | 5,59286E-44 |
| 341 | ENSG00000152990 | *ADGRA3* | -1,965738855 | 6,2783E-195 |
| 342 | ENSG00000223812 | *AC125608.1* | -1,963535114 | 5,16664E-08 |
| 343 | ENSG00000109618 | *SEPSECS* | -1,963377532 | 3,50023E-90 |
| 344 | ENSG00000123560 | *PLP1* | -1,959538094 | 7,6875E-261 |
| 345 | ENSG00000173406 | *DAB1* | -1,958087448 | 2,09273E-66 |
| 346 | ENSG00000133216 | *EPHB2* | -1,956215961 | 2,27769E-32 |
| 347 | ENSG00000132692 | *BCAN* | -1,953955417 | 0 |
| 348 | ENSG00000254139 | *AC104051.2* | -1,951360874 | 1,03467E-19 |
| 349 | ENSG00000116147 | *TNR* | -1,950905733 | 6,1025E-245 |
| 350 | ENSG00000197705 | *KLHL14* | -1,949453388 | 1,414E-07 |
| 351 | ENSG00000214999 | *AC129492.1* | -1,943362672 | 7,70631E-05 |
| 352 | ENSG00000232239 | *RBPJP5* | -1,94152415 | 2,3184E-06 |
| 353 | ENSG00000151287 | *TEX30* | -1,936329024 | 5,88768E-12 |
| 354 | ENSG00000140522 | *RLBP1* | -1,9362882 | 2,5272E-86 |
| 355 | ENSG00000166206 | *GABRB3* | -1,930011113 | 2,34099E-64 |
| 356 | ENSG00000272512 | *AL645608.8* | -1,925065749 | 7,37798E-10 |
| 357 | ENSG00000068903 | *SIRT2* | -1,924377565 | 1,0324E-231 |
| 358 | ENSG00000112394 | *SLC16A10* | -1,921232325 | 1,55852E-07 |
| 359 | ENSG00000128710 | *HOXD10* | -1,9183883 | 2,0373E-45 |
| 360 | ENSG00000180596 | *HIST1H2BC* | -1,915229008 | 8,24167E-09 |
| 361 | ENSG00000205810 | *KLRC3* | -1,909210965 | 4,90009E-06 |
| 362 | ENSG00000113763 | *UNC5A* | -1,900388529 | 2,10798E-12 |
| 363 | ENSG00000175352 | *NRIP3* | -1,891300765 | 6,78512E-77 |
| 364 | ENSG00000167995 | *BEST1* | -1,889283513 | 2,7907E-35 |
| 365 | ENSG00000118160 | *SLC8A2* | -1,882229416 | 1,54635E-05 |
| 366 | ENSG00000128713 | *HOXD11* | -1,880424793 | 1,88764E-15 |
| 367 | ENSG00000181409 | *AATK* | -1,877871534 | 7,82626E-30 |
| 368 | ENSG00000145794 | *MEGF10* | -1,871635802 | 9,75194E-90 |
| 369 | ENSG00000158270 | *COLEC12* | -1,861919438 | 5,76648E-13 |
| 370 | ENSG00000170962 | *PDGFD* | -1,853327611 | 0,000627464 |
| 371 | ENSG00000101188 | *NTSR1* | -1,852538 | 0,000493312 |
| 372 | ENSG00000134376 | *CRB1* | -1,852379761 | 6,41037E-32 |
| 373 | ENSG00000165443 | *PHYHIPL* | -1,851353662 | 8,75604E-31 |
| 374 | ENSG00000153071 | *DAB2* | -1,846805495 | 6,95397E-07 |
| 375 | ENSG00000128594 | *LRRC4* | -1,842893554 | 3,1468E-43 |
| 376 | ENSG00000143867 | *OSR1* | -1,837988299 | 2,88766E-84 |
| 377 | ENSG00000186479 | *RGS7BP* | -1,836715243 | 9,47307E-07 |
| 378 | ENSG00000186472 | *PCLO* | -1,834865782 | 1,28326E-06 |
| 379 | ENSG00000176641 | *RNF152* | -1,827800376 | 6,37088E-20 |
| 380 | ENSG00000175785 | *PRIMA1* | -1,826742614 | 6,59128E-06 |
| 381 | ENSG00000187773 | *FAM69C* | -1,800020556 | 6,24577E-54 |
| 382 | ENSG00000107736 | *CDH23* | -1,798722619 | 9,75999E-17 |
| 383 | ENSG00000260398 | *AC068700.1* | -1,789924906 | 0,000519386 |
| 384 | ENSG00000259417 | *LINC01314* | -1,783023951 | 8,22262E-27 |
| 385 | ENSG00000152192 | *POU4F1* | -1,780366138 | 4,24041E-13 |

| 386 | ENSG00000188848 | *BEND4* | -1,772740654 | 0,001220579 |
|---|---|---|---|---|
| 387 | ENSG00000104324 | *CPQ* | -1,770129518 | 0,001048912 |
| 388 | ENSG00000183542 | *KLRC4* | -1,768557977 | 0,001265058 |
| 389 | ENSG00000197816 | *CCDC180* | -1,768332762 | 0,000380542 |
| 390 | ENSG00000141622 | *RNF165* | -1,767643695 | 3,25505E-43 |
| 391 | ENSG00000115194 | *SLC30A3* | -1,766002348 | 3,37898E-28 |
| 392 | ENSG00000187323 | *DCC* | -1,7656766 | 9,3388E-42 |
| 393 | ENSG00000137393 | *RNF144B* | -1,761437465 | 5,14042E-07 |
| 394 | ENSG00000171757 | *LRRC34* | -1,760618358 | 0,00036284 |
| 395 | ENSG00000163362 | *C1orf106* | -1,755394374 | 2,06106E-40 |
| 396 | ENSG00000154822 | *PLCL2* | -1,754017089 | 2,08248E-19 |
| 397 | ENSG00000240184 | *PCDHGC3* | -1,753742352 | 2,64892E-07 |
| 398 | ENSG00000133067 | *LGR6* | -1,752046357 | 0,00086357 |
| 399 | ENSG00000143443 | *C1orf56* | -1,747905988 | 2,94061E-11 |
| 400 | ENSG00000160678 | *S100A1* | -1,744589492 | 1,07592E-09 |
| 401 | ENSG00000198598 | *MMP17* | -1,743451778 | 2,09941E-31 |
| 402 | ENSG00000136842 | *TMOD1* | -1,739782601 | 2,77764E-43 |
| 403 | ENSG00000150594 | *ADRA2A* | -1,738369623 | 0,000680292 |
| 404 | ENSG00000259218 | *LINC00928* | -1,738144527 | 8,23108E-05 |
| 405 | ENSG00000162614 | *NEXN* | -1,737760761 | 2,41664E-09 |
| 406 | ENSG00000198208 | *RPS6KL1* | -1,736025772 | 2,71035E-24 |
| 407 | ENSG00000118276 | *B4GALT6* | -1,732462757 | 5,49121E-66 |
| 408 | ENSG00000205592 | *MUC19* | -1,730761319 | 0,001733013 |
| 409 | ENSG00000114019 | *AMOTL2* | -1,7305732 | 1,6474E-124 |
| 410 | ENSG00000213222 | *AC093724.1* | -1,728569473 | 7,82488E-12 |
| 411 | ENSG00000182022 | *CHST15* | -1,724956122 | 5,05805E-08 |
| 412 | ENSG00000137571 | *SLCO5A1* | -1,720233245 | 3,55352E-12 |
| 413 | ENSG00000090932 | *DLL3* | -1,720148524 | 1,5026E-146 |
| 414 | ENSG00000001626 | *CFTR* | -1,718937385 | 0,000385615 |
| 415 | ENSG00000139915 | *MDGA2* | -1,71892529 | 1,44085E-12 |
| 416 | ENSG00000145779 | *TNFAIP8* | -1,718073674 | 6,88673E-11 |
| 417 | ENSG00000164938 | *TP53INP1* | -1,711530574 | 2,57492E-26 |
| 418 | ENSG00000132669 | *RIN2* | -1,707816867 | 2,66406E-45 |
| 419 | ENSG00000197927 | *C2orf27A* | -1,704478415 | 1,02564E-22 |
| 420 | ENSG00000163923 | *RPL39L* | -1,701520473 | 6,37312E-20 |
| 421 | ENSG00000183873 | *SCN5A* | -1,688164246 | 1,42705E-09 |
| 422 | ENSG00000188486 | *H2AFX* | -1,6863056 | 1,3617E-171 |
| 423 | ENSG00000235903 | *CPB2-AS1* | -1,683721195 | 0,000643735 |
| 424 | ENSG00000065809 | *FAM107B* | -1,68059948 | 3,17282E-73 |
| 425 | ENSG00000182109 | *AL365277.1* | -1,677982487 | 0,000263852 |
| 426 | ENSG00000264575 | *LINC00526* | -1,674467641 | 0,00185732 |
| 427 | ENSG00000259953 | *AL138756.1* | -1,674466163 | 0,000534664 |
| 428 | ENSG00000154975 | *CA10* | -1,671794861 | 1,6561E-128 |
| 429 | ENSG00000136859 | *ANGPTL2* | -1,67173431 | 2,6093E-146 |
| 430 | ENSG00000121440 | *PDZRN3* | -1,671260001 | 4,67069E-62 |
| 431 | ENSG00000071991 | *CDH19* | -1,667896426 | 0,002728276 |
| 432 | ENSG00000185477 | *GPRIN3* | -1,665030455 | 0,001039624 |
| 433 | ENSG00000261478 | *AC013391.3* | -1,661039166 | 2,6351E-06 |
| 434 | ENSG00000127955 | *GNAI1* | -1,660438351 | 2,50442E-62 |
| 435 | ENSG00000013293 | *SLC7A14* | -1,659464393 | 0,002384919 |
| 436 | ENSG00000176438 | *SYNE3* | -1,658966508 | 4,94449E-06 |
| 437 | ENSG00000166342 | *NETO1* | -1,65835722 | 2,37556E-26 |
| 438 | ENSG00000101665 | *SMAD7* | -1,65434049 | 4,83022E-12 |
| 439 | ENSG00000118513 | *MYB* | -1,647373926 | 1,08452E-08 |
| 440 | ENSG00000088970 | *KIZ* | -1,642621927 | 6,94185E-72 |
| 441 | ENSG00000218739 | *CEBPZOS* | -1,642471933 | 8,13151E-34 |
| 442 | ENSG00000168234 | *TTC39C* | -1,642046489 | 5,19737E-57 |
| 443 | ENSG00000164398 | *ACSL6* | -1,639659622 | 9,7943E-23 |
| 444 | ENSG00000142611 | *PRDM16* | -1,639296991 | 0,000125677 |
| 445 | ENSG00000148053 | *NTRK2* | -1,638417661 | 2,6247E-216 |
| 446 | ENSG00000012171 | *SEMA3B* | -1,638034157 | 3,32768E-71 |
| 447 | ENSG00000037280 | *FLT4* | -1,63196704 | 0,000100372 |
| 448 | ENSG00000197965 | *MPZL1* | -1,629238041 | 3,0664E-151 |
| 449 | ENSG00000162630 | *B3GALT2* | -1,625608189 | 7,45501E-07 |
| 450 | ENSG00000106477 | *CEP41* | -1,622612267 | 3,35349E-31 |
| 451 | ENSG00000226508 | *LINC01918* | -1,622435152 | 8,78443E-05 |
| 452 | ENSG00000187098 | *MITF* | -1,622010468 | 1,5892E-35 |
| 453 | ENSG00000246528 | *AC079089.1* | -1,617207777 | 0,000640832 |
| 454 | ENSG00000196421 | *C20orf204* | -1,615192349 | 0,000933454 |
| 455 | ENSG00000161048 | *NAPEPLD* | -1,612845634 | 1,69673E-25 |
| 456 | ENSG00000164125 | *FAM198B* | -1,607233762 | 1,93206E-05 |
| 457 | ENSG00000116254 | *CHD5* | -1,606037651 | 2,31691E-06 |
| 458 | ENSG00000182010 | *RTKN2* | -1,601767297 | 8,51797E-38 |
| 459 | ENSG00000253159 | *PCDHGA12* | -1,600800851 | 2,82913E-39 |
| 460 | ENSG00000226380 | *AC016831.1* | -1,597968731 | 0,000111985 |
| 461 | ENSG00000073861 | *TBX21* | -1,595296356 | 1,90719E-06 |
| 462 | ENSG00000139364 | *TMEM132B* | -1,59495964 | 4,01077E-54 |
| 463 | ENSG00000171714 | *ANO5* | -1,593903809 | 6,51963E-28 |

| 464 | ENSG00000015568 | *RGPD5* | -1,59355909 | 2,65102E-06 |
|---|---|---|---|---|
| 465 | ENSG00000005513 | *SOX8* | -1,586519492 | 4,4986E-180 |
| 466 | ENSG00000127084 | *FGD3* | -1,585866741 | 8,19933E-15 |
| 467 | ENSG00000137177 | *KIF13A* | -1,580514879 | 3,17078E-97 |
| 468 | ENSG00000179477 | *ALOX12B* | -1,580012754 | 0,00389115 |
| 469 | ENSG00000144366 | *GULP1* | -1,57709165 | 7,54511E-05 |
| 470 | ENSG00000127152 | *BCL11B* | -1,576399435 | 0,003748708 |
| 471 | ENSG00000176746 | *MAGEB6* | -1,575391654 | 0,004351083 |
| 472 | ENSG00000164050 | *PLXNB1* | -1,573138827 | 5,2753E-155 |
| 473 | ENSG00000117791 | *MARC2* | -1,572142335 | 0,003308242 |
| 474 | ENSG00000137877 | *SPTBN5* | -1,571193003 | 1,31685E-07 |
| 475 | ENSG00000171368 | *TPPP* | -1,568085183 | 3,66345E-59 |
| 476 | ENSG00000248587 | *GDNF-AS1* | -1,568015164 | 3,32975E-07 |
| 477 | ENSG00000079102 | *RUNX1T1* | -1,56327982 | 6,04507E-14 |
| 478 | ENSG00000089177 | *KIF16B* | -1,560946426 | 3,98708E-08 |
| 479 | ENSG00000116132 | *PRRX1* | -1,560841968 | 7,3962E-106 |
| 480 | ENSG00000036565 | *SLC18A1* | -1,559858489 | 8,52984E-05 |
| 481 | ENSG00000156959 | *LHFPL4* | -1,559466528 | 8,00643E-09 |
| 482 | ENSG00000134775 | *FHOD3* | -1,558102361 | 9,37297E-76 |
| 483 | ENSG00000109255 | *NMU* | -1,5531869 | 7,65731E-10 |
| 484 | ENSG00000241527 | *CA15P1* | -1,54936418 | 0,00360088 |
| 485 | ENSG00000125845 | *BMP2* | -1,541975721 | 4,16434E-17 |
| 486 | ENSG00000144476 | *ACKR3* | -1,541619495 | 4,38928E-40 |
| 487 | ENSG00000267121 | *AC008105.3* | -1,540866159 | 0,000139588 |
| 488 | ENSG00000064989 | *CALCRL* | -1,540637388 | 4,01204E-30 |
| 489 | ENSG00000122971 | *ACADS* | -1,539355615 | 1,30486E-09 |
| 490 | ENSG00000101349 | *PAK5* | -1,537296089 | 0,002010219 |
| 491 | ENSG00000205927 | *OLIG2* | -1,534809201 | 1,0383E-159 |
| 492 | ENSG00000164303 | *ENPP6* | -1,531425357 | 0,00498006 |
| 493 | ENSG00000203472 | *AC009163.1* | -1,528932377 | 0,005882379 |
| 494 | ENSG00000085276 | *MECOM* | -1,526831 | 1,32616E-16 |
| 495 | ENSG00000136943 | *CTSV* | -1,518056305 | 4,55107E-14 |
| 496 | ENSG00000168484 | *SFTPC* | -1,517342938 | 0,002748851 |
| 497 | ENSG00000140368 | *PSTPIP1* | -1,516025553 | 0,006665831 |
| 498 | ENSG00000160179 | *ABCG1* | -1,515547716 | 0,005205002 |
| 499 | ENSG00000124406 | *ATP8A1* | -1,515524587 | 8,59809E-16 |
| 500 | ENSG00000164106 | *SCRG1* | -1,514407396 | 1,12404E-88 |
| 501 | ENSG00000273032 | *DGCR9* | -1,509718289 | 0,000340534 |
| 502 | ENSG00000233822 | *HIST1H2BN* | -1,508822277 | 3,00551E-06 |
| 503 | ENSG00000203814 | *HIST2H2BF* | -1,508524554 | 0,006067574 |
| 504 | ENSG00000250312 | *ZNF718* | -1,508411248 | 8,41716E-06 |
| 505 | ENSG00000197496 | *SLC2A10* | -1,507990881 | 0,003607449 |
| 506 | ENSG00000221716 | *SNORA11* | -1,507192146 | 6,35233E-05 |
| 507 | ENSG00000153162 | *BMP6* | -1,501579551 | 0,005535406 |
| 508 | ENSG00000115159 | *GPD2* | -1,500780883 | 4,23942E-92 |
| 509 | ENSG00000135636 | *DYSF* | -1,496931239 | 4,1235E-18 |
| 510 | ENSG00000073910 | *FRY* | -1,496319661 | 1,41003E-32 |
| 511 | ENSG00000079819 | *EPB41L2* | -1,49589666 | 1,0439E-151 |
| 512 | ENSG00000197903 | *HIST1H2BK* | -1,494702556 | 1,1973E-26 |
| 513 | ENSG00000189221 | *MAOA* | -1,493015921 | 7,79823E-05 |
| 514 | ENSG00000167654 | *ATCAY* | -1,491846979 | 2,1887E-124 |
| 515 | ENSG00000118515 | *SGK1* | -1,488599991 | 5,914E-52 |
| 516 | ENSG00000185664 | *PMEL* | -1,485705916 | 0,00015503 |
| 517 | ENSG00000100311 | *PDGFB* | -1,483889407 | 1,07669E-05 |
| 518 | ENSG00000273297 | *AC009275.1* | -1,483741398 | 0,001043017 |
| 519 | ENSG00000080854 | *IGSF9B* | -1,483655243 | 2,20981E-32 |
| 520 | ENSG00000176402 | *GJC3* | -1,481447981 | 0,003165651 |
| 521 | ENSG00000250039 | *AC096719.1* | -1,480540806 | 0,00884405 |
| 522 | ENSG00000182247 | *UBE2E2* | -1,479353666 | 2,50378E-30 |
| 523 | ENSG00000260423 | *LINC02367* | -1,479343383 | 7,46708E-05 |
| 524 | ENSG00000206077 | *ZDHHC11B* | -1,479271943 | 6,17742E-21 |
| 525 | ENSG00000255864 | *AC069208.1* | -1,475981418 | 0,000284258 |
| 526 | ENSG00000176463 | *SLCO3A1* | -1,475588747 | 4,57903E-29 |
| 527 | ENSG00000092969 | *TGFB2* | -1,475240459 | 0,002646264 |
| 528 | ENSG00000197959 | *DNM3* | -1,475021043 | 3,14015E-64 |
| 529 | ENSG00000105251 | *SHD* | -1,474161258 | 1,34177E-30 |
| 530 | ENSG00000171451 | *DSEL* | -1,472594441 | 7,98231E-74 |
| 531 | ENSG00000175556 | *LONRF3* | -1,472395369 | 0,006111522 |
| 532 | ENSG00000198133 | *TMEM229B* | -1,471657347 | 2,13419E-42 |
| 533 | ENSG00000133878 | *DUSP26* | -1,471437205 | 0,000118532 |
| 534 | ENSG00000124570 | *SERPINB6* | -1,470832235 | 2,11114E-25 |
| 535 | ENSG00000109846 | *CRYAB* | -1,468753897 | 2,45772E-36 |
| 536 | ENSG00000196090 | *PTPRT* | -1,468479436 | 7,27974E-33 |
| 537 | ENSG00000178031 | *ADAMTSL1* | -1,466963264 | 8,87722E-07 |
| 538 | ENSG00000150625 | *GPM6A* | -1,466924974 | 1,1392E-123 |
| 539 | ENSG00000081148 | *IMPG2* | -1,463393284 | 0,006341105 |
| 540 | ENSG00000215612 | *HMX1* | -1,463116858 | 1,82607E-11 |
| 541 | ENSG00000232815 | *DUX4L50* | -1,462646256 | 0,007552872 |

| | | | | |
|---|---|---|---|---|
| 542 | ENSG00000157399 | *ARSE* | -1,461984122 | 2,04405E-12 |
| 543 | ENSG00000248690 | *HAS2-AS1* | -1,461256572 | 2,46135E-05 |
| 544 | ENSG00000109680 | *TBC1D19* | -1,457410051 | 7,55097E-20 |
| 545 | ENSG00000179348 | *GATA2* | -1,456551575 | 6,11792E-07 |
| 546 | ENSG00000104327 | *CALB1* | -1,455151224 | 0,000485544 |
| 547 | ENSG00000167900 | *TK1* | -1,455068311 | 9,92137E-57 |
| 548 | ENSG00000064393 | *HIPK2* | -1,454470221 | 3,8829E-106 |
| 549 | ENSG00000237515 | *SHISA9* | -1,451139665 | 1,29266E-09 |
| 550 | ENSG00000184221 | *OLIG1* | -1,448829604 | 1,456E-141 |
| 551 | ENSG00000196787 | *HIST1H2AG* | -1,446729569 | 6,00316E-05 |
| 552 | ENSG00000184160 | *ADRA2C* | -1,445817549 | 0,001178151 |
| 553 | ENSG00000265579 | *AC023301.1* | -1,444097329 | 2,76491E-08 |
| 554 | ENSG00000105699 | *LSR* | -1,441766176 | 0,00195986 |
| 555 | ENSG00000104388 | *RAB2A* | -1,440958284 | 1,4646E-108 |
| 556 | ENSG00000197409 | *HIST1H3D* | -1,440381961 | 0,006174882 |
| 557 | ENSG00000177103 | *DSCAML1* | -1,440141578 | 1,0467E-11 |
| 558 | ENSG00000117266 | *CDK18* | -1,439609397 | 6,14133E-10 |
| 559 | ENSG00000101417 | *PXMP4* | -1,436010335 | 6,89235E-11 |
| 560 | ENSG00000180573 | *HIST1H2AC* | -1,435852389 | 1,37585E-34 |
| 561 | ENSG00000163376 | *KBTBD8* | -1,433593495 | 6,90438E-08 |
| 562 | ENSG00000213785 | *AKR1B1P3* | -1,433444857 | 0,01157169 |
| 563 | ENSG00000256973 | *AC053513.1* | -1,428517568 | 0,004934465 |
| 564 | ENSG00000184564 | *SLITRK6* | -1,428293804 | 0,011335863 |
| 565 | ENSG00000136099 | *PCDH8* | -1,427957505 | 0,011749634 |
| 566 | ENSG00000131773 | *KHDRBS3* | -1,426995205 | 6,93342E-96 |
| 567 | ENSG00000104490 | *NCALD* | -1,424038368 | 6,78728E-66 |
| 568 | ENSG00000156475 | *PPP2R2B* | -1,420382614 | 5,85882E-81 |
| 569 | ENSG00000145569 | *FAM105A* | -1,420256376 | 9,33548E-07 |
| 570 | ENSG00000169184 | *MN1* | -1,415419422 | 2,66429E-24 |
| 571 | ENSG00000069188 | *SDK2* | -1,415103587 | 1,293E-06 |
| 572 | ENSG00000121690 | *DEPDC7* | -1,414754257 | 2,65657E-08 |
| 573 | ENSG00000162836 | *ACP6* | -1,414126729 | 0,005988542 |
| 574 | ENSG00000215417 | *MIR17HG* | -1,413826337 | 0,001052674 |
| 575 | ENSG00000184260 | *HIST2H2AC* | -1,412499754 | 0,000456989 |
| 576 | ENSG00000173175 | *ADCY5* | -1,411842647 | 3,26621E-18 |
| 577 | ENSG00000126500 | *FLRT1* | -1,410698094 | 2,29513E-08 |
| 578 | ENSG00000109814 | *UGDH* | -1,409970181 | 1,89811E-54 |
| 579 | ENSG00000080986 | *NDC80* | -1,40951151 | 1,44589E-62 |
| 580 | ENSG00000163072 | *NOSTRIN* | -1,408622765 | 0,000582918 |
| 581 | ENSG00000068615 | *REEP1* | -1,407767781 | 6,59386E-27 |
| 582 | ENSG00000254377 | *MIR124-2HG* | -1,407340606 | 2,31877E-05 |
| 583 | ENSG00000163520 | *FBLN2* | -1,406029753 | 0,000160672 |
| 584 | ENSG00000168621 | *GDNF* | -1,404728388 | 0,002428956 |
| 585 | ENSG00000227693 | *GSTM3P1* | -1,40425343 | 8,78216E-11 |
| 586 | ENSG00000148120 | *C9orf3* | -1,403010383 | 4,3684E-24 |
| 587 | ENSG00000136869 | *TLR4* | -1,401888205 | 8,80915E-15 |
| 588 | ENSG00000108384 | *RAD51C* | -1,401642513 | 2,97609E-23 |
| 589 | ENSG00000176136 | *MC5R* | -1,400678067 | 0,00630708 |
| 590 | ENSG00000112414 | *ADGRG6* | -1,400302088 | 1,41763E-29 |
| 591 | ENSG00000172667 | *ZMAT3* | -1,394397456 | 1,67939E-51 |
| 592 | ENSG00000134532 | *SOX5* | -1,394310508 | 1,27076E-69 |
| 593 | ENSG00000154358 | *OBSCN* | -1,393552226 | 7,89771E-05 |
| 594 | ENSG00000229151 | *AC233976.1* | -1,391752369 | 0,014418226 |
| 595 | ENSG00000145416 | *MARCH1* | -1,387204036 | 1,53205E-05 |
| 596 | ENSG00000100842 | *EFS* | -1,386795037 | 1,46275E-66 |
| 597 | ENSG00000154928 | *EPHB1* | -1,385926944 | 9,80911E-32 |
| 598 | ENSG00000137834 | *SMAD6* | -1,384497826 | 1,0361E-10 |
| 599 | ENSG00000175928 | *LRRN1* | -1,384304113 | 8,7107E-108 |
| 600 | ENSG00000086570 | *FAT2* | -1,379288982 | 0,000579823 |
| 601 | ENSG00000219773 | *RPSAP45* | -1,377515442 | 0,001073376 |
| 602 | ENSG00000154493 | *C10orf90* | -1,376079317 | 0,00212644 |
| 603 | ENSG00000140519 | *RHCG* | -1,374039328 | 0,011624842 |
| 604 | ENSG00000170293 | *CMTM8* | -1,374036582 | 4,22557E-06 |
| 605 | ENSG00000141665 | *FBXO15* | -1,371363129 | 0,00192375 |
| 606 | ENSG00000094755 | *GABRP* | -1,371246045 | 0,00845153 |
| 607 | ENSG00000132185 | *FCRLA* | -1,370905889 | 1,07378E-41 |
| 608 | ENSG00000154316 | *TDH* | -1,368852962 | 0,012887978 |
| 609 | ENSG00000005189 | *REXO5* | -1,365116945 | 2,33963E-31 |
| 610 | ENSG00000152661 | *GJA1* | -1,364655411 | 1,10372E-06 |
| 611 | ENSG00000229953 | *AL590666.2* | -1,360798066 | 3,40835E-06 |
| 612 | ENSG00000109686 | *SH3D19* | -1,359626177 | 3,34137E-65 |
| 613 | ENSG00000170162 | *VGLL2* | -1,356503462 | 0,006416161 |
| 614 | ENSG00000101938 | *CHRDL1* | -1,355935559 | 4,1151E-99 |
| 615 | ENSG00000139926 | *FRMD6* | -1,353660841 | 9,15719E-56 |
| 616 | ENSG00000271387 | *AL445228.2* | -1,351052043 | 0,00750068 |
| 617 | ENSG00000134595 | *SOX3* | -1,350926475 | 1,04797E-05 |
| 618 | ENSG00000175445 | *LPL* | -1,349962643 | 1,54105E-68 |
| 619 | ENSG00000256616 | *AP002414.2* | -1,346619454 | 0,00044661 |

| | | | | |
|---|---|---|---|---|
| 620 | ENSG00000106078 | *COBL* | -1,341350824 | 1,74553E-77 |
| 621 | ENSG00000114757 | *PEX5L* | -1,339475545 | 0,003526494 |
| 622 | ENSG00000233846 | *AL133480.2* | -1,338803896 | 0,000461514 |
| 623 | ENSG00000127252 | *HRASLS* | -1,337242313 | 1,64156E-12 |
| 624 | ENSG00000169955 | *ZNF747* | -1,333966574 | 1,22858E-08 |
| 625 | ENSG00000119547 | *ONECUT2* | -1,332879404 | 4,43243E-19 |
| 626 | ENSG00000089225 | *TBX5* | -1,332235429 | 1,65245E-14 |
| 627 | ENSG00000007062 | *PROM1* | -1,331457219 | 2,03899E-16 |
| 628 | ENSG00000072952 | *MRVI1* | -1,330507504 | 0,002009901 |
| 629 | ENSG00000150510 | *FAM124A* | -1,330337957 | 5,71093E-06 |
| 630 | ENSG00000182255 | *KCNA4* | -1,330204296 | 0,003477931 |
| 631 | ENSG00000189212 | *DPY19L2P1* | -1,328903636 | 6,11718E-06 |
| 632 | ENSG00000204446 | *C9orf170* | -1,325675552 | 0,015299373 |
| 633 | ENSG00000142871 | *CYR61* | -1,325080758 | 2,75252E-16 |
| 634 | ENSG00000254221 | *PCDHGB1* | -1,323724383 | 1,34326E-05 |
| 635 | ENSG00000144407 | *PTH2R* | -1,319645668 | 0,020940651 |
| 636 | ENSG00000111199 | *TRPV4* | -1,319546995 | 0,001040236 |
| 637 | ENSG00000169371 | *SNUPN* | -1,317185465 | 6,49573E-11 |
| 638 | ENSG00000096433 | *ITPR3* | -1,312926775 | 3,98838E-37 |
| 639 | ENSG00000100033 | *PRODH* | -1,311480607 | 2,62612E-53 |
| 640 | ENSG00000130720 | *FIBCD1* | -1,311084586 | 5,70008E-06 |
| 641 | ENSG00000125726 | *CD70* | -1,308585928 | 1,74294E-36 |
| 642 | ENSG00000128652 | *HOXD3* | -1,306118337 | 8,09288E-07 |
| 643 | ENSG00000103381 | *CPPED1* | -1,305771775 | 6,53923E-09 |
| 644 | ENSG00000150627 | *WDR17* | -1,304775949 | 4,67262E-14 |
| 645 | ENSG00000237380 | *HOXD-AS2* | -1,304239219 | 0,001555097 |
| 646 | ENSG00000174171 | *AC020659.1* | -1,303850724 | 0,000708783 |
| 647 | ENSG00000146094 | *DOK3* | -1,303287789 | 0,003531103 |
| 648 | ENSG00000101198 | *NKAIN4* | -1,303235202 | 1,31508E-08 |
| 649 | ENSG00000114541 | *FRMD4B* | -1,302845868 | 6,83551E-28 |
| 650 | ENSG00000171766 | *GATM* | -1,301960644 | 0,000174834 |
| 651 | ENSG00000167680 | *SEMA6B* | -1,301639514 | 2,05866E-52 |
| 652 | ENSG00000101746 | *NOL4* | -1,300670112 | 1,93828E-10 |
| 653 | ENSG00000255399 | *TBX5-AS1* | -1,298530552 | 2,08489E-06 |
| 654 | ENSG00000198944 | *SOWAHA* | -1,298356404 | 0,001931529 |
| 655 | ENSG00000198843 | *SELENOT* | -1,298053722 | 5,95669E-80 |
| 656 | ENSG00000100276 | *RASL10A* | -1,298035535 | 0,010095017 |
| 657 | ENSG00000167588 | *GPD1* | -1,297326516 | 0,000659986 |
| 658 | ENSG00000163082 | *SGPP2* | -1,297166173 | 0,009361151 |
| 659 | ENSG00000198585 | *NUDT16* | -1,296365589 | 1,23089E-59 |
| 660 | ENSG00000131386 | *GALNT15* | -1,295656764 | 1,55486E-19 |
| 661 | ENSG00000162944 | *RFTN2* | -1,293496694 | 9,62561E-47 |
| 662 | ENSG00000224597 | *SVIL-AS1* | -1,29285832 | 5,41398E-13 |
| 663 | ENSG00000125898 | *FAM110A* | -1,292680072 | 2,02682E-14 |
| 664 | ENSG00000143816 | *WNT9A* | -1,292524763 | 3,3598E-10 |
| 665 | ENSG00000134594 | *RAB33A* | -1,291706537 | 4,64607E-36 |
| 666 | ENSG00000253764 | *AC019257.1* | -1,289668965 | 0,025181505 |
| 667 | ENSG00000176244 | *ACBD7* | -1,288966531 | 4,82967E-13 |
| 668 | ENSG00000239268 | *AC092691.1* | -1,288594196 | 0,009350167 |
| 669 | ENSG00000134330 | *IAH1* | -1,286712584 | 0,010362155 |
| 670 | ENSG00000251396 | *LINC01301* | -1,286233292 | 1,3937E-09 |
| 671 | ENSG00000124508 | *BTN2A2* | -1,285085175 | 7,25193E-26 |
| 672 | ENSG00000156298 | *TSPAN7* | -1,2849699 | 1,02215E-66 |
| 673 | ENSG00000180269 | *GPR139* | -1,284563138 | 0,005496431 |
| 674 | ENSG00000007968 | *E2F2* | -1,282234647 | 2,37804E-27 |
| 675 | ENSG00000163697 | *APBB2* | -1,27947771 | 1,23991E-71 |
| 676 | ENSG00000231187 | *AL356056.2* | -1,276564668 | 0,014223192 |
| 677 | ENSG00000225472 | *AL136366.1* | -1,275738357 | 8,35733E-05 |
| 678 | ENSG00000149090 | *PAMR1* | -1,275076935 | 1,17351E-05 |
| 679 | ENSG00000156103 | *MMP16* | -1,274961659 | 1,73351E-97 |
| 680 | ENSG00000206199 | *ANKUB1* | -1,274022123 | 0,026811836 |
| 681 | ENSG00000273492 | *AP000229.1* | -1,272696751 | 0,00186509 |
| 682 | ENSG00000145721 | *LIX1* | -1,272300433 | 0,000248735 |
| 683 | ENSG00000176658 | *MYO1D* | -1,27178954 | 0,004934465 |
| 684 | ENSG00000235413 | *KRT18P63* | -1,271713143 | 0,027630593 |
| 685 | ENSG00000138639 | *ARHGAP24* | -1,27090156 | 0,00903145 |
| 686 | ENSG00000151276 | *MAGI1* | -1,269215628 | 2,32341E-73 |
| 687 | ENSG00000196782 | *MAML3* | -1,26910238 | 2,9205E-05 |
| 688 | ENSG00000181218 | *HIST3H2A* | -1,26824481 | 2,93775E-14 |
| 689 | ENSG00000130066 | *SAT1* | -1,267731253 | 2,61028E-91 |
| 690 | ENSG00000176771 | *NCKAP5* | -1,267074497 | 6,88513E-08 |
| 691 | ENSG00000198157 | *HMGN5* | -1,266627501 | 3,63479E-11 |
| 692 | ENSG00000167094 | *TTC16* | -1,265758838 | 0,029038185 |
| 693 | ENSG00000243069 | *ARHGEF26-AS1* | -1,265700965 | 3,42163E-08 |
| 694 | ENSG00000204176 | *SYT15* | -1,265630611 | 0,001071362 |
| 695 | ENSG00000226650 | *KIF4B* | -1,264974006 | 1,99203E-05 |
| 696 | ENSG00000197122 | *SRC* | -1,264726214 | 2,81587E-17 |
| 697 | ENSG00000115112 | *TFCP2L1* | -1,264280933 | 0,022924474 |

| 698 | ENSG00000170153 | *RNF150* | -1,264166777 | 1,00879E-16 |
|---|---|---|---|---|
| 699 | ENSG00000169515 | *CCDC8* | -1,263003236 | 0,010355868 |
| 700 | ENSG00000229585 | *AC110792.1* | -1,258927135 | 0,029051828 |
| 701 | ENSG00000171791 | *BCL2* | -1,257727948 | 1,56204E-25 |
| 702 | ENSG00000176890 | *TYMS* | -1,257421155 | 8,53796E-68 |
| 703 | ENSG00000061938 | *TNK2* | -1,255672155 | 3,43624E-81 |
| 704 | ENSG00000175305 | *CCNE2* | -1,255542613 | 1,20646E-17 |
| 705 | ENSG00000006740 | *ARHGAP44* | -1,255339885 | 0,002064576 |
| 706 | ENSG00000125249 | *RAP2A* | -1,255284105 | 1,16992E-58 |
| 707 | ENSG00000110900 | *TSPAN11* | -1,254578676 | 2,73791E-41 |
| 708 | ENSG00000260249 | *AC007608.3* | -1,252821454 | 0,020914142 |
| 709 | ENSG00000103460 | *TOX3* | -1,250810522 | 1,08295E-22 |
| 710 | ENSG00000157017 | *GHRL* | -1,245673321 | 0,028221191 |
| 711 | ENSG00000064886 | *CHI3L2* | -1,244101322 | 0,029998619 |
| 712 | ENSG00000229589 | *ACVR2B-AS1* | -1,242412955 | 1,10531E-05 |
| 713 | ENSG00000214776 | *AC092821.1* | -1,238467163 | 0,000239445 |
| 714 | ENSG00000222044 | *AL031587.1* | -1,237154907 | 0,026275497 |
| 715 | ENSG00000257337 | *AC068888.1* | -1,236117499 | 6,48583E-15 |
| 716 | ENSG00000104413 | *ESRP1* | -1,23329679 | 0,032333812 |
| 717 | ENSG00000106537 | *TSPAN13* | -1,233136829 | 2,47891E-39 |
| 718 | ENSG00000159899 | *NPR2* | -1,232840292 | 0,000290028 |
| 719 | ENSG00000231407 | *AL354732.1* | -1,232529042 | 0,024000393 |
| 720 | ENSG00000198429 | *ZNF69* | -1,231118553 | 7,904E-11 |
| 721 | ENSG00000101306 | *MYLK2* | -1,23009253 | 0,023952804 |
| 722 | ENSG00000224243 | *LINC00403* | -1,229528555 | 0,033611627 |
| 723 | ENSG00000070761 | *CFAP20* | -1,229440059 | 2,09268E-36 |
| 724 | ENSG00000224376 | *AC017104.1* | -1,224937263 | 3,40112E-08 |
| 725 | ENSG00000153823 | *PID1* | -1,222127904 | 7,00767E-33 |
| 726 | ENSG00000154040 | *CABYR* | -1,221900994 | 0,034820495 |
| 727 | ENSG00000188064 | *WNT7B* | -1,218049089 | 2,5607E-34 |
| 728 | ENSG00000145087 | *STXBP5L* | -1,217329235 | 1,28455E-18 |
| 729 | ENSG00000125780 | *TGM3* | -1,216627726 | 0,015148484 |
| 730 | ENSG00000185774 | *KCNIP4* | -1,216510924 | 0,001000321 |
| 731 | ENSG00000164188 | *RANBP3L* | -1,214921419 | 0,036884888 |
| 732 | ENSG00000171320 | *ESCO2* | -1,214750806 | 1,912E-34 |
| 733 | ENSG00000217275 | *AL031777.1* | -1,214654769 | 0,033611897 |
| 734 | ENSG00000104219 | *ZDHHC2* | -1,211111073 | 7,32517E-51 |
| 735 | ENSG00000188039 | *NWD1* | -1,210177954 | 0,009631937 |
| 736 | ENSG00000151490 | *PTPRO* | -1,210038339 | 3,94436E-24 |
| 737 | ENSG00000120742 | *SERP1* | -1,207722235 | 1,52823E-67 |
| 738 | ENSG00000154118 | *JPH3* | -1,206786175 | 1,04685E-05 |
| 739 | ENSG00000172995 | *ARPP21* | -1,206689601 | 0,000774463 |
| 740 | ENSG00000176678 | *FOXL1* | -1,206463722 | 4,26149E-05 |
| 741 | ENSG00000228623 | *ZNF883* | -1,203896565 | 2,24852E-07 |
| 742 | ENSG00000162951 | *LRRTM1* | -1,201433938 | 0,039951701 |
| 743 | ENSG00000112561 | *TFEB* | -1,195511206 | 2,68605E-15 |
| 744 | ENSG00000247131 | *AC025263.1* | -1,190864821 | 0,041662855 |
| 745 | ENSG00000198759 | *EGFL6* | -1,189937795 | 0,037543029 |
| 746 | ENSG00000187634 | *SAMD11* | -1,189834433 | 1,66808E-07 |
| 747 | ENSG00000099282 | *TSPAN15* | -1,189174226 | 3,01801E-32 |
| 748 | ENSG00000076826 | *CAMSAP3* | -1,187821987 | 1,00008E-10 |
| 749 | ENSG00000206549 | *PRSS50* | -1,186937497 | 0,042135047 |
| 750 | ENSG00000198093 | *ZNF649* | -1,186593519 | 6,60221E-30 |
| 751 | ENSG00000269416 | *LINC01224* | -1,185681816 | 8,22399E-14 |
| 752 | ENSG00000184481 | *FOXO4* | -1,185295715 | 3,46016E-21 |
| 753 | ENSG00000183346 | *C10orf107* | -1,181896246 | 0,043629254 |
| 754 | ENSG00000049089 | *COL9A2* | -1,181008928 | 1,46218E-28 |
| 755 | ENSG00000128714 | *HOXD13* | -1,179538301 | 6,51196E-08 |
| 756 | ENSG00000164116 | *GUCY1A3* | -1,179472048 | 0,001166395 |
| 757 | ENSG00000095261 | *PSMD5* | -1,17896972 | 2,37734E-11 |
| 758 | ENSG00000272086 | *AC025181.2* | -1,178484035 | 0,000595682 |
| 759 | ENSG00000154655 | *L3MBTL4* | -1,178394757 | 5,74421E-06 |
| 760 | ENSG00000171848 | *RRM2* | -1,176390386 | 7,28279E-67 |
| 761 | ENSG00000117148 | *ACTL8* | -1,174433537 | 0,045208248 |
| 762 | ENSG00000123384 | *LRP1* | -1,173364298 | 1,11809E-13 |
| 763 | ENSG00000223461 | *AC004471.1* | -1,172219581 | 0,045052095 |
| 764 | ENSG00000260139 | *CSPG4P13* | -1,172007901 | 0,001844606 |
| 765 | ENSG00000123892 | *RAB38* | -1,171701975 | 9,27993E-09 |
| 766 | ENSG00000174611 | *KY* | -1,170923116 | 0,04242254 |
| 767 | ENSG00000163539 | *CLASP2* | -1,170154562 | 2,29677E-65 |
| 768 | ENSG00000196562 | *SULF2* | -1,169902548 | 9,62562E-35 |
| 769 | ENSG00000124479 | *NDP* | -1,168793329 | 3,14631E-06 |
| 770 | ENSG00000076770 | *MBNL3* | -1,168694167 | 2,62616E-28 |
| 771 | ENSG00000255020 | *AF131216.3* | -1,168265889 | 0,013478287 |
| 772 | ENSG00000196345 | *ZKSCAN7* | -1,167142686 | 3,01071E-05 |
| 773 | ENSG00000267500 | *ZNF887P* | -1,166375175 | 0,005763432 |
| 774 | ENSG00000204682 | *CASC10* | -1,166278586 | 0,00014008 |
| 775 | ENSG00000213398 | *LCAT* | -1,165813011 | 8,09084E-13 |

| | | | | |
|---|---|---|---|---|
| 776 | ENSG00000125637 | *PSD4* | -1,164628572 | 0,002191477 |
| 777 | ENSG00000183248 | *PRR36* | -1,162902842 | 4,62349E-25 |
| 778 | ENSG00000163932 | *PRKCD* | -1,160659479 | 5,11308E-22 |
| 779 | ENSG00000259207 | *ITGB3* | -1,160512123 | 0,003431212 |
| 780 | ENSG00000226752 | *PSMD5-AS1* | -1,159190445 | 3,77196E-10 |
| 781 | ENSG00000264278 | *AC027575.2* | -1,158795046 | 0,02055748 |
| 782 | ENSG00000148773 | *MKI67* | -1,157286277 | 5,17144E-73 |
| 783 | ENSG00000177453 | *NIM1K* | -1,157130157 | 2,48789E-08 |
| 784 | ENSG00000185565 | *LSAMP* | -1,157037895 | 2,91404E-86 |
| 785 | ENSG00000231252 | *AC099792.1* | -1,156801848 | 0,000398612 |
| 786 | ENSG00000106066 | *CPVL* | -1,155975432 | 3,01069E-15 |
| 787 | ENSG00000213621 | *RPSAP54* | -1,155105714 | 0,000143703 |
| 788 | ENSG00000164647 | *STEAP1* | -1,153286525 | 0,034970515 |
| 789 | ENSG00000260572 | *AC069224.1* | -1,151864429 | 0,004360359 |
| 790 | ENSG00000157404 | *KIT* | -1,151174383 | 0,023920424 |
| 791 | ENSG00000245648 | *AC022075.1* | -1,148455457 | 0,003560035 |
| 792 | ENSG00000092068 | *SLC7A8* | -1,147889817 | 0,000990025 |
| 793 | ENSG00000269486 | *AC011455.2* | -1,14666564 | 0,010447043 |
| 794 | ENSG00000120549 | *KIAA1217* | -1,146488727 | 1,21059E-11 |
| 795 | ENSG00000213186 | *TRIM59* | -1,14405017 | 0,002223871 |
| 796 | ENSG00000111405 | *ENDOU* | -1,143951925 | 0,007418186 |
| 797 | ENSG00000148082 | *SHC3* | -1,143681833 | 3,06647E-45 |
| 798 | ENSG00000169122 | *FAM110B* | -1,143019054 | 9,13141E-37 |
| 799 | ENSG00000248890 | *HHIP-AS1* | -1,142846049 | 0,036093117 |
| 800 | ENSG00000170891 | *CYTL1* | -1,142706935 | 1,72028E-05 |
| 801 | ENSG00000133863 | *TEX15* | -1,141244735 | 0,000561814 |
| 802 | ENSG00000048740 | *CELF2* | -1,140802357 | 1,54968E-49 |
| 803 | ENSG00000144278 | *GALNT13* | -1,139882274 | 3,02477E-19 |
| 804 | ENSG00000178184 | *PARD6G* | -1,138085011 | 7,94337E-17 |
| 805 | ENSG00000196172 | *ZNF681* | -1,137875852 | 0,000267457 |
| 806 | ENSG00000260742 | *AC009962.1* | -1,137684528 | 0,033439692 |
| 807 | ENSG00000142632 | *ARHGEF19* | -1,137474348 | 0,006029818 |
| 808 | ENSG00000136997 | *MYC* | -1,137375594 | 1,828E-56 |
| 809 | ENSG00000103260 | *METRN* | -1,135427155 | 4,60307E-80 |
| 810 | ENSG00000123570 | *RAB9B* | -1,135148875 | 1,72725E-13 |
| 811 | ENSG00000132205 | *EMILIN2* | -1,13496596 | 5,34768E-35 |
| 812 | ENSG00000168874 | *ATOH8* | -1,133877755 | 1,81333E-16 |
| 813 | ENSG00000071282 | *LMCD1* | -1,133677536 | 6,32462E-12 |
| 814 | ENSG00000161082 | *CELF5* | -1,133550261 | 1,465E-07 |
| 815 | ENSG00000149654 | *CDH22* | -1,131998631 | 0,000186118 |
| 816 | ENSG00000224945 | *AL353150.1* | -1,130994453 | 2,18019E-16 |
| 817 | ENSG00000272767 | *JMJD1C-AS1* | -1,129371314 | 0,010776691 |
| 818 | ENSG00000164300 | *SERINC5* | -1,129079738 | 3,80977E-26 |
| 819 | ENSG00000168297 | *PXK* | -1,128783295 | 8,61593E-28 |
| 820 | ENSG00000225511 | *LINC00475* | -1,127756579 | 0,038484169 |
| 821 | ENSG00000231607 | *DLEU2* | -1,126273661 | 2,28434E-06 |
| 822 | ENSG00000253457 | *SMIM18* | -1,126199152 | 0,017034801 |
| 823 | ENSG00000198846 | *TOX* | -1,125470089 | 6,97214E-19 |
| 824 | ENSG00000183496 | *MEX3B* | -1,12531 | 8,49033E-17 |
| 825 | ENSG00000183067 | *IGSF5* | -1,124456104 | 0,008066898 |
| 826 | ENSG00000151612 | *ZNF827* | -1,12379215 | 1,20168E-32 |
| 827 | ENSG00000261770 | *AC006504.1* | -1,123775058 | 0,000440733 |
| 828 | ENSG00000104381 | *GDAP1* | -1,123455737 | 1,2881E-26 |
| 829 | ENSG00000164796 | *CSMD3* | -1,122897573 | 2,41076E-06 |
| 830 | ENSG00000180113 | *TDRD6* | -1,122019692 | 0,027882937 |
| 831 | ENSG00000134508 | *CABLES1* | -1,121366046 | 0,000556047 |
| 832 | ENSG00000149929 | *HIRIP3* | -1,120160788 | 3,30168E-32 |
| 833 | ENSG00000177363 | *LRRN4CL* | -1,120001834 | 0,002696112 |
| 834 | ENSG00000230454 | *U73166.1* | -1,117796878 | 0,009386645 |
| 835 | ENSG00000188266 | *HYKK* | -1,117471384 | 0,029763947 |
| 836 | ENSG00000261857 | *MIA* | -1,114949407 | 0,009524953 |
| 837 | ENSG00000112576 | *CCND3* | -1,114097684 | 2,82228E-31 |
| 838 | ENSG00000106034 | *CPED1* | -1,112588363 | 0,024561192 |
| 839 | ENSG00000188818 | *ZDHHC11* | -1,111145724 | 2,14169E-07 |
| 840 | ENSG00000046604 | *DSG2* | -1,110870059 | 4,06899E-10 |
| 841 | ENSG00000031081 | *ARHGAP31* | -1,110768412 | 4,14242E-72 |
| 842 | ENSG00000064225 | *ST3GAL6* | -1,109499744 | 1,43621E-32 |
| 843 | ENSG00000146147 | *MLIP* | -1,108983719 | 0,003529183 |
| 844 | ENSG00000115468 | *EFHD1* | -1,104066343 | 3,51256E-22 |
| 845 | ENSG00000177599 | *ZNF491* | -1,103011581 | 2,87355E-07 |
| 846 | ENSG00000176406 | *RIMS2* | -1,101715804 | 4,52353E-09 |
| 847 | ENSG00000162676 | *GFI1* | -1,10161985 | 0,023776984 |
| 848 | ENSG00000198312 | *BMS1P9* | -1,099846951 | 0,031633271 |
| 849 | ENSG00000118193 | *KIF14* | -1,099462674 | 6,67988E-37 |
| 850 | ENSG00000261829 | *AC009407.1* | -1,098663057 | 0,003157314 |
| 851 | ENSG00000172264 | *MACROD2* | -1,098020051 | 2,61996E-05 |
| 852 | ENSG00000114166 | *KAT2B* | -1,096883718 | 6,78353E-48 |
| 853 | ENSG00000127241 | *MASP1* | -1,096419205 | 1,5702E-52 |

| | | | | |
|---|---|---|---|---|
| 854 | ENSG00000123096 | *SSPN* | -1,09514327 | 0,001566436 |
| 855 | ENSG00000213638 | *ADAT3* | -1,094541505 | 9,05647E-06 |
| 856 | ENSG00000267041 | *ZNF850* | -1,094181641 | 3,15153E-14 |
| 857 | ENSG00000221955 | *SLC12A8* | -1,090949733 | 0,012720987 |
| 858 | ENSG00000118946 | *PCDH17* | -1,089079785 | 6,01309E-18 |
| 859 | ENSG00000073111 | *MCM2* | -1,087352102 | 1,11446E-70 |
| 860 | ENSG00000152583 | *SPARCL1* | -1,085756422 | 8,12742E-77 |
| 861 | ENSG00000148677 | *ANKRD1* | -1,084737478 | 0,026912451 |
| 862 | ENSG00000164104 | *HMGB2* | -1,082188802 | 1,20048E-60 |
| 863 | ENSG00000140451 | *PIF1* | -1,08074595 | 6,30983E-23 |
| 864 | ENSG00000162878 | *PKDCC* | -1,07811601 | 2,86393E-13 |
| 865 | ENSG00000180592 | *SKIDA1* | -1,077998821 | 0,03031749 |
| 866 | ENSG00000169554 | *ZEB2* | -1,077893839 | 1,20949E-58 |
| 867 | ENSG00000131747 | *TOP2A* | -1,077403565 | 7,37914E-89 |
| 868 | ENSG00000117724 | *CENPF* | -1,076808542 | 6,5412E-58 |
| 869 | ENSG00000163808 | *KIF15* | -1,076046397 | 4,53785E-41 |
| 870 | ENSG00000166432 | *ZMAT1* | -1,074268534 | 2,65951E-19 |
| 871 | ENSG00000179403 | *VWA1* | -1,074123513 | 4,34276E-33 |
| 872 | ENSG00000075945 | *KIFAP3* | -1,070945499 | 3,81307E-33 |
| 873 | ENSG00000184678 | *HIST2H2BE* | -1,070812448 | 5,78582E-31 |
| 874 | ENSG00000133131 | *MORC4* | -1,070477864 | 1,57606E-19 |
| 875 | ENSG00000105963 | *ADAP1* | -1,068711432 | 0,00667825 |
| 876 | ENSG00000178999 | *AURKB* | -1,068007021 | 5,14544E-30 |
| 877 | ENSG00000254122 | *PCDHGB7* | -1,067938984 | 1,53651E-45 |
| 878 | ENSG00000154188 | *ANGPT1* | -1,066829751 | 2,65085E-10 |
| 879 | ENSG00000227487 | *NCAM1-AS1* | -1,066323745 | 0,014847434 |
| 880 | ENSG00000163935 | *SFMBT1* | -1,065348588 | 6,64874E-15 |
| 881 | ENSG00000111077 | *TNS2* | -1,063771698 | 1,49908E-51 |
| 882 | ENSG00000198947 | *DMD* | -1,063689189 | 1,10329E-12 |
| 883 | ENSG00000221990 | *EXOC3-AS1* | -1,06138633 | 3,92086E-05 |
| 884 | ENSG00000175105 | *ZNF654* | -1,060830242 | 3,14575E-14 |
| 885 | ENSG00000124613 | *ZNF391* | -1,060777995 | 4,52944E-07 |
| 886 | ENSG00000175611 | *LINC00476* | -1,060207031 | 1,00918E-06 |
| 887 | ENSG00000118939 | *UCHL3* | -1,059209921 | 0,028994206 |
| 888 | ENSG00000269793 | *ZIM2-AS1* | -1,058990335 | 1,35036E-07 |
| 889 | ENSG00000188290 | *HES4* | -1,058554022 | 2,62754E-19 |
| 890 | ENSG00000198797 | *BRINP2* | -1,056925765 | 7,86935E-34 |
| 891 | ENSG00000115525 | *ST3GAL5* | -1,055840092 | 3,25428E-45 |
| 892 | ENSG00000198131 | *ZNF544* | -1,055596096 | 2,70882E-06 |
| 893 | ENSG00000137812 | *KNL1* | -1,054765619 | 1,73869E-29 |
| 894 | ENSG00000170873 | *MTSS1* | -1,054299683 | 1,80475E-56 |
| 895 | ENSG00000152578 | *GRIA4* | -1,053516751 | 9,44983E-42 |
| 896 | ENSG00000188897 | *AC099489.1* | -1,053335298 | 0,046056739 |
| 897 | ENSG00000080839 | *RBL1* | -1,053334345 | 2,44607E-20 |
| 898 | ENSG00000169964 | *TMEM42* | -1,053272871 | 0,016607621 |
| 899 | ENSG00000102109 | *PCSK1N* | -1,052924379 | 1,2372E-23 |
| 900 | ENSG00000233429 | *HOTAIRM1* | -1,05095186 | 7,54511E-05 |
| 901 | ENSG00000164109 | *MAD2L1* | -1,050562038 | 9,59642E-31 |
| 902 | ENSG00000228522 | *AL845321.1* | -1,050335252 | 0,018104795 |
| 903 | ENSG00000136603 | *SKIL* | -1,049717105 | 8,34627E-09 |
| 904 | ENSG00000164920 | *OSR2* | -1,049388086 | 1,68193E-06 |
| 905 | ENSG00000112852 | *PCDHB2* | -1,049245121 | 1,25033E-17 |
| 906 | ENSG00000250486 | *FAM218A* | -1,047985932 | 0,005517033 |
| 907 | ENSG00000105825 | *TFPI2* | -1,04750729 | 0,025379245 |
| 908 | ENSG00000170961 | *HAS2* | -1,046451784 | 4,85615E-26 |
| 909 | ENSG00000082781 | *ITGB5* | -1,046015404 | 3,24991E-53 |
| 910 | ENSG00000100784 | *RPS6KA5* | -1,045897473 | 2,67889E-12 |
| 911 | ENSG00000076604 | *TRAF4* | -1,043460371 | 1,0382E-57 |
| 912 | ENSG00000087303 | *NID2* | -1,042295098 | 1,05767E-51 |
| 913 | ENSG00000230359 | *TPI1P2* | -1,041226753 | 0,022069131 |
| 914 | ENSG00000168386 | *FILIP1L* | -1,041090851 | 0,027694364 |
| 915 | ENSG00000173598 | *NUDT4* | -1,039018764 | 3,78202E-65 |
| 916 | ENSG00000154839 | *SKA1* | -1,035503236 | 1,19089E-20 |
| 917 | ENSG00000245571 | *AP001258.1* | -1,034976094 | 0,000558051 |
| 918 | ENSG00000116299 | *KIAA1324* | -1,03341273 | 0,024718484 |
| 919 | ENSG00000183230 | *CTNNA3* | -1,033118981 | 0,044464215 |
| 920 | ENSG00000001617 | *SEMA3F* | -1,032856022 | 0,0205753 |
| 921 | ENSG00000176912 | *TYMSOS* | -1,032019308 | 0,000835237 |
| 922 | ENSG00000185442 | *FAM174B* | -1,029588957 | 0,026265639 |
| 923 | ENSG00000035499 | *DEPDC1B* | -1,028783231 | 4,30265E-18 |
| 924 | ENSG00000137166 | *FOXP4* | -1,027883869 | 4,79056E-27 |
| 925 | ENSG00000119866 | *BCL11A* | -1,02771829 | 0,000429336 |
| 926 | ENSG00000170396 | *ZNF804A* | -1,027306592 | 0,029873866 |
| 927 | ENSG00000215190 | *LINC00680* | -1,026983539 | 9,22212E-06 |
| 928 | ENSG00000165169 | *DYNLT3* | -1,025239843 | 2,33031E-21 |
| 929 | ENSG00000134758 | *RNF138* | -1,025214519 | 1,21109E-21 |
| 930 | ENSG00000170681 | *CAVIN4* | -1,02503519 | 0,001613946 |
| 931 | ENSG00000271614 | *ATP2B1-AS1* | -1,023745633 | 0,001470421 |

| | | | | |
|---|---|---|---|---|
| 932 | ENSG00000122042 | *UBL3* | -1,02317198 | 7,71103E-38 |
| 933 | ENSG00000149633 | *KIAA1755* | -1,022787724 | 3,01798E-19 |
| 934 | ENSG00000231160 | *KLF3-AS1* | -1,022704748 | 0,022664167 |
| 935 | ENSG00000158234 | *FAIM* | -1,02009993 | 4,98541E-07 |
| 936 | ENSG00000101463 | *SYNDIG1* | -1,02003464 | 2,27534E-08 |
| 937 | ENSG00000156395 | *SORCS3* | -1,019381369 | 3,70406E-14 |
| 938 | ENSG00000080503 | *SMARCA2* | -1,019246846 | 1,8965E-31 |
| 939 | ENSG00000165359 | *INTS6L* | -1,018575936 | 8,35595E-09 |
| 940 | ENSG00000110092 | *CCND1* | -1,017716106 | 3,30359E-47 |
| 941 | ENSG00000157557 | *ETS2* | -1,0163748 | 2,55415E-11 |
| 942 | ENSG00000088035 | *ALG6* | -1,015783317 | 2,61712E-17 |
| 943 | ENSG00000260633 | *AC010207.1* | -1,015096513 | 0,044780681 |
| 944 | ENSG00000100625 | *SIX4* | -1,01505943 | 3,96482E-11 |
| 945 | ENSG00000111554 | *MDM1* | -1,013122814 | 5,22381E-08 |
| 946 | ENSG00000166851 | *PLK1* | -1,012891876 | 5,51955E-40 |
| 947 | ENSG00000268362 | *AC092279.1* | -1,012700033 | 3,57358E-05 |
| 948 | ENSG00000140534 | *TICRR* | -1,012644948 | 7,12751E-28 |
| 949 | ENSG00000140807 | *NKD1* | -1,012281062 | 1,22797E-06 |
| 950 | ENSG00000165795 | *NDRG2* | -1,010650421 | 4,63421E-48 |
| 951 | ENSG00000203819 | *HIST2H2BC* | -1,0103519 | 0,049898102 |
| 952 | ENSG00000115350 | *POLE4* | -1,010284471 | 9,03636E-10 |
| 953 | ENSG00000198794 | *SCAMP5* | -1,010261415 | 2,55291E-27 |
| 954 | ENSG00000129810 | *SGO1* | -1,009462293 | 1,31024E-13 |
| 955 | ENSG00000168078 | *PBK* | -1,008909205 | 2,14157E-41 |
| 956 | ENSG00000163507 | *KIAA1524* | -1,008560185 | 2,41613E-27 |
| 957 | ENSG00000178878 | *APOLD1* | -1,006613327 | 5,35411E-16 |
| 958 | ENSG00000175548 | *ALG10B* | -1,005684784 | 0,00012887 |
| 959 | ENSG00000112290 | *WASF1* | -1,004678902 | 2,88957E-25 |
| 960 | ENSG00000114346 | *ECT2* | -1,00344333 | 2,16593E-46 |
| 961 | ENSG00000145075 | *CCDC39* | -1,003255067 | 0,000102997 |
| 962 | ENSG00000167964 | *RAB26* | -1,003154732 | 0,000320998 |
| 963 | ENSG00000167912 | *AC090152.1* | -1,003090802 | 1,84082E-06 |
| 964 | ENSG00000155970 | *MICU3* | -1,002945469 | 3,90396E-05 |
| 965 | ENSG00000182118 | *FAM89A* | -1,002828412 | 3,16804E-14 |
| 966 | ENSG00000256463 | *SALL3* | -1,002024558 | 5,15305E-37 |
| 967 | ENSG00000138160 | *KIF11* | -1,001694832 | 3,59566E-37 |
| 968 | ENSG00000142303 | *ADAMTS10* | -1,001456978 | 2,90898E-11 |
| 969 | ENSG00000213190 | *MLLT11* | -1,000298206 | 2,22478E-29 |
| 970 | ENSG00000109805 | *NCAPG* | -0,999802695 | 2,29589E-28 |
| 971 | ENSG00000184661 | *CDCA2* | -0,998933884 | 4,51945E-24 |
| 972 | ENSG00000121211 | *MND1* | -0,998347706 | 1,54282E-06 |
| 973 | ENSG00000112773 | *FAM46A* | -0,996934331 | 4,19063E-08 |
| 974 | ENSG00000076706 | *MCAM* | -0,995653626 | 1,00494E-62 |
| 975 | ENSG00000007402 | *CACNA2D2* | -0,993325954 | 2,31228E-06 |
| 976 | ENSG00000159023 | *EPB41* | -0,992813163 | 4,73928E-32 |
| 977 | ENSG00000134343 | *ANO3* | -0,992755185 | 0,019340199 |
| 978 | ENSG00000167861 | *HID1* | -0,99259227 | 4,01076E-12 |
| 979 | ENSG00000264364 | *DYNLL2* | -0,992493076 | 2,0296E-48 |
| 980 | ENSG00000170540 | *ARL6IP1* | -0,991965006 | 6,84025E-67 |
| 981 | ENSG00000272817 | *AL359198.1* | -0,989511981 | 0,030657038 |
| 982 | ENSG00000255153 | *TOLLIP-AS1* | -0,989163842 | 0,033380462 |
| 983 | ENSG00000177842 | *ZNF620* | -0,988992086 | 1,75995E-10 |
| 984 | ENSG00000092964 | *DPYSL2* | -0,988482544 | 2,1416E-63 |
| 985 | ENSG00000227124 | *ZNF717* | -0,987523282 | 0,015138911 |
| 986 | ENSG00000186446 | *ZNF501* | -0,986836754 | 2,3803E-07 |
| 987 | ENSG00000187764 | *SEMA4D* | -0,985319913 | 3,65512E-20 |
| 988 | ENSG00000189057 | *FAM111B* | -0,985091374 | 1,04811E-19 |
| 989 | ENSG00000229676 | *ZNF492* | -0,984594866 | 0,021826731 |
| 990 | ENSG00000197381 | *ADARB1* | -0,984436283 | 2,08722E-13 |
| 991 | ENSG00000173811 | *CCDC13-AS1* | -0,983600705 | 0,041735331 |
| 992 | ENSG00000164574 | *GALNT10* | -0,982757983 | 1,50863E-48 |
| 993 | ENSG00000156398 | *SFXN2* | -0,982093564 | 4,9536E-07 |
| 994 | ENSG00000084628 | *NKAIN1* | -0,980747232 | 9,97368E-11 |
| 995 | ENSG00000182575 | *NXPH3* | -0,98044867 | 0,000119963 |
| 996 | ENSG00000103044 | *HAS3* | -0,980134382 | 6,0819E-27 |
| 997 | ENSG00000110693 | *SOX6* | -0,979337356 | 2,70518E-55 |
| 998 | ENSG00000228630 | *HOTAIR* | -0,979169951 | 0,02671191 |
| 999 | ENSG00000101447 | *FAM83D* | -0,978690496 | 8,0276E-23 |
| 1000 | ENSG00000263146 | *LINC01896* | -0,977960793 | 1,418E-18 |
| 1001 | ENSG00000166689 | *PLEKHA7* | -0,977901691 | 6,56618E-09 |
| 1002 | ENSG00000144868 | *TMEM108* | -0,976871153 | 3,74961E-16 |
| 1003 | ENSG00000236499 | *LINC00896* | -0,975710035 | 0,030329363 |
| 1004 | ENSG00000100596 | *SPTLC2* | -0,974824024 | 2,24503E-25 |
| 1005 | ENSG00000196081 | *ZNF724* | -0,974729847 | 1,97579E-07 |
| 1006 | ENSG00000117569 | *PTBP2* | -0,97454883 | 3,43819E-12 |
| 1007 | ENSG00000052795 | *FNIP2* | -0,97283337 | 2,31554E-11 |
| 1008 | ENSG00000158352 | *SHROOM4* | -0,972534129 | 2,2007E-25 |
| 1009 | ENSG00000182568 | *SATB1* | -0,97229392 | 5,13427E-32 |

| | | | | |
|---|---|---|---|---|
| 1010 | ENSG00000151883 | *PARP8* | -0,971985817 | 1,04153E-15 |
| 1011 | ENSG00000072134 | *EPN2* | -0,971573541 | 2,69348E-47 |
| 1012 | ENSG00000141298 | *SSH2* | -0,971165696 | 2,46849E-22 |
| 1013 | ENSG00000103037 | *SETD6* | -0,971072695 | 0,000108954 |
| 1014 | ENSG00000214940 | *NPIPA8* | -0,968566925 | 0,01990221 |
| 1015 | ENSG00000171316 | *CHD7* | -0,968064694 | 7,16031E-50 |
| 1016 | ENSG00000137804 | *NUSAP1* | -0,966776255 | 5,04911E-61 |
| 1017 | ENSG00000183856 | *IQGAP3* | -0,966564846 | 3,30934E-42 |
| 1018 | ENSG00000273274 | *ZBTB8B* | -0,965840543 | 7,72797E-08 |
| 1019 | ENSG00000130997 | *POLN* | -0,965736346 | 0,003718624 |
| 1020 | ENSG00000259877 | *AC009113.1* | -0,965647706 | 0,000191463 |
| 1021 | ENSG00000114993 | *RTKN* | -0,964723154 | 1,82952E-45 |
| 1022 | ENSG00000189283 | *FHIT* | -0,964237102 | 0,000177074 |
| 1023 | ENSG00000136938 | *ANP32B* | -0,96409853 | 4,46739E-59 |
| 1024 | ENSG00000171681 | *ATF7IP* | -0,963510308 | 4,76738E-28 |
| 1025 | ENSG00000213988 | *ZNF90* | -0,96320001 | 1,70268E-05 |
| 1026 | ENSG00000183963 | *SMTN* | -0,963188062 | 1,38245E-18 |
| 1027 | ENSG00000164093 | *PITX2* | -0,963034691 | 0,010388506 |
| 1028 | ENSG00000173546 | *CSPG4* | -0,962664693 | 6,72933E-13 |
| 1029 | ENSG00000169607 | *CKAP2L* | -0,962456777 | 8,25011E-27 |
| 1030 | ENSG00000163083 | *INHBB* | -0,962232925 | 0,000112194 |
| 1031 | ENSG00000269821 | *KCNQ1OT1* | -0,961064966 | 1,55581E-06 |
| 1032 | ENSG00000162063 | *CCNF* | -0,960874892 | 1,66072E-18 |
| 1033 | ENSG00000169562 | *GJB1* | -0,960577489 | 5,46538E-09 |
| 1034 | ENSG00000066279 | *ASPM* | -0,959201966 | 2,1929E-09 |
| 1035 | ENSG00000150275 | *PCDH15* | -0,959077417 | 6,90889E-37 |
| 1036 | ENSG00000196507 | *TCEAL3* | -0,958613228 | 1,02378E-20 |
| 1037 | ENSG00000095203 | *EPB41L4B* | -0,957301205 | 0,000103681 |
| 1038 | ENSG00000105767 | *CADM4* | -0,956635499 | 2,06554E-68 |
| 1039 | ENSG00000150907 | *FOXO1* | -0,955011195 | 1,29192E-13 |
| 1040 | ENSG00000260807 | *AC009041.2* | -0,953224142 | 9,51354E-36 |
| 1041 | ENSG00000095383 | *TBC1D2* | -0,953083977 | 9,1498E-05 |
| 1042 | ENSG00000100225 | *FBXO7* | -0,95272056 | 1,54104E-58 |
| 1043 | ENSG00000080573 | *COL5A3* | -0,952685283 | 1,17355E-21 |
| 1044 | ENSG00000109654 | *TRIM2* | -0,952671758 | 2,18207E-14 |
| 1045 | ENSG00000101347 | *SAMHD1* | -0,952643896 | 2,02199E-16 |
| 1046 | ENSG00000186871 | *ERCC6L* | -0,950819237 | 5,16402E-10 |
| 1047 | ENSG00000155629 | *PIK3AP1* | -0,950029493 | 0,019678487 |
| 1048 | ENSG00000136824 | *SMC2* | -0,950006716 | 3,80409E-41 |
| 1049 | ENSG00000270964 | *AC016355.1* | -0,948716909 | 0,047676615 |
| 1050 | ENSG00000102221 | *JADE3* | -0,948242872 | 1,85306E-23 |
| 1051 | ENSG00000186193 | *SAPCD2* | -0,948040087 | 2,81152E-43 |
| 1052 | ENSG00000146281 | *PM20D2* | -0,947705804 | 3,40027E-21 |
| 1053 | ENSG00000165424 | *ZCCHC24* | -0,947209213 | 3,38563E-42 |
| 1054 | ENSG00000185614 | *FAM212A* | -0,946533928 | 0,007905656 |
| 1055 | ENSG00000079482 | *OPHN1* | -0,943346082 | 7,89835E-25 |
| 1056 | ENSG00000177359 | *AC024940.1* | -0,943011178 | 1,3324E-05 |
| 1057 | ENSG00000120251 | *GRIA2* | -0,942184508 | 1,05224E-29 |
| 1058 | ENSG00000188783 | *PRELP* | -0,941762835 | 9,58792E-10 |
| 1059 | ENSG00000169306 | *IL1RAPL1* | -0,941450982 | 0,010950268 |
| 1060 | ENSG00000134779 | *TPGS2* | -0,941416223 | 1,26005E-47 |
| 1061 | ENSG00000272121 | *AC006058.3* | -0,940452741 | 0,032456384 |
| 1062 | ENSG00000172426 | *RSPH9* | -0,937328427 | 0,02811578 |
| 1063 | ENSG00000147364 | *FBXO25* | -0,937173235 | 7,40354E-09 |
| 1064 | ENSG00000138316 | *ADAMTS14* | -0,936564331 | 0,00042986 |
| 1065 | ENSG00000166801 | *FAM111A* | -0,935285476 | 2,23911E-30 |
| 1066 | ENSG00000101412 | *E2F1* | -0,933778905 | 3,83382E-27 |
| 1067 | ENSG00000163576 | *EFHB* | -0,932164044 | 0,000549727 |
| 1068 | ENSG00000030419 | *IKZF2* | -0,93178689 | 0,006065442 |
| 1069 | ENSG00000237238 | *BMS1P10* | -0,931440901 | 1,07419E-05 |
| 1070 | ENSG00000139344 | *AMDHD1* | -0,931267179 | 0,046517548 |
| 1071 | ENSG00000148541 | *FAM13C* | -0,930323453 | 0,00017352 |
| 1072 | ENSG00000011332 | *DPF1* | -0,930243241 | 5,87502E-16 |
| 1073 | ENSG00000180611 | *MB21D2* | -0,929470087 | 8,32911E-06 |
| 1074 | ENSG00000156802 | *ATAD2* | -0,929308255 | 2,20567E-45 |
| 1075 | ENSG00000051341 | *POLQ* | -0,92808807 | 1,98959E-18 |
| 1076 | ENSG00000154429 | *CCSAP* | -0,92783709 | 1,84391E-27 |
| 1077 | ENSG00000164850 | *GPER1* | -0,926801267 | 0,001687689 |
| 1078 | ENSG00000049192 | *ADAMTS6* | -0,92666256 | 0,014860022 |
| 1079 | ENSG00000184588 | *PDE4B* | -0,926438369 | 2,27955E-46 |
| 1080 | ENSG00000096092 | *TMEM14A* | -0,92584623 | 1,19957E-09 |
| 1081 | ENSG00000166816 | *LDHD* | -0,92534725 | 0,035526376 |
| 1082 | ENSG00000175048 | *ZDHHC14* | -0,925048006 | 1,70506E-10 |
| 1083 | ENSG00000272447 | *AL135925.1* | -0,924823271 | 0,002410115 |
| 1084 | ENSG00000177511 | *ST8SIA3* | -0,922934167 | 0,004775875 |
| 1085 | ENSG00000134030 | *CTIF* | -0,922068283 | 4,42416E-27 |
| 1086 | ENSG00000128923 | *MINDY2* | -0,920894966 | 3,3842E-12 |
| 1087 | ENSG00000143476 | *DTL* | -0,919404548 | 7,63297E-28 |

| | | | | |
|---|---|---|---|---|
| 1088 | ENSG00000112541 | *PDE10A* | -0,91903624 | 7,30878E-09 |
| 1089 | ENSG00000196935 | *SRGAP1* | -0,918396639 | 2,92271E-21 |
| 1090 | ENSG00000158769 | *F11R* | -0,91566045 | 0,003379847 |
| 1091 | ENSG00000068078 | *FGFR3* | -0,914495101 | 9,48434E-35 |
| 1092 | ENSG00000067445 | *TRO* | -0,913857845 | 2,19548E-41 |
| 1093 | ENSG00000100105 | *PATZ1* | -0,913667231 | 4,23887E-26 |
| 1094 | ENSG00000239445 | *ST3GAL6-AS1* | -0,913354042 | 0,007022502 |
| 1095 | ENSG00000108821 | *COL1A1* | -0,913094951 | 0,000619283 |
| 1096 | ENSG00000167608 | *TMC4* | -0,912781638 | 0,033586344 |
| 1097 | ENSG00000065989 | *PDE4A* | -0,912643867 | 2,96813E-09 |
| 1098 | ENSG00000072571 | *HMMR* | -0,911295924 | 4,19619E-16 |
| 1099 | ENSG00000178764 | *ZHX2* | -0,910907627 | 1,21438E-18 |
| 1100 | ENSG00000197872 | *FAM49A* | -0,910058884 | 3,04855E-18 |
| 1101 | ENSG00000134954 | *ETS1* | -0,909154234 | 2,6185E-34 |
| 1102 | ENSG00000115339 | *GALNT3* | -0,907078758 | 0,011484218 |
| 1103 | ENSG00000157152 | *SYN2* | -0,906054776 | 5,05734E-05 |
| 1104 | ENSG00000196381 | *ZNF781* | -0,905843923 | 0,003667562 |
| 1105 | ENSG00000101439 | *CST3* | -0,905658824 | 9,81201E-47 |
| 1106 | ENSG00000129521 | *EGLN3* | -0,904491944 | 5,6144E-07 |
| 1107 | ENSG00000131831 | *RAI2* | -0,902133495 | 0,007172101 |
| 1108 | ENSG00000137574 | *TGS1* | -0,901780235 | 1,45844E-14 |
| 1109 | ENSG00000137767 | *SQOR* | -0,901476322 | 0,034110412 |
| 1110 | ENSG00000104368 | *PLAT* | -0,901166058 | 6,09457E-46 |
| 1111 | ENSG00000056736 | *IL17RB* | -0,900985233 | 4,16555E-08 |
| 1112 | ENSG00000165480 | *SKA3* | -0,90075986 | 2,92905E-12 |
| 1113 | ENSG00000165478 | *HEPACAM* | -0,898105904 | 1,66125E-19 |
| 1114 | ENSG00000233237 | *LINC00472* | -0,897889761 | 0,005921273 |
| 1115 | ENSG00000135916 | *ITM2C* | -0,897698902 | 1,97057E-55 |
| 1116 | ENSG00000184602 | *SNN* | -0,897492506 | 1,71645E-28 |
| 1117 | ENSG00000256673 | *AC141557.1* | -0,896188367 | 0,005595849 |
| 1118 | ENSG00000109472 | *CPE* | -0,896061159 | 1,81333E-20 |
| 1119 | ENSG00000231305 | *AC112484.2* | -0,895254927 | 0,041744992 |
| 1120 | ENSG00000129646 | *QRICH2* | -0,894679432 | 3,79197E-08 |
| 1121 | ENSG00000153310 | *FAM49B* | -0,891653948 | 8,3202E-23 |
| 1122 | ENSG00000105088 | *OLFM2* | -0,890611658 | 4,65882E-33 |
| 1123 | ENSG00000122952 | *ZWINT* | -0,890256326 | 4,0604E-22 |
| 1124 | ENSG00000170802 | *FOXN2* | -0,890034266 | 1,80841E-19 |
| 1125 | ENSG00000088325 | *TPX2* | -0,890009746 | 2,38839E-46 |
| 1126 | ENSG00000101608 | *MYL12A* | -0,889745567 | 7,34326E-25 |
| 1127 | ENSG00000198948 | *MFAP3L* | -0,889177303 | 0,000232682 |
| 1128 | ENSG00000177565 | *TBL1XR1* | -0,889165725 | 1,64504E-34 |
| 1129 | ENSG00000135045 | *C9orf40* | -0,888880028 | 9,47351E-10 |
| 1130 | ENSG00000013810 | *TACC3* | -0,888040112 | 1,29645E-29 |
| 1131 | ENSG00000134900 | *TPP2* | -0,88783967 | 4,99569E-28 |
| 1132 | ENSG00000259683 | *AC243562.2* | -0,887591661 | 0,029234075 |
| 1133 | ENSG00000175322 | *ZNF519* | -0,886964593 | 6,58222E-09 |
| 1134 | ENSG00000165813 | *CCDC186* | -0,885060984 | 3,69737E-05 |
| 1135 | ENSG00000112149 | *CD83* | -0,884878714 | 1,00931E-09 |
| 1136 | ENSG00000130675 | *MNX1* | -0,883779214 | 1,17741E-05 |
| 1137 | ENSG00000196724 | *ZNF418* | -0,881883366 | 8,59525E-05 |
| 1138 | ENSG00000171462 | *DLK2* | -0,881785622 | 0,001110371 |
| 1139 | ENSG00000186767 | *SPIN4* | -0,881539876 | 2,22019E-10 |
| 1140 | ENSG00000262246 | *CORO7* | -0,881230501 | 5,70473E-07 |
| 1141 | ENSG00000184349 | *EFNA5* | -0,879870992 | 0,044396071 |
| 1142 | ENSG00000101057 | *MYBL2* | -0,879162352 | 1,68226E-32 |
| 1143 | ENSG00000154914 | *USP43* | -0,878499736 | 6,72181E-05 |
| 1144 | ENSG00000206560 | *ANKRD28* | -0,877601455 | 4,55769E-30 |
| 1145 | ENSG00000118298 | *CA14* | -0,877296182 | 6,82291E-20 |
| 1146 | ENSG00000175130 | *MARCKSL1* | -0,876988963 | 2,95085E-51 |
| 1147 | ENSG00000112759 | *SLC29A1* | -0,87609857 | 3,17482E-14 |
| 1148 | ENSG00000141428 | *C18orf21* | -0,875688205 | 1,4801E-12 |
| 1149 | ENSG00000016391 | *CHDH* | -0,875212249 | 8,25896E-10 |
| 1150 | ENSG00000141384 | *TAF4B* | -0,874993588 | 0,000120215 |
| 1151 | ENSG00000257167 | *TMPO-AS1* | -0,874705272 | 0,000115044 |
| 1152 | ENSG00000075218 | *GTSE1* | -0,874590725 | 6,02345E-31 |
| 1153 | ENSG00000100167 | *SEPT3* | -0,873808832 | 5,39419E-43 |
| 1154 | ENSG00000167536 | *DHRS13* | -0,872434327 | 3,85698E-08 |
| 1155 | ENSG00000154217 | *PITPNC1* | -0,871856483 | 2,23493E-09 |
| 1156 | ENSG00000163781 | *TOPBP1* | -0,871802466 | 3,11677E-35 |
| 1157 | ENSG00000113368 | *LMNB1* | -0,870500866 | 4,49573E-45 |
| 1158 | ENSG00000109062 | *SLC9A3R1* | -0,870212276 | 6,15098E-18 |
| 1159 | ENSG00000051180 | *RAD51* | -0,869361443 | 7,13298E-11 |
| 1160 | ENSG00000158402 | *CDC25C* | -0,869150422 | 1,23287E-13 |
| 1161 | ENSG00000176393 | *RNPEP* | -0,869075757 | 7,60504E-21 |
| 1162 | ENSG00000101888 | *NXT2* | -0,867470065 | 9,15027E-10 |
| 1163 | ENSG00000224728 | *IMPDH1P8* | -0,866326335 | 0,043592665 |
| 1164 | ENSG00000175155 | *YPEL2* | -0,866236991 | 2,93485E-11 |
| 1165 | ENSG00000100908 | *EMC9* | -0,866017916 | 7,85217E-08 |

| 1166 | ENSG00000165152 | *TMEM246* | -0,865731101 | 8,7586E-22 |
|---|---|---|---|---|
| 1167 | ENSG00000142512 | *SIGLEC10* | -0,864055152 | 0,006128612 |
| 1168 | ENSG00000159263 | *SIM2* | -0,863668313 | 9,71495E-14 |
| 1169 | ENSG00000149503 | *INCENP* | -0,862922689 | 5,6036E-28 |
| 1170 | ENSG00000226742 | *HSBP1L1* | -0,862846609 | 0,03657379 |
| 1171 | ENSG00000154917 | *RAB6B* | -0,861813021 | 4,60461E-08 |
| 1172 | ENSG00000141401 | *IMPA2* | -0,861355623 | 3,61912E-14 |
| 1173 | ENSG00000127564 | *PKMYT1* | -0,861095419 | 2,12447E-13 |
| 1174 | ENSG00000168056 | *LTBP3* | -0,86107602 | 2,38828E-29 |
| 1175 | ENSG00000166974 | *MAPRE2* | -0,860101293 | 1,17102E-29 |
| 1176 | ENSG00000187049 | *TMEM216* | -0,859911278 | 0,001054817 |
| 1177 | ENSG00000150471 | *ADGRL3* | -0,859647796 | 2,04252E-34 |
| 1178 | ENSG00000166803 | *PCLAF* | -0,859457521 | 4,90111E-13 |
| 1179 | ENSG00000186868 | *MAPT* | -0,859092661 | 2,03088E-13 |
| 1180 | ENSG00000156970 | *BUB1B* | -0,854852179 | 2,82809E-28 |
| 1181 | ENSG00000121152 | *NCAPH* | -0,853721814 | 4,34094E-23 |
| 1182 | ENSG00000081913 | *PHLPP1* | -0,85274376 | 2,01467E-38 |
| 1183 | ENSG00000183250 | *LINC01547* | -0,8525044 | 0,005920194 |
| 1184 | ENSG00000116016 | *EPAS1* | -0,851938344 | 2,68056E-19 |
| 1185 | ENSG00000131437 | *KIF3A* | -0,851919058 | 6,9829E-16 |
| 1186 | ENSG00000140396 | *NCOA2* | -0,851345241 | 4,26878E-21 |
| 1187 | ENSG00000235919 | *ASH1L-AS1* | -0,851106626 | 0,048949968 |
| 1188 | ENSG00000115163 | *CENPA* | -0,850936469 | 1,10612E-11 |
| 1189 | ENSG00000147234 | *FRMPD3* | -0,850788869 | 1,00055E-05 |
| 1190 | ENSG00000157150 | *TIMP4* | -0,848520806 | 6,70455E-29 |
| 1191 | ENSG00000104331 | *IMPAD1* | -0,848010201 | 1,49788E-40 |
| 1192 | ENSG00000197622 | *CDC42SE1* | -0,847335091 | 3,09651E-32 |
| 1193 | ENSG00000178966 | *RMI1* | -0,846330417 | 5,32944E-12 |
| 1194 | ENSG00000038382 | *TRIO* | -0,845647065 | 1,59176E-52 |
| 1195 | ENSG00000119686 | *FLVCR2* | -0,845176397 | 0,013771179 |
| 1196 | ENSG00000121454 | *LHX4* | -0,844866336 | 0,001354614 |
| 1197 | ENSG00000024526 | *DEPDC1* | -0,844359834 | 2,13957E-16 |
| 1198 | ENSG00000267325 | *LINC01415* | -0,844060666 | 0,011668539 |
| 1199 | ENSG00000104218 | *CSPP1* | -0,842237731 | 1,31112E-10 |
| 1200 | ENSG00000180964 | *TCEAL8* | -0,840678459 | 5,25363E-17 |
| 1201 | ENSG00000129534 | *MIS18BP1* | -0,839879691 | 7,21572E-16 |
| 1202 | ENSG00000010282 | *HHATL* | -0,839279965 | 0,04970852 |
| 1203 | ENSG00000261455 | *LINC01003* | -0,83834827 | 0,002655403 |
| 1204 | ENSG00000204128 | *C2orf72* | -0,837799964 | 5,14079E-19 |
| 1205 | ENSG00000177873 | *ZNF619* | -0,836948685 | 2,36855E-07 |
| 1206 | ENSG00000164045 | *CDC25A* | -0,836679632 | 1,19292E-14 |
| 1207 | ENSG00000148604 | *RGR* | -0,836656405 | 0,007408533 |
| 1208 | ENSG00000196678 | *ERI2* | -0,836262391 | 3,34837E-11 |
| 1209 | ENSG00000125378 | *BMP4* | -0,836211295 | 0,022587153 |
| 1210 | ENSG00000139597 | *N4BP2L1* | -0,834892762 | 0,003140823 |
| 1211 | ENSG00000081154 | *PCNP* | -0,833839585 | 3,18788E-30 |
| 1212 | ENSG00000090238 | *YPEL3* | -0,833795809 | 1,1105E-06 |
| 1213 | ENSG00000130962 | *PRRG1* | -0,83280575 | 0,000247793 |
| 1214 | ENSG00000154548 | *SRSF12* | -0,832534564 | 5,5431E-07 |
| 1215 | ENSG00000272933 | *AL391121.1* | -0,83160555 | 0,013929966 |
| 1216 | ENSG00000075340 | *ADD2* | -0,830957035 | 7,59568E-22 |
| 1217 | ENSG00000228801 | *AC064807.1* | -0,829850697 | 0,019303489 |
| 1218 | ENSG00000176597 | *B3GNT5* | -0,829466808 | 3,20715E-13 |
| 1219 | ENSG00000167771 | *RCOR2* | -0,829381881 | 4,86889E-17 |
| 1220 | ENSG00000171817 | *ZNF540* | -0,827969858 | 0,027462952 |
| 1221 | ENSG00000183337 | *BCOR* | -0,827902893 | 7,91843E-18 |
| 1222 | ENSG00000077152 | *UBE2T* | -0,825490102 | 1,35687E-18 |
| 1223 | ENSG00000163531 | *NFASC* | -0,824963495 | 2,58029E-18 |
| 1224 | ENSG00000181467 | *RAP2B* | -0,824630951 | 9,80853E-14 |
| 1225 | ENSG00000242539 | *AC007620.2* | -0,824627018 | 1,68108E-08 |
| 1226 | ENSG00000066735 | *KIF26A* | -0,824067683 | 0,049103544 |
| 1227 | ENSG00000133138 | *TBC1D8B* | -0,823950631 | 0,000235831 |
| 1228 | ENSG00000005249 | *PRKAR2B* | -0,823586758 | 2,55628E-11 |
| 1229 | ENSG00000157456 | *CCNB2* | -0,822377096 | 8,16677E-29 |
| 1230 | ENSG00000116990 | *MYCL* | -0,822075481 | 8,85368E-07 |
| 1231 | ENSG00000168461 | *RAB31* | -0,822029695 | 4,60319E-45 |
| 1232 | ENSG00000164418 | *GRIK2* | -0,820715819 | 1,66507E-15 |
| 1233 | ENSG00000168952 | *STXBP6* | -0,820118631 | 0,000288939 |
| 1234 | ENSG00000174371 | *EXO1* | -0,819588306 | 1,33663E-12 |
| 1235 | ENSG00000166845 | *C18orf54* | -0,817910051 | 9,38168E-13 |
| 1236 | ENSG00000145386 | *CCNA2* | -0,817743406 | 1,01302E-19 |
| 1237 | ENSG00000081320 | *STK17B* | -0,817236769 | 1,38861E-05 |
| 1238 | ENSG00000102316 | *MAGED2* | -0,817174191 | 3,83736E-53 |
| 1239 | ENSG00000182481 | *KPNA2* | -0,81710958 | 3,38487E-44 |
| 1240 | ENSG00000164082 | *GRM2* | -0,815866427 | 0,039201858 |
| 1241 | ENSG00000196517 | *SLC6A9* | -0,814756416 | 5,74006E-13 |
| 1242 | ENSG00000142149 | *HUNK* | -0,814591975 | 2,25528E-14 |
| 1243 | ENSG00000206417 | *H1FX-AS1* | -0,814264931 | 0,003360917 |

| 1244 | ENSG00000100162 | *CENPM* | -0,814134837 | 5,2074E-16 |
|---|---|---|---|---|
| 1245 | ENSG00000205704 | *LINC00634* | -0,813156267 | 0,005841504 |
| 1246 | ENSG00000172361 | *CFAP53* | -0,812883763 | 0,040293359 |
| 1247 | ENSG00000034533 | *ASTE1* | -0,812308469 | 1,14082E-05 |
| 1248 | ENSG00000113645 | *WWC1* | -0,812077666 | 1,42895E-21 |
| 1249 | ENSG00000213347 | *MXD3* | -0,812051902 | 2,51735E-25 |
| 1250 | ENSG00000166317 | *SYNPO2L* | -0,810548867 | 0,006494403 |
| 1251 | ENSG00000164754 | *RAD21* | -0,810462339 | 1,74521E-44 |
| 1252 | ENSG00000149294 | *NCAM1* | -0,809971915 | 1,21508E-51 |
| 1253 | ENSG00000120802 | *TMPO* | -0,808998739 | 2,86773E-36 |
| 1254 | ENSG00000137478 | *FCHSD2* | -0,808750047 | 7,69137E-20 |
| 1255 | ENSG00000205268 | *PDE7A* | -0,807993722 | 2,27811E-10 |
| 1256 | ENSG00000109674 | *NEIL3* | -0,805627168 | 6,39029E-06 |
| 1257 | ENSG00000085719 | *CPNE3* | -0,804848614 | 1,15144E-32 |
| 1258 | ENSG00000170312 | *CDK1* | -0,804487784 | 5,66281E-28 |
| 1259 | ENSG00000103145 | *HCFC1R1* | -0,803911121 | 2,0228E-09 |
| 1260 | ENSG00000180834 | *MAP6D1* | -0,802683357 | 2,61479E-09 |
| 1261 | ENSG00000213888 | *LINC01521* | -0,802556243 | 0,009367796 |
| 1262 | ENSG00000139946 | *PELI2* | -0,801262071 | 1,92393E-08 |
| 1263 | ENSG00000117906 | *RCN2* | -0,800595477 | 5,25185E-32 |
| 1264 | ENSG00000114853 | *ZBTB47* | -0,800118696 | 2,96857E-21 |
| 1265 | ENSG00000171408 | *PDE7B* | -0,799885927 | 2,13198E-07 |
| 1266 | ENSG00000249859 | *PVT1* | -0,799804371 | 3,11044E-05 |
| 1267 | ENSG00000036448 | *MYOM2* | -0,799023842 | 0,015104105 |
| 1268 | ENSG00000175029 | *CTBP2* | -0,797127685 | 1,14584E-19 |
| 1269 | ENSG00000164506 | *STXBP5* | -0,795467925 | 0,000735973 |
| 1270 | ENSG00000154639 | *CXADR* | -0,795293062 | 2,81938E-26 |
| 1271 | ENSG00000239521 | *GATS* | -0,794830271 | 3,97226E-07 |
| 1272 | ENSG00000163939 | *PBRM1* | -0,794731355 | 6,58797E-28 |
| 1273 | ENSG00000151725 | *CENPU* | -0,794351577 | 7,13298E-11 |
| 1274 | ENSG00000134049 | *IER3IP1* | -0,794074555 | 8,12321E-11 |
| 1275 | ENSG00000247081 | *BAALC-AS1* | -0,793995204 | 0,006737761 |
| 1276 | ENSG00000125871 | *MGME1* | -0,793427837 | 6,45758E-12 |
| 1277 | ENSG00000109458 | *GAB1* | -0,792544424 | 5,9927E-18 |
| 1278 | ENSG00000270504 | *AL391422.3* | -0,792147277 | 0,000223044 |
| 1279 | ENSG00000144647 | *POMGNT2* | -0,791020518 | 8,45344E-28 |
| 1280 | ENSG00000103485 | *QPRT* | -0,790985822 | 1,24776E-06 |
| 1281 | ENSG00000173786 | *CNP* | -0,790863543 | 2,19204E-44 |
| 1282 | ENSG00000105011 | *ASF1B* | -0,790768542 | 5,15417E-23 |
| 1283 | ENSG00000103257 | *SLC7A5* | -0,790374453 | 7,58017E-16 |
| 1284 | ENSG00000121542 | *SEC22A* | -0,79029391 | 1,32104E-06 |
| 1285 | ENSG00000244274 | *DBNDD2* | -0,790105479 | 0,039228752 |
| 1286 | ENSG00000031003 | *FAM13B* | -0,789401691 | 7,14324E-11 |
| 1287 | ENSG00000073849 | *ST6GAL1* | -0,788956986 | 7,71892E-20 |
| 1288 | ENSG00000185920 | *PTCH1* | -0,788414712 | 3,75681E-23 |
| 1289 | ENSG00000122824 | *NUDT10* | -0,787744668 | 2,78899E-07 |
| 1290 | ENSG00000122547 | *EEPD1* | -0,787348456 | 4,6124E-08 |
| 1291 | ENSG00000105519 | *CAPS* | -0,787329341 | 4,34837E-17 |
| 1292 | ENSG00000101856 | *PGRMC1* | -0,787063647 | 4,088E-31 |
| 1293 | ENSG00000166123 | *GPT2* | -0,786850803 | 2,70688E-30 |
| 1294 | ENSG00000088808 | *PPP1R13B* | -0,786138942 | 2,7135E-05 |
| 1295 | ENSG00000172014 | *ANKRD20A4* | -0,786136741 | 0,004123567 |
| 1296 | ENSG00000115884 | *SDC1* | -0,785469671 | 2,06212E-23 |
| 1297 | ENSG00000159915 | *ZNF233* | -0,785329788 | 0,017211914 |
| 1298 | ENSG00000092096 | *SLC22A17* | -0,783165675 | 4,93192E-29 |
| 1299 | ENSG00000065154 | *OAT* | -0,782732618 | 8,17314E-21 |
| 1300 | ENSG00000178567 | *EPM2AIP1* | -0,782544619 | 3,79096E-21 |
| 1301 | ENSG00000149636 | *DSN1* | -0,782468955 | 1,0056E-10 |
| 1302 | ENSG00000163946 | *FAM208A* | -0,7822145 | 1,11068E-20 |
| 1303 | ENSG00000164989 | *CCDC171* | -0,779543264 | 0,031172719 |
| 1304 | ENSG00000188706 | *ZDHHC9* | -0,779055475 | 2,90603E-21 |
| 1305 | ENSG00000114857 | *NKTR* | -0,778980102 | 1,8304E-27 |
| 1306 | ENSG00000260018 | *AC040169.1* | -0,77841432 | 0,035983408 |
| 1307 | ENSG00000070413 | *DGCR2* | -0,777529249 | 3,49655E-39 |
| 1308 | ENSG00000146263 | *MMS22L* | -0,777229036 | 1,58845E-08 |
| 1309 | ENSG00000173599 | *PC* | -0,777074399 | 1,31004E-17 |
| 1310 | ENSG00000102931 | *ARL2BP* | -0,776453582 | 1,17228E-26 |
| 1311 | ENSG00000183444 | *OR7E38P* | -0,775965869 | 0,031645184 |
| 1312 | ENSG00000139211 | *AMIGO2* | -0,775955172 | 0,006957032 |
| 1313 | ENSG00000146005 | *PSD2* | -0,775609092 | 0,00274732 |
| 1314 | ENSG00000065413 | *ANKRD44* | -0,775370161 | 5,91239E-09 |
| 1315 | ENSG00000166377 | *ATP9B* | -0,774892916 | 1,00991E-16 |
| 1316 | ENSG00000136243 | *NUPL2* | -0,774527392 | 1,61377E-14 |
| 1317 | ENSG00000182504 | *CEP97* | -0,774103073 | 5,90899E-16 |
| 1318 | ENSG00000157349 | *DDX19B* | -0,774021355 | 3,02012E-05 |
| 1319 | ENSG00000138778 | *CENPE* | -0,773822308 | 2,14353E-15 |
| 1320 | ENSG00000203952 | *CCDC160* | -0,773768288 | 0,042566781 |
| 1321 | ENSG00000189319 | *FAM53B* | -0,773529283 | 4,74357E-09 |

| | | | | |
|---|---|---|---|---|
| 1322 | ENSG00000170579 | *DLGAP1* | -0,773216844 | 6,13788E-14 |
| 1323 | ENSG00000064300 | *NGFR* | -0,773124544 | 1,67213E-19 |
| 1324 | ENSG00000164087 | *POC1A* | -0,773118601 | 3,55995E-15 |
| 1325 | ENSG00000160229 | *ZNF66* | -0,771857264 | 0,021595617 |
| 1326 | ENSG00000187391 | *MAGI2* | -0,77148237 | 3,1574E-11 |
| 1327 | ENSG00000154080 | *CHST9* | -0,771358675 | 0,017912223 |
| 1328 | ENSG00000119900 | *OGFRL1* | -0,77129471 | 3,47281E-09 |
| 1329 | ENSG00000198300 | *PEG3* | -0,771090251 | 9,80138E-18 |
| 1330 | ENSG00000156531 | *PHF6* | -0,77071798 | 1,46765E-27 |
| 1331 | ENSG00000113790 | *EHHADH* | -0,770128193 | 0,00439801 |
| 1332 | ENSG00000144285 | *SCN1A* | -0,769095834 | 6,56716E-21 |
| 1333 | ENSG00000273329 | *AC078846.1* | -0,767956094 | 0,00179594 |
| 1334 | ENSG00000104738 | *MCM4* | -0,767705079 | 3,444E-36 |
| 1335 | ENSG00000159958 | *TNFRSF13C* | -0,767644924 | 0,021846174 |
| 1336 | ENSG00000083097 | *DOPEY1* | -0,767334032 | 7,92097E-11 |
| 1337 | ENSG00000162458 | *FBLIM1* | -0,767313586 | 2,26337E-07 |
| 1338 | ENSG00000111206 | *FOXM1* | -0,766560654 | 1,96913E-26 |
| 1339 | ENSG00000106617 | *PRKAG2* | -0,765719278 | 0,000756461 |
| 1340 | ENSG00000164611 | *PTTG1* | -0,765132064 | 8,42505E-26 |
| 1341 | ENSG00000086300 | *SNX10* | -0,765109524 | 1,82509E-08 |
| 1342 | ENSG00000130224 | *LRCH2* | -0,7651059 | 1,91127E-06 |
| 1343 | ENSG00000122545 | *SEPT7* | -0,764968282 | 1,81171E-39 |
| 1344 | ENSG00000271936 | *AC012073.1* | -0,764734406 | 0,010672266 |
| 1345 | ENSG00000131242 | *RAB11FIP4* | -0,764351153 | 0,000125329 |
| 1346 | ENSG00000205413 | *SAMD9* | -0,76375255 | 9,96337E-07 |
| 1347 | ENSG00000173801 | *JUP* | -0,763194827 | 0,001390223 |
| 1348 | ENSG00000272870 | *AC097534.2* | -0,76285746 | 0,036083792 |
| 1349 | ENSG00000126778 | *SIX1* | -0,762301684 | 8,03713E-10 |
| 1350 | ENSG00000151466 | *SCLT1* | -0,762153933 | 0,000167934 |
| 1351 | ENSG00000124795 | *DEK* | -0,761440813 | 5,48035E-34 |
| 1352 | ENSG00000109832 | *DDX25* | -0,759995531 | 0,006306709 |
| 1353 | ENSG00000204839 | *MROH6* | -0,759863682 | 0,037150615 |
| 1354 | ENSG00000186185 | *KIF18B* | -0,759834576 | 8,25953E-23 |
| 1355 | ENSG00000112742 | *TTK* | -0,759702577 | 1,36456E-18 |
| 1356 | ENSG00000109046 | *WSB1* | -0,759598082 | 3,3908E-31 |
| 1357 | ENSG00000118200 | *CAMSAP2* | -0,758784553 | 3,93602E-25 |
| 1358 | ENSG00000041515 | *MYO16* | -0,758612222 | 0,000148238 |
| 1359 | ENSG00000197696 | *NMB* | -0,758259974 | 0,02671191 |
| 1360 | ENSG00000090097 | *PCBP4* | -0,75730662 | 3,2959E-36 |
| 1361 | ENSG00000100479 | *POLE2* | -0,756911443 | 0,000760745 |
| 1362 | ENSG00000272899 | *AC025594.3* | -0,756559376 | 0,0481601 |
| 1363 | ENSG00000187952 | *HS6ST1P1* | -0,75652167 | 0,019614379 |
| 1364 | ENSG00000183077 | *AFMID* | -0,756354687 | 4,77758E-06 |
| 1365 | ENSG00000167088 | *SNRPD1* | -0,75625477 | 1,15451E-20 |
| 1366 | ENSG00000163788 | *SNRK* | -0,755255737 | 8,38685E-13 |
| 1367 | ENSG00000103056 | *SMPD3* | -0,755039563 | 0,006532891 |
| 1368 | ENSG00000138311 | *ZNF365* | -0,754372565 | 9,55456E-06 |
| 1369 | ENSG00000170049 | *KCNAB3* | -0,753555326 | 0,034393232 |
| 1370 | ENSG00000196741 | *LINC01560* | -0,75353954 | 0,031398048 |
| 1371 | ENSG00000113810 | *SMC4* | -0,753359602 | 8,48924E-29 |
| 1372 | ENSG00000138468 | *SENP7* | -0,752619414 | 3,19544E-13 |
| 1373 | ENSG00000272758 | *AC083798.2* | -0,752580646 | 0,021902406 |
| 1374 | ENSG00000104369 | *JPH1* | -0,752552154 | 9,84263E-05 |
| 1375 | ENSG00000196693 | *ZNF33B* | -0,752458854 | 0,00025465 |
| 1376 | ENSG00000132613 | *MTSS1L* | -0,751837133 | 7,14925E-25 |
| 1377 | ENSG00000206561 | *COLQ* | -0,751017681 | 0,024350557 |
| 1378 | ENSG00000167363 | *FN3K* | -0,750980418 | 0,037840074 |
| 1379 | ENSG00000084070 | *SMAP2* | -0,750750424 | 4,81164E-16 |
| 1380 | ENSG00000140948 | *ZCCHC14* | -0,750737404 | 2,85948E-16 |
| 1381 | ENSG00000141753 | *IGFBP4* | -0,750328086 | 7,84237E-25 |
| 1382 | ENSG00000272686 | *AC006333.2* | -0,750220594 | 0,000273619 |
| 1383 | ENSG00000164402 | *SEPT8* | -0,750051133 | 6,98836E-36 |
| 1384 | ENSG00000182158 | *CREB3L2* | -0,749801028 | 1,29705E-18 |
| 1385 | ENSG00000012983 | *MAP4K5* | -0,749142467 | 1,79635E-20 |
| 1386 | ENSG00000160539 | *PLPP7* | -0,748553197 | 0,034544297 |
| 1387 | ENSG00000179314 | *WSCD1* | -0,748007999 | 1,94487E-30 |
| 1388 | ENSG00000102409 | *BEX4* | -0,747878284 | 2,89922E-18 |
| 1389 | ENSG00000160447 | *PKN3* | -0,747172329 | 1,5978E-11 |
| 1390 | ENSG00000184939 | *ZFP90* | -0,746840965 | 2,13973E-15 |
| 1391 | ENSG00000123473 | *STIL* | -0,746817346 | 3,1114E-11 |
| 1392 | ENSG00000142945 | *KIF2C* | -0,745776952 | 6,68556E-23 |
| 1393 | ENSG00000101333 | *PLCB4* | -0,745559357 | 5,25186E-07 |
| 1394 | ENSG00000151929 | *BAG3* | -0,744884425 | 1,65814E-11 |
| 1395 | ENSG00000112029 | *FBXO5* | -0,744766358 | 3,04922E-15 |
| 1396 | ENSG00000185269 | *NOTUM* | -0,744507345 | 0,014153691 |
| 1397 | ENSG00000214756 | *METTL12* | -0,744457389 | 0,045291392 |
| 1398 | ENSG00000132646 | *PCNA* | -0,743755465 | 2,167E-27 |
| 1399 | ENSG00000206579 | *XKR4* | -0,743275481 | 0,012850913 |

| 1400 | ENSG00000272655 | *POLR2J4* | -0,741932916 | 0,045305309 |
|---|---|---|---|---|
| 1401 | ENSG00000070087 | *PFN2* | -0,740020962 | 1,56876E-41 |
| 1402 | ENSG00000088387 | *DOCK9* | -0,740008194 | 1,32237E-09 |
| 1403 | ENSG00000116667 | *C1orf21* | -0,739980427 | 6,25659E-34 |
| 1404 | ENSG00000145284 | *SCD5* | -0,739689179 | 1,4678E-37 |
| 1405 | ENSG00000140945 | *CDH13* | -0,739685245 | 6,01949E-28 |
| 1406 | ENSG00000114631 | *PODXL2* | -0,739564291 | 5,20591E-31 |
| 1407 | ENSG00000143842 | *SOX13* | -0,739287403 | 4,05455E-23 |
| 1408 | ENSG00000168243 | *GNG4* | -0,738466884 | 2,01758E-17 |
| 1409 | ENSG00000053747 | *LAMA3* | -0,737759245 | 0,034858662 |
| 1410 | ENSG00000267100 | *ILF3-AS1* | -0,737670536 | 1,93053E-10 |
| 1411 | ENSG00000197712 | *FAM114A1* | -0,73764301 | 1,95763E-06 |
| 1412 | ENSG00000164070 | *HSPA4L* | -0,737495391 | 2,6213E-05 |
| 1413 | ENSG00000129195 | *PIMREG* | -0,737052475 | 4,2562E-26 |
| 1414 | ENSG00000156735 | *BAG4* | -0,736906065 | 4,78953E-07 |
| 1415 | ENSG00000148835 | *TAF5* | -0,736423324 | 0,001689131 |
| 1416 | ENSG00000203880 | *PCMTD2* | -0,735368627 | 9,08705E-24 |
| 1417 | ENSG00000168300 | *PCMTD1* | -0,735296813 | 9,1134E-07 |
| 1418 | ENSG00000214016 | *RPSAP61* | -0,735079483 | 0,036129459 |
| 1419 | ENSG00000106799 | *TGFBR1* | -0,734845547 | 2,42576E-20 |
| 1420 | ENSG00000197563 | *PIGN* | -0,734079338 | 9,2975E-12 |
| 1421 | ENSG00000122966 | *CIT* | -0,733146831 | 4,35347E-24 |
| 1422 | ENSG00000206573 | *THUMPD3-AS1* | -0,732661044 | 4,08839E-11 |
| 1423 | ENSG00000162415 | *ZSWIM5* | -0,732335594 | 0,000227192 |
| 1424 | ENSG00000163535 | *SGO2* | -0,731739242 | 1,85898E-15 |
| 1425 | ENSG00000069712 | *KIAA1107* | -0,731416536 | 0,021259397 |
| 1426 | ENSG00000172602 | *RND1* | -0,731293915 | 0,007771946 |
| 1427 | ENSG00000171067 | *C11orf24* | -0,731161422 | 3,22378E-16 |
| 1428 | ENSG00000089685 | *BIRC5* | -0,73091772 | 3,52115E-14 |
| 1429 | ENSG00000081189 | *MEF2C* | -0,730451559 | 4,94173E-08 |
| 1430 | ENSG00000146278 | *PNRC1* | -0,730398796 | 3,84998E-18 |
| 1431 | ENSG00000110047 | *EHD1* | -0,730218012 | 1,04689E-18 |
| 1432 | ENSG00000053524 | *MCF2L2* | -0,729823153 | 0,022383816 |
| 1433 | ENSG00000095209 | *TMEM38B* | -0,729126293 | 3,38284E-09 |
| 1434 | ENSG00000070882 | *OSBPL3* | -0,72904691 | 1,61754E-12 |
| 1435 | ENSG00000214530 | *STARD10* | -0,728737394 | 0,000281407 |
| 1436 | ENSG00000145675 | *PIK3R1* | -0,728401357 | 9,65669E-20 |
| 1437 | ENSG00000085274 | *MYNN* | -0,727274949 | 3,29041E-07 |
| 1438 | ENSG00000163378 | *EOGT* | -0,726616705 | 0,001327846 |
| 1439 | ENSG00000259623 | *AC125257.1* | -0,725701137 | 1,34729E-05 |
| 1440 | ENSG00000235423 | *AC068768.1* | -0,725307146 | 0,01920025 |
| 1441 | ENSG00000108039 | *XPNPEP1* | -0,724816286 | 4,23669E-19 |
| 1442 | ENSG00000186106 | *ANKRD46* | -0,722604079 | 7,21698E-07 |
| 1443 | ENSG00000186907 | *RTN4RL2* | -0,72244167 | 5,86722E-06 |
| 1444 | ENSG00000185697 | *MYBL1* | -0,722431183 | 4,57055E-13 |
| 1445 | ENSG00000141646 | *SMAD4* | -0,721564297 | 1,55656E-17 |
| 1446 | ENSG00000146054 | *TRIM7* | -0,721518317 | 0,001768544 |
| 1447 | ENSG00000131797 | *CLUHP3* | -0,721030574 | 0,000795616 |
| 1448 | ENSG00000091157 | *WDR7* | -0,720486433 | 1,8335E-10 |
| 1449 | ENSG00000144152 | *FBLN7* | -0,720297546 | 0,041902533 |
| 1450 | ENSG00000215018 | *COL28A1* | -0,719512291 | 0,001265585 |
| 1451 | ENSG00000076716 | *GPC4* | -0,719324161 | 1,69077E-20 |
| 1452 | ENSG00000131389 | *SLC6A6* | -0,71911499 | 1,87104E-13 |
| 1453 | ENSG00000104969 | *SGTA* | -0,718603549 | 2,61884E-30 |
| 1454 | ENSG00000183778 | *B3GALT5* | -0,718198839 | 0,000424615 |
| 1455 | ENSG00000165238 | *WNK2* | -0,71755518 | 8,64999E-05 |
| 1456 | ENSG00000158560 | *DYNC1I1* | -0,71754635 | 0,027582356 |
| 1457 | ENSG00000133111 | *RFXAP* | -0,717175216 | 0,000507202 |
| 1458 | ENSG00000182054 | *IDH2* | -0,716876773 | 1,67549E-24 |
| 1459 | ENSG00000102984 | *ZNF821* | -0,716657009 | 1,26098E-05 |
| 1460 | ENSG00000102384 | *CENPI* | -0,716109268 | 1,7758E-08 |
| 1461 | ENSG00000146938 | *NLGN4X* | -0,716063426 | 5,10581E-31 |
| 1462 | ENSG00000154845 | *PPP4R1* | -0,715808192 | 2,20701E-21 |
| 1463 | ENSG00000153391 | *INO80C* | -0,715469801 | 7,19756E-05 |
| 1464 | ENSG00000161542 | *PRPSAP1* | -0,715135516 | 2,14034E-22 |
| 1465 | ENSG00000128805 | *ARHGAP22* | -0,714658771 | 1,10489E-05 |
| 1466 | ENSG00000134755 | *DSC2* | -0,714396962 | 0,012316879 |
| 1467 | ENSG00000087301 | *TXNDC16* | -0,713986723 | 8,99287E-10 |
| 1468 | ENSG00000121864 | *ZNF639* | -0,713811197 | 3,20176E-12 |
| 1469 | ENSG00000035664 | *DAPK2* | -0,71360453 | 0,015270375 |
| 1470 | ENSG00000119969 | *HELLS* | -0,713309797 | 1,28554E-07 |
| 1471 | ENSG00000168899 | *VAMP5* | -0,712827832 | 0,008705362 |
| 1472 | ENSG00000149599 | *DUSP15* | -0,71168316 | 0,002552417 |
| 1473 | ENSG00000165476 | *REEP3* | -0,711600564 | 2,14941E-13 |
| 1474 | ENSG00000105613 | *MAST1* | -0,711185595 | 2,87679E-09 |
| 1475 | ENSG00000124193 | *SRSF6* | -0,710297629 | 1,30274E-28 |
| 1476 | ENSG00000198087 | *CD2AP* | -0,709854268 | 4,47314E-06 |
| 1477 | ENSG00000067141 | *NEO1* | -0,709477615 | 1,03511E-22 |

| 1478 | ENSG00000136492 | *BRIP1* | -0,708772162 | 2,58981E-10 |
|---|---|---|---|---|
| 1479 | ENSG00000082212 | *ME2* | -0,708289555 | 1,02185E-17 |
| 1480 | ENSG00000134690 | *CDCA8* | -0,707619682 | 8,29387E-14 |
| 1481 | ENSG00000132561 | *MATN2* | -0,706959973 | 1,76238E-38 |
| 1482 | ENSG00000079435 | *LIPE* | -0,705988582 | 0,00043224 |
| 1483 | ENSG00000169330 | *KIAA1024* | -0,705889948 | 0,017546535 |
| 1484 | ENSG00000162174 | *ASRGL1* | -0,705813463 | 1,38499E-07 |
| 1485 | ENSG00000160957 | *RECQL4* | -0,704966301 | 7,40736E-18 |
| 1486 | ENSG00000240024 | *LINC00888* | -0,704597787 | 1,55178E-07 |
| 1487 | ENSG00000079134 | *THOC1* | -0,703663375 | 8,35198E-12 |
| 1488 | ENSG00000197535 | *MYO5A* | -0,703482606 | 6,65206E-20 |
| 1489 | ENSG00000101596 | *SMCHD1* | -0,703383313 | 3,30145E-20 |
| 1490 | ENSG00000176971 | *FIBIN* | -0,70332985 | 1,95771E-29 |
| 1491 | ENSG00000003436 | *TFPI* | -0,701987718 | 8,36422E-18 |
| 1492 | ENSG00000213853 | *EMP2* | -0,701971596 | 1,48275E-13 |
| 1493 | ENSG00000067177 | *PHKA1* | -0,701961211 | 1,85461E-05 |
| 1494 | ENSG00000158987 | *RAPGEF6* | -0,701569995 | 0,000688733 |
| 1495 | ENSG00000135476 | *ESPL1* | -0,701487062 | 5,16291E-13 |
| 1496 | ENSG00000234420 | *ZNF37BP* | -0,701485179 | 6,60731E-12 |
| 1497 | ENSG00000221883 | *ARIH2OS* | -0,701037954 | 0,03956487 |
| 1498 | ENSG00000097046 | *CDC7* | -0,700187235 | 1,48205E-13 |
| 1499 | ENSG00000130203 | *APOE* | -0,700126505 | 0,000382941 |
| 1500 | ENSG00000136542 | *GALNT5* | -0,700085603 | 0,028477354 |
| 1501 | ENSG00000127589 | *TUBBP1* | -0,699940812 | 8,81458E-24 |
| 1502 | ENSG00000188191 | *PRKAR1B* | -0,699901026 | 1,85825E-07 |
| 1503 | ENSG00000059573 | *ALDH18A1* | -0,69983634 | 2,62754E-19 |
| 1504 | ENSG00000176720 | *BOK* | -0,699777069 | 3,24321E-06 |
| 1505 | ENSG00000137135 | *ARHGEF39* | -0,699307241 | 0,011302941 |
| 1506 | ENSG00000154832 | *CXXC1* | -0,698962387 | 5,27642E-17 |
| 1507 | ENSG00000047579 | *DTNBP1* | -0,698544682 | 4,51622E-08 |
| 1508 | ENSG00000176170 | *SPHK1* | -0,698431981 | 5,37125E-17 |
| 1509 | ENSG00000182923 | *CEP63* | -0,69823711 | 2,46448E-13 |
| 1510 | ENSG00000171824 | *EXOSC10* | -0,69801235 | 3,60614E-22 |
| 1511 | ENSG00000091622 | *PITPNM3* | -0,69661803 | 0,000358106 |
| 1512 | ENSG00000182195 | *LDOC1* | -0,695696581 | 5,03568E-13 |
| 1513 | ENSG00000167397 | *VKORC1* | -0,695569645 | 0,00015656 |
| 1514 | ENSG00000174672 | *BRSK2* | -0,695194283 | 1,21713E-14 |
| 1515 | ENSG00000143674 | *MAP3K21* | -0,694475166 | 0,018201367 |
| 1516 | ENSG00000112333 | *NR2E1* | -0,694238726 | 0,020719261 |
| 1517 | ENSG00000135766 | *EGLN1* | -0,694137858 | 1,10902E-13 |
| 1518 | ENSG00000166147 | *FBN1* | -0,693994023 | 2,13973E-15 |
| 1519 | ENSG00000187068 | *C3orf70* | -0,693895425 | 1,69001E-13 |
| 1520 | ENSG00000164684 | *ZNF704* | -0,693798779 | 4,16077E-22 |
| 1521 | ENSG00000269834 | *ZNF528-AS1* | -0,693798663 | 9,57734E-06 |
| 1522 | ENSG00000095739 | *BAMBI* | -0,693466893 | 1,38951E-12 |
| 1523 | ENSG00000103966 | *EHD4* | -0,693293842 | 1,02998E-11 |
| 1524 | ENSG00000101187 | *SLCO4A1* | -0,693000116 | 2,7749E-10 |
| 1525 | ENSG00000137364 | *TPMT* | -0,692600608 | 1,15273E-07 |
| 1526 | ENSG00000146247 | *PHIP* | -0,692259971 | 2,57211E-16 |
| 1527 | ENSG00000112144 | *ICK* | -0,692090139 | 4,69286E-13 |
| 1528 | ENSG00000157500 | *APPL1* | -0,691998702 | 6,62622E-18 |
| 1529 | ENSG00000163584 | *RPL22L1* | -0,691979407 | 0,000138698 |
| 1530 | ENSG00000145908 | *ZNF300* | -0,691129485 | 1,19363E-12 |
| 1531 | ENSG00000182013 | *PNMA8A* | -0,690542689 | 3,03933E-15 |
| 1532 | ENSG00000064666 | *CNN2* | -0,690401346 | 3,59872E-11 |
| 1533 | ENSG00000128283 | *CDC42EP1* | -0,690284978 | 3,99664E-13 |
| 1534 | ENSG00000143942 | *CHAC2* | -0,689991188 | 0,019448115 |
| 1535 | ENSG00000198185 | *ZNF334* | -0,689880533 | 2,07527E-05 |
| 1536 | ENSG00000108055 | *SMC3* | -0,689705451 | 5,55833E-18 |
| 1537 | ENSG00000050344 | *NFE2L3* | -0,688493656 | 0,003891477 |
| 1538 | ENSG00000148143 | *ZNF462* | -0,686744954 | 6,46173E-17 |
| 1539 | ENSG00000185818 | *NAT8L* | -0,686343918 | 2,09208E-17 |
| 1540 | ENSG00000266208 | *AC080112.2* | -0,686019412 | 0,00874556 |
| 1541 | ENSG00000158457 | *TSPAN33* | -0,685909169 | 0,009516289 |
| 1542 | ENSG00000118523 | *CTGF* | -0,685755127 | 0,005651607 |
| 1543 | ENSG00000082397 | *EPB41L3* | -0,68547765 | 2,19906E-20 |
| 1544 | ENSG00000105750 | *ZNF85* | -0,685475256 | 1,8737E-06 |
| 1545 | ENSG00000149679 | *CABLES2* | -0,684817839 | 5,49217E-06 |
| 1546 | ENSG00000175063 | *UBE2C* | -0,684357412 | 5,66332E-17 |
| 1547 | ENSG00000100242 | *SUN2* | -0,684335786 | 5,17106E-21 |
| 1548 | ENSG00000196812 | *ZSCAN16* | -0,683800514 | 0,002144953 |
| 1549 | ENSG00000182372 | *CLN8* | -0,682946041 | 8,13074E-11 |
| 1550 | ENSG00000137124 | *ALDH1B1* | -0,682554383 | 5,89657E-16 |
| 1551 | ENSG00000079337 | *RAPGEF3* | -0,682464197 | 0,000763222 |
| 1552 | ENSG00000226711 | *FAM66C* | -0,682358353 | 0,003848539 |
| 1553 | ENSG00000125354 | *SEPT6* | -0,682267889 | 3,90671E-14 |
| 1554 | ENSG00000130830 | *MPP1* | -0,681533374 | 2,59446E-06 |
| 1555 | ENSG00000123130 | *ACOT9* | -0,681526172 | 5,05753E-09 |

| 1556 | ENSG00000161800 | *RACGAP1* | -0,680684181 | 2,76669E-23 |
|---|---|---|---|---|
| 1557 | ENSG00000120693 | *SMAD9* | -0,680642252 | 8,55426E-06 |
| 1558 | ENSG00000125772 | *GPCPD1* | -0,679277884 | 3,2898E-07 |
| 1559 | ENSG00000171724 | *VAT1L* | -0,678573505 | 0,000649255 |
| 1560 | ENSG00000120324 | *PCDHB10* | -0,67848325 | 7,70986E-05 |
| 1561 | ENSG00000164327 | *RICTOR* | -0,678399337 | 8,36319E-09 |
| 1562 | ENSG00000188322 | *SBK1* | -0,678117685 | 2,40605E-11 |
| 1563 | ENSG00000176593 | *AC008969.1* | -0,677983136 | 6,89115E-07 |
| 1564 | ENSG00000187257 | *RSBN1L* | -0,675639067 | 3,24312E-09 |
| 1565 | ENSG00000165312 | *OTUD1* | -0,674865135 | 0,013162824 |
| 1566 | ENSG00000188312 | *CENPP* | -0,673661615 | 0,000190342 |
| 1567 | ENSG00000233369 | *GTF2IP4* | -0,672287596 | 0,000426075 |
| 1568 | ENSG00000108375 | *RNF43* | -0,671651665 | 0,014693434 |
| 1569 | ENSG00000198729 | *PPP1R14C* | -0,670648086 | 2,09208E-17 |
| 1570 | ENSG00000152253 | *SPC25* | -0,670315643 | 1,92393E-08 |
| 1571 | ENSG00000162086 | *ZNF75A* | -0,670253103 | 1,18554E-07 |
| 1572 | ENSG00000198168 | *SVIP* | -0,668374388 | 1,10805E-09 |
| 1573 | ENSG00000092470 | *WDR76* | -0,668271563 | 8,22982E-10 |
| 1574 | ENSG00000235257 | *ITGA9-AS1* | -0,667987547 | 0,026274982 |
| 1575 | ENSG00000241360 | *PDXP* | -0,667732242 | 0,034742517 |
| 1576 | ENSG00000001461 | *NIPAL3* | -0,667073677 | 1,07993E-16 |
| 1577 | ENSG00000272143 | *FGF14-AS2* | -0,666801493 | 0,021653556 |
| 1578 | ENSG00000077684 | *JADE1* | -0,666672577 | 7,65683E-08 |
| 1579 | ENSG00000165124 | *SVEP1* | -0,666638749 | 1,03727E-07 |
| 1580 | ENSG00000108312 | *UBTF* | -0,665929349 | 1,77322E-20 |
| 1581 | ENSG00000145198 | *VWA5B2* | -0,665682721 | 0,041306225 |
| 1582 | ENSG00000187193 | *MT1X* | -0,665618984 | 0,000496252 |
| 1583 | ENSG00000148700 | *ADD3* | -0,665387121 | 1,66421E-20 |
| 1584 | ENSG00000259865 | *AL390728.6* | -0,664912959 | 0,048832215 |
| 1585 | ENSG00000136451 | *VEZF1* | -0,664860338 | 5,15561E-19 |
| 1586 | ENSG00000185219 | *ZNF445* | -0,664859331 | 1,6418E-14 |
| 1587 | ENSG00000001084 | *GCLC* | -0,663836054 | 0,000867682 |
| 1588 | ENSG00000136108 | *CKAP2* | -0,663466964 | 8,06473E-22 |
| 1589 | ENSG00000066739 | *ATG2B* | -0,663193092 | 1,26208E-14 |
| 1590 | ENSG00000115129 | *TP53I3* | -0,662835528 | 7,33883E-08 |
| 1591 | ENSG00000150867 | *PIP4K2A* | -0,662634543 | 1,51442E-12 |
| 1592 | ENSG00000141068 | *KSR1* | -0,662435504 | 2,58324E-10 |
| 1593 | ENSG00000172687 | *ZNF738* | -0,661972237 | 3,12181E-07 |
| 1594 | ENSG00000134901 | *KDELC1* | -0,661960485 | 5,19953E-05 |
| 1595 | ENSG00000188338 | *SLC38A3* | -0,661851592 | 1,34447E-09 |
| 1596 | ENSG00000121904 | *CSMD2* | -0,66175852 | 8,84713E-13 |
| 1597 | ENSG00000138640 | *FAM13A* | -0,661721792 | 5,3862E-05 |
| 1598 | ENSG00000100031 | *GGT1* | -0,659869548 | 0,000175095 |
| 1599 | ENSG00000019144 | *PHLDB1* | -0,659002151 | 5,56548E-27 |
| 1600 | ENSG00000145194 | *ECE2* | -0,658619028 | 0,048394376 |
| 1601 | ENSG00000141664 | *ZCCHC2* | -0,658545493 | 8,34898E-07 |
| 1602 | ENSG00000271270 | *TMCC1-AS1* | -0,657923816 | 6,66178E-05 |
| 1603 | ENSG00000142178 | *SIK1* | -0,657866327 | 0,00091721 |
| 1604 | ENSG00000188732 | *FAM221A* | -0,656598438 | 0,001717665 |
| 1605 | ENSG00000186814 | *ZSCAN30* | -0,655884346 | 6,09796E-08 |
| 1606 | ENSG00000123975 | *CKS2* | -0,655285822 | 6,67606E-17 |
| 1607 | ENSG00000165113 | *GKAP1* | -0,654912963 | 8,56235E-05 |
| 1608 | ENSG00000167005 | *NUDT21* | -0,654606399 | 3,76387E-23 |
| 1609 | ENSG00000167118 | *URM1* | -0,654352053 | 8,09666E-21 |
| 1610 | ENSG00000117632 | *STMN1* | -0,654019783 | 5,59726E-34 |
| 1611 | ENSG00000080819 | *CPOX* | -0,653180633 | 1,3021E-07 |
| 1612 | ENSG00000060656 | *PTPRU* | -0,653147965 | 3,23765E-10 |
| 1613 | ENSG00000102383 | *ZDHHC15* | -0,653057015 | 6,89578E-08 |
| 1614 | ENSG00000116191 | *RALGPS2* | -0,652893738 | 2,86605E-09 |
| 1615 | ENSG00000130822 | *PNCK* | -0,652397158 | 0,034344805 |
| 1616 | ENSG00000188157 | *AGRN* | -0,652307042 | 9,83145E-26 |
| 1617 | ENSG00000122068 | *FYTTD1* | -0,651531033 | 6,80818E-19 |
| 1618 | ENSG00000000460 | *C1orf112* | -0,651360191 | 2,89084E-06 |
| 1619 | ENSG00000006459 | *KDM7A* | -0,651265942 | 0,010471259 |
| 1620 | ENSG00000198826 | *ARHGAP11A* | -0,650584828 | 1,76583E-16 |
| 1621 | ENSG00000260804 | *LINC01963* | -0,650572716 | 2,13822E-05 |
| 1622 | ENSG00000228716 | *DHFR* | -0,650416754 | 1,64461E-18 |
| 1623 | ENSG00000079616 | *KIF22* | -0,650281234 | 5,1865E-20 |
| 1624 | ENSG00000096080 | *MRPS18A* | -0,648861091 | 1,70263E-10 |
| 1625 | ENSG00000198960 | *ARMCX6* | -0,648820322 | 1,37457E-14 |
| 1626 | ENSG00000179406 | *LINC00174* | -0,648690658 | 0,014804407 |
| 1627 | ENSG00000177303 | *CASKIN2* | -0,646355379 | 3,91747E-13 |
| 1628 | ENSG00000135245 | *HILPDA* | -0,646169391 | 0,000640615 |
| 1629 | ENSG00000163686 | *ABHD6* | -0,645107385 | 1,58773E-08 |
| 1630 | ENSG00000186310 | *NAP1L3* | -0,643229136 | 0,000130606 |
| 1631 | ENSG00000104147 | *OIP5* | -0,643155584 | 5,71653E-05 |
| 1632 | ENSG00000160307 | *S100B* | -0,642808767 | 1,21046E-26 |
| 1633 | ENSG00000267544 | *AC007229.1* | -0,642358724 | 0,040715868 |

| 1634 | ENSG00000152749 | *GPR180* | -0,642276435 | 0,000323811 |
|---|---|---|---|---|
| 1635 | ENSG00000076242 | *MLH1* | -0,641744323 | 7,01801E-14 |
| 1636 | ENSG00000168283 | *BMI1* | -0,64134513 | 2,5294E-07 |
| 1637 | ENSG00000162402 | *USP24* | -0,640554851 | 1,06345E-17 |
| 1638 | ENSG00000090661 | *CERS4* | -0,640112952 | 3,35326E-13 |
| 1639 | ENSG00000214222 | *TUBBP2* | -0,639376651 | 4,93414E-16 |
| 1640 | ENSG00000150477 | *KIAA1328* | -0,639154843 | 0,005488849 |
| 1641 | ENSG00000075336 | *TIMM21* | -0,639073478 | 6,54303E-09 |
| 1642 | ENSG00000099284 | *H2AFY2* | -0,639039678 | 6,65498E-09 |
| 1643 | ENSG00000177602 | *GSG2* | -0,638894183 | 0,000390697 |
| 1644 | ENSG00000144724 | *PTPRG* | -0,638545763 | 7,66262E-16 |
| 1645 | ENSG00000134057 | *CCNB1* | -0,63846466 | 4,32462E-20 |
| 1646 | ENSG00000129757 | *CDKN1C* | -0,637952514 | 0,008228096 |
| 1647 | ENSG00000139352 | *ASCL1* | -0,637711079 | 1,81568E-21 |
| 1648 | ENSG00000247627 | *MTND4P12* | -0,637704188 | 4,76001E-16 |
| 1649 | ENSG00000052126 | *PLEKHA5* | -0,637448451 | 0,002152765 |
| 1650 | ENSG00000028528 | *SNX1* | -0,636452621 | 5,06079E-23 |
| 1651 | ENSG00000138764 | *CCNG2* | -0,634985969 | 5,63958E-10 |
| 1652 | ENSG00000143409 | *MINDY1* | -0,634814194 | 1,40885E-05 |
| 1653 | ENSG00000126709 | *IFI6* | -0,634215947 | 6,06848E-06 |
| 1654 | ENSG00000145022 | *TCTA* | -0,633894257 | 1,91384E-10 |
| 1655 | ENSG00000170017 | *ALCAM* | -0,633554083 | 1,88644E-28 |
| 1656 | ENSG00000110841 | *PPFIBP1* | -0,633291959 | 6,40503E-21 |
| 1657 | ENSG00000149548 | *CCDC15* | -0,632981745 | 0,000497594 |
| 1658 | ENSG00000162817 | *C1orf115* | -0,632654155 | 0,023720358 |
| 1659 | ENSG00000114127 | *XRN1* | -0,632558633 | 2,14689E-10 |
| 1660 | ENSG00000273015 | *AC008124.1* | -0,632252555 | 1,86971E-06 |
| 1661 | ENSG00000104472 | *CHRAC1* | -0,632128413 | 7,62763E-07 |
| 1662 | ENSG00000133424 | *LARGE1* | -0,631953787 | 7,64187E-11 |
| 1663 | ENSG00000203760 | *CENPW* | -0,631706664 | 0,000621363 |
| 1664 | ENSG00000110042 | *DTX4* | -0,631612101 | 5,99397E-05 |
| 1665 | ENSG00000225733 | *FGD5-AS1* | -0,631564914 | 1,21029E-26 |
| 1666 | ENSG00000130558 | *OLFM1* | -0,630966788 | 1,99695E-15 |
| 1667 | ENSG00000076513 | *ANKRD13A* | -0,630965588 | 1,66494E-10 |
| 1668 | ENSG00000177733 | *HNRNPA0* | -0,630894031 | 1,84644E-24 |
| 1669 | ENSG00000256223 | *ZNF10* | -0,630583401 | 6,84139E-05 |
| 1670 | ENSG00000164086 | *DUSP7* | -0,630456378 | 2,31862E-09 |
| 1671 | ENSG00000153395 | *LPCAT1* | -0,630364411 | 5,73055E-18 |
| 1672 | ENSG00000144395 | *CCDC150* | -0,630284256 | 0,001986655 |
| 1673 | ENSG00000182796 | *TMEM198B* | -0,630122956 | 9,1405E-09 |
| 1674 | ENSG00000166508 | *MCM7* | -0,629657416 | 1,21508E-27 |
| 1675 | ENSG00000152092 | *ASTN1* | -0,628746791 | 6,08308E-21 |
| 1676 | ENSG00000163320 | *CGGBP1* | -0,627702299 | 9,85433E-23 |
| 1677 | ENSG00000147459 | *DOCK5* | -0,627667711 | 0,00126014 |
| 1678 | ENSG00000083799 | *CYLD* | -0,627517459 | 6,11792E-07 |
| 1679 | ENSG00000224189 | *HAGLR* | -0,627364545 | 0,004652709 |
| 1680 | ENSG00000152154 | *TMEM178A* | -0,626681405 | 0,014455446 |
| 1681 | ENSG00000196220 | *SRGAP3* | -0,626216323 | 1,17185E-14 |
| 1682 | ENSG00000130193 | *THEM6* | -0,626202908 | 3,32791E-07 |
| 1683 | ENSG00000184897 | *H1FX* | -0,626055246 | 7,23724E-21 |
| 1684 | ENSG00000100297 | *MCM5* | -0,625389018 | 1,19053E-21 |
| 1685 | ENSG00000225792 | *AC004540.2* | -0,625022866 | 0,002482765 |
| 1686 | ENSG00000181555 | *SETD2* | -0,624648065 | 4,62164E-17 |
| 1687 | ENSG00000165449 | *SLC16A9* | -0,624526744 | 7,57048E-06 |
| 1688 | ENSG00000123358 | *NR4A1* | -0,62418242 | 2,88913E-11 |
| 1689 | ENSG00000176978 | *DPP7* | -0,623736744 | 0,000274932 |
| 1690 | ENSG00000197275 | *RAD54B* | -0,623730776 | 0,007897409 |
| 1691 | ENSG00000124374 | *PAIP2B* | -0,62350701 | 0,024561192 |
| 1692 | ENSG00000122359 | *ANXA11* | -0,623375092 | 0,021419759 |
| 1693 | ENSG00000184014 | *DENND5A* | -0,623316597 | 4,64656E-26 |
| 1694 | ENSG00000184986 | *TMEM121* | -0,621873027 | 2,79712E-07 |
| 1695 | ENSG00000164548 | *TRA2A* | -0,621871723 | 1,79799E-11 |
| 1696 | ENSG00000127423 | *AUNIP* | -0,621778837 | 0,004258333 |
| 1697 | ENSG00000179455 | *MKRN3* | -0,621545594 | 0,001470639 |
| 1698 | ENSG00000136040 | *PLXNC1* | -0,621537768 | 0,004371248 |
| 1699 | ENSG00000231770 | *TMEM44-AS1* | -0,620907742 | 0,008785166 |
| 1700 | ENSG00000198039 | *ZNF273* | -0,62073173 | 0,000495457 |
| 1701 | ENSG00000163873 | *GRIK3* | -0,620584569 | 2,2355E-22 |
| 1702 | ENSG00000235109 | *ZSCAN31* | -0,619984605 | 0,021577276 |
| 1703 | ENSG00000104356 | *POP1* | -0,619920996 | 2,30068E-06 |
| 1704 | ENSG00000177628 | *GBA* | -0,61971002 | 1,65812E-11 |
| 1705 | ENSG00000178700 | *DHFR2* | -0,61956707 | 5,51901E-05 |
| 1706 | ENSG00000172037 | *LAMB2* | -0,619525894 | 9,46296E-24 |
| 1707 | ENSG00000185158 | *LRRC37B* | -0,619443321 | 3,71005E-05 |
| 1708 | ENSG00000152240 | *HAUS1* | -0,619091496 | 8,25896E-10 |
| 1709 | ENSG00000154473 | *BUB3* | -0,618602218 | 1,78051E-18 |
| 1710 | ENSG00000152433 | *ZNF547* | -0,618209981 | 0,015388526 |
| 1711 | ENSG00000178917 | *ZNF852* | -0,617181576 | 0,017351365 |

| 1712 | ENSG00000101558 | *VAPA* | -0,617087214 | 1,13533E-18 |
|---|---|---|---|---|
| 1713 | ENSG00000015133 | *CCDC88C* | -0,616698329 | 7,54464E-13 |
| 1714 | ENSG00000198901 | *PRC1* | -0,616469218 | 1,01146E-22 |
| 1715 | ENSG00000136754 | *ABI1* | -0,615649652 | 6,86062E-11 |
| 1716 | ENSG00000273270 | *AC090114.2* | -0,615090322 | 0,035904836 |
| 1717 | ENSG00000163659 | *TIPARP* | -0,613780799 | 1,58981E-10 |
| 1718 | ENSG00000134444 | *KIAA1468* | -0,613669987 | 5,36026E-09 |
| 1719 | ENSG00000237940 | *LINC01238* | -0,613444787 | 0,01447202 |
| 1720 | ENSG00000142686 | *C1orf216* | -0,613193424 | 0,015312795 |
| 1721 | ENSG00000198890 | *PRMT6* | -0,613093125 | 2,07047E-07 |
| 1722 | ENSG00000182606 | *TRAK1* | -0,612212527 | 5,98356E-18 |
| 1723 | ENSG00000213160 | *KLHL23* | -0,612155058 | 7,81869E-09 |
| 1724 | ENSG00000204899 | *MZT1* | -0,611723462 | 8,99037E-05 |
| 1725 | ENSG00000054654 | *SYNE2* | -0,610952941 | 8,78555E-13 |
| 1726 | ENSG00000198373 | *WWP2* | -0,61075958 | 1,45335E-14 |
| 1727 | ENSG00000069974 | *RAB27A* | -0,61051121 | 0,00134296 |
| 1728 | ENSG00000077942 | *FBLN1* | -0,610450087 | 1,62435E-07 |
| 1729 | ENSG00000168496 | *FEN1* | -0,610238096 | 5,05362E-15 |
| 1730 | ENSG00000178585 | *CTNNBIP1* | -0,609780203 | 2,75055E-11 |
| 1731 | ENSG00000170364 | *SETMAR* | -0,609195822 | 1,9339E-05 |
| 1732 | ENSG00000129173 | *E2F8* | -0,609184256 | 0,000589373 |
| 1733 | ENSG00000021300 | *PLEKHB1* | -0,606826639 | 4,98243E-20 |
| 1734 | ENSG00000107338 | *SHB* | -0,606718676 | 0,002587718 |
| 1735 | ENSG00000114698 | *PLSCR4* | -0,606353174 | 0,000431687 |
| 1736 | ENSG00000181544 | *FANCB* | -0,605963831 | 0,011909396 |
| 1737 | ENSG00000140199 | *SLC12A6* | -0,605647819 | 0,000107169 |
| 1738 | ENSG00000108387 | *SEPT4* | -0,605163814 | 6,51931E-09 |
| 1739 | ENSG00000146670 | *CDCA5* | -0,604660985 | 5,78774E-15 |
| 1740 | ENSG00000168374 | *ARF4* | -0,604333074 | 2,04651E-20 |
| 1741 | ENSG00000126970 | *ZC4H2* | -0,603317402 | 9,8419E-06 |
| 1742 | ENSG00000100504 | *PYGL* | -0,6020543 | 8,13617E-14 |
| 1743 | ENSG00000272593 | *AL359091.2* | -0,602026618 | 0,022578569 |
| 1744 | ENSG00000204934 | *ATP6V0E2-AS1* | -0,602000576 | 0,011241408 |
| 1745 | ENSG00000152642 | *GPD1L* | -0,601958989 | 4,30498E-15 |
| 1746 | ENSG00000101003 | *GINS1* | -0,601616583 | 3,79639E-11 |
| 1747 | ENSG00000138092 | *CENPO* | -0,601575357 | 4,92326E-09 |
| 1748 | ENSG00000125675 | *GRIA3* | -0,601508233 | 2,26245E-10 |
| 1749 | ENSG00000128944 | *KNSTRN* | -0,601071961 | 2,19402E-09 |
| 1750 | ENSG00000106588 | *PSMA2* | -0,600977401 | 0,01932934 |

# Erklärung

Ich versichere, dass ich die von mir vorgelegte Dissertation selbstständig angefertigt, die benutzten Quellen und Hilfsmittel vollständig angegeben und die Stellen der Arbeit -einschließlich Tabellen, Karten und Abbildungen -, die anderen Werken im Wortlaut oder dem Sinn nach entnommen sind, in jedem Einzelfall als Entlehnung kenntlich gemacht habe; dass diese Dissertation noch keiner anderen Fakultät oder Universität zur Prüfung vorgelegen hat; dass sie - abgesehen von unten angegebenen Teilpublikationen - noch nicht veröffentlicht worden ist sowie, dass ich eine solche Veröffentlichung vor Abschluss des Promotionsverfahrens nicht vornehmen werde. Die Bestimmungen dieser Promotionsordnung sind mir bekannt. Die von mir vorgelegte Dissertation ist von Prof. Dr. Jay Gopalakrishnan betreut worden.

Übersicht der Publikationen: Siehe “List of publications” (Seite 119)

Ich versichere, dass ich alle Angaben wahrheitsgemäß nach bestem Wissen und Gewissen gemacht habe und verpflichte mich, jedmögliche, die obigen Angaben betreffenden Veränderungen, dem Promotionsausschuss unverzüglich mitzuteilen.

..... .....

Datum Unterschrift